TRANSIENT POSTNATAL PULMONARY ARTERIAL SMOOTH MUSCLE CYTOSKELETAL DISASSEMBLY AND ITS FUNCTIONAL IMPLICATIONS

by

Dr A A Chaudhry

A thesis submitted for the degree of

Doctor of Philosophy

in the University of London

August 1999

Institute of Child Health

University College London

30 Guilford Street

London WCIN 1EH

Abstract

In the human at birth the flow of blood through the pulmonary arteries increases ten-fold as a consequence of an acute fall in pulmonary vascular resistance followed by a gradual remodelling of vessels which occurs over the first weeks of life. These changes are essential for normal gaseous exchange to occur in the lungs. The initial part of the process may be halted by perinatal hypoxia, acidosis, or sepsis and causes the clinical syndrome of persistent pulmonary hypertension of the newborn (PPHN).

This thesis explores the changes in the cytoskeleton of the smooth muscle cells (SMCs) which help mediate the normal fall in pulmonary vascular resistance and are abnormal in PPHN. These studies were carried out using normal pigs and a hypobaric hypoxic model of PPHN.

A series of cytoskeletal SMC phenotypes were identified within the intact intrapulmonary artery wall dependant upon different combinations of certain cytoskeletal proteins (α smooth muscle actin, β actin, γ actin SM1 myosin heavy chain isoform, calponin, caldesmon and desmin). This classification demonstrated an outer to inner medial progression of SMC phenotype during development. This was punctuated by a transient reduction in α smooth muscle actin, β actin and calponin staining at three days of age, which was considered to represent phenotypic modulation of the SMC phenotype. The total actin content and the proportion present in the monomeric form was found to remain constant during this time, using a highly specific fluorometric DNAse I inhibition assay. However, using simultaneously permeabilised and phalloidin treated preparations, the filamentous actin cytoskeleton of the SMCs was shown to re-organise to finer filaments after birth which may help explain the change in staining pattern within the inner media at three days.

Functional studies using isolated segments of intrapulmonary artery indicated that the reorganisation of the actin cytoskeleton after birth was not associated with a significant reduction in contractile potential. Studies on the vessels from fetal and full term piglets indicated that changes in the actin organisation occurred within

minutes of the onset of breathing and were associated with significant increases in contractile potential.

The possibility that changes in morphologically distinct SMC phenotypes could be responsible for the cytoskeletal changes seen in the intact vessel was investigated by primary cell culture. Epithelioid and spindle-shaped SMC phenotypes were isolated from intrapulmonary arteries throughout development and from both inner and outer parts of the media. Although not responsible for the changes within the inner media of the intact vessel wall at three days of age, an increase in the proportion of epithelioid cells was noted to occur following birth. Spindle-shaped and epithelioid SMCs were obtained by dilutional cloning from intrapulmonary arteries from normal 14 day old and neonatal piglets exposed to hypobaric hypoxia. These cell lines were then characterised in terms of cytoskeletal protein content, replication properties, contractile properties and migrational potential. Distinct differences between the different morphological phenotypes were observed, suggesting differences in function within the intact vessel wall and perturbation of normal function following hypobaric hypoxia.

Acknowledgements

My first thoughts are to my friend Professor David Harvey, whose continuing support throughout my paediatric training is much appreciated.

I would also like to thank Professor S.G. Haworth and Dr Susan Hall for their supervision and the British Heart Foundation for funding this period of study. Many people at the Institute of Child Health, University College London, and the University of Manchester have helped me with kind advice, technical expertise and reagents during the course of these experiments. In particular I must thank Dr Alison Hislop, Dr Stephen Greenwald and Dr Durward Lawson. I am indebted to Dr Alison North, who taught me to cut semi-thin sections and looked after me at the Meeting of the European Cytoskeletal Forum in Siena, in 1998.

Finally I thank my wife, Dr Deborah Henderson, for scientific advice and support and together with my son, Jamey, for being my family.

Abbreviations

ANOVA	Analysis of variation
ATP	Adenosine tri-phosphate
bET-1	Big Endothelin 1
BrdU	5-bromo-2'-deoxy uridine
BSA	Bovine serum albumin
CHD	Congenital heart disease
CLSM	Confocal laser scanning microscopy
CRBP	Cellular retinol binding protein
D	Diameter of vessel ring
DNA	Deoxyribonucleic acid
Dnase I	Deoxyribonuclease I
Δh	increase in hemi-circumference
eNOS	endothelial Nitric oxide synthase
ECMO	Extra corporal membrane oxygenation
EDRF	Endothelium dependent relaxing factor
EDTA	Ethylenediaminetetraacetic acid
epSMC	epithelioid smooth muscle cell
ET-A, B	Endothelin receptor A and B
ET-1, 2, and 3	Endothelins 1, 2, and 3
E	Young's Modulus
E_{inc}	Incremental elastic modulus
EVG	Elastin van Giesen
F	Force

FAC	Focal adhesion complex
FAK	Focal adhesion kinase
F actin	Filamentous actin
FCS	Fetal calf serum
FITC	Fluorescein isothiocyanate
G actin	Globular or monomeric actin
h	hemi-circumference
hyepSMC	hypoxic epithelioid smooth muscle cell
hyspSMC	hypoxic spindle-shaped smooth muscle cell
kDa	KiloDaltons
kPa	KiloPascals
L	Length of experimental vessel rings
MHC	Myosin heavy chain
MLC	Myosin light chain
MMPs	Matrix metaloproteinases
NO	Nitric oxide
P	Percentage circumferential wall stress
Pr	Pressure
PO_2	Partial pressure of oxygen
PBS	Phosphate buffered saline
PCO_2	Partial pressure of carbon dioxide
PGI_2	Prostacyclin
PSS	Physiological saline solution
PVP	Polyvinylpyrrolidone
PPHN	Persistent pulmonary hypertension of the newborn

R	Radius
S	Strain
SD	Standard deviation from the mean
SE	Standard error of the means
SE%	Standard error of percentage
SM1	204 kDa myosin heavy chain isoform
SM2	200 kDa myosin heavy chain isoform
SMC	Smooth muscle cell
Smemb	Non-smooth muscle specific myosin heavy chain isoform (198kDa)
SpSMC	Spindle-shaped smooth muscle cell
SR	Stress ratio
T	Tension
TRITC	Tetramethylrhodamine isothiocyanate
w	Wall thickness
τ	Wall stress

Contents

List of figures

List of tables

Chapter 1. Introduction and background

The purpose of this thesis was to investigate changes in smooth muscle cell (SMC) appearance during adaptation of the pulmonary arteries to the extra-uterine environment. In particular it focused on the cytoskeletal proteins within the pulmonary arterial SMCs, both in the intact vessel wall and following tissue culture. It is proposed that alterations in SMC morphology facilitate the normal process of postnatal adaptation and that PPHN, represented by a hypobaric hypoxic model, is associated with expression of abnormal SMC phenotype(s).

The introduction to this thesis outlines what is known about the structure and function of the normal pulmonary circulation in the fetus, and how adaptation to the extra-uterine environment occurs. The humoral controlling mechanisms that initially maintain the fetal circulation, and are then associated with the transition to the extra-uterine circulation, are discussed. Abnormal development of the pulmonary circulation is seen in persistent pulmonary hypertension of the newborn. The pathophysiology, histological findings, clinical picture and management of this condition are discussed and a porcine hypobaric hypoxic model of PPHN is described. A brief review of the SMC phenotypes in the systemic and pulmonary circulations, and possible markers of SMC phenotype is given. Extra-cellular matrix proteins which may influence SMC phenotype, and other contractile cells of the vasculature which might be confused with SMC phenotypes are discussed. Finally, the mechanical properties of the pulmonary arterial wall, which alter during adaptation to the extra-uterine environment are addressed.

1.1 THE NORMAL PULMONARY CIRCULATIONS

William Harvey took the first step towards a modern physiology in proposing how the heart pumped blood through a circulation of arteries and veins, and predicted the discovery of "pores" that connected the arterial and venous systems (Harvey, 1628). It was the Italian physician and anatomist Marcello Malpighi (1661) who with the aid of a microscope, discovered capillaries and described the pulmonary microvasculature: "I could clearly see that the blood is divided and flows through tortuous vessels, and that it is not poured into spaces, but is always driven through tubules and distributed through manifold bendings of the vessels"

It was not until 1939 that the fetal circulation was first visualised in vivo, when Barclay, Barcroft, Barron and Franklin (Barclay et al., 1939) performed cineangiographic studies on the exteriorised fetal lamb. Following on from these initial investigations we now know the intra-uterine pulmonary circulation is very different from the extra-uterine pulmonary circulation, and that at birth major alterations of the circulation must occur to allow a change from a totally placental to a totally pulmonary-dependent system of gas exchange. Impairment of this immediate transition, as seen in persistent pulmonary hypertension of the newborn (PPHN) is a leading cause of mortality and morbidity in the neonatal period, in both term and preterm infants, whilst disordered remodelling and growth of the pulmonary circulation is a key problem in children with structural congenital heart disease.

1.1.1 The fetal circulation

The nutritional and oxygen requirements of the fetus are met entirely by the placenta. The fetal circulation (Figure 1) serves to direct nutritionally-rich oxygenated blood directly into the systemic circulation. Enriched blood from the placenta enters the fetus via the umbilical vein and passes through the hepatic portal system towards the liver, where it directly enters the inferior vena cava via the ductus venosus. This stream of blood is directed through the foramen ovale, into the left side of the heart, and out to the systemic circulation to supply the

metabolic needs of the fetus. Some of this nutritionally-rich blood from the inferior vena cava mixes with blood flow from the superior vena cava and passes into the pulmonary arteries via the right ventricle. Most of the blood entering the main pulmonary artery bypasses the lungs through the ductus arteriosus and passes into the descending aorta. Thus, pulmonary blood flow in the near term fetal lamb is only about 10% of the total cardiac output of the heart, but is sufficient to supply the lungs with nutritional requirements for growth and metabolic functions (Rudolph and Heymann, 1970).

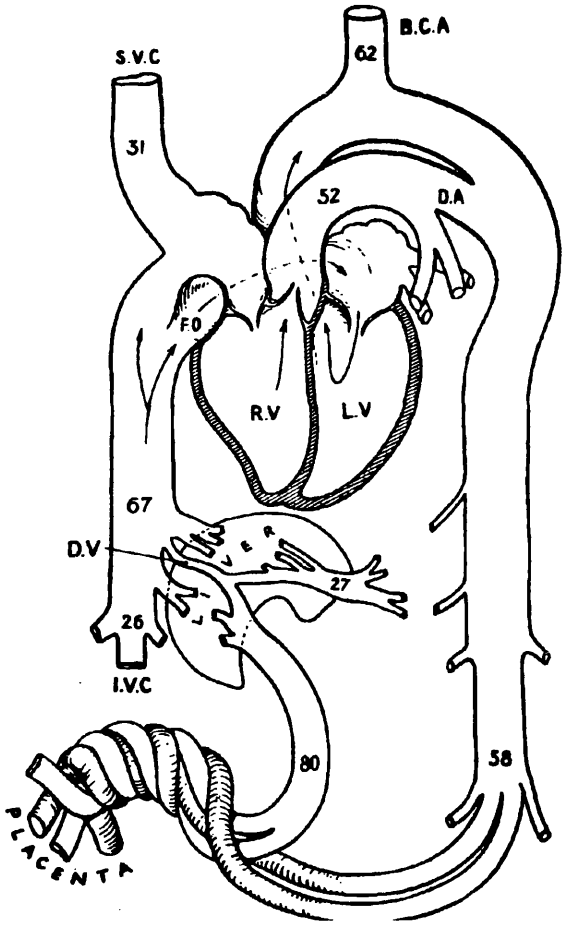

Figure 1. The fetal circulation. The numbers represent the mean oxygen saturation in the sheep. BCA brachiocephalic artery, DA ductus arteriosus, DV ductus venosus, FO foramen ovale, IVC inferior vena cava, LV left ventricle, RV right ventricle, SVC superior vena cava. (Adapted from Dawes et al., 1953).

1.1.2 The postnatal pulmonary circulation

The lungs receive de-oxygenated venous blood through the pulmonary arteries and function to replete the haemoglobin within red blood cells, by bringing them into close proximity with oxygen-containing inspired air at the alveolar surface. There is also an additional but small bronchial blood flow (1% of cardiac output) which originates from the systemic circulation and provides oxygen and nutrition to the airways.

The pulmonary circulation, in contrast to the systemic, is a low resistance, high flow circulation which can accommodate large increases in cardiac output (such as during exercise) without elevations in arterial pressure. The site of control of pressure is thought to reside in the small pre-alveolar muscular arteries (Fike and Kaplowitz, 1992). Poiseuille's law explains how small changes in the radius of these vessels can produce large reductions in flow (the laminar flow of a liquid through a rigid tube is inversely proportional to the fourth power of the radius of the tube). Thus these small vessels can regulate pulmonary artery pressure under changing flow conditions and also can act to control the distribution of blood within the lung, directing it to well oxygenated areas and diverting it away from poorly ventilated areas (West, 1974). Alveolar hypoxia is the most potent stimulus for vasoconstriction and acts synergistically with acidosis, of either respiratory or metabolic origin (Julian et al., 1996).

1.2 PULMONARY ADAPTATION TO EXTRA-UTERINE LIFE

Normal postnatal pulmonary arterial adaptation to extra-uterine life in higher mammals can be divided into three overlapping stages:

1. Initial adaptation to extrauterine life - in which the pulmonary vasculature is rapidly remodelled to effect an abrupt reduction in pulmonary vascular resistance. This stage lasts from birth to approximately four days of age.
2. Continued remodelling and stabilisation - of the altered structure, which begins at birth and continues until 3-4 weeks of age.
3. Growth - which continues more slowly as the vessels grow into adulthood.

These changes can be seen in the human and have been fully characterised in the pig.

1.2.1 Initial adaptation to extrauterine life

Following birth, pulmonary vascular resistance falls eight-to-tenfold allowing half of the combined ventricular output to pass through the lungs (Figure 2). (Cassin et al., 1964). Mean pulmonary arterial pressure continues to fall, and by 25 hours after birth is at 50% of systemic pressure (Moss et al., 1963) (Figure 3).

The process by which the pulmonary vasculature suddenly adapts to extrauterine life, and accepts the massive increase in blood flow, involves the entire arterial pathway, from the large elastic and muscular conducting arteries to the resistance arteries which are just proximal to the respiratory units (Hall and Haworth, 1987). The most dramatic structural changes are seen in the precapillary arteries (Haworth et al., 1987). At birth the endothelial and smooth muscle cells are brick-like, with considerable overlap of cell borders. The endothelial cells almost, or completely, occlude the vessel lumen. Within five minutes of birth the surface-to-volume ratio of the endothelial cells and SMCs has increased and the endothelial cells, pericytes and SMCs have spread, such that the vessel wall becomes thinner and the lumen larger. This process continues to affect the

remainder of the precapillary arteries over the next few days until they are all dilated. A similar series of changes occurs in the large elastic arteries, such that there is a reduction in the wall thickness, and the diameter of smooth muscle cells is reduced (Hall and Haworth, 1987).

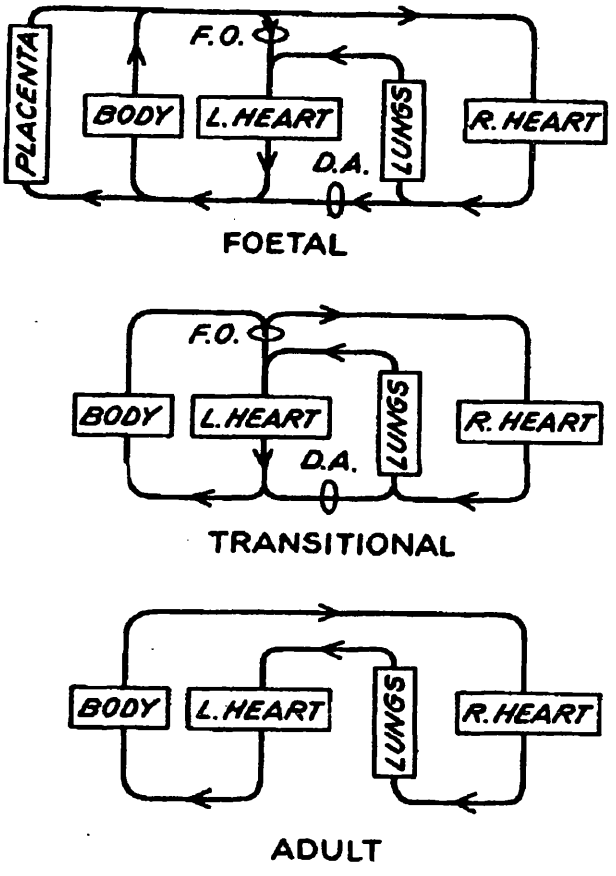

Figure 2. Schematic representation of the fetal, transitional and adult circulations. Removal of the placenta from the fetal circulation increases systemic resistance and the increase in pulmonary blood flow raises left atrial pressure. Progression from the transitional to the adult circulation occurs by the closure of the flap like foramen ovale (FO), and functional closure of the ductus arteriosus (DA). This prevents any significant right-to-left shunting of blood and effectively separates the two circulations (adapted from Dawes et al., 1954).

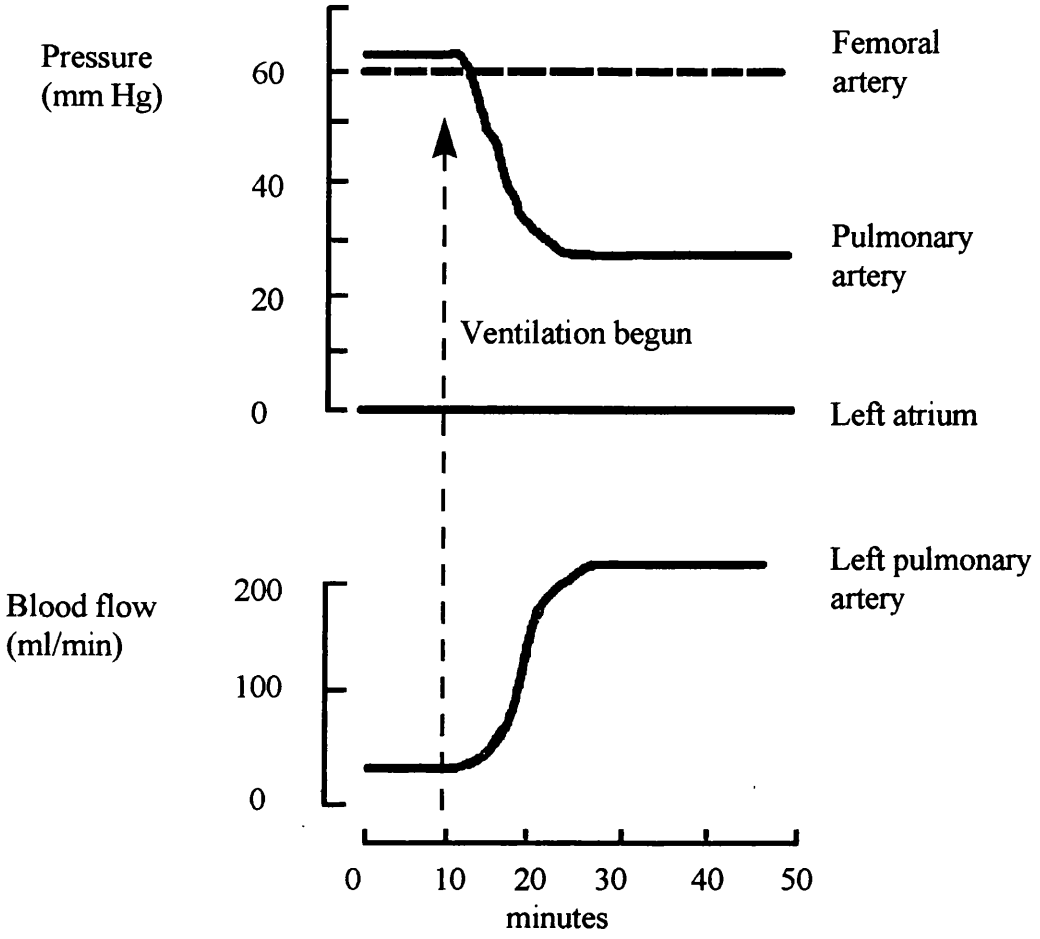

Figure 3. The effect of positive pressure ventilation on pulmonary blood flow and pressures in a mature fetal lamb. Prior to ventilation of the lungs at birth the pulmonary and systemic arterial pressures are similar and pulmonary blood flow is low. On inflation of the lungs pulmonary arterial pressure immediately falls by 50% and pulmonary blood flow increases ten fold (adapted from Dawes et al., 1953).

1.2.2 Stabilisation of structure

The myofilament volume density of the SMCs is relatively low at birth and increases with age. The myofilaments are particularly prominent in SMCs of the outer third of the vessel media, with the inner layer of SMCs containing fewer myofilaments (Hall and Haworth, 1987). This difference may be related to uneven stress and strain loading of the vessel wall, as it is at this point that dissecting aortic aneurysm is found to occur in systemic vessels (Berry et. al., 1993). Although the

myofilament density in all regions of the wall increases with age there is a transient reduction in myofilaments occurring three days after birth (Hall and Haworth, 1987). Subsequently when the endothelial and smooth muscle cells appear to have taken up their definitive position within the vessel wall, they begin to deposit connective tissue around themselves and stabilise the new wall structure. Initially the internal elastic lamina consists of amorphous patches of elastin, but by three weeks of age a definite elastic lamina is present. Throughout the wall elastin and collagen fibres become larger (Hall and Haworth, 1987; Haworth et al., 1987). Collagen types III and V are abundant at birth, whilst there is relatively little of the stiffer collagen type I. This composition helps to explain why the newborn vessels are more plastic than those of the adult (Mills and Haworth, 1987). During this period of stabilisation the pulmonary arterial pressure continues to fall and adult values are achieved by 2 - 6 weeks after birth.

1.2.3 Growth

Although the pulmonary arterial pressure has fallen to adult values by 2 to 6 weeks of age, the animal continues to grow and must accommodate a progressive increase in cardiac output. Thus, with somatic growth, the overall size of the intrapulmonary arteries and the amount of the components within the wall also increases. SMCs increase in size and number, and connective tissue is deposited around them. The balance of collagen shifts towards type I explaining the increasing structural stiffness of the pulmonary arteries with age (Mills and Haworth, 1987; Greenwald et al., 1982). The wall thickness is related to external diameter. Therefore, small peripheral vessels which initially have only a single layer of pericytes become coated with one or more layers of SMCs as they increase in size. These changes in the structure and dimensions of the pulmonary arteries within the lung are particularly important as they influence, and are related to, the intramural stress and the tone required to be generated by the SMCs themselves.

1.3 NORMAL MECHANISMS OF CONTROL IN THE FETAL PULMONARY CIRCULATION

The mechanisms responsible for maintenance of a high fetal pulmonary vasculature resistance, and the rapid remodelling which occurs within minutes of birth, are poorly understood. The initial experiments were performed on late gestation fetal sheep, examining the factors which produce an increase in pulmonary blood flow (Dawes, 1968). Following from this work, fetal sheep were implanted with flow and pressure measuring devices (chronically instrumented) and then investigated. This work has yielded more information about the variations in normal fetal pulmonary arterial pressure and flow.

1.3.1 Humoral factors involved in maintenance of the fetal state

The site of resistance to blood flow in the fetal lung is thought to reside in the small pre-alveolar arteries. The occluded lumens seen on histological section begin to dilate within minutes of birth, but the controlling factors that maintain narrow/occluded arteriolar lumens within the fetus are not clear. A variety of vasoconstricting mediators that may maintain the high fetal pulmonary vascular resistance have been investigated. Pharmacological blockage of mediators such as sympathetic nervous tone (Colebatch et al., 1965), prostaglandins, thromboxane and leukotrienes (Cassin, 1987) have not resulted in pulmonary arterial vasodilatation.

It is possible that a low oxygen tension might directly contribute to the high pulmonary vascular resistance in the fetus. The nature of the oxygen sensor remains unknown but is has been shown that endothelial cells (Stevens et al., 1994) and pulmonary arterial SMCs within the fetus respond to changes in oxygen tension (Cornfield et al., 1993). Experiments have indicated that alterations in the fetal oxygen tension during the early part of gestation do not affect fetal pulmonary vascular resistance, but by 135 days (ovine gestation - 147 days) an increase in oxygen increased the ovine fetal pulmonary blood flow to the newborn level

(Morin et al., 1988), and a decrease in oxygen tension can double pulmonary vascular resistance (Lewis et al., 1976).

In addition to these pharmacological vasoconstrictors, a series of potent vasodilatory substances present in the fetus do not seem to have significant effects until after birth. For example, the response to acetylcholine in the fetal lamb is poor (Abman et al., 1991) and the response to bradykinin is absent at birth. After birth, these and other agonists produce endothelial dependent relaxation via the generation of nitric oxide.

1.3.2 Humoral factors mediating the transition from the fetal to extrauterine circulation

From the elegant work of Dawes and Strang (1968) the key factors associated with the increase in pulmonary blood flow at the time of birth are known to include: physical expansion of the lung without oxygenation (Cassin et al., 1964); an increase in oxygen tension in the alveoli or an increase in arterial oxygen tension (Enhorning et al., 1966); and fall in carbon dioxide tension (Teitel et al., 1990). However the mechanisms underlying these factors have been more difficult to understand. The most extensively studied potential mediators of these changes are the prostaglandins and in particular prostacyclin (PGI_2), nitric oxide (endothelium-derived relaxing factor or EDRF) and the endothelins.

1.3.2.1 Prostaglandins

The prostaglandins, in particular PGI_2, have been proposed as important mediators of the postnatal fall in pulmonary arterial pressure. Inhibitors of prostacyclin synthesis, such as indomethacin and meclofenamate, blunt the fall in pulmonary vascular resistance seen when the fetal lung is ventilated (Leffler et al., 1978). PGI_2 synthesis, as measured by its stable metabolite 6-keto-$PGF_{1\alpha}$, also increases during late fetal and early newborn life (Leffler et al., 1984). However, the magnitude of the PGI_2 effect has been questioned. The production of PGI_2 within the lung declines after birth and may revert to clearance of PGI_2 in the following days (Morin, 1986). Similarly, after birth the effect of indomethacin

becomes less marked with time (Redding et al., 1984). Although the prostaglandin pathway does not seem to mediate the vasodilation produced by increasing oxygen tension (Morin et al., 1988), it does seem to protect against vasoconstriction in the postnatal period (Gordon et al., 1999).

1.3.2.2 Nitric oxide (NO)

Nitric oxide (Figure 4) has been shown to be important in the oxygen-dependent fall in pulmonary vascular resistance that occurs during birth.

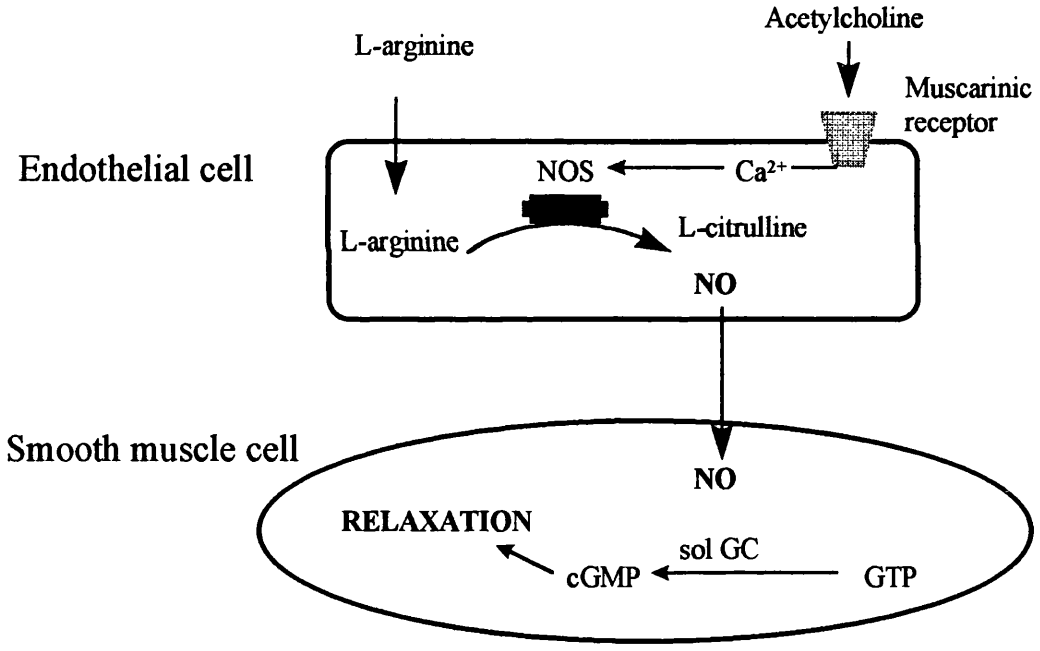

Figure 4. The nitric oxide pathway. Stimulation of muscarinic receptors on the endothelial cell activates nitric oxide synthase (NOS) to produce nitric oxide (NO) from L-arginine. NO then activates soluble guanylyl cyclase (sol GC), leading to an increase in guanosine 3'5'-monophosphate (cGMP) and relaxation of the smooth muscle cell.

In the lamb, pharmacological blockage of NO synthesis in the days prior to birth markedly blunts the normal increase in pulmonary blood flow and fall in resistance (Tiktinsky and Morin, 1993). In the sheep, throughout gestation and until at least

six days after birth, there is abundant endothelial nitric oxide synthase (eNOS) within the pulmonary circulation (Halbower et al., 1994). However, there is diminished endothelium-derived relaxation factor activity when vessel rings are stimulated with acetylcholine or adenosine di-phosphate. In contrast, sodium nitroprusside which directly donates NO to the SMCs, produces good relaxation. This suggests that, despite the presence of eNOS in the pulmonary endothelium, the endothelial production of NO is relatively low in the fetus (Abman et al., 1991).

1.3.2.3 Endothelin-1.

The endothelins (endothelin-1, 2 and 3) are a family of circulating endothelium-derived peptides with vasoactive properties. They are all originally produced from preproendothelin (203 amino acids), which is then cleaved to make big ET-1 (bET-1, 92 amino acids). Endothelin-1 (21 amino acids) is finally produced from bET-1 by the action of endothelin converting enzyme.

ET-1 binds with two types of receptor, ET-A and ET-B. The ET-A receptor is predominantly expressed in vascular smooth muscle and on binding with ET-1 mediates vasoconstriction. The ET-B receptor is more widely expressed and is also found on endothelial cells. In mature vessels, when the ET-B receptor on the SMC is stimulated there is vasoconstriction, but when the ET-B receptors on endothelial cells are stimulated there is vasodilation. It has been shown that pharmacological stimulation of ET-B receptors or pharmacological blockade of ET-A receptors in late gestation fetal sheep produce an increase in pulmonary blood flow and that these effects are mediated via release of nitric oxide (Ivy et al., 1994). In addition at the time of birth there is transient expression of ET-B receptors on the porcine pulmonary endothelium (Hislop et al., 1995) and ET-1 itself is found at high levels. It is possible that enhanced ET-B receptor stimulation at birth could favour a shift in pulmonary arterial tone from vasoconstriction to vasodilatation.

It is particularly interesting to note that endothelin-1 has been shown to alter the contractile phenotypic of cultured embryonic SMCs. Embryonic chick gizzard SMCs demonstrate a clonic, or rhythmical, contractile pattern whilst aortic SMCs have a tonic, or continuous, contractile response to stimulation. Aortic SMCs also produce large amounts of ET-1, and when gizzard SMCs are cultured in the presence of ET-1 they change their contractile pattern from a clonic to a tonic

response. This change in contractility is biochemically related to alterations in the splice variants of myosin light chain 17 (Fisher et al., 1997).

1.4 PULMONARY HYPERTENSION IN THE NEWBORN (PPHN)

Persistent pulmonary hypertension of the newborn is a clinical syndrome, the key feature of which is an elevated pulmonary arterial pressure that is equal or greater than that of the systemic circulation. The aetiology of PPHN is unknown but although up to 20% of cases are idiopathic, it is associated with a variety of different factors including fetal and perinatal hypoxia, abnormal lung development, parenchymal lung disease such as hyaline membrane disease and sepsis. The pathogenesis of PPHN is not understood but these various conditions probably represent defects in the cellular pathways producing and maintaining the normal postnatal fall in pulmonary vascular resistance. However, experimental and clinical studies suggest that this may not be the entire explanation, and the role of the SMC has not been fully evaluated in this disease process. All these conditions produce similar histopathological and pathophysiological changes.

Congenital heart disease (CHD) that is associated with an obligatory postnatal increase in pulmonary blood flow is associated with the presence of a sustained high pulmonary arterial pressure after birth. This may occur in infancy, for example in children with atrio-ventricular septal defects.

1.4.1 Histological findings in PPHN and pulmonary hypertension secondary to CHD

1.4.1.1 Hypoxia and pulmonary hypertension

In babies who died soon after birth with persistent pulmonary hypertension, precipitated by severe intrauterine or intrapartum hypoxia (but with essentially normal lung parenchyma), the distal arteries were observed to be thick walled and undilated (McKenzie and Haworth, 1981; Haworth and Reid, 1976). In babies who survive for a few days, the vessels seem to be fixed by excessive collagen I and elastin in an incompletely dilated state. The SMCs also show an excessive myofilament density and abnormal extension along the arterial pathway (Raine et al., 1991). These changes are also seen in newborn animals exposed to chronic

hypoxia. Piglets exposed to chronic hypobaric hypoxia show medial hypertrophy, increased myofilament density of SMCs and increased connective tissue (Smith et al., 1985; Haworth and Hislop, 1982). The findings are similar to those seen in fetal sheep with umbilical cord compression (Soifer et al., 1987), or hypoxia (Abman et al., 1987) and in the offspring of pregnant rats exposed to chronic hypoxia (Fox and Duara, 1983)

1.4.1.2 Congenital lung abnormalities and pulmonary hypertension

Pulmonary hypoplasia is most commonly seen in association with congenital diaphragmatic hernia. As well as impairment of airway development, the pulmonary arterial bed is disrupted and there is a reduction in the number of peripheral arteries and increase in the muscularity of the existing vessels (Bohn et al., 1987; Kitagawa et al., 1971). A particular problem in understanding the histopathology of this group is that the barotrauma of mechanical ventilation invariably leads to alveolar damage and emphysematous change.

Rarely, infants with alveolar dysplasia are seen. Their presentation is often identical to idiopathic PPHN and they may transiently respond to conventional therapies, including nitric oxide. The histological findings of thick walled dysplastic alveoli are seen in the lung biopsies.

1.4.1.3 Idiopathic pulmonary hypertension

In this condition the behaviour of the pulmonary circulation is abnormal and there are no obvious factors that can be held responsible for failure of adaptation to the extrauterine environment. Typically the pregnancy and birth is unremarkable and the baby is noted to be tachypnoeic and cyanosed some hours after birth (Roberton, 1992). In babies that die, the pulmonary arteries have the features of hypoxic pulmonary hypertension with thick walled arteries and progression to increased pulmonary arterial muscularity (Raine et al., 1991; McKenzie and Haworth, 1981). However, it is important to note that the lung pathology of survivors cannot be studied and infants with idiopathic PPHN may be a heterogeneous group.

1.4.1.4 Pulmonary hypertension secondary to congenital heart disease

Although in severe forms of congenital heart disease the pulmonary vasculature is abnormal before birth, for most lesions vascular remodelling over the first 2-3 months of life is most seriously affected. In conditions of increased flow with little increase in pulmonary pressure, as in some babies with an isolated ventricular septal defect, there is premature development of SMCs in the distal arteries. This extension of smooth muscle is accompanied by excessive production of extracellular matrix together with hyperplasia and hypertrophy of SMCs in the proximal arteries. The normal postnatal increase in density of the myofilaments within the SMCs is also accelerated, so that the myofilament concentration at a few weeks of age is that which would normally be achieved after several months (Hall and Haworth, 1992).

Similar changes are seen in obstructive lesions involving the left heart such as mitral stenosis and obstructed total anomalous pulmonary venous drainage, although the impact on the capillary and venous beds is greater.

1.4.2 Pathophysiology

The initial mediators of postnatal adaptation, and the abnormalities that might produce pulmonary hypertension of the newborn, are unknown. The pathophysiology resulting from this is however well understood. Maintenance of high resistance increases right ventricular afterload, and the ventricle maintains cardiac output by increasing power output which eventually produces right ventricular hypertrophy. When the pulmonary artery pressure is greater than systemic, shunting of blood into the systemic circulation occurs either at the level of the arterial duct or through the foramen ovale, or both. Reduced pulmonary blood flow results in hypoxia and acidosis, which further increases pulmonary resistance and a deterioration in ventricular performance (Soifer and Heymann, 1997). Untreated, there is a spiralling clinical decline, leading to death.

1.4.3 Management of pulmonary hypertension

The diagnosis of persistent pulmonary hypertension of the newborn, whether idiopathic or in association with other conditions such as asphyxia, is a clinical one. Diagnosis relies chiefly on the exclusion of other conditions that produce central cyanosis in the newborn, such as primary lung disease and structural heart disease. Similarly, the treatment of the condition is largely empirical, ameliorating the effects of hypoxia or other insult and sustaining life, whilst waiting for the underlying condition to correct itself.

1.4.3.1 Clinical picture

Some infants with PPHN immediately come to medical attention because of distress before or at the time of birth. Others, particularly those without a recognised associating cause, are seen some hours after an apparently normal birth. Diagnosis in these infants is based on the recognition of cyanosis, which can be difficult in the newborn. The demonstration that cyanosis is not due to primary lung disease or PPHN is shown by the nitrogen washout, or hyperventilation-hyperoxia, test (Fox and Duara, 1983). In primary lung disease or PPHN, hypoxia can be corrected by an increased inspired concentration of oxygen and hyperventilation, whereas in cyanotic heart disease this has no effect. Comparison of arterial blood gases obtained from the right arm (pre-ductal) in comparison with arterial blood from the legs will indicate right to left shunting of blood across the arterial duct, which often remains patent.

Similarly tachypnoea is often noted before cyanosis is obvious. Although it is a non-specific sign, more commonly associated with pulmonary surfactant deficiency or sepsis, it will alert the paediatrician.

1.4.3.2 General treatment

Initial management on the neonatal intensive care unit is directed at identifying and treating alternative conditions, such as hyaline membrane disease and sepsis, by septic screen (including lumbar puncture and chest X-ray), antibiotics and ventilatory support or oxygen as required (Roberton, 1992).

Infants are likely to be ventilated because of hypoxia and acidosis, and it is important to do this early before metabolic derangements occur. It is important to realise that expansion of the lung is an important part of treatment.

At some stage an echocardiogram should be carried out to exclude intra-cardiac anomalies and anomalous drainage of the pulmonary veins. Often there is tricuspid regurgitation which allows an estimation of elevated pulmonary arterial pressures. Similarly right to left shunting at atrial level or across the arterial duct indicates a high pulmonary arterial pressure.

Much of the treatment of PPHN is based on good neonatal intensive care procedures. Fluid intake is restricted and electrolyte imbalances and hypoglycaemia corrected. Sedation and paralysis are an important part of treatment as elevations of pulmonary arterial pressure occur with agitation and stress.

1.4.3.3 Specific treatment

Several specific strategies have been suggested and used to treat PPHN. They all aim to increase pulmonary blood flow by reducing pulmonary vascular resistance in relation to systemic vascular resistance.

The main roles of artificial ventilation are to correct hypoxia by delivering high concentrations of oxygen at high mean airway pressures, and to ensure optimal lung expansion. Oxygen is a potent pulmonary vasodilator and hence increases pulmonary blood flow. This in turn improves oxygenation of blood and further improves pulmonary blood flow. The pulmonary arteries are also sensitive to the vasoconstrictor effects of acidosis. One of the most effective treatments for PPHN used to be hyperventilation, which caused low levels of arterial carbon dioxide tension and therefore alkalosis. Unfortunately, the cerebral effect of this manoeuvre is severe vasoconstriction. Currently a normal arterial pH is sought by use of fluids and inotropes to ensure adequate perfusion, with sodium bicarbonate if necessary. The PCO_2 is held in the normal range (greater than 4.5kPa). Newer forms of ventilation, such as high frequency oscillation, are useful when oxygenation is particularly difficult and is used in association with nitric oxide therapy when trying to achieve adequate lung expansion for the optimal delivery of the nitric oxide within the lung (Kinsella and Abman, 1998).

Magnesium infusion has been used to treat pulmonary hypertension of the newborn. It causes smooth muscle relaxation at high concentrations. Although there are anecdotal reports of its efficacy, the results of clinical trials are equivocal (Abu-Osba et al., 1990a; Abu-Osba et al., 1990b). Currently, it is reasonable to correct hypomagnesaemia, but not to produce un-physiologically high magnesium levels.

Traditionally, intravenous vasodilators have been used to dilate the pulmonary arteries, with the aim of dilating the pulmonary vessels to a greater extent than the systemic vessels. Tolazoline is frequently used in the treatment of neonatal pulmonary hypertension. It appears to work via a histaminergic mechanism but is often ineffective after 24 hours of age. This refractoriness may be mediated by calcium and alpha adrenergic mechanisms (Abman et al., 1986). The main problem is that the use of tolazoline is associated with precipitous falls in systemic blood pressure and experience suggests that it should be given after augmentation of the circulating volume and concomitant use of an inotropic agent. Prostacyclin, although less hazardous in use, often produces little benefit and is very expensive.

The greatest breakthrough in the pharmacological treatment of pulmonary hypertension has been the use of nitric oxide (NO), which has become a mainstay of therapy in the UK (Kinsella et al., 1992), following establishment of optimal lung inflation, systemic blood volume and systemic vascular resistance (Kinsella and Abman, 1995). NO is given via the ventilator circuit at concentrations of up to 40 ppm, but can often be equally effective at 1 - 2 ppm. It is delivered to the areas of the lung being ventilated and produces vasodilatation, but on contact with haemoglobin is immediately inactivated. Thus, it is a specific pulmonary, rather than systemic, vasodilator and specifically improves the pulmonary ventilation/perfusion ratio. Although nitrogen dioxide, a degradation product, is toxic it is not produced in significant quantities at levels of nitric oxide below 40 ppm. The levels of methaemoglobin produced are usually low but should be monitored. Unfortunately some babies, even with a clear diagnosis of pulmonary hypertension, do not respond to nitric oxide.

Although extra corporal membrane oxygenation (ECMO) was the mainstay of treatment for PPHN in the USA, it is now generally used if NO therapy and high

frequency oscillation has failed. It is in effect cardiopulmonary bypass and provides oxygen for the body (and lungs) whilst the underlying pathology improves. It is invasive, requiring carotid artery ligation, and can only be performed in specialist enters. It is also expensive, uses large quantities of blood products and requires specialised personnel. In the UK nitric oxide and high frequency oscillation are widely used but ECMO is restricted to a few specialist centres.

1.4.3.4 Prognosis

The clinical course of successfully managed PPHN is recovery within approximately one week. Non-response at this point should probably lead to an open lung biopsy to exclude developmental abnormalities of the lung and establish whether histological features suggest that recovery is possible. If recovery has not occurred by one week, then barotrauma to the lungs from artificial ventilation is usually associated with deterioration and death.

1.5 THE PIG AS A MODEL OF NORMAL HUMAN ADAPTATION TO THE EXTRA-UTERINE ENVIRONMENT AND OF PPHN

The pig is an ideal large animal model for the investigation of adaptation to the extra-uterine environment because of the similarity in pulmonary arterial structure and the availability of a hypobaric hypoxic model which closely resembles PPHN.

1.5.1 The structure of normal porcine and human pulmonary arteries

The pulmonary arteries arise from a common trunk and then divide to supply the left and right lungs. In both the human and the pig, the pulmonary arteries enter the lung with the main bronchus, pulmonary vein and nervous supply at the hilum. In the human the bronchi and accompanying pulmonary arterial tree sequentially bifurcate until they form the acinus - or gas exchange area of the lung. However, branching of the intrapulmonary arteries in the pig is asymmetrical, such that there is a long conduit artery with large side-branches and the porcine airways are cartilaginous almost to the level of the acini, (Figure 5). Despite these differences, the arterial structure of the human and pig is similar and both have elastic as well as muscular pulmonary arteries (Figure 6). Innermost there is a lining of endothelial cells, and surrounding this are a series of layers of smooth muscle cells. The internal elastic lamina is a sheet of elastin which separates the SMCs of the media from the endothelial cell layer. It is incomplete at the time of birth but the lamina becomes thicker and more continuous by adulthood. In the larger vessels elastin sheets are interspersed in between the muscle cell layers. Between the smooth muscle cells of the media and the adventitial tissues there is another layer of elastin known as the external elastic lamina (Haworth, 1995).

Human

Pig

Figure 5. Schematic representation of the acinus in the newborn human and pig. Length of acinus in pig is 0.5 mm and in human is 1.1 mm. AD alveolar duct, AS alveolar sac, RB respiratory bronchiolus, TB terminal bronchiolus (Haworth and Hislop, 1981)

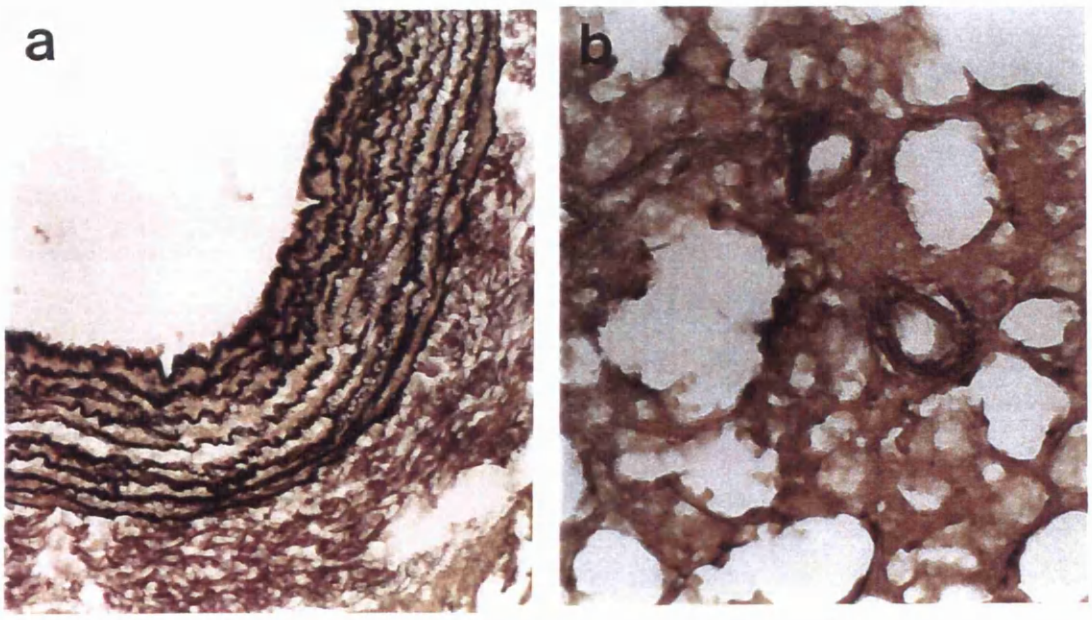

Figure 6. Histological structure of (a) an elastic artery, (b) a muscular artery.

1.5.2 The hypobaric hypoxic porcine model of PPHN

A variety of animal models have been used to study PPHN, for example chronic umbilical clamping (Soifer et al., 1987)and intra-uterine ligation of the arterial duct (Abman et al., 1989) in fetal lambs. Animals that are born at altitude have histological features of pulmonary hypertension, such as muscularisation of distal pulmonary arteries, and some animals become ill and die (Stenmark et al., 1987).

The hypoxic hypobaric oxygen chamber mimics the effect of altitude on the porcine lung. Using a vacuum pump, the air is rarefied to 0.5 atmospheres (50.4 kPa), and the partial pressure of oxygen is halved (10.5 kPa). The use of chronic hypobaric hypoxia produces pathophysiological changes and histological changes in keeping with human PPHN. The animals are cyanosed and shunt right to left through persistent fetal channels. There is right ventricular hypertrophy indicated at autopsy by an increase in the right ventricular to left ventricular weight ratio (Haworth and Hislop, 1982). Histological examination of the lungs shows an increase in pulmonary artery wall thickness with muscularisation of small distal pre-alveolar arteries. Electron microscopy shows an increase in SMC myofilaments (Allen and Haworth, 1986). Similar findings are produced in piglets exposed to chronic hypoxia due to a reduction in inspired oxygen concentration (Fike and Kaplowitz, 1994).

Piglets are used to investigate the pathophysiology of PPHN because both their size and pulmonary arterial structure are similar to human babies. They have elasticated conduit pulmonary arteries which rats and mice do not, but the elastic laminae and adventitia are not excessively thick like the bovine pulmonary arteries. A further advantage of using the pig as a model for PPHN is the size of the litter. Since pigs produce between 8 - 16 piglets there are usually sufficient animals in each litter for both experimental and control studies. The main problem with the porcine model is the relatively small number of animals produced at high cost, when compared to the cost of small mammals such as mice and rats. In practise the pig is a successful model in which to study adaptation to the extra-uterine environment.

1.6 THE VASCULAR SMOOTH MUSCLE CELL (SMC)

The smooth muscle cell is histologically defined as a spindle-shaped contractile cell completely surrounded by a basement membrane (basal lamina) except at gap junctions. It is found in certain typical situations, for example the blood vessel wall, the uterus and the bowel wall. The smooth muscle cell is characteristically capable of slow sustained contraction; but in contrast to cardiac myocytes and skeletal muscle does not have organised bands of contractile apparatus (Stevens and Lowe 1997). In cell culture, SMCs also have a typical appearance. Individual cells have a spindle-shaped morphology, prominent myofilaments, and when confluent tend to produce a characteristic "hill and valley"-like contour. The cytoskeletal proteins which characterise the SMC are α smooth muscle actin and smooth muscle specific myosin (Chamley-Campbell et al., 1979). Fully differentiated SMCs within the vessel wall or in culture also contain intermediate filament proteins (desmin or vimentin), and actin-associated proteins such as calponin and SM22 (Duband et al., 1993).

1.6.1 SMC phenotypes in the systemic circulation

The word "phenotype" in general histology refers to the characteristic appearance of a cell, for example a smooth muscle cell, which differentiates it from other cells of the body. Recently "phenotype" has been used in vascular biology to describe sub-types of smooth muscle cells which differ from each other because of distinctive features. For example, cells derived from human systemic vessels with atherosclerosis (Babaev et al., 1990) and from human embryos (Mironov et al., 1995) show an epithelioid appearance rather than the spindle-shaped appearance of SMCs obtained from the adult arterial media. There continues to be speculation as to the functional role of these SMC phenotypes.

1.6.2 SMC phenotypes within the intact systemic arterial wall

The normal media of the systemic vessel is comprised of spindle-shaped contractile SMCs. They contain myofilament bundles, but Golgi, rough endoplasmic reticulum and ribosomes are not a prominent feature (Chamley-Campbell et al., 1979). The cells have a different appearance in the areas of intimal proliferation seen in arteriosclerosis. The origins of arteriosclerosis, and why the appearance of the SMCs is different are not clear. The SMCs may have an aetiological role in the development of arteriosclerosis, or the neo-intimal formation by SMCs may be the result of repair mechanisms - possibly occurring to an excessive degree. In contrast to normal SMCs of the media, the atheromatous plaque SMCs contain more cellular organelles of protein synthesis, fewer myofilaments and reduced amounts of α smooth muscle actin, smooth muscle specific myosin and desmin. There are in addition, other cells which although completely lacking classical markers of smooth muscle cells, morphologically resemble spindle-shaped contractile smooth muscle cells that have been modulated by prolonged cell culture (Gabbiani et al., 1984b).

1.6.3 Culture of the SMCs from systemic vessels - the synthetic and contractile phenotypes

Further experimental work on cell phenotypes has been carried out on SMCs obtained from a variety of sources, such as rat and rabbit aorta and human coronary arteries, which have been maintained in culture. The relevance of cell culture experiments is limited because the cells being studied are not in their natural habitat and have been placed in an artificial environment. This undoubtedly leads to changes in their behaviour which after extended periods, and cycles of cell replication, can mean that the final cells bear little resemblance to those within the original tissue. Despite these limitations, cell culture does allow better control of experimental variables and provides a plentiful source of consistent material.

Two methods are generally used to obtain SMCs from the vessel wall (Chamley-Campbell et al., 1979). The tissue can be minced and the extracellular matrix proteins digested with elastase and collagenase to release cells, or pieces of

vessel wall (explants) which can be placed in cell culture medium and smooth muscle cells allowed to migrate out. The cells obtained then replicate and are used to seed further cell culture flasks. After several cycles of replication the cells obtained using either method appear very similar on gross morphological examination. The majority of cells isolated from the normal arterial wall are spindle-shaped and form a typical "hill and valley" appearance when confluence has been reached. However, if individual cells are examined then variations in their intracellular architecture and responses are evident. The extremes of these SMC appearances have been designated as the synthetic and contractile phenotypes (Campbell and Burnstock, 1974). The designation of "phenotypes" suggests two completely different forms, but in fact the cellular appearances are a continuum and it is more correct to say the contractile spindle-shaped cells have "undergone modulation" to a synthetic spindle-shaped cell (Chamley-Campbell et al., 1979).

The contractile spindle-shaped phenotype is a SMC that contains a high myofilament density and can spontaneously, and when stimulated, undergo contraction. The contractile function has been demonstrated by wrinkling of silastic membranes by cultured SMCs in response to contractile agonists. However, up to 30% of cells with a contractile phenotype, and a greater proportion of cells which have been in prolonged culture, fail to demonstrate this effect (Murray et al., 1990). The contractile SMCs exhibit low rates of replication and relatively poor synthesis of extracellular matrix proteins. The contractile phenotype is considered to represent the mature, fully differentiated SMC. In contrast, the synthetic spindle-shaped SMC contains fewer myofilaments and instead is filled with rough endoplasmic reticulum, Golgi apparatus and ribosomes (the cellular machinery of protein synthesis) (Chamley-Campbell et al., 1979). Abundant production of extracellular matrix and high replication rates are features of these cells (Palmberg et al., 1985).

1.6.4 Modulation of the synthetic and contractile SMC phenotypes by cell culture conditions

Variation in cell culture conditions can induce a population of smooth muscle cells to express a more synthetic or a more contractile appearance. For example, when SMCs are placed in cell culture in high concentrations they retain a higher proportion of original α smooth muscle actin content, (i.e. more contractile phenotype) than if plated in sparse numbers (Campbell et al., 1989; Owens et al., 1986). Sub-confluent cultures also exhibit higher rates of replication as compared to higher cell density cultures (Kato et al., 1996), but also express lower levels of α smooth muscle actin (Owens et al., 1986). Although this suggests that in order for cell division to occur, the SMC must exist as a synthetic phenotype, it has been shown that SMCs in culture can synthesise DNA and progress through the cell cycle whilst continuing to express contractile cytoskeletal proteins (Blank et al., 1988). Serum deprivation of sparse cultures up-regulates α smooth muscle actin synthesis, an effect which can be dramatically reversed by re-exposure to serum (Owens et al., 1986). Smooth muscle cells can also maintain high levels of α smooth muscle actin expression and undergo co-ordinate rhythmic contraction if neuronal cells contaminate the culture, but this effect is not seen when the cells are only exposed to neuronal cell conditioned medium (Chamley and Campbell, 1973).

In cell culture, both low cell density and mitogenic stimulation with serum are associated with enhanced matrix production, reduced contractile protein content, and increased fibroblastic growth factor receptor -1 expression (Kato et al., 1996). The effects of serum stimulation and reduced cell density are additive (Kato et al., 1996). The process of attachment and spreading is essential for cellular survival in cell culture conditions and those cells that are not allowed to do this rapidly apoptose (Chen et al., 1997).

Much research has been carried out to study the expression of matrix proteins in the intact wall in atheroma and the interactions between SMCs and matrix proteins in the cell culture environment have been investigated. Fibronectin is associated with migrating cells and its increased expression in neointimal lesions after balloon injury has lead to the suggestion that it acts as a gradient for cell migration into the

neointima. SMCs within the intact vessel make contact with fibronectin via the αvβ3 integrin and this mechanism is probably important in maintaining the stability of the SMC as when fibronectin is used as a substrate in the primary culture of SMCs, it facilitates the attachment and spreading of cells. SMCs grown on other substrates secrete fibronectin which then facilitates attachment (Hedin et al., 1988). However, the use of fibronectin is associated with a transient modulation of the SMC phenotype, with reduction of alpha smooth muscle actin mRNA and protein production (Hedin et al., 1990). There is a reduction in myofilament density and an increase in rough endoplasmic reticulum and Golgi apparatus.

Collagen type I is as effective in promoting adhesion and spreading of cultured SMCs as fibronectin. SMCs cultured on a substrate of laminin or collagen type IV demonstrate a higher myofilament density (Hayward et al., 1995), and produce more αSM actin mRNA and αSM actin protein than SMCs grown on fibronectin. Both laminin and collagen type IV also retard the mitotic burst normally elicited by exposure to PDGF-BB and serum (Thyberg and Hultgardh-Nilsson, 1994). Elastin suppresses cell attachment and spreading and maintains SMCs in a contractile state (Yamamoto et al., 1993). These observations suggests that basal lamina and extra cellular matrix proteins are important in modulating the vascular SMC phenotype between a contractile, non-replicating state, and a migratory synthetic one.

1.6.5 Epithelioid and spindle-shaped SMC phenotypes in the systemic circulation.

The phenotypes of SMCs present within the intact vessel wall and in culture are related. For example, if the intimal thickening produced following balloon injury is dissociated and the cells placed in culture, the majority of cells are seen to exhibit an epithelioid morphological phenotype. These cultured SMCs continue to exhibit reduced myofilament densities and increased synthetic organelle content. They also show the reduced levels of cytoskeletal proteins that characterised the intimal thickening of the intact vessel wall, affecting α smooth muscle actin, smooth muscle specific-myosin and desmin (Orlandi et al., 1994).

The characteristics of systemic SMCs derived from juvenile and adult animals have been compared in culture and the same pattern has emerged in studies of a number of species, including the mouse (Ehler et al., 1995), rat (Rothman et al., 1992), and human (Fujita et al., 1993). Systemic vascular structures in the adult are primarily composed of typical, contractile spindle-shaped smooth muscle cells forming the "hill and valley" contour in culture. They also contain abundant α smooth muscle actin, smooth muscle specific myosin type II, desmin, calponin, caldesmon and SM22. In contrast, cultured juvenile cells derived from fetal or neonatal animals give rise to epithelioid-shaped cells in culture, which form a monolayer rather than three dimensional structures. The cellular composition of the epithelioid cells also contrasts with that of the normal spindle-shaped cells as they contain fewer myofilaments, express low levels of α smooth muscle actin and smooth muscle specific myosin, and in general do not express desmin, SM22 or calponin. In place of the contractile apparatus, there is abundant synthetic machinery and the ability to produce extracellular matrix proteins.

Within the systemic circulation, the spindle-shaped and epithelioid-shaped SMCs are considered to be the principle stable and distinct SMC phenotypes. Although the synthetic spindle-shaped SMC has similar features to the epithelioid phenotype, for example reduced contractile cytoskeletal protein content, the epithelioid SMCs are distinctly different and stable in their overall properties (Lemire et al., 1994). It is interesting to note that in epithelioid cultures obtained from juvenile animals or from atherosclerotic plaques arising from balloon injury, there are often some spindle-shaped cells. These few spindle cells arise even if cells are obtained by cloning from a single original epithelioid cell (Bochaton-Piallat et al., 1996), suggesting that transformation of cell phenotype occurs, at least in vitro.

1.6.6 The balloon injury model of atherosclerosis

Much work on SMC phenotypes has been carried out investigating atherosclerosis, using the balloon injury model. The pathogenesis of atherosclerosis probably involves endothelial damage or dysfunction, as proposed by Ross (1986). Similar lesions to those seen in human atherosclerosis can be produced

experimentally in the systemic vessels of adult animals by inflation of an intra-luminal balloon. Following damage to the endothelium, proliferation of sub-intimal SMCs occurs to produce a neointima of longitudinally orientated cells (Manderson et al., 1989; Kocher et al., 1994). This lesion eventually resolves as the cells of the neo-intima take on the appearance of normal mature vascular SMCs within 90 days after the initial injury. The neo-intimal thickening is comprised of cells of epithelioid morphology, which are similar to the epithelioid cells derived from juvenile animals (Orlandi et al., 1994).

1.6.7 SMC phenotypes in the pulmonary arteries

The SMC of the pulmonary circulation has not been studied as thoroughly as that in the systemic circulation. Ultrastructural studies of the intact porcine pulmonary arterial wall have shown a transient reduction in myofilament volume density following birth, principally affecting the adluminal SMCs of the conduit artery. Following this there was a progressive increase in myofilament volume density with age, which affected all SMCs of the media. However, phenotypically distinct SMCs could not be distinguished in any region of the media (Hall and Haworth, 1987).

Much of the work identifying different SMC phenotypes has been carried out on the main pulmonary artery using the bovine model (Frid et. al., 1994). Four distinct appearances of cells have been identified on the basis of their spatial distribution, orientation of long axis and expression of smooth muscle-specific cytoskeletal proteins, particularly meta-vinculin. The initial descriptions described a sub-luminal sheet of small irregular cells, which do not express smooth muscle-specific actin or myosin (L1 cells); spindle-shaped medial cells expressing αSM actin and SM myosin found throughout the inner media (L2 cells); similar spindle -shaped cells dispersed throughout the outer media but not expressing αSM actin and SM myosin (L3 interstitial cells); and thick longitudinally orientated cells which were found in compact clusters in the outer part of the media (L4 cells). The L4 cells expressed meta-vinculin protein as well as αSM actin and SM myosin (Frid et al., 1994). Tissue culture experiments have suggested that the L2 medial spindle cells

and the L4 outer longitudinal cells have similar typical spindle-shaped SMC appearance in cell culture and the L1 and L3 cells have a non-spindle appearance. The L2 and L4 cells also demonstrated greater serum dependence than the L1 and L3 cells (Frid et al., 1997). This raises the possibility that there may be two SMC phenotypes in bovine main pulmonary artery, epithelioid and spindle-shaped. Experiments using chick-quail chimeras to study SMC lineage has similarly demonstrated two types of smooth muscle cell in the walls of the ascending aorta with phenotypic behaviour related to their embryonic origins. Neural crest-derived SMCs demonstrated serum independent growth in confluent culture, whilst SMCs of mesodermal origin were inhibited by these conditions (Topouzis and Majesky, 1996).

1.6.8 Ontology of the SMC

The model of development favoured for vascular smooth muscle is the determination, differentiation and maturation model (Owens, 1995). Determination is the process by which a multipotent cell becomes committed to cell lineage, and differentiation the process during which the cell acquires cell specific features. Maturation can be seen as the terminal part of differentiation. There are several sources for the multipotent cell. The majority of SMCs that make up the media of any large vessel, pulmonary or systemic, appear as condensations of apparently undifferentiated cells, derived from primitive mesenchyme, which become determined and applied to endothelial cell tubes (Le Lievre and Le Douarin, 1975). Progressive differentiation and maturation then takes place. Alternatively new vessels that have formed by angiogenesis may develop an arterial media from pre-existing SMCs that have migrated along the wall from proximal vessels (Price et al., 1994), or the media may derive from pericytes surrounding the developing endothelial cells of the vessel. A particularly intriguing source is the neural crest. Neural crest cells are responsible for the formation of many structures in the head, neck and upper part of the thorax and there is evidence for their migration and subsequent differentiation to produce the SMCs of the great vessels arising from the heart (Topouzis and Majesky, 1996). In addition, there is an in vitro model demonstrating differentiation of smooth muscle cells from neural crest cells (Jain et

al., 1998). But whilst there is good evidence for a neural crest component in the main pulmonary trunk and ascending aorta there is no evidence to prove that neural crest cells contribute to the pulmonary vessels contained within the parenchyma of the lung.

Experiments to investigate the origins of vascular SMCs are difficult because there is no definitive early marker of determined smooth muscle progenitor cells. Thus the strategy for studying the embryological origins of the vasculature has been to follow the temporal expression of cellular proteins within cells that occupy the positions that will later be held by vascular SMCs. For example, development of SMCs in the embryonic chick systemic vasculature has been followed with a variety of smooth muscle specific markers. Expression of alpha smooth muscle actin and desmin can be seen as early as day two in developing chicken embryos and precede myosin light chain kinase / myosin light and heavy chain expression which appear on day three. SM22 appears later on day four and calponin on day six (Duband et al., 1993). However, all these proteins are found in several cell types, either at specific times during development or in the mature tissue. For example, alpha smooth muscle actin, SM22 and calponin are not limited to smooth muscle but are also expressed transiently in early skeletal and cardiac muscle tissue (Duband et al., 1993). Desmin is found in adult skeletal muscle and vimentin is widespread in tissues of mesodermal origin (Alberts et al., 1999). Furthermore within the same vessel wall there is considerable heterogeneity of cytoskeletal protein expression as some SMCs may express vimentin, some desmin, and others neither (Kocher et al., 1985).

Phenotypic modulation of SMCs, as seen in atherosclerotic plaques or in cell culture, may also occur during development. Thus, SMCs may not always express typical lineage markers (alpha smooth muscle actin or smooth muscle specific myosin). The distinction of these modulated cells from other cells, such as fibroblasts, can then be difficult. Conversely, since expression of alpha smooth muscle actin and contractile properties have been demonstrated in fibroblasts (Darby et al., 1990), and endothelial cells (DeRuiter et al., 1997), it may be difficult to designate a cell that lies within the vessel wall and expresses these markers as a definitive SMC.

The common expression of these contractile proteins also raises the possibility of SMCs originating by lateral differentiation from endothelial cells (DeRuiter et al., 1997) and fibroblasts. A number of studies in the transplantation biology and bone marrow literature have also described a population of haematological CD44 (a receptor for hyaluronic acid) positive cells that have the potential to form several cell types including SMCs (Li et al., 1995).

1.7 MARKERS OF VASCULAR SMC DIFFERENTIATION AND PHENOTYPE IN THE SYSTEMIC AND PULMONARY CIRCULATIONS

The search for appropriate markers of smooth muscle cell phenotype has encompassed consideration of the gross morphological features (epithelioid and spindle-shapes), the cytoplasmic myofilament and organelle content of cells (contractile or synthetic phenotypes), and the expression of a variety of intra-cellular cytoskeletal, and extra-cellular matrix proteins. Most of the proteins examined are cytoskeletal elements and although they may not provide convincing markers of different phenotype they do serve to emphasise the wide degree of variation within the extremes of the contractile/synthetic SMC phenotype model. Information on the transition between epithelioid and spindle-shaped SMC phenotypes has been obtained by examining the morphology of SMCs obtained when the media of normal rat aortic media is cultured. Two distinct SMC subtypes are observed - spindle-shaped and epithelioid SMC phenotypes. Cell lines produced from individual cells seen in primary culture produce pure lines of each phenotype (Bochaton-Pillat et al., 1992). The epithelioid appearance has been noted to be similar to that of SMCs that comprise the neo-intimal thickening produced after endothelial balloon injury. Cellular protein maps produced by two dimensional electrophoresis of the epithelioid and normal spindle-shaped cells have demonstrated a series of differentially expressed proteins. One of these proteins, expressed in the epithelioid SMCs but not in the spindle-shaped cells, is cellular retinol binding protein-1 (CRBP-1) (Neuville et al., 1997). An antibody to rat CRBP-1 has been used to identify the epithelioid cells from the spindle-shaped cells in culture, and more importantly to identify cells in the intact vessel wall that also express CRBP and relate to the epithelioid phenotype. The antibody has been used to track the cellular events after endothelial balloon injury in the rat. Immediately after endothelial damage the neo-intimal cells stain with anti-CRBP-1 but once the endothelium is healed this staining pattern disappears, supporting a role for retinoids in modulating SMC phenotype and a role for epithelioid phenotype cells in repair. Treatment of epithelioid cells with retinoic acid is associated with a rapid and complete change to the spindle-shaped phenotype (Neuville et al., 1997).

1.7.1 Actin

Actin is a highly conserved structural protein that is found in high concentrations in almost all eukaryotic cells. It can exist in a monomeric form (globular or G actin) associated with actin-binding proteins, or it can assemble into robust filaments (filamentous or F actin). The assembly of filaments from monomers is a dynamic process known as treadmilling and is dependent on hydrolysis of ATP. Accessory proteins such as gelsolin and profilin control the state of the actin (Alberts et al., 1999).

The evolutionary path of the actins is intriguing. Alpha smooth muscle actin is found in the most primitive of invertebrates, such as the small amoeba *Naegleria gruberi* that use actin for propulsion (Fulton, 1983). There is also remarkable conservation of α smooth muscle actin in all species. This conservation is similarly seen with β actin which is the predominant scaffolding protein of eukaryotic cells. γ actin is equally ubiquitous and so although it is possible that γ actin exists as a redundant actin polymorphism it may have subtle functions within the cell. It is important to note that α smooth muscle actin is expressed before γ actin during vascular development, indicating different control mechanisms, and that whilst αSM actin predominates in the vasculature, γ actin is the main isoform found in gut smooth muscle (McHugh and Lessard, 1988).

The actins have three principle roles within the smooth muscle cell. Firstly, they have a structural role in helping to maintain a rigid cell shape - although this is primarily the role of the intermediate filaments. The actin filaments are held under tension and are balanced by compressive forces directed through the rigid intermediate filaments. These together produce a stable mechanical framework (Ingber, 1997). The main isoform associated with this role is β actin. It is found in the cytoplasm of all cells and in cultured cells is particularly deposited in the newly formed leading edge in motile cells (Gimola et al., 1994),(Hill and Gunning, 1993). Because of their high concentrations, α actin and γ actin may also be involved in this process. The second role of the actins is in the generation of force and cell

movement (Figure 7). Alpha actin is predominantly involved in SMC contraction in association with SM specific type II myosin (Alberts et al. 1999).

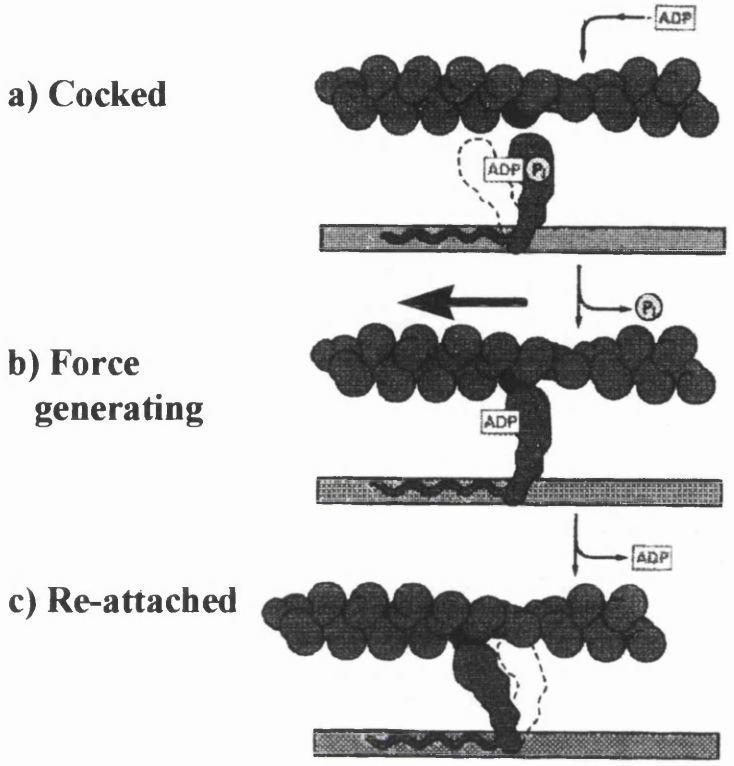

Figure 7. The cycle of changes by which a myosin molecule walks along an actin filament. Binding of ATP allows the myosin head to move along the actin filament (a). Hydrolysis of ATP and subsequent release of inorganic phosphate (Pi) produces a conformational change in the myosin head and the power stroke which moves the myosin molecule in relation to the actin head. ADP is released in this process.

The role of γ actin in all cells and in smooth muscle cells in particular is not clear. Two isoforms of γ actin have been found; one which is specific to smooth muscle cells and another which is found in all cells. The relative abundance of γ actin in gastrointestinal smooth muscle cells suggests it may have a functional role peculiar to the gut (Liddell et al., 1993)

The third role of the actin cytoskeleton is in intra-cellular communication. This is not only via myosin motors and the delivery of cargo proteins to different parts of the cell, but also by the transduction of forces from the external environment to the cell nucleus (Ingber, 1997).

In the experiments performed for this thesis immunolabelling for α, β and γ actin was carried out.

1.7.2 Actin binding proteins - gelsolin, thymosin and profilin

The dynamic instability of the actin cytoskeleton is controlled by a series of proteins that bind to filamentous or monomeric actin, allowing net filament formation or breakdown to occur in different parts of the same cell at the same time (Fechheimer and Zigmond, 1993) (Figure 8). For example, gelsolin binds to the barbed (plus or growing) end of the actin filament and stabilises it such that growth or diminution of the filament length is reduced. This is termed actin capping (Figure 8). The binding can also occur with actin monomers, so that in certain circumstances gelsolin can stabilise the monomeric actin pool, preventing filament formation. Gelsolin can also break actin filaments - called severing.

Thymosin and profilin are abundant small proteins which regulate actin polymerisation in the cell, for example during movement. When filaments are capped they bind to and buffer the pool of actin monomers. If however the filament end is uncapped they promote rapid addition of actin monomers to the established filament (Pantaloni and Carlier, 1993). Actin depolymerising factor also binds actin monomers but can stabilise or sever filaments, depending on the cellular pH (Sun et al., 1995).

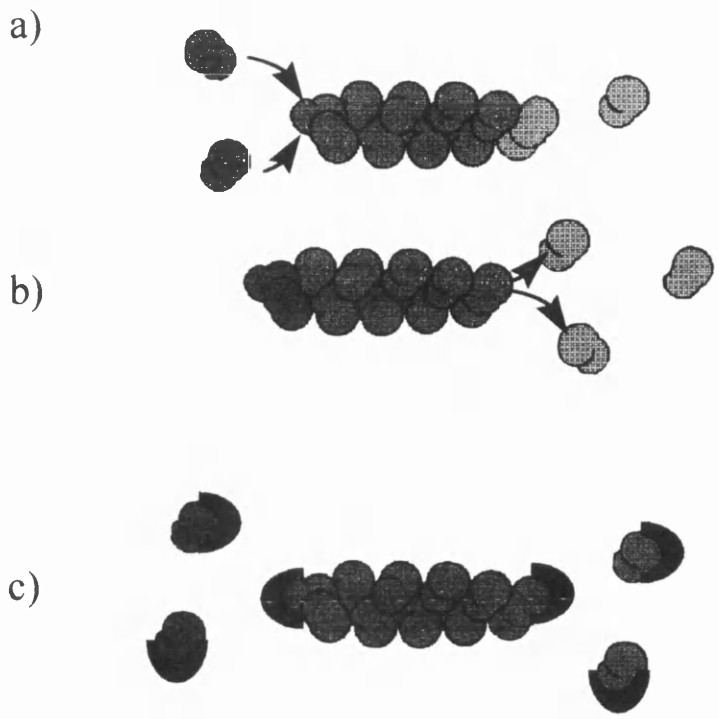

Figure 8. Actin treadmilling and capping. Actin filaments maintain a constant length although there is a net flux of subunits through the polymer (a) and (b). Capping proteins stabilise the end of established filaments, but also cap monomers preventing formation of new filaments (c).

An important class of proteins controlling cell shape and the actin cytoskeleton are the rho GTPase proteins. These are members of the p21 Ras superfamily of small GTPases. Two important sub-groups of the rho GTPase family are the Rho and Rac proteins. Activation of the Rac pathway leads to sequestration of capping proteins such as gelsolin and monomer binding proteins, such as thymosin and profilin. The overall effect, as seen in cultured fibroblasts, is the promotion of cortical actin polymerisation and ruffling. In contrast, fibroblasts in which Rho is activated show dramatic reorganisation of actin cytoskeleton into bundled stress fibres containing myosin filaments (Hall, 1998).

1.7.3 Myosin

The myosins are molecular motors that interact with actin filaments to generate force. Of the seven families of myosin, most are associated with molecular

transport around the cell, but class II myosins (Figure 9) are of particular interest as they are responsible for the contractile function of SMCs (Alberts et al., 1999).

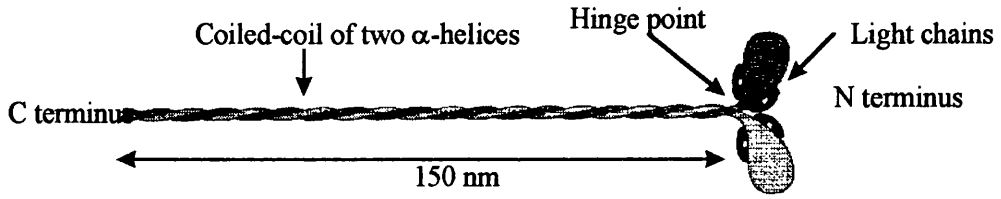

Figure 9. Diagram of an individual myosin molecule. The two heavy chains form an α-helical coiled-coil, and each myosin head contains two light chains.

1.7.3.1 Myosin heavy chains (MHC)

Experimental work has consistently shown that two MHC isoforms, SM1 and SM2 are specific for smooth muscle cells(Nagai et al., 1989). These are produced by alternative splicing of the same gene producing 204 and 200 kDa proteins. SM1 (204 kDa) is present at all stages of development but SM2 (200 kDa) is up-regulated at the end of the neonatal period in the SMCs of porcine carotid and rabbit aorta (Kuro-o et al., 1989). In these examples, the appearance of SM1 is preceded by transient expression of a 198 kDa non-muscle specific MHC isoform known as SMemb. In the human aorta however, SM2 appears only transiently in the late fetal and neonatal period, whilst SM1 and the SMemb predominate at all stages (Aikawa et al., 1993; Frid et al., 1993).

The heavy chain myosin molecules have not been successful markers of different SMC phenotypes. Whilst SM1 and SM2 expression affects the SMCs of the whole mature vessel wall, it is only SMemb (the non-smooth muscle specific isoform) that can identify cells within particular regions of the vessel such as the intima, small nests of cells within the media (Frid et al., 1993), and the cells produced by experimental and human atherosclerosis (Aikawa et al., 1993). In primary cell culture, non-confluent SMCs almost exclusively express non-muscle myosin, whereas confluent cells express increased amounts of non-muscle myosin as well as

SM1 myosin. This pattern of SM1 expression mirrors that of αSM actin (Rovner et al., 1986).

In the studies described in this thesis, SM1 immunolabelling was used to identify SMCs. Anti-SM2 antibody was not available for study and it has been suggested that this antibody is not entirely specific for the 200 kDa MHC isoform. SMemb antibody was also unavailable for use in these studies.

1.7.3.2 Myosin light chains (MLC)

There are many isoforms of the phosphorylatable 20 kDa regulatory MLCs. $L_{20\text{-}A}$ and $L_{20\text{-}B}$ are specific for smooth muscle but both are widely expressed in other tissues. None of these isoforms appear to have different effects on myosin function (Somlyo, 1993).

There are two known isoforms of the 17 kDa myosin light chain molecule, L_{17a} and L_{17b}. Both are found in vascular smooth muscle cells but the L_{17a} form predominates in gut SMCs and fibroblasts. Variations in the ratio of these two light chain isoforms may modulate the affinity of the myosin molecule for filamentous actin and also regulate actin activated ATPase activity (Owens, 1995).

1.7.4 Calponin

Calponin is a basic protein of approximately 33 kDa that is specifically expressed in smooth muscle cells in adult animals. Its developmental expression occurs later than that of other smooth muscle determinants and it is widely regarded as a marker of the fully differentiated SMC phenotype (Gimona et al., 1990), although it is transiently expressed during early embryonic development of the heart and skeletal muscle (Li et al., 1996; Moessler et al., 1996; Duband et al., 1993). Its physiological role remains to be elucidated, but its characteristics in cultured cells suggests that it is an actin filament-based regulator of actin-myosin interaction. Under physiological conditions it has been shown to bind avidly to actin and is able to inhibit the Mg^{2+} dependent actinomyosin ATPase activity which underpins contraction. In the presence of Ca^{2+}, calponin will bind to calmodulin (although not avidly) and the resulting complex is then unable to interact with F

actin or inhibit Mg^{2+}-ATPase activity. Similarly, if calponin is phosphorylated, it is unable to bind to actin or inhibit Mg^{2+}-ATPase (Winder et al., 1991).

Calponin expression was studied in the experiments performed for this thesis.

1.7.5 SM22

SM22 is a 22 kDa protein that exhibits sequence motifs which are homologous with parts of the calponin molecule (Lees-Miller et al., 1987). In vivo it is a major component of mature smooth muscle and its expression follows that of the other smooth muscle cell markers. It is widely expressed in many cell lines. It has been cloned from a variety of cell types but most frequently from fibroblasts (Lawson et al., 1997) In cultured cells it is up-regulated by serum stimulation or ageing, and down regulated by viral transformation. Its functional role is yet to be elucidated.

1.7.6 Caldesmon

Caldesmon is a protein that is found in both smooth muscle and non-smooth muscle cells (Sobue and Sellers, 1991). Two isoforms, which are produced by alternative splicing of a single gene, have so far been characterised and have different roles within the cell. The low molecular weight caldesmon isoform (59-63 kDa) is distributed throughout the cellular network and is involved in the regulation of the actin cytoskeleton. The high molecular weight isoform(89-93kDa) is exclusively found in fully differentiated smooth muscle cells (Sobue and Sellers, 1991). Like calponin, the caldesmons are potent inhibitors of the actin-tropomyosin activated Mg^{2+} dependent ATPase. The physiological role of caldesmon is not clear but it has been suggested that in contracting actin structures, the caldesmon may inhibit force generation and play a role in stabilising the cytoskeleton (Huber, 1997).

Caldesmon expression was examined by immunolabelling in this thesis.

1.7.7 Vinculin, metavinculin and the focal adhesion complex (FAC)

The FAC mechanically couples the cytoplasmic portion of integrin molecules to the internal actin cytoskeleton. Vinculin is a 17kDa actin-associated molecule found in the FAC, together with talin, α-actinin and a variety of other signalling molecules that mediate stimulus-response coupling (Chicurel et al., 1998). There are a series of vinculin isoforms which show tissue specific expression. Meta-vinculin is a 150 kDa protein which is also found in the FAC, that is antigenically related to vinculin and has been shown to identify a particular subset of "L4" spindle-shaped SMCs in the bovine main pulmonary artery (Frid et al., 1994).

Vinculin was immunolabelled to show the position of focal adhesions on cultured SMCs in experiments performed for this thesis (porcine anti-metavinculin antibodies were not available).

1.7.8 Integrins

Integrins are heterodimeric cell-surface adhesion receptors that transduce mechanical signals from the extracellular environment into the cell (Figure 10). The integrin molecule is composed of α and β subunits, with at least 15 α subunits and 8 β subunits capable of forming 21 different heterodimers. Unbound integrins are mobile in the cell membrane and accumulate at focal contacts and areas of the backward moving cytoskeleton of motile cells. This mechanism may involve tyrosine kinase^{FAK} (focal adhesion kinase) (Schaller and Parsons, 1993).

Many integrins are specific receptors for extracellular matrix proteins. For example α1β1bind laminin and α2β1 is a receptors for fibrillar collagen and is expressed on human vascular smooth muscle cells. Integrins can also control the formation of matrix; this has been clearly demonstrated for fibronectin (Mosher, 1993). Although some integrins are expressed in several types of cell, for example, αvβ3, others are specific for different cell types. The α6β4 integrin, whose ligand is laminin, has been described as being specifically localised to SMCs in small arteries and venules in human tissue (Cremona et al., 1994). The heterogeneity of the integrin receptor has suggested different functional roles. β1 integrins are

important for SMC adhesion, whilst cell migration over matrix depends to a large extent on αvβ3 receptors (Clyman et al., 1992).

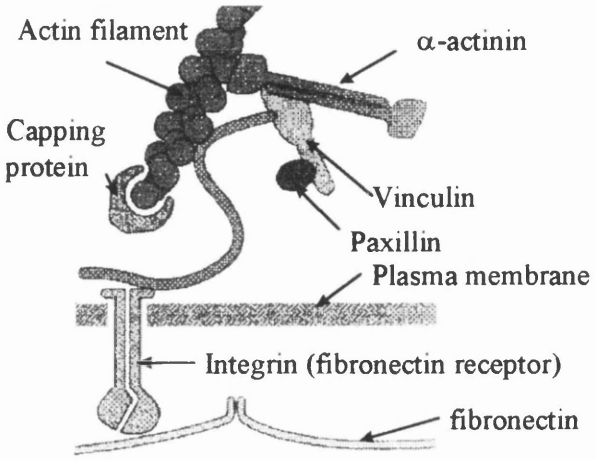

Figure 10. The focal adhesion complex. The extracellular matrix (fibronectin) communicates with the actin cytoskeleton via the focal adhesion complex, allowing changes outside the cell to be communicated to cytoplasm and the nucleus.

1.7.9 Intermediate filament proteins: desmin and the cytokeratins

1.7.9.1 Desmin

Desmin is considered a marker of the mature contractile SMC phenotype (Gabbiani, 1987). Practically all SMCs (and other cells of mesenchymal derivation) contain intermediate filaments composed of vimentin which provide the cell with structural strength. In addition, up to 50% of cells in the mature arterial wall of systemic vessels also contain the intermediate filament protein desmin. The production of a mouse null mutant for desmin (Li et al., 1996) has led to improved understanding of the functional role of desmin. In particular, the expression of desmin is associated with improved resilience to repeated stress in frequently contracting muscles, and its absence leads to degeneration of the systemic vessels and heart (Galou et al., 1997). Desmin is not expressed in cells of the neointima formed after balloon injury, cells in atheromatous plaques or juvenile cells.

The expression of desmin within SMCs was investigated in experiments carried out for this thesis, both in the intact vessel wall and in cultured SMCs.

1.7.9.2 Cytokeratins

Cytokeratins are the intermediate filament found in epithelia, which gives these cells their mechanical strength. Interestingly, cytokeratins 8 and 18 are also found in human atheromatous plaques (Jahn et al., 1993). Cytokeratin 8 is also expressed in rat epithelioid phenotype SMCs derived from the normal aorta of the adult rat, juvenile animals and the neo-intima after balloon injury (Ehler et al., 1995: Milo et al., 1979).

1.8 THE OTHER CONTRACTILE CELLS

Several cell types are specialised to generate motile forces through contraction via the actin-myosin interaction. Cardiac and skeletal myocytes and myoepithelial cells are not relevant to this thesis and will not be discussed.

1.8.1 Pericytes

Pericytes are distinctively shaped contractile cells that are associated with the endothelial cell lining of blood vessels from arteries to post-capillary venules. Pericytes lining the capillaries have cell bodies containing prominent nuclei but little surrounding cytoplasm, surrounded by a basal lamina. The basal lamina is continuous with that of the underlying endothelial cells. They give off extensively branched longitudinal and circumferential processes which envelop the abluminal surface of the endothelial cells (Stevens and Lowe, 1998). Pericytes contain abundant alpha smooth muscle actin, non-smooth muscle specific actins, and myosin, as well as vimentin or desmin (Kapanci et al., 1992). The role of these cells is not certain but along with endothelial cells they are thought to play a role in the control of microvascular blood flow (Hirschi and D'Amore, 1996). The relationship of pericytes to SMCs is also poorly understood. Pericytes may give rise to SMCs during formation of the blood vessel media, but conversely, SMCs may become pericytes (Nicosia and Villaschi, 1995).

1.8.2 Myofibroblasts

Myofibroblasts are fibroblast-like cells that secrete collagen but also have well defined contractile properties which are similar to SMCs. In normal tissues myofibroblasts are inconspicuous and frequently remain inactive. They are found in the alveolar septae of the lung and also sparsely in the loose collagenous support tissue of other organs. Following tissue damage they become active and proliferate. They secrete collagen to consolidate a damaged area, and as healing progresses the myofibroblast contracts and pulls the edges of the wound together (Stevens and

Lowe, 1998). Myofibroblasts have not been described within the blood vessel media. This is because in conventional histological sections it can be hard to distinguish myofibroblasts from SMCs. Like SMCs, myofibroblasts contain myofilaments and can express alpha smooth muscle actin and desmin (Gabbiani, 1992). Myofibroblasts however, do not generally have a complete basal lamina and lack smooth muscle-specific heavy chain myosin isoforms which are considered to be hallmarks of true SMCs. In the absence of alpha smooth muscle actin and desmin, the myofibroblasts may be indistinguishable from fibroblasts.

The origin of myofibroblasts is not clear but it is likely they derive from fibroblasts (Sappino et al., 1990). Populations of fibroblasts in culture always contain a variable proportion of cells that express alpha smooth muscle actin - even if clonally derived from an alpha smooth muscle actin-negative cell. Similarly, fibroblasts may express vimentin, desmin, or both proteins in conjunction with alpha smooth muscle actin. Gabbianni (Gabbiani, 1992) has characterised the expression of vimentin (V), α smooth muscle actin (A) and desmin (D) and described four main patterns of protein expression in fibroblasts/myofibroblasts;. V cells, VD cells, VA cells and VAD cells.

There may be a close relationship between SMCs and myofibroblasts. A rat model of pulmonary hypertension indicated that cells with the electron microscopic appearance of fibroblasts were recruited from the interstitium and migrated into the vessel wall to produce more muscularisation of the pulmonary arteries (Milo et al., 1980). Similarly, a transition from myofibroblasts to SMCs has been proposed in an experimental model producing obstructive hypertrophy of the rabbit bladder (Buoro et al., 1993). During smooth muscle hypertrophy within the bladder wall, serosal myofibroblasts expressing vimentin, αSM actin and in part desmin, were seen to express SM specific myosin.

1.8.3 Endothelial cells

Endothelial cells found in the micro-vasculature, in conjunction with the pericytes, may exhibit some contractile properties to regulate blood flow. This is

not a feature of endothelial cells derived from large vessels such as the aorta (Kelley et al., 1987).

Although endothelial cells in the intact vessel do not normally express SMC markers, cerebral endothelial cells in cell culture have been shown to modulate their appearance towards that of SMCs. Cultured cerebral endothelial cells maintain a cobblestone morphology if endothelial cell growth factors (derived from bovine hypothalamus) and heparin are present. If these two factors are missing the cells elongate, become spindle-shaped and express αSM actin mRNA and protein (Amberger et al., 1991). Although this is an artificial situation the behaviour of these cerebral endothelial cells may provide a model for trans-differentiation of endothelial cells to SMCs.

1.9 VASCULAR MECHANICS

The principle function of the pulmonary arteries in extra-uterine life is to carry blood to the alveoli and regulate their perfusion in relation to ventilation of local respiratory units. Before birth the pulmonary arteries have a low flow and high total resistance. The immediate increase in pulmonary blood flow at birth occurs because of intrinsic changes to the lungs. These changes are probably the initial inflation of the lungs, followed by a progressive dilatation of the pre-alveolar arteries. At any age, the behaviour of blood flowing through the pulmonary circulation can be modelled in theoretical terms by analogy with the flow of current through an electrical circuit (Nichols and O'Rourke, 1998).

1.9.1 Resistance and impedance

The pulmonary circulation can be modelled as a branching network of rigid tubes with a viscous liquid (blood) flowing through them under the constant force generated by a pump (the right ventricle). The analogy of direct current electrical circuits has been applied to describe this system, where Ohms law gives a relationship between resistance to flow, potential difference and flow of current:

Resistance = Potential difference/Current

This relationship is used in clinical medicine to calculate cardiac output (flow) or conversely the resistance of the pulmonary or systemic vascular beds:

Resistance = pressure gradient across circulation/ flow through circulation.

However, in reality the pumping of blood through the pulmonary (and systemic) arteries is cyclical, occurring during systole, and the vessels are distensible which allows energy to be absorbed during systole and released during diastole. The effect of this is to produce a pulsatile but continuous blood flow. The analogy with alternating current provides a useful model of this (Figure 11). The fluctuating

potential difference can be described as a single waveform with frequency and amplitude. In this system the opposition to flow of current is termed impedance (when the frequency of the potential difference is zero frequency, i.e. as in direct current, impedance is exactly the same as resistance). Because pulsatile flow behaves as a waveform, the summation of waveforms depends on their phase. If the peaks and troughs are in phase, the resultant wave form will be the addition of the amplitudes of the contributing waveforms (Figure 11a and c). However, if the peak of one waveform is in phase with the trough of another, i.e. the waveforms are 180° out of phase with each other, they will oppose each other and the resulting waveform will have a reduced amplitude (Figure 11b).

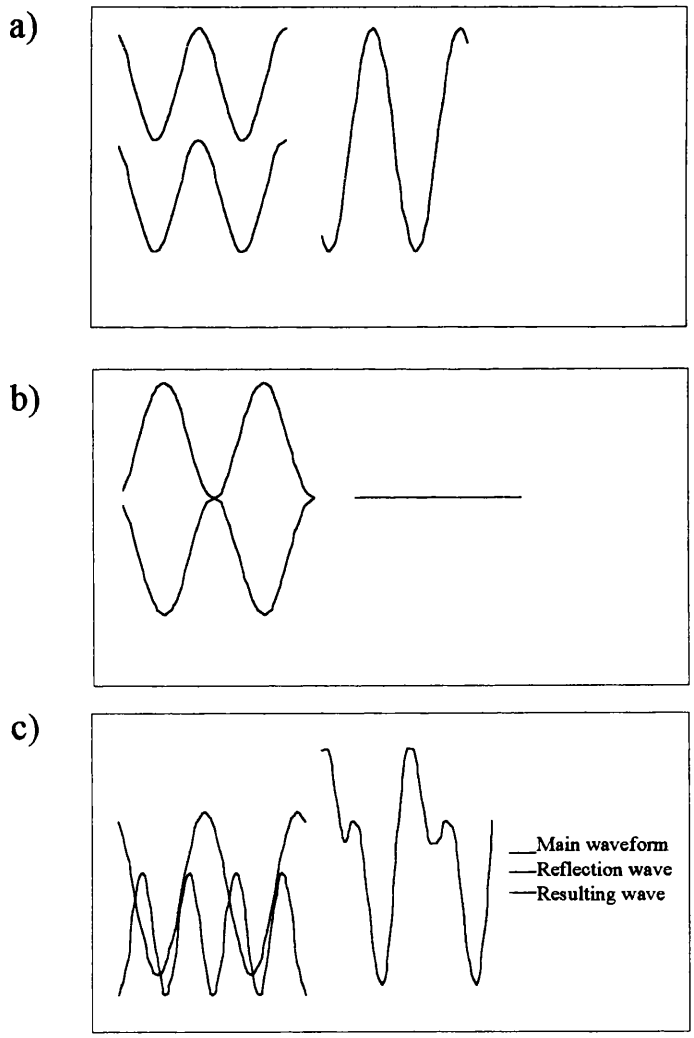

Figure 11. Diagram showing summation of waveforms depending on their phase. Summation of (a) two waveforms in phase, (b) two waveforms 180 ° out of phase and (c) waves of different frequency.

The main arterial wave form can be attenuated by the effects of other waveforms generated at points throughout the vasculature. These contributing waveforms are called reflectance waves and occur when the main waveform is reflected by a discontinuity (change of impedance) in the system. Examples of such points are: firstly, branches in the tubular system; secondly, the proximal effect of distal high resistance arteries; and thirdly, areas where there is a change in the elasticity in the wall of the conduit vessel.

The pattern of branching of the intrapulmonary arterial system and particularly the size of the angles at which side-branches arise can have significant effects on the forward flow of blood into the lung.

The effect of the distal arteries can be envisaged in two extremes; as a tube completely blocked at its end (high resistance of arteries) and subjected to pulsatile flow or as a tube that is completely open and drains into a large reservoir (collection of low resistance arteries). In the tube with a closed end there is total reflection of the wave which enhances the main waveform to produce a standing wave with no forward flow of blood. However, with an open ended tube the reflection wave is 180° out of phase with the main wave. This reduces the amplitude of the composite waveform but also produces continuous forward flow.

The forward flow of blood through the lung can be altered by a series of physical characteristics of the conduit vessel itself. Increasing the tone of SMCs within the media of the artery can constrict the lumen, increase resistance and reduce flow. An additional effect of contraction can also be to stiffen, and therefore reduce the impedance of the vessel wall.

In adaptation of the pulmonary circulation to extra-uterine life all of these factors may be relevant: changes in the angulation of side branches during lung inflation, dilatation of distal vessels to enhance forward flow and cytoskeletal re-organisation of SMCs to produce changes in wall tone and overall elasticity of the conduit vessel wall might be important. This study is particularly concerned with the effect of cytoskeletal reorganisation on SMC contraction and hence tone of the vessel wall.

1.9.2 Stress-strain and the elastic modulii

In order to assess the contractile or elastic properties of the vessel wall it is necessary to consider the relationship between force and distortion. When a force is applied to any solid body without displacing it in space, the parts of the body must move in relation to one another. If the body regains exactly its initial form when the force is removed then the material is said to be perfectly *elastic*, but if it retains the deformation it is said to be *plastic*. The ability to withstand an applied force is a property that distinguishes a solid from a liquid - as a liquid will undergo a *viscous flow*. The vessel wall however behaves with properties of an elastic solid and also a viscous liquid and is said to be *visco-elastic*. If force is applied slowly to the vessel wall the viscous effects are not seen and the vessel behaves elastically.

In describing materials undergoing deformation, the terms stress and strain are used. Stress is defined as the quantity of force per unit area that produces the deformation. Strain is the ratio of the dimensions of the material after deformation in comparison to its original dimensions. Strain has no units because it is a ratio. No material is perfectly elastic when exposed to large forces. As strain increases, so will the stress generated within the material, until it snaps. For small forces the deformation produced is proportional to the force applied (Hooke's law), or the strain produced is proportional to the stress applied. The ratio of stress to strain, in one dimension, is known as Young's modulus (E). A characteristic feature of blood vessels is that with increasing distension, the relationship between stress and strain becomes non-linear. By taking tangents of the stress-strain curve the incremental elastic modulus, for that strain (E_{inc}) can be evaluated. E_{inc} has been evaluated for non-contracted pulmonary vessels in the pig and shown to fall between birth and two days of age, before rising to a maximal value in the second week of life (Greenwald et al., 1982).

The effect of smooth muscle cell contraction in the systemic vessel is mainly in a circumferential direction, mirroring the orientation of the SMCs. Recent experiments have shown the SMCs are capable of exerting significant forces to reduce the resting length by 25 - 30%. Most vessels exhibit their greatest capacity for constriction at transmural pressures comparable to those to which they are exposed in vivo (Dobrin, 1978).

In this thesis, the wall stress generated in isolated segments of intrapulmonary artery by passive stretching (increasing strains) is measured. The additional stress generated at these strains during generated at these strains during potassium chloride induced contraction of the SMCs is also measured and the ratio of stresses used to give an index of contractile function. This is then correlated with the cytoskeletal appearances of SMCs within the vessel wall.

1.9.3 Wall stress

As discussed above, increasing the strain of the vessel wall will result in an increase in passive stress contained in the wall. The law of Laplace describes the intramural stress of a vessel from a knowledge of the distending pressure. The internal distending pressure produces a tension (force per unit length) within the wall that is proportional to the radius.

Tension=Pressure X Radius

If the wall thickness is known then the force per unit area, or circumferential wall stress (τ) can be calculated from this tension:

τ=Pressure X Radius /wall thickness

Thus, if the intraluminal pressure (pulmonary arterial pressure) is known, the wall stress due to this pressure can be calculated for a given radius (measured from the intrapulmonary artery) of vessel. This is important, as it ensures experiments can be carried out at strain values sufficient to generate passive wall stress similar in magnitude to those encountered in life. However it is difficult to extrapolate in vivo wall stress to dissected and isolated vessel rings. To overcome this, the contractile behaviour of intrapulmonary artery was investigated over a range of strains from 1.0 - 1.7 which represents a reasonable physiological range (Greenwald et. al., 1982).

1.9.4 Edge effects and alterations in vessel length during contraction

The theory of stress and strain in vessels specifically excludes effects due to the edge of the ring where stress distribution is not linear. These are more important during measurement of the passive qualities of vessels and have less bearing on the active contractile properties of vessels (Cox, 1983). As these edge effects cannot be quantified it is important to ensure the length of the rings is sufficient with regards to their diameter such that these errors are minimised by use of cylindrical shapes of vessel (Nichols and O'Rourke, 1998). Similarly when a ring is stretched, in order to maintain the same volume, its cross sectional area will narrow, increasing the stress in this area. This phenomenon is known as necking and can be adjusted for by multiplying stress values by the reciprocal of their strains.

The effect of changing vessel dimensions during contraction in vivo is very difficult to model. This is especially so in the pulmonary vessels as these are subject to periodic longitudinal as well as radial forces during respiration. It is not possible to model these changes in a simple system.

1.9.5 Stress Ratio

Whilst investigating the contractile capacity of intrapulmonary arterial segments at increasing strain, it became clear that there was significant variation in the magnitude of result obtained between different animals, which made evaluating the data difficult. At the suggestion of Dr Stephen Greenwald, the stress ratio of these vessels was calculated. Passive wall stress must increase with increasing strains (unless the vessel simply stretches). If there is no additional increase in stress of the stretched vessel wall upon contraction with potassium chloride, the stress ratio will remain at 1.0. If there is additional stress generated by contraction, the stress ratio will increase. The important advantage of this ratio is that all dimensions used in the calculation of stress cancel out in the calculation of stress ratio. This leaves the absolute force from passive stretching and the absolute force obtained upon contraction at each strain value as the measurements that comprise the stress ratio.

1.10 SUMMARY

The adaptation of the pulmonary circulation to the extra-uterine environment is a fundamental and critical event in mammalian life yet little is known about the process. Immediate failure of adaptation is manifest as pulmonary hypertension in the newborn which continues to carry a high mortality. Disturbed adaptation as a result of congenital structural heart disease remains as an obstacle to successful corrective surgery for many children leading to early death.

The mechanisms underlying adaptation to the extrauterine environment are not well understood. In diseases of the systemic arteries, such as atherosclerosis, the presence of multiple SMC phenotypes have been and implicated in their pathophysiology. Multiple SMC phenotypes have described in the bovine main pulmonary trunk. The purpose of this study was identify whether normal postnatal adaptation of the intrapulmonary artery in the pig is associated with modulation or change of SMC phenotypes within the vessel wall, and whether failure of adaptation as seen in the porcine hypobaric hypoxia model of PPHN is associated with alteration of SMC phenotype. To do this SMC phenotypes were initially identified on the basis of their cytoskeletal protein expression, within the intact intrapulmonary arterial wall. Following this initial survey, a more detailed examination of the actin cytoskeleton, was performed. In addition to these structural investigations, the functional implications of these phenotypic changes were evaluated by measuring the contractile ability of the artery as reflected in contractile stress ratio. Finally, SMC phenotypes from the intrapulmonary arteries of normal and hypoxic animals were cloned, and their structural and functional characteristics identified and related to the vessels from which they were obtained.

Chapter 2. Materials and methods

The investigation of SMC cytoskeletal remodelling, within the intact intrapulmonary artery required the use of a variety of different techniques which were each used to address a specific question. Immunocytochemical staining was initially performed on cryo-ultramicrotomy sections to map the expression of cytoskeletal proteins within individual SMCs. The organisation of actin was then examined using fixation methods to stabilise the filamentous actin cytoskeleton. A specific biochemical assay was employed to determine the total quantity of actin present, and the proportion comprising the filamentous cytoskeleton. The functional implications of these findings were explored by measuring the passive wall stress generated within isolated rings of vessel, compared with the stress produced during contraction at increasing strains (stress ratio).

Individual SMCs were isolated from intrapulmonary arteries and maintained in tissue culture. It was possible to identify different SMC phenotypes on the basis of their morphological appearance. The cytoskeletal changes seen within the SMCs of the intact vessel wall during development were related to these in vitro phenotypes. A selection of SMC phenotypes, from the vessels of normal pigs and those that had been exposed to hypobaric hypoxia for 3 days, were then cloned by serial dilution and their characteristics investigated.

2.1 SOURCES OF ANIMAL TISSUE

Large White pigs were used throughout this study. These were chosen because their lung development and pulmonary adaptation to extra-uterine life is similar to that of the human (Haworth and Hislop, 1981). This model has been used extensively for studies of postnatal adaptation and pulmonary hypertension, making it possible to consider the findings in the present study against an extensive experience already gained in the cell biology and pharmacology of the developing porcine intrapulmonary arteries. Familiarity with the physiology and the general management of both the normal piglets and those exposed to hypobaric hypoxia increased the ease with which the animals could be handled and therefore the rapidity with which the animals could be killed. This was important in that at birth or on removal from exposure to hypobaric hypoxia delays were avoided which could otherwise of allowed adaptation or regression of hypoxia induced changes to occur.

One of the common problems in animal studies is the great variation in the behaviour of different animals - even when normal. Specifically in relation to these experiments, the rate of adaptation to the extra-uterine environment although progressing in a similar fashion does probably occur at slightly different rates in different animals as it does in human infants. The relatively wide variation in the rate of fall in pulmonary arterial pressure and in the structural changes occurring at this time reflects this normal and unavoidable process. The implication for the scientist is that more animals must be examined at younger than older ages, and unfortunately these animals are the most difficult to acquire due to the ethical and logistical constraints.

Normal adult lungs were obtained from a commercial abattoir; 3 and 14 day old piglets were obtained from Selbourne Biological Supplies Ltd, Basingstoke, UK and killed at the Institute of Child Health; and lungs from fetal piglets, breathing and non-breathing, were collected from Selbourne Biological supplies Ltd.

Although tissue from animals at most of the required ages were easily obtained from sources outside the Institute, newborn animals could only be obtained after animals had farrowed at the Institute of Child Health. The care and maintenance of

these animals was carried out in accordance with the rules and regulations of the Home Office.

A total of 130 animals, ranging in age from fetal to adult pigs, were used in this study.

2.1.1 Adult animals

Lungs from adult animals were obtained from Fresh Tissue Supplies Ltd, Horsham Surrey. These animals were killed in a commercial abattoir by electrical stunning followed by exsanguination. The lungs were immediately removed and placed in physiological saline solution. They were then transported by motorcycle courier to the laboratory. This interval was no longer than two hours.

2.1.2 Three, fourteen and 21 day old piglets

These animals were delivered live to the Institute of Child Health 24 hours before use. They were kept in conditions dictated by the Home Office and those animals too young to feed themselves were gavage fed. They were killed with an intra-peritoneal injection of pentobarbitone (Expirol) at a dose of 100mg/Kg. The thoracic cavity was opened, the heart and lungs removed as a block, and transported to the laboratory in physiological saline for dissection of the pulmonary arteries.

2.1.3 Normal newborn piglets

To obtain newborn piglets, pregnant sows were farrowed at the Institute of Child Health. Some newborn piglets were allowed to breath for five minutes before being killed by an intra-peritoneal injection of. Others were prevented from breathing by placing a rubber condom over the snout, immediately after birth, before they could take a breath. The animals were then killed immediately, with phenobarbitone as described previously. The lungs were removed and taken to the laboratory in physiological saline.

2.1.4 Fetal piglets

Fetal piglets were obtained from Selbourne Biological Supplies Ltd, Basingstoke UK, by killing a pregnant sow one week before the expected date of farrowing. The sow was stunned and killed by exsanguination and the fetal piglets were removed from the uterus one at a time. In some animals breathing was prevented (called fetal non-breathers) by immediately placing a rubber condom over the snout and then killing them by an intra-peritoneal injection of pentobarbitone, as above. Animals allowed to breath (called fetal breathers) were removed from the uterus as soon as possible after death of the sow. The membranes were wiped from the snout and the piglets rubbed dry. By five minutes of age they had become pink, had regular respiratory patterns and were walking around. They were then killed by an intra-peritoneal injection of phenobarbitone as described previously, and the lungs removed. The lungs from the fetal animals were transported back to the laboratory in physiological saline within two hours of death.

2.1.5 Hypoxic piglets (0 - 3 days)

When a sow farrowed at the Institute of Child Health, four of the piglets were placed in a hypobaric, hypoxic chamber (pressure 50.8 kPa) within 15 minutes of birth. Before entering, the piglets were dried, allowed to obtain colostrum from the sow and also gavage fed with milk. Inside the chamber they were kept warm with a heating lamp and had ample straw for bedding. Piglet feed and milk were also provided. Because they were not always able to feed themselves, they were gavage fed with modified cows milk four to six times per day. They were kept under these conditions for up to three days. At the end of this period they showed evidence of pulmonary hypertension, as indicated by central cyanosis due to right to left shunting through persistent fetal channels. There was also right ventricular and pulmonary arterial medial hypertrophy at death (Haworth and Hislop, 1982). They were immediately killed by an intra-peritoneal injection of pentobarbitone. The lungs were removed and taken to the laboratory in physiological saline.

2.2 Origin of tissue specimens taken for experiments

The samples for all the experiments were taken from the same area of the intrapulmonary artery (Figure 12). This was to allow comparison between microscopy studies, biochemical analyses, cell culture experiments and mechanical studies. For cell culture and biochemical estimations the entire middle 50% of the intrapulmonary artery was used (Figure 12).

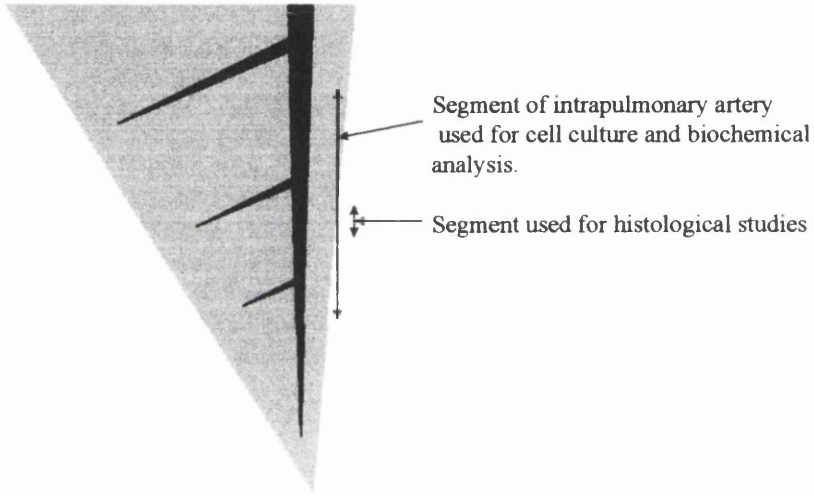

Figure 12. Origin of segments of intrapulmonary artery used for experiments.

2.3 SMC CYTOSKELETAL PROTEIN EXPRESSION WITHIN THE INTACT VESSEL WALL STUDIED USING IMMUNOLABLLED CRYO-ULTRAMICROTOMY SECTIONS

In order to study the cytoskeletal proteins of the SMCs within the intact wall of the vessel, it was necessary to improve on conventional immunolabelling techniques. Conventional fluorescent immunohistochemistry is limited by the ability of light to resolve fine differences in structure. This can be overcome by utilising the shorter wavelength of the electron, as with scanning and transmission electron microscopy. Unfortunately the rigorous fixation and dehydration methods essential for these techniques reduces the antigenicity of the material. Immunolabelling is also limited to heavy metal particles, for example gold. However, the resolution of immunofluorescent microscopy can be improved if stray light signals, from tissue above and below the plane of view, can be removed. This can either be done optically via a pinhole aperture (confocal microscopy) or mechanically by cutting a very thin section within the depth of field of the lens. Confocal microscopy was attempted, but because light did not penetrate the dense tissue of the vessel wall, this approach was found to be unsuitable for our purpose. Instead, 250 nm frozen sections were cut, immunolabelled and viewed with a microscope equipped with epifluorescence and a digital camera (Unpublished method of Dr A North, University of Manchester).

Tissue from fetal (non-breathing), 3 day old, 14 day old, adult and 0 - 3 day old hypoxic animals was studied in these experiments. In total 15 animals were examined.

2.3.1 Embedding of tissue

Tissue for sectioning was lightly fixed and infused with 2.3 M sucrose solution, as a cryoprotectant, before mounting on aluminium stubs and freezing in liquid nitrogen. Polyvinylpyrrolidone (PVP) was added to the sucrose to give plasticity to the blocks and improve cutting conditions. The procedure was as follows:

1. Five mm segments of intrapulmonary artery were dissected from the lower lobe of left or right lung, using a binocular microscope where necessary (see Figure 12).
2. The segments were further trimmed, using a razor blade, to blocks of 1 - 2 mm diameter.
3. The blocks were fixed in 2% paraformaldehyde for one hour at room temperature and then washed three times in PBS.
4. The blocks were then immersed in PVP/sucrose (100 ml of PVP/sucrose was made by adding 20g of PVP and 4 ml of 1.1 M sodium carbonate (Na_2CO_3) to a 2.3 M solution of sucrose in PBS) for four hours at room temperature.
5. The blocks were orientated on aluminium stubs, plunged into liquid nitrogen and stored for up to four weeks until used.

2.3.2 Cutting of sections

The prepared blocks were cut at temperatures of approximately -100 °C, using glass knives on a modified ultramicrotome (Sorvall). Sections were lifted using a droplet of sucrose/gelatin on a wire loop. The sections were placed on prepared coverslips, and stored on gelatin until use. The procedure was as follows

1. 5 cm diameter plastic petri dishes were filled with a solution of 2% gelatin in distilled water and allowed to solidify at 4 °C.
2. 13 mm diameter glass coverslips were prepared by first coating with Bacitracin (40μg/ml in distilled water). The excess was drained off and the coverslips were then dipped into poly L-lysine. After drying they were stored on clean filter paper in a sterile plastic petri dish.
3. The cryo-ultramicrotome (Sorvall) was cooled from room temperature to -70 °C. A mounted block was removed from liquid nitrogen and placed in the specimen chuck. After the temperature of the block had equilibrated, the face was manually trimmed to reveal the tissue. 500nm sections were cut initially and picked up with a wire loop holding sucrose/gelatin solution. The droplets froze as the sections were lifted. After thawing, the droplet containing the section, was placed on a plain glass slide and stained with 1% toluidine blue (w/v in

water). The excess was washed off with distilled water and the section examined under a microscope (Leica).

4. The specimen was then cooled to -90 °C. 250 nm sections were cut at a knife speed of 0.4 mm/second.
5. The sections were picked up as before with sucrose/gelatin and a wire loop but this time deposited on coated 13 mm glass coverslips. The coverslip was then inverted onto a gelatin containing petri dish.
6. The coverslips were stored for up to one week at 4 °C until use.

2.3.3 Immunolabelling of sections

The cryo-ultramicrotomy sections were examined using a variety of antibodies against cytoskeletal proteins and anti-mouse FITC-labelled secondary antibodies (Table 1). The nuclei were stained using Hoechst 33528 (2 μg/ml), and the basal lamina surrounding the cells by a rabbit derived polyclonal anti-laminin antibody, detected with a specific anti-rabbit TRITC-labelled secondary antibody (Table 1). The procedure was as follows:

1. Petri dishes containing gelatin and coverslips were placed in an oven at 37 °C until the gelatin had melted and the coverslips were floating on the surface of the gelatin. After a further 10 minutes the coverslips were washed three times in 0.02M glycine in PBS (glycine was added to reduce non-specific, ionic charge-related antibody binding).
2. Non-specific antibody binding was further prevented by application of 1% BSA/5% normal goat serum in PBS (blocking solution) for 15 minutes at room temperature.
3. This blocking solution was then removed and the primary antibodies, diluted in 1% BSA, mixed with anti-laminin antibody (rabbit) diluted 1:200 (Table 1) were applied for one hour at room temperature in a humidity chamber.
4. The sections were washed three times in PBS and a secondary antibody mixture was then applied for 30 minutes at room temperature in the dark. This consisted

of anti-mouse FITC (1:200); anti-rabbit TRITC (1:50); and Hoechst 33258 (2 μg/ml). All secondary antibodies were diluted in blocking solution.

Table 1. Primary antibodies used against cytoskeletal proteins on cryo-ultramicrotomy sections.

Primary antibody (mouse)	dilution
anti-αSM actin	1:200
anti-β actin	1:200
anti-γ actin	1:200
anti MHC SM1	1:100
anti-desmin	1:10
anti-calponin	1:200
anti-caldesmon	1:200

5. The coverslips were washed three times with PBS, before air drying in the dark and mounting with Vectormount fluorescent microscopy mounting medium.
6. Coverslips were kept in the dark at 4 °C, but examined on the same day using a Zeiss microscope with epifluorescence and a digital camera system (Openlab Ltd).

2.3.4 Semiquantitative scoring of staining pattern

The staining pattern of the cytoskeletal antibodies was assessed in a semi-quantitative manner, scoring from absent (-) to complete (+++), depending on the area of the cytoplasm that was labelled with antibody. The cytoplasmic area was defined as the area around a nucleus limited by anti-laminin antibody staining. The intensity of staining was not used as it is unreliable when attempting to quantify immunofluorescence (Keller and Bebie, 1996).

2.4 THE ACTIN CYTOSKELETON IN THE INTACT VESSEL WALL - HISTOLOGICAL STUDIES OF STABILISED ACTIN FILAMENTS

Experiments were performed to see if there was a significant change in the organisation of the actin in the SMCs within the intact vessel wall during development.

To improve visualisation of the actin cytoskeleton, segments of pulmonary artery were treated with detergents and phalloidin. This stabilised the filamentous structure of the actin cytoskeleton, and removed monomeric and very short filaments. The tissue was then fixed and sectioned, and the actin visualised with rhodamine (TRITC)-phalloidin conjugate. Once the tissue had been permeablised, an intracellular buffer solution (Hirokawa and Tilney, 1982) was used. This was important as the cytoskeleton is prone to disruption under changing salt concentrations. Similarly, Taxol was used to stabilise the microtubular structures to ensure that its disruption did not alter the appearance of the SMCs.

In order to ensure that the technique was suitable for detecting changes in the actin cytoskeleton, the effect of contraction was assessed by exposing vessels from 14 day old piglets to a thromboxane analogue, U46619, and to sodium azide (which elicits a maximal contraction by depleting cellular ATP). Having found the technique to be satisfactory, the effect of postnatal adaptation on the appearance of intrapulmonary elastic conduit arteries from fetal (breathing and non breathing), newborn (breathing and non breathing), 3 day old, 14 day old, adult and 0 - 3 day old hypoxic pigs was examined. In these experiments a single intra pulmonary arterial segment was used from each of three animals at each age. The procedure was as follows:

2.4.1 Preparation of tissue sections

1. 5 mm segments of intrapulmonary artery were dissected from the lower lobe of left or right lung as previously described (Figure 12). However to prevent proteolysis, during dissection, the lung was bathed in PBS containing protease inhibitor tablets (Amersham) at room temperature.

2. Segments were then randomly allocated either to PBS solution alone, PBS containing sodium azide (10mM), or PBS containing the thromboxane analogue U46619 (0.1μM) for 30 minutes at room temperature.
3. The segments were dipped in Hirokawa's solution (an intracellular physiological buffer containing 70 mM potassium chloride, 5 mM magnesium chloride, 3 mM EGTA, 30 mM HEPES in distilled water) containing one Complete Anti-protease Tablet per 10 ml at room temperature, either alone or containing the sodium azide (10 mM) or U46619 (0.1 μM) for 30 minutes at room temperature.
4. 3.7% formaldehyde was added to fresh aliquots of these, and the segments fixed for 10 minutes at room temperature, whilst still exposed to U46619 or sodium azide.
5. The segments were rinsed three times in Hirokawa solution before orientating in OCT compound on cork discs. The OCT was snap frozen in melting iso-pentane (cooled by liquid nitrogen).
6. 5μm sections were cut using a cryostat (Bright) and transferred to glass slides coated with tissue adhesive (Vectabond).
7. The slides were covered in kitchen foil and stored at -70 °C, and used within one month.

2.4.2 Staining of tissue sections

1. The slides were wrapped within foil until completely defrosted to avoid condensation damage.
2. The slides were rehydrated in PBS for five minutes, then plunged into cold acetone (-20°C) for 20 minutes.
3. The slides were rehydrated with three washes of PBS
4. Non-specific antibody binding was prevented by application of 1% BSA/0.1 M lysine in PBS for 15 minutes. This blocking solution was then tapped from the slide.

5. Phalloidin-TRITC conjugate (1:200) diluted in blocking solution was applied for 20 minutes at 4°C in the dark.
6. The coverslips were washed three times with PBS before air drying in the dark and mounting with Vectormount fluorescent microscopy mounting medium.
7. Coverslips were kept in the dark at 4° C until examined, on the same day, using a microscope with epifluorescence (Nikon).
8. Black and white photographs using Kodak 400 ASA panther film were obtained using the automatic spot metering exposure system of the microscope. Four photographs were taken of the inner half of the media.

2.4.3 Analysis of data

Images were taken at random from each rhodamine-phalloidin stained section, in a blind fashion by Dr D Lawson (University of London). Each set of photographs were coded at random and then sorted into groups with similar appearances as described above. This was also carried out, again in a blind manner, by Dr D Lawson and myself. Although the appearance of sections cut from blocks of the same age of animal were similar, the longitudinal or transverse arrangement of filamentous actin within the SMCs of each section was variable. Thus sorting could not be carried out based on the appearances of filaments. Therefore, the sections were scored using the degree of actin compaction, from an arbitrary score of (+) indicating extensive distribution of actin filaments between the main margins of the SMCs, to (+++) indicating no extension of filaments away from the cell outline and compact cytoskeleton.

2.5 THE ACTIN CYTOSKELETON IN THE INTACT VESSEL WALL - BIOCHEMICAL ESTIMATION OF TOTAL AND MONOMERIC/TOTAL ACTIN RATIO

The total actin contained within a tissue sample can be easily determined by electrophoresis, but determining the proportion of monomeric actin is more difficult. Although filamentous (F) actin is stable under the influence of mild detergents, the short filaments can be washed out of cells together with monomeric actin. These problems make the calculation of the monomeric to total actin ratio difficult. An alternative approach is to use Triton X-100 extraction to strip the cell of its membrane and produce a suspension of cellular monomeric actin and filamentous actin. The actin present in the monomeric state can be measured by a sensitive and specific fluorometric method using an aliquot of this tissue suspension. The filamentous actin in a second aliquot can then be chemically broken down into monomeric actin and assayed to give the total cellular actin content. Thus by measuring the monomeric and total actin content of the same sample a monomeric/total actin ratio can be calculated.

The total actin content of the tissue must be standardised to allow comparison between animals of different ages, and those exposed to hypobaric hypoxia. A DNA assay was also used to indicate quantity of actin per cell, and a protein assay was carried out to indicate the intra-cellular concentration of actin at each age.

These experiments were carried out on: fetal (breathing and non breathing), newborn (breathing and non breathing), 3 day old, 14 day old, adult, and 0 - 3 day old hypoxic pigs. A total of 28 animals were used in these experiments.

2.5.1 Measurement of monomeric to total actin ratio in whole tissue samples

Inhibition of bovine pancreatic deoxyribonuclease 1 (DNAse I) is a standard method for quantification of monomeric actin. The enzyme tightly and selectively binds to monomeric actin, in the presence of F actin, with demonstrable loss of the enzyme's DNA hydrolysis properties. DNA hydrolysis can be followed by

monitoring the reduction in fluorescent signal from a nucleic acid stain which is specific for intact double-stranded DNA, for example ethidium bromide or Yo-Pro (a thiazole orange derivative). Within the assay, inhibition of DNase I by monomeric actin causes a reduction in the rate of DNA hydrolysis per minute, and hence a slower attenuation of the fluorescent signal (Huang et al., 1993). Unknown monomeric actin concentrations can be determined by comparison with a standard curve. Inhibition of DNAse I hydrolysis was preferable to protein electrophoresis of differentially centrifuged samples because of the small size of the tissue samples available from young animals. The main consideration in using the actin assay was to ensure that the readings from the samples were obtained in the sensitive part of the calibration curve (between 0.5 and 2.5μg/ml actin). Outside these limits the curve becomes more parallel with the adjacent axis and the measurements inaccurate. Used appropriately, this assay is very reproducible and the differences in "change of fluorescence" readings obtained on the same sample were at most 1 %. Thus, the variation in actin concentration that could be attributed to the method was 0.02 μg/ml actin at the part of the curve relating to 0.5μg/ml actin standard, and 0.08 μg/ml at the part of the curve relating to 2.5 μg/ml actin standard. These figures are in keeping with published sensitivities (Huang et al., 1993). A commercial assay (Molecular Probes) was modified for use in these experiments. The procedure was as follows

2.5.1.1 Preparation of standard curve

1. Monomeric actin standards were prepared by addition of 10μl of actin standard (provided with the Molecular Probes assay kit) to 10μl of actin depolymerising buffer. After 10 minutes at room temperature, the mixture was diluted by the addition of 2ml of working buffer (10 mM Tris buffer pH 7.6) to give a 20μg/ml standard solution of monomeric actin. Standard mixtures were prepared and allowed to stand for five minutes at room temperature before use (Table 2).
2. A fluorometer (Perkin-Elmer) was set to excite at 480 nm and record fluorescence at 520 nm. The excitation slit was set at 10nm and the emission slit

at 20nm. The standard mixtures were split into 1ml aliquots and duplicate experiments performed in 1 ml volume quartz cuvettes.

Table 2. Actin standards used to generate standard curve of monomeric actin concentration /rate of DNA hydrolysis.

Concentration of monomeric actin (μg/ml)	Volume (μl) of 20 μg/μl monomeric actin standard	Volume (μl) of working buffer	Volume (μl) of DNA/dye complex
0 (blank)	0	500	1500
0 (blank)	0	500	1500
0.25	25	475	1500
0.5	50	450	1500
1	100	400	1500
2	200	300	1500
3	300	200	1500
4	400	100	1500
5	500	0	1500

3. For each measurement, 1ml of the DNA/dye-monomeric actin standard mixture was placed in a cuvette and the fluorescence measured. 25μl of DNAse I solution was then added, the cuvette inverted to mix, and a stopwatch started. The fluorescence reading at two minutes was recorded and the percentage drop in fluorescence (initial - final reading/initial reading X 100) was calculated.
4. Using the standard mixtures containing no monomeric actin, the quantity of the DNAse I enzyme solution needed to produce a 50% fall from the initial reading was determined. This was typically between 20 - 25μl.
5. Using this volume of DNAse I, the other reaction mixtures were measured and a standard curve produced.

2.5.1.2 Sample preparation

1. The whole length of the main intrapulmonary conduit artery was dissected from the lower lobe of left or right lung, using a binocular microscope where necessary to remove the adventitial layer. The length of the excised intrapulmonary conduit artery was measured and only the central 50% was

used. The vessel was weighed, immediately frozen in liquid nitrogen, and stored at -70 °C until used.

2. The defrosted tissue was mechanically broken down using an Eppendorf grinding tool in a minimal volume of cold lysis buffer (2% Triton X-100 in 10mM Tris buffer). It was sonicated on ice and the tissue suspension frozen in liquid nitrogen before storage at -70 °C.

2.5.1.3 Measurement of tissue actin - monomeric and total

1. 15 µl of thawed tissue suspension was added to 15 µl of actin depolymerising buffer. After 10 minutes at room temperature this was diluted to 300 µl with working buffer. 200 µl was immediately frozen in liquid nitrogen and used for DNA (**experiment 2.5.2**) and protein (**experiment 2.5.3**) estimations. The remaining 100 µl was diluted to 1.0 ml total volume with working buffer. 750 µl of this was added to 2250 µl of DNA/dye and allowed to stand for five minutes at room temperature. This final 3 ml volume was then used to perform three separate measurements and the mean value calculated. This gave the total actin concentration of the sample
2. To measure the monomeric actin concentration of the samples, 90 -150 µl of the original tissue suspension was added to 2250 µl of DNA/dye and made up to 3 ml with working buffer. This was used to perform three measurements and the mean value calculated.

These measurements were carried out at the same time, for the complete range of experimental age groups, and using the same reagents, in order to minimise variations in the methodology.

2.5.2 Measurement of DNA in whole tissue samples

The DNA content of tissue was measured using the Hoechst 33258 dye-binding spectrofluorimetric method (LaBarca and Paigen, 1980). This method allows an estimation of total DNA content in the presence of protein and other potentially interfering substances such as detergents. A standard curve is generated with

known concentrations of DNA, and is used to interpret readings from tissue samples. Preliminary experiments were performed to demonstrate that no interference resulted from the guanidine hydrochloride contained in the actin depolymerising buffer, or from Triton X-100. The procedure was as follows:

1. A spectrofluorometer (Perkin-Elmer) was set to excite at 365 nm and record fluorescence at 458 nm. The excitation slit was set at 10 nm and the emission slit at 20 nm.
2. Known concentrations of DNA were produced using a commercially obtained solution of herring sperm DNA (10 mg/ml - diluted 1:1000 in distilled water) as in the table below (Table 3), and 100 µl of Hoechst 33258 (2 µg/ml in distilled water) was added to each 2 ml standard.

Table 3. DNA standards used to construct the standard curve of concentration of DNA/fluorescence with Hoechst 33258.

Concentration of DNA (ng/ml)	Volume (µl) of DNA stock 10 ng/µl	Volume (µl) of DNA assay buffer	Volume (µl) of 2µg/ml Hoechst 33528
0 (blank)	0	1000	100
200	20	1000	100
400	40	1000	100
600	60	1000	100
800	80	1000	100
1000	100	1000	100

3. The blank adjustment of the spectrofluorometer was set to obtain a relative fluorescence using the blank, as above.
4. The standard samples were measured using a 1 ml quartz cuvette and the mean of the two readings used to create a standard curve.
5. 100 µl of Hoechst 33258 (2µg/ml) and 3 ml of DNA assay buffer (40 mM Na_2HPO_4, 10 mM NaH_2PO_4, 2M NaCl, and 2 mM EDTA) was added to 150 µl of the total actin samples from **experiment 2.5.1.3**. These were samples of tissue that had been treated with Triton X-100 and guanidine hydrochloride and had been saved for use in the protein assay below. Triplicate measurements of

each sample were taken and the concentration of DNA determined using the standard curve.

2.5.3 Measurement of soluble protein content of whole tissue

The measurement of protein in the tissue was carried out on samples that had been treated with Triton X-100 and guanidine hydrochloride. This treatment solublised the cytoplasmic cytoskeletal proteins and allowed their measurement, but did not solublise proteins such as collagen and elastin (**experiment 2.5.1.3**). Hence the protein estimation could be used to standardise the actin concentration. A commercially available method (Pierce Chemicals BCA protein assay) was used for convenience and on account of its compatibility with guanidine hydrochloride and Triton X-100. Preliminary experiments were performed to demonstrate that no interference resulted from either substance. The procedure was as follows:

1. A set of protein standards of known concentration were prepared by diluting a 2mg/ml stock solution of BSA, as below (Table 4).

Table 4. Protein standards used to create a standard curve for protein estimation of tissue samples.

Concentration of BSA (μg/ml)	Volume (μl) of 2mg/ml BSA solution	Working buffer (μl)
0	0	50
2	1	49
4	2	48
6	3	47
8	4	46
10	5	45
12	6	44
14	7	43
16	8	42
18	9	41
20	10	40

2. 1ml of BCA reagent was added to these standards and the solution incubated at 37°C for 30 minutes.

3. The absorbance of the cuvette filled with standard 0 μg/ml BSA was used to set a spectrophotometer to zero, measuring absorbance at a wavelength of 562 nm. Each of the standards were placed in a glass cuvette and the absorbance of light measured at this wavelength.
4. 20 μl of each sample (from **experiment 2.5.1.3**) mixed with 30μl of working buffer (10 mM Tris buffer pH 7.6) was added to 1 ml of BCA reagent, and the absorbance measured as in **steps 2 and 3**.
5. The concentration of protein was determined by reference to the standard curve.

2.5.4 Statistical analysis

The mean values of protein, DNA and actin content were calculated for each group of animals and the variation expressed as standard deviation.

2.6 STUDIES OF CONTRACTION

The functional effects of changes in the actin cytoskeleton, during normal development and in the hypoxic model of pulmonary hypertension, were investigated by assessing the stress ratio of segments of intrapulmonary artery, before and after contraction with potassium chloride, at increasing physiological strain values. A total of 41 animals were used in these studies. The proportions of smooth muscle, collagen and elastin within the media were then measured morphometrically using sections cut from adjacent segments of intrapulmonary artery, stained with Millers elastin van Giesen stain.

2.6.1 Principles of deriving stress strain relationships for contraction studies

2.6.1.1 Stress and strain

The determination of wall stress in blood vessels is difficult. There is potential for error at several of the stages involved in the determination of wall stress. There are, for example, potential problems associated with the use of a pharmacological organ bath to measure force production of isolated vessel rings. The ring may become damaged as it is dissected free from the surrounding tissue (Furchgott and Zawadzki, 1980). Also, the stress loading of an isolated ring must be different to the loading of an intact vessel because the structural effects of the surrounding tissue on the vessel wall are lost. However, the advantage of the method is its simplicity. Despite the problems with the technique we used, it was possible to reproducibly measure the force produced within the vessel wall and to calculate wall stress in order to evaluate SMC function. Because the diameter, wall thickness and composition of the intrapulmonary artery changes between fetal life and adulthood it was important to standardise the force generated during contraction. To do this, forces generated within the vessel rings were calculated as wall stress (force per unit cross sectional area. Note: 1 g/cm^2 = 100 N/M^2). Strain, which is

the ratio of new dimension of the vessel wall to its original resting dimension, was also determined to take into account variation in vessel size.

To calculate these parameters, it was necessary to determine the dimensions of each ring (Figure 13). During the experiment; the increase in hemi-circumference (Δh) of the experimental vessel rings was measured with a Vernier scale. The length (L) of the vessel ring was measured after the experiment using a binocular dissecting microscope and stage micrometer. The initial hemi-circumference (h) of the vessels was measured from the adjacent histological rings using a binocular dissecting microscope and a stage micrometer. The wall thickness (w) and hemi-circumference (h) of the actual experimental rings were not measured in order to prevent their damage prior to their use, nor following the experiment as they may have been damaged by stretching. The percentage wall thickness in relation to the external diameter of the vessel expressed in fractional form (P) was determined from sections cut from the histology vessel ring following wax embedding (P = wall thickness of section/external diameter of vessel in section). This parameter was used in conjunction with the actual initial hemi-circumference of the adjacent rings (h) to calculate the wall thickness (w) of each vessel as $D = 2h/\pi$. The use of P also eliminated the effect of any shrinkage artefact during the wax embedding process.

Figure 30. Measurements of rings and calculation of strain, stress and stress ratio

a) Source of histology and experimental rings

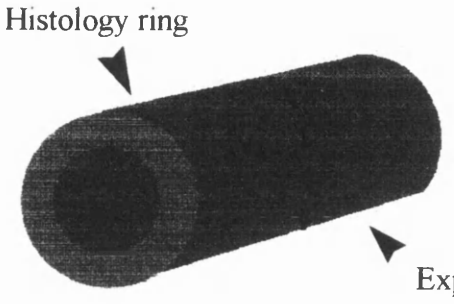

Segment of intrapulmonary artery divided into experimental and histology rings

b) Measurement of hemicircumference and calculation of percentage wall thickness

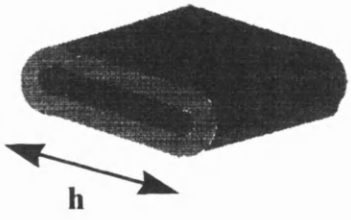

Histology ring is flattened to measure hemicircumference (h) prior to fixation

Note: circumference = πD
and circumference = $2h$
thus, $h = \pi D/2$

c)

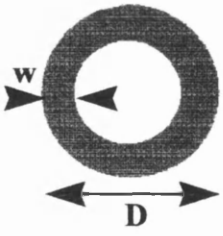

Histology ring is then fixed and sectioned. Itis then used to determine mean percentage wall thickness, in fractional form (P) for each age of animal (where w' and D' are dimensions from fixed sections:

Percentage wall thickness (P) = $\frac{\text{wall thickness (w')}}{\text{external diameter (D')}}$

Combining these equations, the wall thickness (w) can be calculated for each vessel ring from the hemicircumference of each ring (h) and the percentage wall thickness of each age group of animals (P): $w = 2Ph/\pi$

Use of percentage wall thickness, with hemicircumference measurements minimises artifact due to fixation shrinkage.

Figure 30. continued. Measurements of rings and calculation of strain, stress and stress ratio

d) Calculation of strain

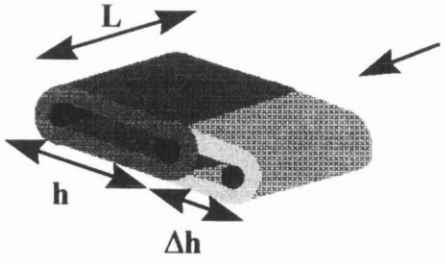

Experimental ring suspended by tungsten wires and stretched by Δh from original hemicircumference (h). Strain is calculated using the hemicircumference (h) which is measured from the adjacent histology ring and Δh which is measured using an integral Vernier scale during the experiment.
The length of the ring (L) is measured after the experiment using a dissecting microscope and stage micrometer.

$$\text{Strain} = \frac{h + \Delta h}{h}$$

e) Calculation of stress

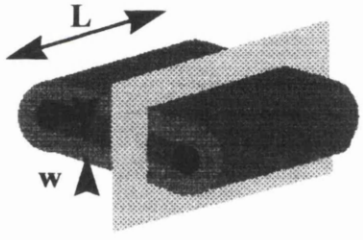

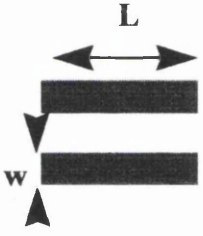

The forces generated by passive stretching and by contraction with potassium chloride are directed through the cross sectional area of the two sides of the vessel ring. Length (L) is measured directly. The wall thickness (w) is determined from a knowledge of the percentage wall thickness (P) for each age group and the hemicircumference (h) of each ring. Because the cross sectional area of the ring becomes smaller as the ring is progressively stretched, each stress value must be adjusted for this by multiplying by 1/strain:

The total cross sectional area = 2wL
Therefore cross sectional area = $4PhL/\pi$

for each age group $w = 2Ph/\pi$

$$\text{Stress} = \frac{\text{Force}}{\text{area}}$$

$$\text{Stress} = \frac{0.79\ F}{PhL\ \text{strain}}$$

F = force
P = percentage wall thickness (as a fraction)
h = hemicircumference
L = length

Figure 30. continued. Measurements of rings and calculation of strain, stress and stress ratio

f) Calculation of stress ratio

$$\text{Stress ratio (SR)} = \frac{\text{Active stress (stress}_A\text{)}}{\text{Passive stress (stress}_P\text{)}}$$

$$\text{Stress ratio} = \frac{\dfrac{0.79\,F_A}{\text{PhL strain}}}{\dfrac{0.79\,F_P}{\text{PhL strain}}}$$

In this ratio all the terms except force cancel each other out hence:

$$\text{Stress ratio} = \frac{F_A}{F_P}$$

F_A = Active force after KCl contraction
F_P = Passive force after stretch

These measurements do not take into account edge effects or errors due to longitudinal changes in vessel dimensions. However, use of stress ratio removes all these variables.

2.6.1.2 Physiological range of strain

If a ring of pulmonary artery is stretched (subjected to increasing strain) the stress passively generated in the tissue increases until the ring eventually snaps. To ensure these studies were physiologically meaningful, the experimental vessel rings were subjected to a range of strain values similar to those encountered during life. Whilst it is impossible to know the exact working strain of each vessel, a reasonable range of 1.0 to 1.6 was assumed for all ages of animal, although measurements were obtained at strains of up to 2.0 where possible.

2.6.1.3 Calculation of stress

Stress was calculated for both the passive and contracted rings by dividing the absolute force generated by the ring by the cross sectional area of the vessel ring (Figure 13). Furthermore, because the volume of the vessel ring is constant, as it is stretched the cross sectional area will diminish. The calculated stress values were adjusted to allow for this by multiplying the stress by the reciprocal of strain. Thus, for each vessel studied a passive and a contracted force measurement at increasing strains was obtained.

2.6.1.4 Stress ratio

In practice, comparison of passive and active data sets from different animals was difficult because of variability in the magnitude of absolute force generated between animals of the same age. However, by dividing the active stress by the passive stress at each strain value, these variations could be removed and an index of contractile capacity produced. This ratio was termed the stress ratio (SR). Hence, when passive stress equalled active stress a stress ratio of one was obtained, and as active stress increased over the passive values the stress ratio increased. This had the additional advantage that when stress ratio was calculated all parameters except absolute force during contraction and at rest were removed. The original data showing the wall stress generated over a range of strains was still

important as is was essential to define a physiological range of vessel strain values at which to examine the stress ratio.

2.6.2 Measurement of stress ratio at increasing strain values in isolated segments of intrapulmonary artery

The experimental procedure was as follows:

1. Lungs were obtained from freshly killed piglets and adult animals. Segments of intrapulmonary artery were obtained from the same anatomical position (Figure 12) within the lower lobe of left or right lung. The cylinders of vessel were divided to produce two identical rings each 1-4 mm in length, depending on the size of the vessel. One ring (histology ring) was placed in 3.7 % formaldehyde for later measurement of initial hemicircumference (h), before embedding in wax and histological examination to measure external diameter (D) and wall thickness (w).
2. The second arterial ring (experimental ring) was suspended between tungsten wire stirrups and mounted in a conventional pharmacology organ bath. The ring was bathed in physiological saline solution (PSS) at 37 °C and gassed with a 95% oxygen/5% carbon dioxide mixture. The stirrups were widened until the ring was fully supported, but not under significant tension, and allowed to equilibrate for one hour. At the start of the experiment the stirrups were again widened to support the ring, but not to such an extent that they exerted significant tension.
3. The position of the clamp adjusting the stirrup diameter was noted to within 0.1 mm using an attached Vernier scale. The force generated by the ring (passive force) was monitored with a calibrated force transducer and recorded on a paper chart recorder.
4. The PSS within the bath was drained off and fresh warmed PSS containing potassium chloride (125mM) was added. When maximal force had been generated (active force), the potassium chloride was washed out and fresh PSS was added to allow the ring to return to a non-contracted state.

5. The stirrups were then widened by 0.1 to 0.2 mm and the ring allowed to rest for up to 10 minutes. The passive force generated by the non-contracted ring was again noted.
6. **Steps 4 and 5** were repeated until the ring had been stretched to approximately 100% of its initial hemicircumference (Figure 13). These limits were arbitrary, set to mimic the physiological range of dilatation and prevent damage to the vessel.
7. At the end of the experiment the experimental vessel rings were inspected to ensure there was no macroscopic damage, and stored in 3.7 % formaldehyde until their length (L) was measured.

2.6.3 Calculations and statistical analysis

Calculations of strain, stress and stress ratio were performed as indicated in Figure 13. Statistical analysis was performed with the assistance of Dr S. Greenwald (University of London), using the JNP data analysis computer program. The fetal and newborn data sets and the 3 day and 0 - 3 day hypoxic data sets were compared using analysis of variance (ANOVA). In order to compare the magnitude of the stress ratios for newborn animals which had breathed, 3 day old, 14 day old and adult animals, the mean of all the stress ratio values within the physiological range of strain values from 1.0 to 2.0 were calculated. These mean values of stress ratio, and the scatter of data points around these means were then analysed using ANOVA.

2.6.4 Histological analysis of rings from mechanical studies

The unstretched rings from the mechanical studies were embedded in wax, sectioned and the collagen, elastin and smooth muscle identified by histological staining. The proportions of each of the three components was measured and the proportion of extracellular matrix calculated by subtraction from 100%. Although other workers have performed similar analyses by staining for individual components on different sections (Berry, 1976), the multiple labelling of elastin, smooth muscle and collagen did have the potential advantage that the total percentage areas obtained would add up to 100%. The procedure was as follows:

2.6.4.1 Embedding of rings in wax and sectioning

1. The fixed rings were washed three times in PBS to remove the buffered formal saline and then passed through increasing concentrations of alcohol: 30%, 50%, 70%, 85%, 95% and absolute ethanol (each step for 30 minutes at room temperature).
2. The absolute alcohol was cleared from the tissue with two 30 minute changes of xylene.
3. The rings were placed in a 1:1 xylene/wax mixture at 60 °C for one hour followed by three changes of wax, each at 60° C for one hour. They were then orientated in moulds, using heated forceps, and the wax allowed to set.
4. 7 μm sections were cut and placed on Vectabond coated slides.

2.6.4.2 Histological staining with Millers elastin van Giesen stain

1. The sections were de-waxed by immersion in xylene for five minutes and then by immersion for a further 1 minute in fresh xylene.
2. The slides were then passed from absolute alcohol to 70 % alcohol over two minutes before immersing in Millers Elastin Stain for 35 minutes.
3. After rinsing well in tap water, they were placed in 3 % ferric chloride solution for 10 minutes, rinsed again and placed in 70 % alcohol for a further 10 minutes.

4. The slides were then dipped into Van Giesen stain for one minute before being rapidly passed through 70 % alcohol, absolute alcohol and xylene before mounting in DPX mountant.

2.6.4.3 Computer aided quantification of collagen, elastin and smooth muscle within rings

1. The stained sections from experiment 5.2.2 were examined using a microscope and X40 objective (Leica) and random photographs taken using 400 ASA colour print film in a blind fashion (by Dr AA Hislop, Institute of Child Health, London). The ratio of the wall thickness to external diameter was measured and calculated using a calibrated eyepiece graticule.
2. The colour prints were scanned into a digital format at 360 pixels per inch using a desktop computer and scanner (Afga). Three 580 X 600 pixel samples were taken at random from across the media in a blind fashion.
3. The images were viewed using Adobe Photoshop 3.0. Using EVG stain, muscle appeared brown, collagen pink/purple and elastin black. It was possible to select areas with particular colour characteristics, and automatically determine the number of pixels within the area selected. The percentage area of each element could then be calculated.

2.6.4.4 Statistical analysis

The mean values of the percentage areas from each sample were calculated and the variation expressed as standard deviation.

2.7 SMOOTH MUSCLE CELL PHENOTYPE: CELL CULTURE STUDIES

Primary pulmonary artery SMC cultures were produced from the entire media of the intrapulmonary artery and the SMCs analysed for phenotypic differences on the basis of morphological appearance and cytoskeletal protein expression. The inner media was then cultured separately from the outer media at selected ages to investigate whether changes in cytoskeletal protein expression seen in the intact vessel were due to specific SMC phenotypes. Pure lines of these different SMC phenotypes were then obtained by dilutional cloning and their characteristics studied. A total of 21 animals were used in the cell culture studies.

2.7.1 Standard method for isolation of SMCs from pulmonary arteries

SMC for primary cultures were isolated by collagenase/elastase digestion of fresh tissue using a modified method of Ives (Ives et al., 1978). The composition of the enzyme mixture and the length of incubation time was optimised by preliminary experiments to ensure maximum yield of viable cells before formal experiments were carried out. It is therefore unlikely that a particular SMC phenotype was favoured over others due to sensitivity to the enzymes. The procedure was as follows:

1. Dissecting dish, scissors, forceps and scalpel were sterilised by immersion in 95% ethanol for at least 15 minutes.
2. Lungs were obtained from freshly killed pigs and the whole length of the main intrapulmonary conduit artery dissected from the lower lobe of left or right lung, using a binocular microscope where necessary to remove the adventitial layer. The lung was bathed in 3X antibiotic PBS solution (3 ml of 100X antibiotic-antibiotic solution in 100 ml sterile PBS) during dissection, and the excised vessel stored in fresh 3X antibiotic-antimycotic/PBS solution for a further 20 minutes at 4 °C to reduce the risk of bacterial or fungal infection.

3. The length of the intrapulmonary conduit artery was measured and only the central 50% was used for the cell culture studies. This was the region that had been examined by cryo-ultramicrotomy as described in section 3 of this chapter. Because these studies had revealed a postnatal reduction in anti-α SM actin, anti-β actin, anti-γ actin and anti-calponin antibody staining, it was thought that this part of the vessel might reveal distinctive SMC phenotypes in culture. The proximal and distal ends of the vessel, together with side-branches were discarded.
4. The remaining vessel was finely diced with a sterile scalpel blade in a fresh sterile glass petri dish and the tissue placed in 1 ml of digestion media (1 mg/ml collagenase, 0.25 mg/ml soya bean-trypsin inhibitor, 0.5 mg/ml elastase) in a rotary water bath at 37 °C for one hour.
5. 9 ml of M199/10% FCS was added to the mixture, and the cells mechanically disaggregated by gentle pipetting, before centrifugation in an IEC centra-8R centrifuge at 800 rpm for eight minutes. The supernatant, containing the digestion enzymes, was removed and the cells resuspended uniformly in 2ml fresh M199/10% FCS.
6. 100 µl of 0.4 % trypan blue solution was added to 100 µl of the resuspended cell suspension and the viable cell count determined by counting five squares of an Improved Neubauer Haemocytometer. The cells were then used in specific experiments.

2.7.2 Characterisation of intrapulmonary arterial SMC phenotypes

Primary SMC isolates were obtained and characterised with regard to their morphology viewed with phase contrast microscopy. They were then examined with endothelial and SMC specific immunofluorescent markers.

2.7.2.1 Preparation of primary cell isolates for characterisation

Primary cell isolates were plated on fibronectin-coated coverslips at sub-confluent density to allow classification of their cell morphology. The initial high FCS concentration was chosen to facilitate settling and spreading on the

fibronectin coated coverslips. This was then reduced to 1% FCS to reduce SMC replication.

The intrapulmonary elastic conduit arteries of fetal (non-breathing), 3 day old, 14 day old, adult, and 0 - 3 day old hypoxic pigs were examined. The procedure was as follows:

1. 13mm diameter round coverslips were sterilised by baking, allowed to cool and then coated by immersion in 20μg/ml fibronectin solution. Individual coverslips were placed in the wells of a 24 well cell culture plate and allowed to dry at 37°C.
2. Primary cell isolates (obtained by enzymatic digestion, **experiment 2.7.1**) were seeded onto the coverslips at a concentration of 8000 trypan blue viable cells/cm^2 coverslip in 1 ml of M199/10% FCS.
3. The plates were incubated in a cell culture incubator, humidified and maintained at 37° C with 5% CO_2 in air.
4. After 48 hours, the medium was changed to M199/1% FCS.
5. At 72 hours the coverslips were washed three times with PBS and the cells fixed in 3.7% formaldehyde for 10 minutes. The coverslips were then washed three times in PBS and used to identify the morphology of the SMCs (**experiment 2.7.2.2**) and exclude endothelial cell contamination (**experiment 7.2.3**).

2.7.2.2 Morphology under phase contrast light microscopy

Fixed cells were lightly stained with haemotoxylin to improve identification of the cells using phase contrast microscopy. The procedure was as follows:

1. Coverslips containing fixed SMCs (**experiment 2.7.2.1**) were placed in dilute filtered Harris's haemotoxylin (4 drops/10ml distilled water). After 16 hours they were washed in running tap water and then dehydrated through alcohol, cleared in xylene and mounted in DPX mountant.

2. The coverslips were examined on an inverted microscope using phase contrast optics (Nikon). The cells were categorised according to their shape and phase contrast appearances. The proportions of cells with different morphologies was then determined.

2.7.2.3 Expression of smooth muscle specific and endothelial cell specific markers

Preliminary experiments demonstrated that pulmonary endothelial cells were unable to settle and spread in the cell culture conditions used in these experiments (designed for culture of SMCs) and so their specific removal was not necessary. As a further check, to ensure there was no endothelial cell contamination, primary SMC isolates were examined for expression of the SMC markers, αSM actin, SM1 MHC isoform, and the endothelial cell markers CD31 and von Willebrand factor. The SMCs, isolated as above (**experiment 2.7.1**), were seeded onto fibronectin coated coverslips and fixed after 72 hours (**experiment 2.7.2.1**). The expression pattern of these proteins was compared to that of cultured intrapulmonary artery endothelial cells. These endothelial cells were obtained by scraping the inner surface of the intrapulmonary artery and seeding the cells onto fibronectin coated coverslips. A commercial endothelium basal medium (Sigma chemical Co.) was used instead of M199. The procedure was as follows:

1. Coverslips containing fixed SMCs (**experiment 2.7.2.1**) were treated with cold acetone (-20°C) for 20 minutes. This permeabilised the cells and precipitated the proteins inside, which enhanced later staining. They were then re-hydrated with three washes of PBS.
2. Non-specific antibody binding was prevented by application of 1% bovine serum albumin/0.1 M lysine in PBS for 15 minutes. This blocking solution was then tapped off.
3. The primary antibody (Table 5) was diluted in 1% bovine serum albumin and applied for one hour at room temperature in a humidity chamber.

Table 5. Antibodies used to exclude endothelial cell contamination and confirm SMC lineage.

Primary antibody	dilution
anti-αSM actin	1:200
anti- MHC SM1	1:200
anti-CD31	1:200
anti-von Willebrand factor	1:200

4. The unbound primary antibody was removed by three washes of PBS .
5. A secondary antibody mixture was then applied for 30 minutes at room temperature in the dark. For the anti-αSM actin and anti-MHC SM1 antibodies this mixture consisted of anti-mouse FITC (1:200), phalloidin-TRITC conjugate (1:200), and Hoechst 33258 (1:1000) diluted in blocking solution. Hoechst 33528 (2 μg/ml) and anti-mouse FITC (1:200) was used for the anti-CD-31 antibody, and Hoechst 33528 (1:1000) and anti-rabbit TRITC (1:50) with the anti-von Willebrand factor antibody.
6. The coverslips were washed 3 times with PBS before air drying in the dark and mounting with Vectormount fluorescent microscopy mounting medium.
7. Coverslips were kept in the dark at 4° C until examined the same day using a microscope with epifluorescence (Zeiss).

2.7.3 Location of different morphological SMC phenotypes within the arterial wall

Additional experiments were carried out, using other vessels, in order to determine whether the inner part of the media and the outer part of the media of the intrapulmonary conduit artery, are composed of a single or different SMC phenotypes as judged by their appearance by phase contrast microscopy. Vessels from 3 day old (two animals) and adult (one animal) pigs were used in these experiments. The procedure was as follows:

1. The central portion of the main intrapulmonary conduit artery was obtained from freshly killed pigs (**experiment 2.7.1, steps 1 - 3.**).

2. At this point the outer half of the media was mechanically stripped from the inner half using fine forceps. SMC were isolated from both the inner and outer portion, by enzymatic digestion (**experiment 2.7.1 steps 4 - 6**).
3. The morphology of the SMCs obtained was examined by phase contrast microscopy as in **experiment 2.7.2.2**.

2.7.4 The effect of different substrates on SMC phenotype

A series of commonly used cell culture substrates were used to determine if the SMC phenotypes identified in the previous experiments were dependent on the plating substrate used. Fourteen day old and adult pigs were used in these experiments. The procedure was as follows:

1. 13mm diameter round coverslips were sterilised by baking and allowed to cool. Coverslips were coated by immersion for one hour in one of the substrate solutions (Table 6) and allowed to dry in a 24 well cell culture plate at 37 °C.

Table 6. Plating substrates used when culturing SMCs from the porcine intrapulmonary conduit artery.

Plating substrate	Concentration of coating solution (in distilled water)
Fibronectin	20μg/ml
Laminin	20μg/ml
Collagen type IV	20μg/ml
Fetal calf serum	undiluted
Gelatin	10mg/ml (1% w/v)
plain glass	uncoated glass coverslip
cell culture plastic	chamber of 24 well cell culture plate

2. SMC isolates from the intrapulmonary artery of 14 day old piglets and adult pigs were obtained **(experiment 2.7.1).**
3. These isolates were plated onto the substrates indicated in table 6 at a density of 8000 cells/cm^2 and cultured for 72 hours as in **experiment 2.7.2**. The morphology of the SMCs obtained was examined by phase contrast microscopy as in **experiment 2.7.2.2**

These experiments indicated that there was no difference in morphology of the SMCs grown on the different substrates, but that settling of cells was more rapid on fibronectin. Fibronectin was used throughout the remainder of the experiments.

2.8 PRODUCTION OF SMC PHENOTYPE CLONES

A dilute suspension of SMCs was prepared from intrapulmonary arteries, and a cell culture plate seeded, such that each well would contain a single SMC. These were then allowed to divide and produce a series of SMC lines, each derived from a single cell, with a uniform phenotype (Lemire et al., 1994). Tissue from 14 day old and 0 - 3 day hypoxic piglets was used in these experiments.

The initial primary culture was performed as in previous experiments to determine the proportion of different phenotypes (**experiments 2.7.1 and 2.7.2**). The 96 well plates were then seeded with an average of one cell/well. Although this resulted in many empty wells (trypan blue counting overestimates the number of viable cells), this did mean that the majority of the remaining wells that were selected for production of clones initially contained a single SMC. An equal number of each SMC phenotype were passaged on to coverslips after approximately two weeks in the 96 well plates. When the SMCs on the remaining coverslips were almost confluent (at approximately one month from initial isolation) they were transferred to 6 well cell culture plates and allowed to spread over the area of the well. At the end of the cloning procedure 7 epSMC clones and 6 spSMC clones were passaged into 75 cm^2 flasks and cells from each taken for characterisation experiments. During the culture of these clones there was a problem with fungal contamination of the cell lines due to building work within the department and many clonal lines, including all the hypoxic spindle-shaped SMCs were infected.

The cloning procedure was as follows (Figure 14 and Figure 15):

1. A 75 cm^2 surface area cell culture flask was coated with 20 μg/ml solution of fibronectin, the excess aspirated, and the flask allowed to dry at 37 °C.
2. SMC isolates were obtained by enzymatic digestion of the intrapulmonary arteries as described previously in **experiment 2.7.1** (trypan blue counting was

not performed). These cells were resuspended in 10 ml M199/10% FCS and placed in a 75 cm^2 flask.

3. After 24 hours the flask was rinsed twice in sterile PBS and 2 ml of cold EDTA-trypsin solution gently swirled over the adherent cells. After resting for two minutes at room temperature the EDTA-trypsin solution was aspirated. The flask was then incubated at 37 °C and examined by phase contrast microscopy every 45 seconds to monitor the lifting off of cells.
4. When all cells had lifted, the EDTA-trypsin was inactivated by the addition of 10 ml of M199/10% FCS. The cells were re-suspended in 2 ml M199/10% FCS as in **experiment 2.5.1 step 5**.
5. Trypan blue counting was performed as in **experiment 2.5.1 step 6**. The SMC suspension was then diluted to 10 trypan blue viable cells/ml of M199/10% FCS.
6. The wells of a 96 well cell culture plate were coated with undiluted FCS, and allowed to dry at 37 °C. 100 µl of the cell suspension was placed in each well and the plate incubated in a cell culture incubator, humidified and maintained at 37° C with 5% CO_2 in air, for one week without disturbance.
7. The cell culture plates were then examined using an inverted microscope fitted with a X40 lens and phase contrast optics (Nikon). The microscope stage was heated to 37° C by a warm air blower. Individual wells with pure growths of a single SMC phenotype were marked. Empty wells, or wells where more than one phenotype was seen, were discarded.
8. As the wells were never confluent at this stage they were incubated for up to one more week after addition of 50 µl of fresh M199/10% FCS to the marked wells.
9. The plates were examined every 48 hours to ensure purity of phenotype and health of culture.
10. As confluence was achieved, the cells from each marked well were passaged by EDTA-trypsinisation as above (**step 3**). The cells were collected, and the enzymes inactivated, by adding 100 µl aliquots of M199/10% FCS to the well, aspirating this solution and repeating with fresh M199/10% FCS until 1 ml of cell-containing media had been collected.

11. A 24 well cell culture plate, containing fibronectin-coated 13 mm coverslips, was prepared (**experiment 2.7.2**), and each 1 ml of cell suspension placed within a single well.
12. The cells were allowed to settle and fresh M199/10% FCS added after 24 hours.
13. When the cells had reached confluence some of the coverslips were used for cell migration studies (**experiment 2.7.2**).
14. Other coverslips were used to produce larger quantities of cells for further experiments. A 6 well cell culture plate was coated with a 20μg/ml solution of fibronectin, the excess aspirated, and the plate allowed to dry at 37° C.
15. Individual confluent coverslips were then placed in these wells and covered with M199/10% FCS. The cells on the coverslip were allowed to grow out, into the area of the six well plate until confluence was achieved.
16. The cells on the coverslip and the well itself were then removed by EDTA-trypsin treatment as in **steps 3 and 4**.
17. Trypan blue counting was performed (**experiment 2.7.1**) and aliquots of the cell suspension diluted to provide cells for the studies of cell replication - serum dependence and contact inhibition, immunocytochemistry, and ability to generate tension described below.
18. The remainder of the cells were placed into a fibronectin coated 75cm^2 cell culture flask **(step 1)** and allowed to grow to confluence. The cells were then rinsed in PBS, scraped and stored at -70 °C for possible examination of cellular protein profile by two dimensional electrophoresis.

Figure 14. Flow diagram showing derivation of epSMC and spSMC phenotypes from the intrapulmonary arteries of 14 day old piglets.

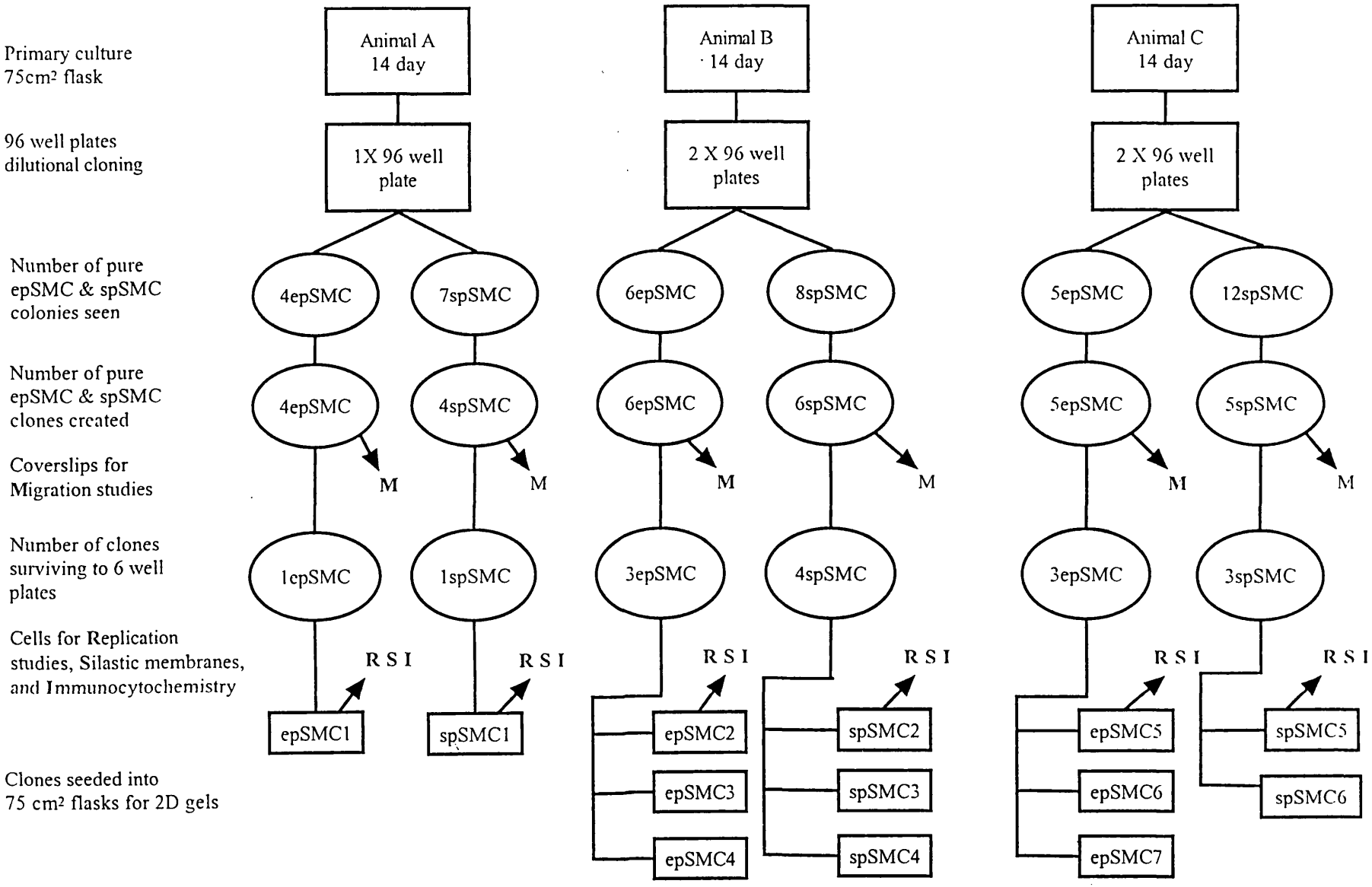
Primary culture
75cm² flask
96 well plates
dilutional cloning
Number of pure
epSMC & spSMC
colonies seen
Number of pure
epSMC & spSMC
clones created
Coverslips for
Migration studies
Number of clones
surviving to 6 well
plates
Cells for Replication
studies, Silastic membranes,
and Immunocytochemistry
Clones seeded into
75 cm² flasks for 2D gels
Animal A
14 day
1X 96 well
plate
4epSMC
7spSMC
4epSMC
4spSMC
M
M
1epSMC
1spSMC
RSI
RSI
epSMC1
spSMC1
Animal B
14 day
2 X 96 well
plates
6epSMC
8spSMC
6epSMC
6spSMC
M
M
3epSMC
4spSMC
RSI
RSI
epSMC2
epSMC3
epSMC4
spSMC2
spSMC3
spSMC4
Animal C
14 day
2 X 96 well
plates
5epSMC
12spSMC
5epSMC
5spSMC
M
M
3epSMC
3spSMC
RSI
RSI
epSMC5
epSMC6
epSMC7
spSMC5
spSMC6

Figure 15. Flow diagram showing derivation of hyepSMC and hyspSMC phenotypes from the intrapulmonary artery of a piglet exposed to hypobaric hypoxia.

Primary culture
75cm² flask

96 well plates
dilutional cloning

Number of pure
epSMC & spSMC
colonies seen

Number of pure
epSMC & spSMC
clones created

Coverslips for
Migration studies

Number of clones
surviving to 6 well
plates

Cells for Replication
studies, Silastic membranes,
and Immunocytochemistry

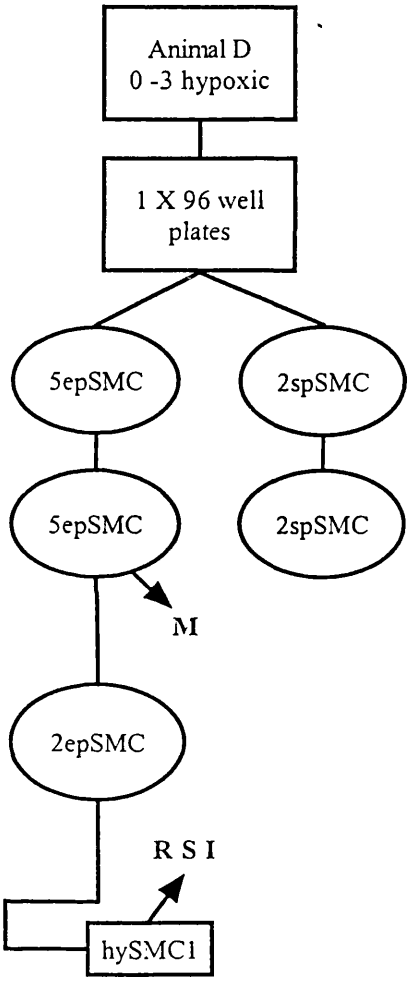

2.9 CHARACTERISATION OF SMC CLONES

The morphological SMC clones produced in **experiment 2.8,** from 14 day old and 0 - 3 day old hypoxic piglets, were characterised with regard to replication rates (serum dependence, contact inhibition), cytoskeletal protein content by immunocytochemistry, contractility by their ability to exert tension on a silicone rubber membrane and capacity to migrate across artificial wounds.

2.9.1 Cell replication - serum dependence and contact inhibition

These experiments were carried out to investigate whether phenotypically different clones of SMCs differ in their replication behaviour when in contact with neighbouring cells and when deprived of FCS in the culture medium.

5-bromo-2'-deoxy uridine (BrdU) incorporation is a non-radioactive method for measuring cell proliferation. It is cheaper and less hazardous than [^{3}H]-thymidine incorporation, but works in a similar way. In cells that are synthesising DNA, i.e. preparing to divide, BrdU added to the culture medium will be incorporated into the new DNA in place of thymidine. The BrdU incorporated into the nuclei of these cells can be visualised by immunofluorescence and the nuclei of the total population of cells can be labelled with a nuclear stain Hoechst 33258.

These experiments were carried out using a commercial BrdU labelling and detection system (Amersham). The procedure was as follows:

1. Glass coverslips were sterilised, coated with fibronectin (20 μg/ml), and placed in a 24 well cell culture plate as in **experiment 2.7.2**.
2. Cells from **experiment 2.8** were seeded at a density of 3000 trypan blue viable cells/cm^2 on each coverslip in M199/10% FCS and incubated for 48 hours under standard conditions.
3. The coverslips were examined by phase contrast microscopy to ensure that the cells were non-confluent (no cell-cell contact).

4. Coverslips containing SMCs were removed to a fresh 24-well cell culture plate. Some of the coverslips were placed in 1 ml of M199/ 1 % FCS and others placed in 1 ml of M199/ 10 % FCS.
5. After 24 hours, BrdU stock solution was added to each well to produce a 10 μM solution of BrdU in M199, and the cells were returned to the incubator for 20 minutes.
6. The media and BrdU was rinsed off by three washes of PBS.
7. The cells were fixed in 70 % acid alcohol (pH 2.0) for 20 minutes at -20°C, and then washed three times in PBS.
8. The coverslips were incubated with an anti-BrdU mouse monoclonal antibody (1:50 diluted in nuclease solution) for 30 minutes at 37 °C in a humidity chamber.
9. The coverslips were washed three times in PBS and incubated for 30 minutes at room temperature in a mixture of anti-mouse-Ig-fluorescein (1:200) and Hoechst 33258 (1:1000) diluted in PBS.
10. The coverslips were washed three times in PBS, air dried and mounted on slides using Vectamount. The coverslips were stored at 4°C in the dark until examined using a Zeiss microscope with X10 lens, epifluorescence, and a digital camera. Random fields were photographed and the number of nuclei labelled with fluorescein and Hoechst 33258 counted separately.
11. Representative coverslips containing each SMC phenotype that had not been exposed to BrdU were processed to act as negative controls for the detection process.
12. Additional coverslips coated with fibronectin were seeded with each SMC phenotype as above but allowed to grow to confluence as assessed by phase contrast microscopy. They were then exposed to BrdU for 20 minutes and processed in an identical fashion as the sub-confluent SMCs. Negative controls for the detection process were also produced.

2.9.2 Immunocytochemistry

The SMC clones were exposed to a panel of antibodies to several cytoskeletal proteins, searching for differences in protein expression. The procedure was as follows:

1. 13 mm diameter coverslips were sterilised by baking and allowed to cool. They were then coated by immersion in fibronectin (20 μg/ml solution in distilled water) or laminin (20 μg/ml solution in distilled water) for 20 minutes. The coverslips were placed into 24 well cell culture plates and allowed to dry at 37°C.
2. SMCs obtained from **experiment 2.8** were seeded on the coverslips at a density of 3000 cells/cm^2 in M199/10% FCS and incubated at 37 °C in humidified air containing 5% CO_2.
3. After 48 hours, the coverslips were washed three times with PBS and fixed for 10 minutes in 3.7% formaldehyde.
4. The coverslips were again washed three times in PBS, before permeabilising in cold acetone (-20 °C) for 20 minutes.
5. The coverslips were rehydrated with three washes of PBS.
6. Non-specific antibody binding was prevented by application of 1% bovine serum albumin/0.1 M lysine in PBS for 15 minutes. This blocking solution was then tapped off.
7. The primary antibody was diluted in blocking solution (Table 7) and was applied for one hour at room temperature using a humidity chamber.
8. The unbound primary antibody was removed by 3 washes of PBS.
9. A secondary antibody mixture was then applied for 30 minutes at room temperature in the dark. This consisted of anti-mouse FITC (1:200); phalloidin-TRITC conjugate (1:200); and Hoechst 33258 (2 μg/ml) diluted in blocking solution.
10. The coverslips were washed 3 times with PBS before air drying in the dark, and mounting with Vectormount fluorescent microscopy mounting medium.

11. Coverslips were kept in the dark at 4 °C until examination using a microscope with epifluorescence and digital camera (Zeiss).

Table 7. Antibodies used to stain the different SMC phenotypes.

Primary antibody	Working dilution
αSM actin	1:200
β actin	1:200
γ actin	1:200
SM1	1:100
Desmin	1:10
Calponin	1:200
Caldesmon	1:200
Vinculin	1:200

2.9.3 Ability to generate tension

The capacity of the different SMC phenotypes to generate tension whilst in culture was examined by growing them on inert silicone rubber membranes, as wrinkling of the silastic membrane is indicative of tension development by the cell. To facilitate attachment and spreading of cells the membranes were coated with fibronectin or laminin. The method of producing membranes and their subsequent coating with attachment substrates is a modification of the method of Harris (Harris et al., 1980). The procedure was as follows:

1. 13 mm diameter coverslips were sterilised by baking and allowed to cool.
2. A solution of 30,000 cp dimethylpolysiloxone solution was prepared by blending 54% by weight of 60,000 cp and 46% by weight of 12,500 cp dimethylpolysiloxone solutions.
3. Ensuring asepsis, a small drop of this was placed on the centre of the 13 mm coverslip. A small disposable plastic weighing boat glued to the base of a 10 cm diameter sterile petri dish was used to house the coverslip whilst it was being spun at 800 rpm for four minutes. This produced a uniform coating of silicone liquid.

4. The coating was heated for two seconds, using a Bunsen burner, to induce cross linking of the dimethylpolysiloxone and to produce a membrane.
5. After cooling, the silastic coverslip was inverted onto a 200µl drop of fibronectin solution (20µg/ml) for 20 minutes. The coverslip was then carefully placed within a 24 well cell culture plate and allowed to dry at 37 °C.
6. Cells from **experiment 2.8** were seeded onto the coverslips at a concentration of 3000 cells/cm^2 in 2 ml of M199/10% FCS and allowed to settle for 72 hours.

2.9.3.1 Effect of potassium chloride and sodium nitroprusside on SMC induced wrinkling of silastic membranes

Unstimulated SMCs wrinkle the underlying silastic membrane. The maximal contractile ability of the SMCs was determined by observing the appearance of additional wrinkles after the addition of potassium chloride. Conversely, the ability of the SMCs to relax in response to nitric oxide was established by the disappearance of wrinkles after addition of sodium nitroprusside. The procedure was as follows:

1. Coverslips from **experiment 2.7.3** were photographed to demonstrate SMCs and wrinkling of the silastic membrane at rest using phase contrast microscopy. Photographs were taken using a Nikon F3 camera body, 400ASA colour print film and automatic exposure mode.
2. A stock solution of potassium chloride 5M (final concentration in medium - 125mM), or sodium nitroprusside 10^{-3} M (final concentration in medium 10^{-5} mM) was added to the medium bathing each coverslip.
3. After five minutes at 37 °C a further photograph was taken to identify any change in the wrinkling pattern.
4. For each SMC phenotype, the experiment was carried out on three coverslips using potassium chloride and on three different coverslips using sodium nitroprusside

2.9.4 Cell migration

The motility of clones of SMC phenotypes was assessed by wounding a confluent layer of cells on a coverslip and monitoring the rate at which the cells moved into the breach using time lapse photography. The procedure was as follows:

1. Confluent coverslips (**experiment 2.8**) were attached to the base of a 5 cm diameter sterile plastic petri dish using silicon grease and covered with M199 HEPES/ 10% FCS.
2. A linear wound was produced on the coverslip with a 21 gauge needle, whilst observing with phase contrast microscopy.
3. The medium was changed for fresh M199 HEPES/10% FCS and the petri dish lid sealed with parafilm.
4. The wound was observed through a X 20 objective lens, under phase contrast optics (Nikon). The microscope was fitted with a perspex cover to allow maintenance of ambient temperature at 37 °C by use of an integral blower/thermostat system.
5. Photographs were taken every two hours for at least 14 hours, using a Nikon F3 camera body with automatic exposure, a timer system and powered film drive (Fuji 400 ASA colour print film).

2.9.5 Statistical analysis

Where necessary, results were expressed as mean percentages and the variation expressed as standard error of a percentage (SE%).

2.10 GENERAL REAGENTS AND ANTIBODIES

All reagents, except where indicated below, were obtained from Sigma Chemicals Co., UK. The cell culture equipment and media used were obtained from Gibco BRL, UK. Vectamount fluorescent mounting medium and Vectabond slide coating were bought from Vector Laboratories, UK. OCT embedding compound was obtained from Bright Ltd, UK. The monomeric actin assay kit was initially obtained as a kit from Molecular Probes (Europe). The components were then bought individually from Sigma Chemical Co and Molecular Probes Ltd. Hoechst 33258 was also purchased from Molecular Probes (Europe) Ltd. The BCA protein assay was obtained from Pierce Chemical Co., USA. The BrdU labelling and detection kit and complete protease inhibitor tablets were purchased from Amersham, UK.

All antibodies were obtained from Sigma Chemical Co., except: anti-MHC SM1antibody, a kind gift from Dr H Katoh, Japan; anti-γ actin antibody, a generous gift from Professor Lessard, USA; anti-desmin antibody, Zymed Ltd; anti-von Willebrand factor antibody, Dako Ltd; and anti-CD31, Serotec Ltd).

Chapter 3. Results: Cytoskeletal SMC phenotypes within the intact intrapulmonary artery

INTRODUCTION

The cytoskeletal composition of individual SMCs within the arterial media, was examined to investigate: firstly what happened to the SMC cytoskeleton following birth; secondly whether one or a multitude of different phenotypes could be identified within the intact vessel wall; thirdly whether the phenotype(s) changed during development; and fourthly whether exposure to hypobaric hypoxia altered the phenotype(s). The antibodies used were directed against those cytoskeletal proteins known to be present in SMCs. These were: α-smooth muscle actin, β-actin, γ-actin, myosin heavy chain isoform SM1, desmin, calponin, and caldesmon.

3.2 GENERAL CONSIDERATIONS

Intrapulmonary elastic conduit arteries from near term fetal piglets (non-breathing), 3 day old piglets, 14 day old piglets and adult animals were examined in these experiments. The ages were chosen to reflect the main stages of adaptation to extra-uterine life: immediate postnatal adaptation (fetal and 3 days); continued remodelling and stabilisation (3 days and 14 days); and growth to adulthood (14 days and adult). Tissue from three animals was examined at each age.

Digital photographs of SMCs were taken of three representative areas of the vessel wall: the inner-medial region, lying beneath the endothelial cells and the internal elastic lamina; the mid-medial region, at the centre of the vessel wall; and the outer-medial region, adjacent to the adventitia (Figure 16). These three regions were chosen as a previous electron microscopic investigation had demonstrated postnatal changes in the myofilament concentration localised to different areas of the media (Hall and Haworth, 1987). The SMCs of the media had shown a transient reduction in myofilament volume density at three days of age in comparison to newborn and 14 day old animals. The outer layer of SMCs had also been noted to contain a greater concentration of myofilaments than the rest of the media, at all ages. This suggested that these were the areas in which different SMC phenotypes might be found. Immunolabelled ultra-thin sections (250 nm) of the vessel wall were studied. The advantages of using this approach and the methodology itself are detailed in **Chapter 2 Materials and Methods** and examples are shown in figures Figure 17 to Figure 23.

The quality and appearance of the sections cut from different blocks at different times was remarkably uniform. In the sections from fetal animals to those from animals aged 14 days, the SMCs of the inner and mid-media were arranged in concentric rings of cells with a circumferential orientation. Some of the outer cells appeared to have a more longitudinal orientation. In sections from the adult, the appearance was of small groups of closely related obliquely lying cells, which along with other groups of similar cells, formed an overall circumferential pattern. The outer layer of cells in the adult, like those in the younger animals, also formed clumps of cells which appeared to be arranged in a more longitudinal direction.

The elastic laminae were not usually seen on these thin sections. The nuclei, stained with Hoechst 33258, within the vessels from fetal (non-breathing), 3 day, 14 day, and 0-3 day hypoxic piglets showed no difference in their appearance or size. The nuclei within the adult vessels appeared to be bigger, which raised the possibility that these cells were polyploid, although it is more likely the larger adult cells simply had larger nuclei.

The use of an anti-laminin antibody was an important part of the protocol as it allowed identification of the basal lamina and hence delineated the cytoplasmic margins of the SMCs. Within sections of the same block of tissue, the basal lamina did not always appear to be complete around each cell, but at least part of this variation was artefactual as experience when cutting sections from the same block showed that much of the variation in the laminin staining and in the amount of space between the SMCs was due to spreading of the sections when they were picked up on the sucrose/gelatin droplets. This problem was common to sections obtained from animals of all ages. As with many histological preparations of the blood vessel wall, the delicate endothelial layer was present in some blocks but absent in others. The internal elastic lamina was not seen in many of these tissue sections as it generally remained on the block. Where it was part of a tissue section, anti-laminin antibodies produced a dense band of stain below the endothelial cells probably reflecting laminin on the internal elastic lamina although there might have been electrostatic attraction of the antibodies to the elastin (for example, Figure 17 α smooth muscle actin, 3 day old).

Figure 16. Low power view of segments of intrapulmonary conduit artery from adult pig showing the areas designated as inner, mid, and outer media. The 7 μm thick sections were cut after wax embedding and were haemotoxylin and eosin. (Bar corresponds to 50 μM).

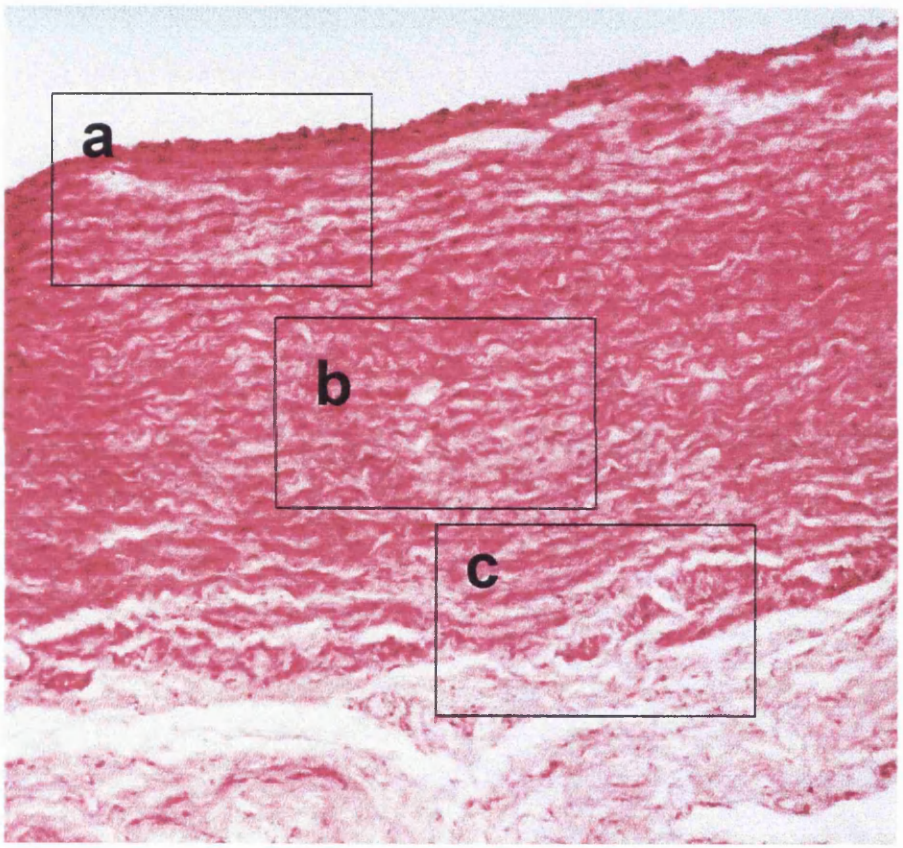

3.3 EXPRESSION OF ALPHA SMOOTH MUSCLE ACTIN DURING ADAPTATION TO EXTRA-UTERINE LIFE

Alpha smooth muscle actin is the actin isoform responsible for the contractile response characteristic of SMCs. Some of the most striking changes in SMC protein expression were seen with this antibody.

Table 8. Semi-quantitative scoring of the α smooth muscle actin expression pattern during postnatal adaptation within the porcine intrapulmonary elastic conduit artery.

	Fetus	0 - 3 hypoxia	3 days	14 days	Adult
Inner-media	++	++	+	+++	+++
Mid-media	++	++	+	+++	+++
Outer-media	+++	+++	+++	+++	+++

The cryo-ultramicrotomy sections were used to reveal the actin content within individual SMCs of the vessel wall, but, as expected, were unable to resolve discrete filament bundles within the cytoplasmic stained area. All the cells contained in the media of the vessels, at all ages, labelled with the anti-α smooth muscle actin antibody (Table 8 and Figure 17). At all ages, the outer SMCs of the media had more labelling of their cytoplasmic compartment than those in the middle or inner media. This effect was more obvious in the sections from fetal, 3 day old and hypoxic piglets and progressively less obvious in the 14 day old piglets and adult animals. In the fetal sections (tissue from non-breathing animals), all the cells of the inner, middle and outer layers had a uniform dense staining for α smooth muscle actin. In contrast, in vessels from the normal 3 day old piglets, the cells of the inner-medial and mid-medial areas contained only flecks of α smooth muscle actin staining found throughout the cytoplasm, whereas the cytoplasm of the outer-medial SMCs continued to label with this antibody. Although not measured, the inner and mid-medial SMCs of the 14 day old piglets appeared larger and to contain much more actin than at 3 days. In many of these cells the whole cytoplasmic compartment was stained with antibody. The adult SMCs were much larger than the SMCs seen at any other age, and the entire cytoplasmic area

delineated by laminin immunostaining was filled with a dense staining for actin. Finally, the hypoxic animals showed dense staining of all SMCs, across the whole media, similar to the appearance in vessels from the fetus and the 14 day old animals but very different to the appearance of vessels from the normal 3 day old piglets (age matched controls) in that the hypoxic animals failed to show a reduction in α actin staining within the inner and mid medial SMCs.

Thus, α smooth muscle actin expression generally increased with age but was punctuated by a transient, large reduction in antibody labelling at 3 days of age, involving the SMCs of the inner half of the media. In animals exposed to hypobaric hypoxia from birth there was persistent immunolabelling across the entire media with anti-α smooth muscle actin antibody with no evidence of the reduction seen at three days in the normal animals.

Figure 17. Anti α-smooth muscle actin immunolabelling in the intrapulmonary conduit artery during development. Actin is labelled green, the basal lamina red and the nuclei blue. The pattern of α-smooth muscle actin expression generally increased with age but was punctuated by a transient, large reduction in antibody labelling, involving the SMCs of the inner and middle part of the media, at 3 days of age (see arrows). This reduction was not seen in animals exposed to hypobaric hypoxia for 3 days following birth. Internal elastic lamina and endothelial cell nuclei (*). Magnification bar = 5 μm

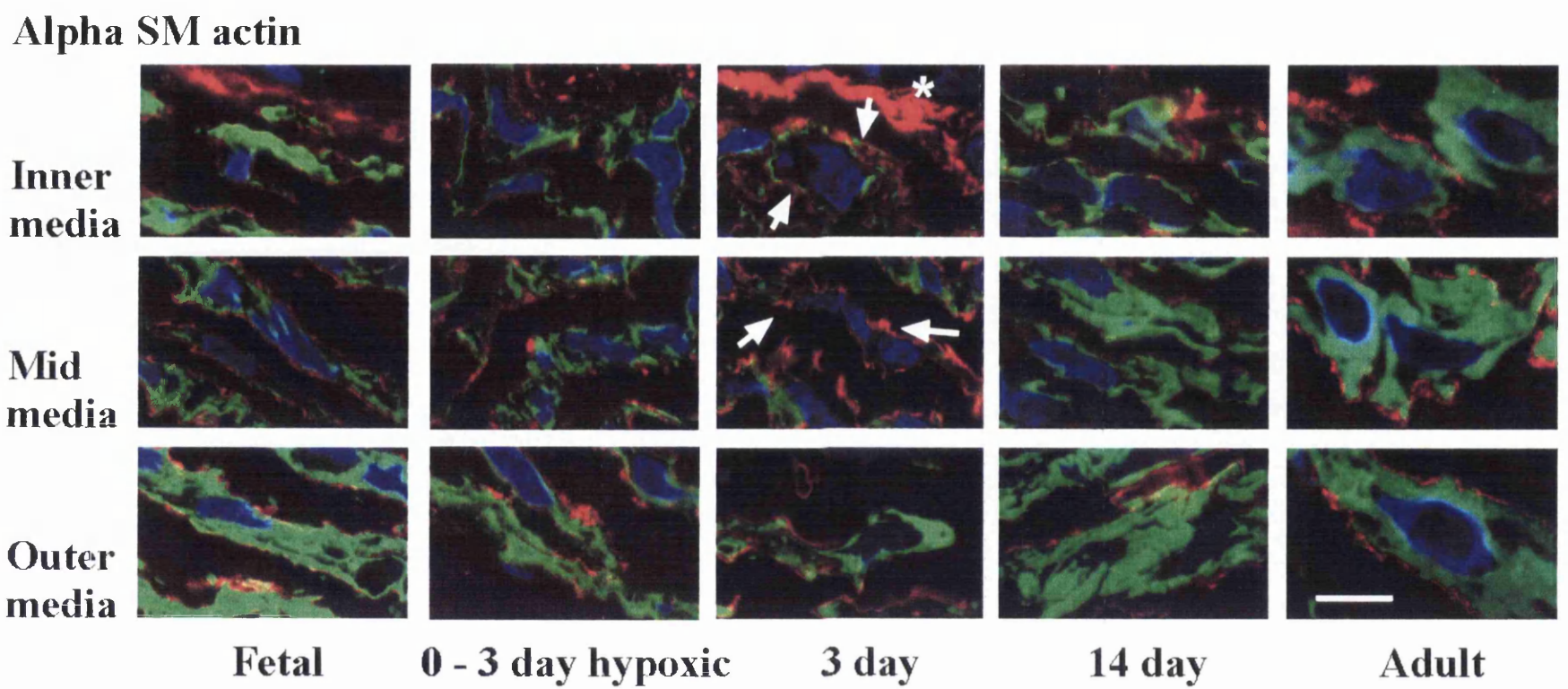
Alpha SM actin
Inner media
Mid media
Outer media
Fetal
0 - 3 day hypoxic
3 day
14 day
Adult

3.4 EXPRESSION OF BETA ACTIN DURING POSTNATAL ADAPTATION

Beta actin is found in all cells and functions as a structural cytoskeletal protein (Alberts et al. 1999). Studies were carried out to see if there was any change in the level of β actin expression associated with the transient reduction in anti-α smooth muscle actin antibody staining noted above.

Table 9. Semi-quantitative scoring of the β actin expression pattern during postnatal adaptation within the porcine intrapulmonary elastic conduit artery.

	Fetus	0 - 3 hypoxia	3 days	14 days	Adult
Inner-media	++	++	+/-	++	+++
Mid-media	++	++	+	++	+++
Outer-media	++	++	+	++	+++

As would be expected, all cells of the media and the endothelial cell layer showed some staining with anti-β actin antibody. At all ages, the staining pattern with the anti-β actin antibody was similar to that of the anti-α smooth muscle actin antibody - although the density of cytoplasmic staining was generally lower at all ages throughout all parts of the media, and produced a speckled rather than solid staining pattern (Table 9 and Figure 18). The sections from the fetal piglets demonstrated a uniform staining pattern throughout the inner, mid and outer media. Compared to the fetus, there was a reduction in the amount of staining in the inner and mid-medial SMCs of the normal vessels at 3 days of age. However, in contrast to the anti-α smooth muscle actin antibody staining, this was also noted to occur in the outer medial layer. Antibody labelling was seen across the entire media at 14 days and the amount of cytoplasmic labelling increased further in sections from the adult. As with the anti-α smooth muscle actin antibody, the anti-β actin antibody labelling in the sections from the hypoxic animals were similar to those from the fetus and 14 day old piglets, and did not show the reduction in staining seen in the normal animals at three days, with immunolabelling across the whole media.

Thus, the pattern of anti-β actin antibody staining was similar to the pattern seen with anti-α smooth muscle actin antibody and similarly revealed a transient reduction in antibody staining within the inner and mid media at 3 days of age in normal vessels and retention of immunostaining in animals exposed to hypoxia from birth.

Figure 18. Anti-β actin immunolabelling within the intrapulmonary conduit artery during development. Actin is labelled green, the basal lamina red and the nuclei blue. The pattern of β actin expression generally increased with age, but was punctuated by a transient, large reduction in antibody labelling, involving the SMCs of the inner and middle regions of the media, at 3 days of age (see arrows). This reduction was not seen in animals exposed to hypobaric hypoxia for 3 days following birth. The single cell in the outer-medial panel at 3 days of age, which stained strongly for β actin but had no laminin staining to suggest a basal lamina, may be a fibroblast (arrowhead). The internal elastic lamina and endothelial cells showing anti-β actin antibody labelling are indicated (*). Magnification bar = 5 μm.

Beta actin

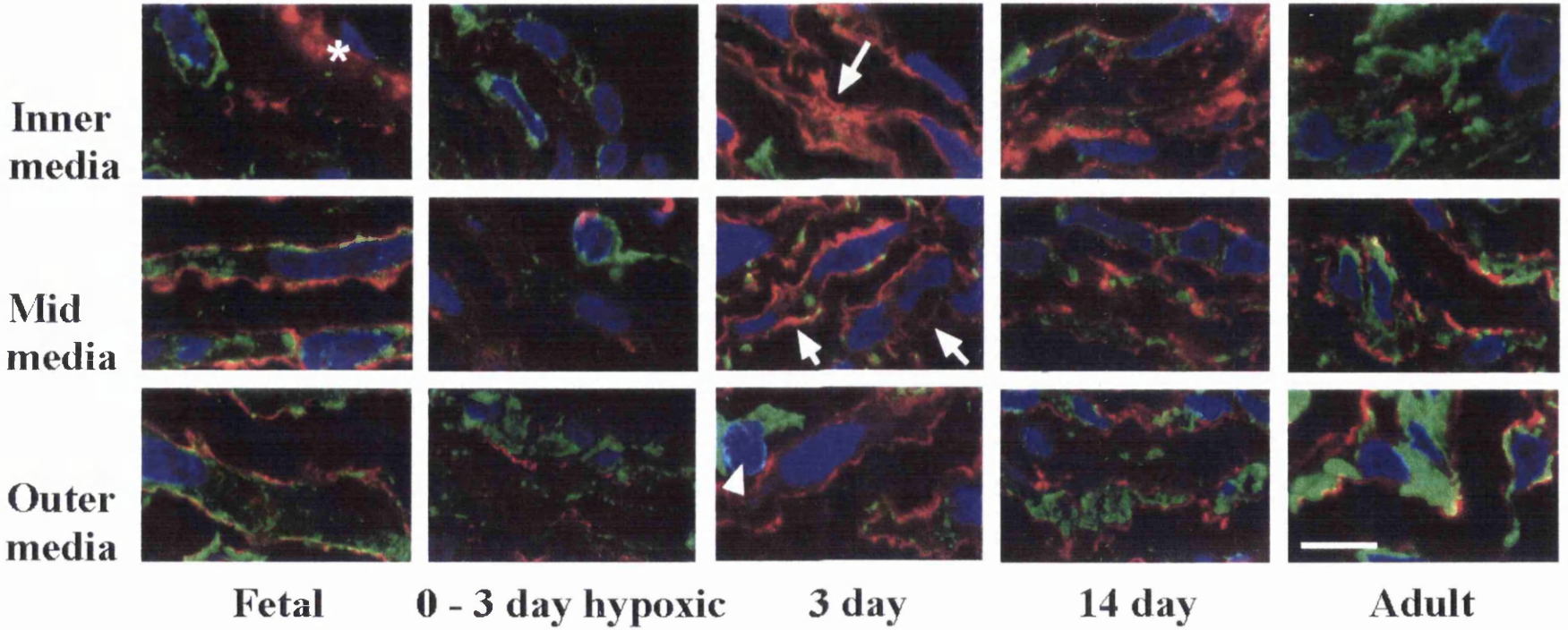
Inner media
Mid media
Outer media
Fetal
0 - 3 day hypoxic
3 day
14 day
Adult

3.5 EXPRESSION OF GAMMA ACTIN DURING POSTNATAL ADAPTATION

The smooth muscle specific γ actin isoform was investigated as it is considered to be a reliable marker of vascular SMCs, being present in SMCs from early stages of development (Owens, 1995).

Table 10. Semi-quantitative scoring of the γ actin expression pattern during postnatal adaptation within the porcine intrapulmonary elastic conduit artery.

	Fetus	0 - 3 hypoxia	3 days	14 days	Adult
Inner-media	+	++	++	++	+++
Mid-media	+++	++	++	+++	+++
Outer-media	+++	+++	+++	+++	+++

As with anti-α smooth muscle and β actin antibodies, the SMCs of the media contained some anti-γ actin staining and the outer SMCs of the vessel wall had more antibody staining than the inner and mid-medial cells at all ages (Table 10 and Figure 19). The pattern of cytoplasmic staining was uniform, like that of anti-α smooth muscle actin antibody, and not speckled like the anti-β actin antibody. The labelling was found generally throughout the cytoplasm of the cell. However, although the outer and mid-medial SMCs of the fetal sections stained well with anti-γ actin antibody, the inner-medial cells did not. This was very different from the pattern seen with anti-α smooth muscle and anti-β actin antibodies. In the normal vessels at 3 days, the inner medial cells had a greater degree of cytoplasmic γ actin immunostaining than on the fetal sections, but the mid-medial cells at 3 days stained less strongly in comparison with the mid-medial cells of the fetus. The anti-γ actin staining density of the outer medial cells was similar to that of the outer medial SMCs in the fetus and at 14 days. In the 14 day old piglets there was increased staining with anti-γ actin antibody in all regions of the media and this was more evident in the adult sections. It was interesting to note that in contrast to the anti-α smooth muscle and anti-β actin antibodies, the anti-γ actin antibody labelling of sections from the hypoxic animals was very similar to that seen in the sections

from normal 3 day old piglets, showing a similar reduction in mid-medial staining and an increase in inner medial staining following exposure to hypoxia.

Figure 19. γ actin immunolabelling in the intrapulmonary conduit artery during development. Actin is labelled green, the basal lamina red and the nuclei blue. The pattern of γ actin expression showed a transient reduction in the mid media and an increase in staining pattern in the inner media at 3 days of age, in both normal and hypoxic animals. Magnification bar = 5 μm.

Gamma actin

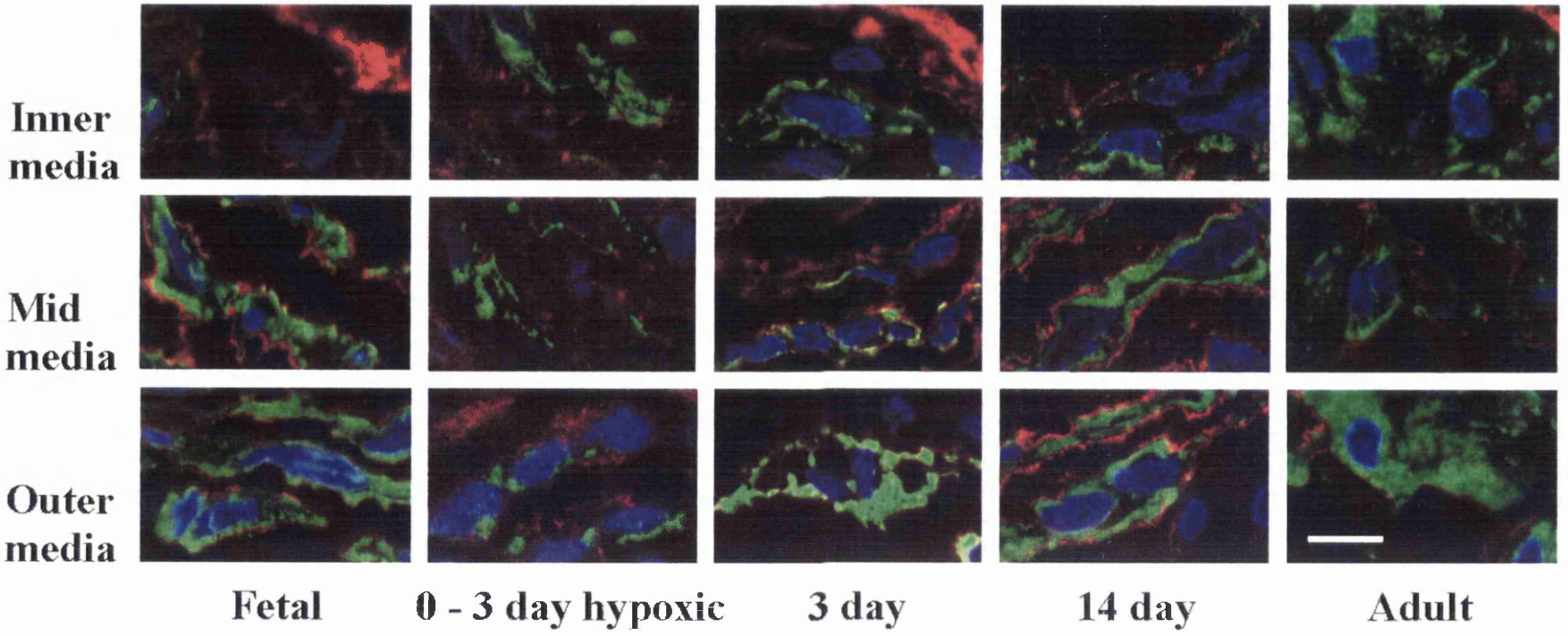
Inner media
Mid media
Outer media
Fetal
0 - 3 day hypoxic
3 day
14 day
Adult

3.6 EXPRESSION OF MYOSIN HEAVY CHAIN ISOFORM SM1 DURING POSTNATAL ADAPTATION

Smooth muscle-specific myosins interact with α smooth muscle actin to produce contraction of the SMC. SM1, the 204 kDa MHC isoform, is characteristic of SMCs (Kuro-o et al., 1989).

Table 11. Semi-quantitative scoring of the MHC isoform SM1 expression pattern during postnatal adaptation in the porcine intrapulmonary elastic conduit artery.

	Fetus	0 - 3 hypoxia	3 days	14 days	Adult
Inner-media	++	++	++	++	+++
Mid-media	++	++	++	++	+++
Outer-media	++	++	++	++	+++

The SMCs within the media at all ages stained with the SM1 antibody which producing a speckled pattern of immunolabelling similar to that noted with the anti-β actin antibody (Table 11 and Figure 20). In contrast to the anti-α smooth muscle, β and γ actin antibodies, the inner, mid and outer media contained the same degree of cytoplasmic staining. This did not change between fetal life, 3 days and 14 days, but the cytoplasmic labelling was uniformly denser throughout the adult media. It is important to note that there was no transient reduction in staining within the media at 3 days of age. The SM1 staining pattern in animals exposed to hypoxia from birth was identical to that of the fetal, 3 day old and 14 day old animals.

Figure 20. SM1 myosin heavy chain immunolabelling in the intrapulmonary conduit artery during development. Myosin is labelled green, the basal lamina red and the nuclei blue. The pattern of SM1 expression remained constant though postnatal development and was unaffected by hypoxia. Magnification bar = 5 μm.

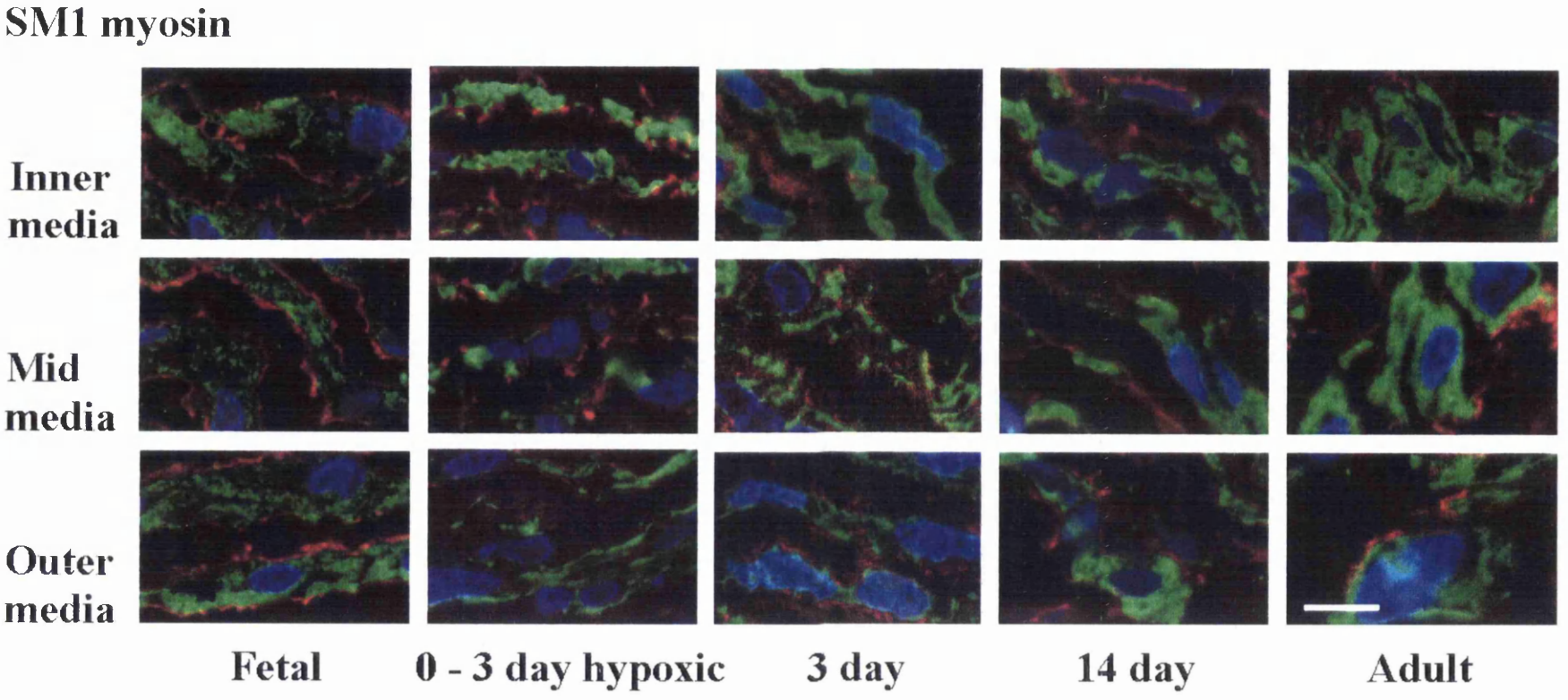
SM1 myosin
Inner media
Mid media
Outer media
Fetal
0 - 3 day hypoxic
3 day
14 day
Adult

3.7 EXPRESSION OF DESMIN DURING POSTNATAL ADAPTATION

Desmin is an intermediate filament protein that is found at high levels in tissues subjected to large repeated stresses. It is accepted as a marker of well differentiated mature SMCs (Duband et al., 1993)

Table 12. Semi-quantitative scoring of the desmin expression pattern during postnatal adaptation in the porcine intrapulmonary elastic conduit artery.

	Fetus	0 - 3 hypoxia	3 days	14 days	Adult
Inner-media	-	++	-	-	++
Mid-media	-	++	-	-	++
Outer-media	+	+++	++	++	+++

Anti-desmin antibody staining was completely absent from the inner and mid-medial regions of the vessel wall of the normal fetus (Table 12 and Figure 21). Only a few cells in the outer media of the fetus labelled with this antibody. The sections taken from 3, and 14 day old piglets showed exactly the same pattern, with labelling confined to a few scattered cells in the outer part of the media. However, the adult vessel contained many positively-stained SMCs scattered across all regions of the vessel wall. Interestingly, the hypoxic vessel revealed a staining pattern that closely resembled the adult, rather than the fetus or 3 day old piglet, with staining of scattered SMCs throughout the media.

Figure 21. Desmin immunolabelling in the intrapulmonary conduit artery during development. Desmin is labelled green, the basal lamina red and the nuclei blue. Desmin staining was confined to a few cells in the outer part of the media in all ages except in the adult animal and in the piglets exposed to hypobaric hypoxia in which cells throughout the entire media were labelled. Magnification bar = 5 μm.

Desmin

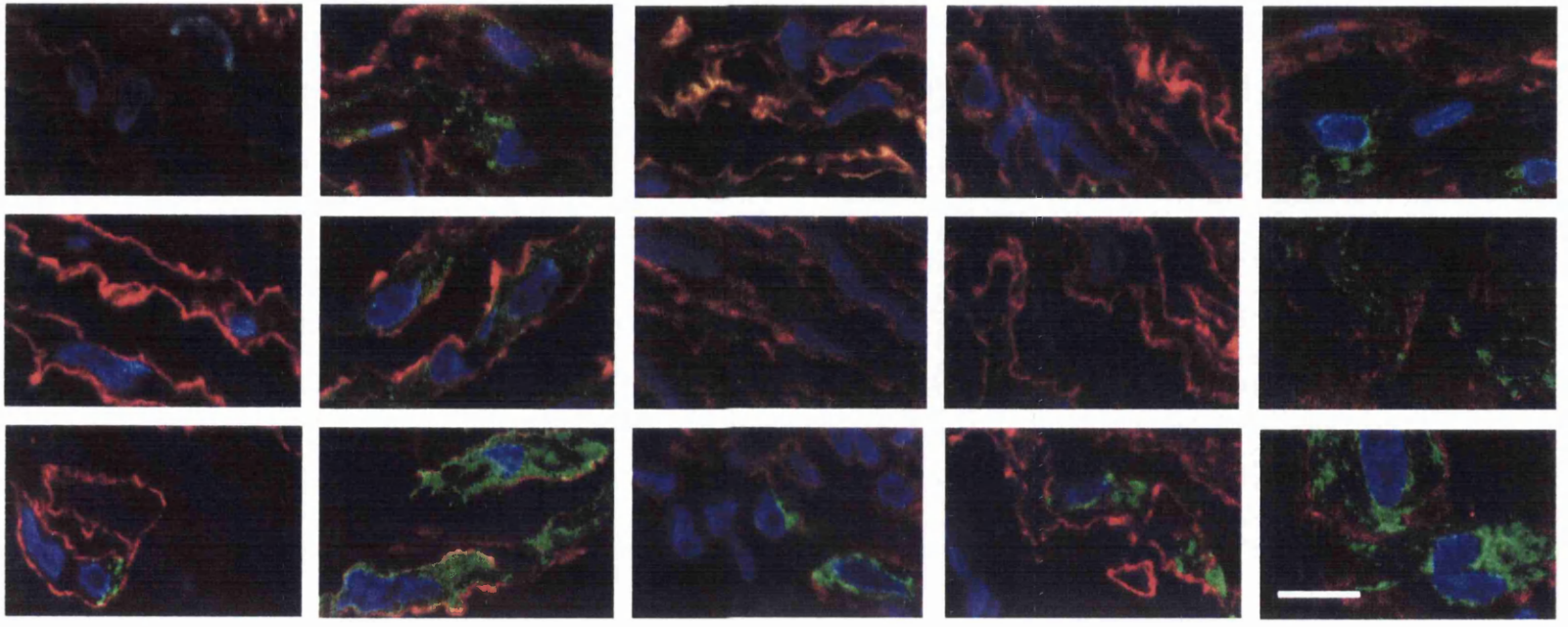
Inner media
Mid media
Outer media
Fetal
0 - 3 day hypoxic
3 day
14 day
Adult

3.8 EXPRESSION OF CALPONIN DURING POSTNATAL ADAPTATION

Calponin is an actin filament-based regulator of the actin-myosin interaction, and is expressed in mature SMCs (Gimona et al., 1990). It inhibits Mg^{2+} dependent actomyosin ATPase activity which underpins contraction.

Table 13. Semi-quantitative scoring of the calponin expression pattern during postnatal adaptation in the porcine intrapulmonary elastic conduit artery.

	Fetus	0 - 3 hypoxia	3 days	14 days	Adult
Inner-media	++	++	-	++	++
Mid-media	+++	++	++	++	++
Outer-media	+++	++	++	++	+++

At all ages, the SMCs of the outer media labelled strongly with anti-calponin antibody (Table 13 and Figure 22). The sections from the fetus showed abundant labelling throughout all areas of the media which had a speckled appearance. At 3 days of age, the cells of the inner media and some adjacent cells in the mid media demonstrated no labelling or weak labelling which was confined to the periphery of the cell. The entire media labelled well at 14 days of age and also in the adult. The sections from hypoxic animals showed staining within all regions of the media. The density of staining was similar to sections from the 14 day old piglets.

Thus, the changes in the staining pattern with the anti-calponin antibody were similar to those seen with anti-α smooth muscle and anti-β actin antibodies, in tissue from both the normal and hypoxic animals.

Figure 22. Calponin immunolabelling in the intrapulmonary conduit artery during development. Calponin is labelled green, the basal lamina red and the nuclei blue. The pattern of calponin expression generally increased with age, but was punctuated by a transient, large reduction in antibody labelling, involving the SMCs of the inner two thirds of the media, at 3 days of age (see arrows). This reduction was not seen in animals exposed to hypobaric hypoxia for 3 days following birth. Magnification bar = 5 μm.

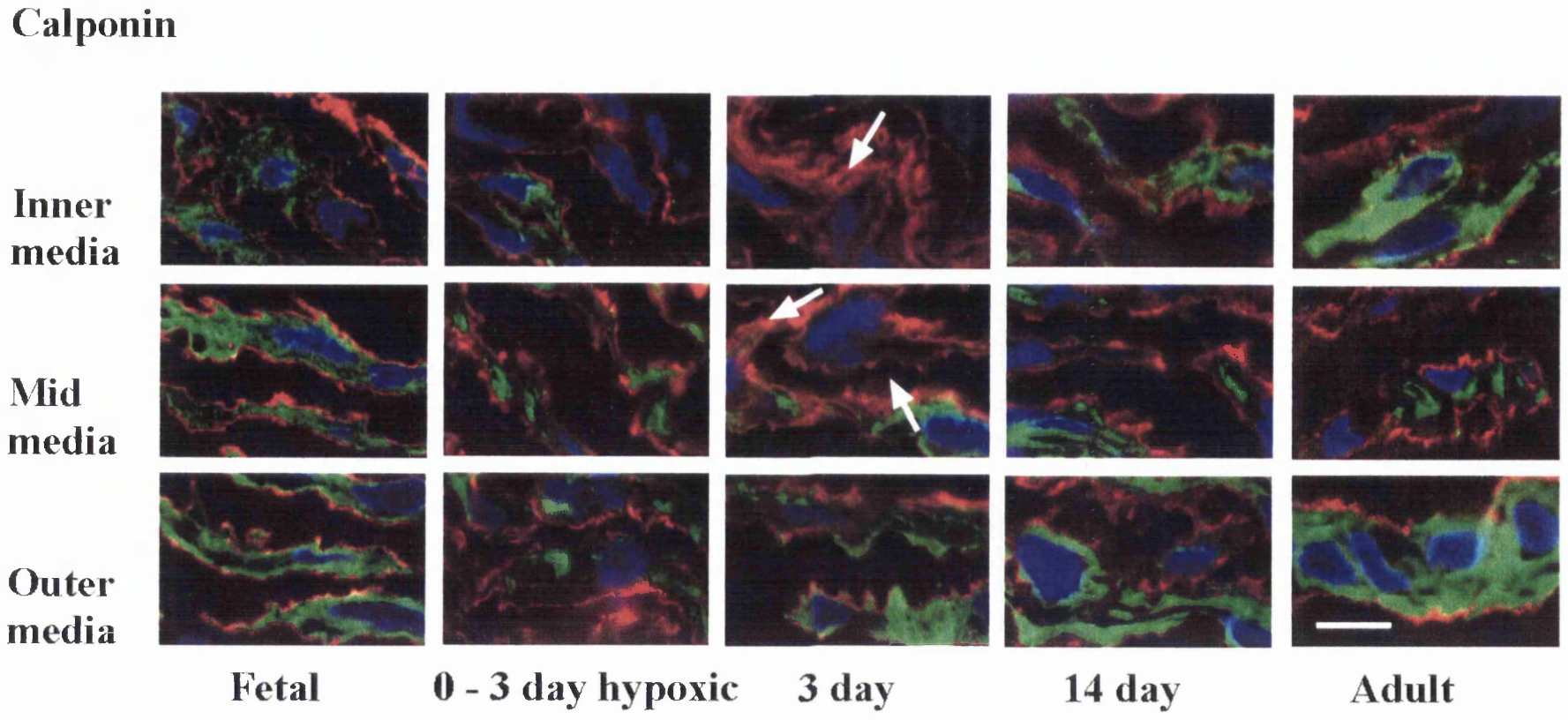
Calponin
Inner media
Mid media
Outer media
Fetal
0 - 3 day hypoxic
3 day
14 day
Adult

3.9 EXPRESSION OF CALDESMON DURING POSTNATAL ADAPTATION

Caldesmon is associated with myosin in mature SMCs and, like calponin, helps to regulate the force of contraction (Owens, 1995).

Table 14. Semi-quantitative scoring of the caldesmon expression pattern during postnatal adaptation in the porcine intrapulmonary elastic conduit artery.

	Fetus	0 - 3 hypoxia	3 days	14 days	Adult
Inner-media	-	-	-	-	++
Mid-media	-	-	-	++	++
Outer-media	+++	+++	+++	+++	+++

The pattern of anti-caldesmon antibody staining was limited to the outer part of the media in vessels from the fetal, normal 3 day old, and hypoxic animals. At 14 days some cells in the outer and mid-media labelled were labelled, and positively stained SMCs were identified in both inner and mid-media in the adult using this antibody (Table 14 and Figure 23).

In the sections from fetal animals the antibody was entirely confined to the SMCs of the outer media where the speckled staining pattern filled the entire cytoplasmic compartment of the cell. The appearances were unchanged at 3 days of age, but at 14 days the sections indicated that cells of the mid-media had strong labelling throughout the cytoplasm. Some scattered cells throughout all areas of the adult media labelled with the anti-caldesmon antibody. The antibody appeared to label the areas of cytoplasm close to the nucleus in the adult sections. The staining pattern seen with sections from the hypoxic animals was similar to that seen in sections from fetal and 3 day old normal animals.

It is interesting to note that the staining pattern of anti-caldesmon, was similar to anti-desmin in that it predominantly labelled the cells of the outer media, but different from anti-desmin antibody in that anti-caldesmon failed to label the cells of the inner and mid-media in sections from the hypoxic animals.

Figure 23. Caldesmon immunolabelling in the intrapulmonary conduit artery during development. Caldesmon is labelled green, the basal lamina red and the nuclei blue. Expression was confined to the outer part of the media prior to 14 days of age, and in the animals exposed to hypobaric hypoxia. The expression progressively spread throughout the whole media in the 14 day and adult animals. Expression appeared to localise to the peri-nuclear areas within the adult sections. Magnification bar = 5 μm.

Caldesmon

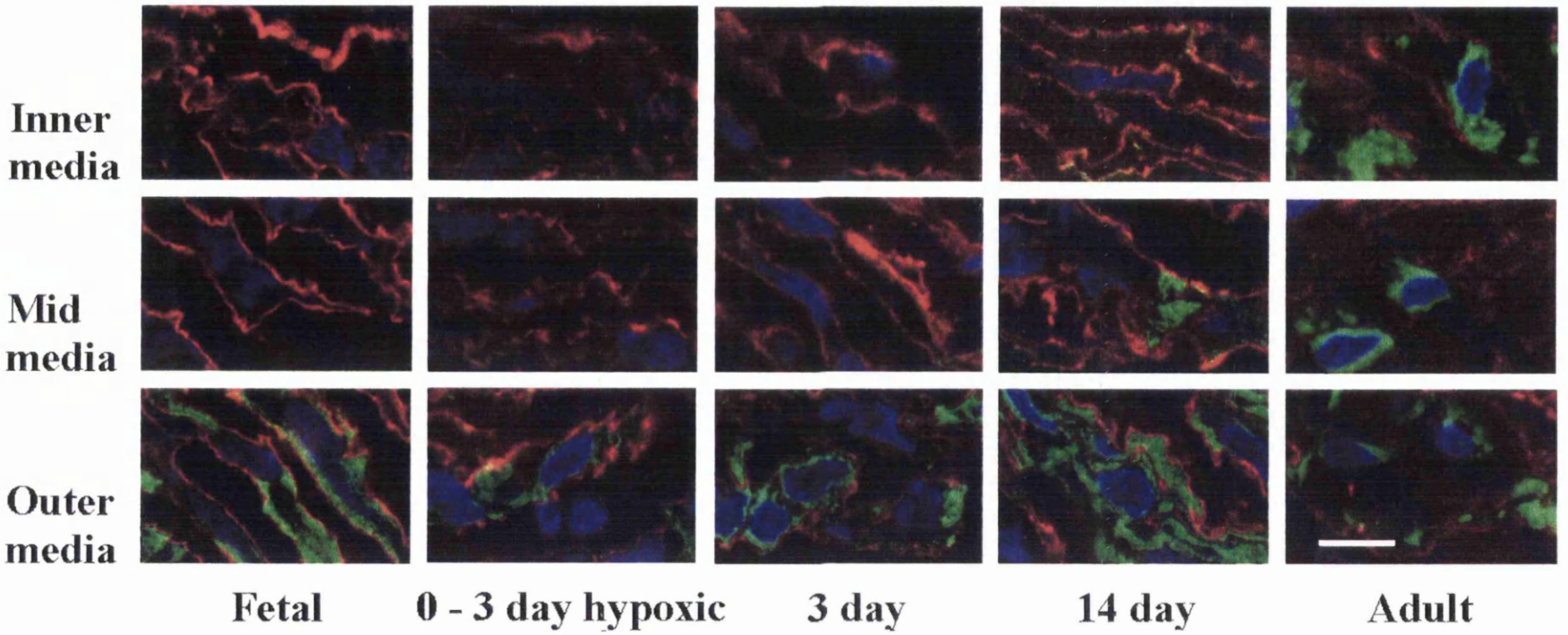
Inner media
Mid media
Outer media
Fetal
0 - 3 day hypoxic
3 day
14 day
Adult

3.10 SUMMARY

The developmental progression of the intrapulmonary arteries from the fetal state to adulthood encompasses adaptation to the extrauterine environment. These immunolabelled cryo-ultramicrotomy sections demonstrated a series of different SMC cytoskeletal protein expression patterns during this process.

Although different age related patterns of SMC cytoskeleton immunostaining were seen in the vessels, SM1 MHC isoform was expressed in all SMCs, throughout the entire media, and at all ages. This unequivocally demonstrated that all the cells within the media were SMCs. In addition to this protein, the basic cytoskeletal profile of the SMCs within the intrapulmonary artery consisted of α, β, and γ actins and calponin. Some cells in the sections contained caldesmon and others desmin. Unfortunately the desmin and caldesmon antibodies did not allow dual immunolabelling to establish whether caldesmon and desmin co-localised to the same cells.

Table 15. SMC phenotypes found in the porcine intrapulmonary artery during normal development and after exposure to hypobaric hypoxia from birth to 3 days of age. B-phenotype SMCs express α, β and γ actins and SM1, C-phenotype cells also express caldesmon, D-phenotype cells also express desmin and CD-phenotype cells may express both. Modulation of B-phenotype cells is indicated in brackets.

	Fetus	0 - 3 d hypoxia	3 dc	14 dc	Adult
Inner	B	B D	B (↓α,β,calp)	B	B /D/CD
Middle	B	B D	B (↓α,β, γ, calp)	B	B /D/CD
Outer	B /D/CD	B /D/CD	B /D/CD	B /D/CD	B /D/CD

Thus, examining the tissue sections from normal and hypoxic animals it was possible to identify at least four different SMC phenotypes and evidence of phenotypic modulation:

SMCs of the inner and middle regions of media in the fetus contained α, β and γ actins, SM1 and calponin. However, SMCs in these areas did not express either caldesmon or desmin. This pattern of cytoskeletal protein expression is represented as the basic (B) intrapulmonary arterial SMC phenotype (Table 15).

At 3 days of age the B-phenotype SMCs (expressing α, β and γ actins, calponin and SM1, but not desmin or caldesmon) within the inner media showed a marked reduction in the immunostaining of α and β actin and calponin. Although the staining pattern of γ-actin was preserved in the inner media it was reduced along with α and β actin and calponin in the middle part of the media. Whilst these changes occurred, the composition and degree of staining of the cells in the outer-media remained unchanged. These findings suggest modulation of the B-phenotype SMCs occurring within the inner and mid-media of normal animals occurring between birth and 3 days of age.

The outer part of the media at all ages, and the entire media in the adult contained cells that, in addition to α, β and γ isoactins, SM1 and calponin, stained with desmin and/or caldesmon antibodies. Depending on whether or not desmin and caldesmon co-localise within individual SMCs, this may represent up to four types of cell. These are caldesmon positive (C), desmin positive (D), caldesmon and desmin positive (CD) or the basic cells (B) which are negative for both caldesmon and desmin. It was not possible to directly demonstrate C or D cells as these antibodies precluded dual labelling. However, it seemed likely that these proteins could be expressed within the same SMC as the high proportion of cells staining for each protein in the adult tissue sections could only occur if some cells express both desmin and caldesmon.

At 14 days, B-phenotype SMCs (containing α, β and γ actins and SM1, but not desmin or caldesmon) were found within the inner media, whilst the outer media was possibly composed of C, D or CD-phenotype cells as discussed above. Some of the cells of the mid-media expressed caldesmon but none expressed desmin. Thus, in addition to B-phenotype SMCs, the mid-media also contains C-phenotype SMCs.

The effect of hypoxia on cytoskeletal protein expression was assessed by comparison with the fetal sections, which reflected the appearances prior to

exposure to hypoxia, and age matched controls - the 3 day old normal vessels. Hypoxia prevented the normal phenotypic modulation (reduction in α and β actin and calponin immunostaining in B-phenotype cells) within the inner and middle regions of the media at 3 days of age. In addition to this , some of the SMCs within the inner and middle parts of the media also immunostained for desmin, but none stained for caldesmon. The presence of desmin positive cells in regions of the vessel wall which did not stain caldesmon positive was only seen in the hypoxic tissue (D phenotype SMCs).

It was interesting to note the similarity of γ-actin staining in the hypoxic and in the normal 3 day old piglets which suggests that hypoxia does not alter the expression of γ actin and furthermore that γ actin is regulated differently from α and β actin.

Thus, a series of site specific cytoskeletal SMC phenotypes could be demonstrated in the normal developing intrapulmonary arterial vessel media and in the intrapulmonary arteries of animals exposed to hypobaric hypoxia. The changing pattern of SMC phenotypes also suggests that the vessel matures, or that the stress load within the vessel wall increases in a direction from adventitia to endothelium. This also highlights the rapidity with which this occurs.

In order to clarify these SMC phenotypes further, it will be important to carry out immunoelectron microscopy of the tissues. This would be of great benefit in showing the relationships between the cytoskeletal proteins within individual cells.

The phenotypic modulation (apparent reduction in α smooth muscle and β actin within the inner and mid-media at 3 days of age) which is associated with normal adaptation, and is not seen in vessels from hypoxic animals which fail to progress through normal adaptation, was investigated in the next experiments (**Chapter 4**). Particular emphasis was placed on determining whether the reduction in actin immunostaining of the inner media at 3 days of age was due to a reduction in total actin content, net depolymerisation of thick actin bundles, a rearrangement of these to finer filament bundles, or a combination of these possibilities. The functional effects associated with these changes in the actin cytoskeleton were evaluated in **Chapter 5.** The possibility that the inner and outer media at three days of age might represent two regions with distinctly different, or modulated, SMC

phenotypes was investigated further in **Chapter 6** by isolation of SMCs from these regions. In **Chapter 7** SMCs isolated from the intrapulmonary arteries of normal and hypoxic animals were cloned to examine the different SMC phenotypes suggested by these results.

Chapter 4. Results: Appearance and content of actin within SMCs of the intact vessel wall during postnatal adaptation.

INTRODUCTION

The transient reduction in anti- α smooth muscle actin and anti-β actin antibody staining, noted in **Chapter 3**, was further investigated in three series of experiments. Firstly, further histological studies were carried out using phalloidin to stabilise the filamentous actin cytoskeleton to try to find out if a change in the architecture from large thick bundles of filaments to finer or shorter bundles of filaments could be responsible for the changes in α and β actin immunostaining patterns within the inner and mid-media at 3 days of age. Secondly, a specific biochemical assay was used to see if there was a reduction in total actin content within the vessel wall at 3 days of age. Thirdly, additional studies were carried out to see if net depolymerisation from filamentous to monomeric actin could be occurring at this time. All three changes might be possible and could help explain changes in actin isoform immunoreactivity and help explain how the SMCs reorganise their cytoskeleton in order to change their shape and accommodate the increased pulmonary blood flow following birth.

In the immunohistochemical studies (**Chapter 3**) the vessel wall had been examined in late fetal life and then at 3 days of age. Earlier ultrastructural studies had shown that the pulmonary arterial SMCs change shape within the first few minutes after birth (Haworth and Hislop, 1981). As these rapid changes might be caused by alterations in the actin cytoskeleton, in the present study intrapulmonary arteries were also examined from animals around the time of birth. In addition to 3 day old, 14 day old adult and hypoxic animals, late gestation fetal piglets (one week prior to term) and newborn piglets born normally at term were used. Some

animals from both groups were killed prior to the onset of breathing and others allowed to establish normal respiration for five minutes before being killed.

4.2 APPEARANCE OF ACTIN FILAMENTS IN WHOLE TISSUE

Before trying to find out whether any changes in actin architecture could be detected which might be associated with normal adaptation to extra-uterine life, or with chronic hypobaric hypoxia, the appearances of a known, and biologically significant change in cell actin architecture - contraction - was investigated. It was reasoned that although the changes in actin cytoskeletal arrangement may be different during contraction and postnatal adaptation, if the method of imaging the cells was unable to reveal changes during contraction, the method would be too insensitive to examine the changes which might occur during adaptation to extrauterine life.

The method used involved permeabilising segments of vessel wall with saponin and simultaneously stabilising the filamentous actin cytoskeleton with phalloidin, whilst allowing other cytoplasmic contents (including non-filamentous actin) to be washed out. The preparations were fixed and 5 μm cryosections cut. These were stained with rhodamine-phalloidin and the inner half of the media visualised with epifluorescence and photographed. These sections were considerably thicker than the cryo-ultramicrotomy sections (250 nm) and contained one or two SMCs in their depth.

4.2.1 The effect of contraction

These experiments were carried out using six randomly chosen segments of intrapulmonary artery from two unrelated 14 day old piglets. Tissue from 14 day old animals was chosen in preference to tissue from adult animals because at 14 days of age the lungs are sufficiently large to produce several pulmonary arterial segments, but produce better quality sections because there is less connective tissue than in adult animals. The same appearances were obtained from different

segments of vessels from each animal and a representative set of images is shown (Figure 24).

Normal relaxed vessel - control

The control vessel wall showed the resting state of the filamentous actin cytoskeleton (Figure 24 (a)). The cell was filled with filaments that appeared to vary in thickness and were relatively disorganised in their arrangement. The apparent space between smooth muscle cells was seen to be almost completely filled with wisps of actin filaments (arrowheads).

Normal contraction with a pharmacological agonist

Contraction with the thromboxane mimetic, U 44619 (0.1 μM), caused the cells to change shape, becoming narrower. The disorganised fine actin filaments seen in the control vessel SMCs underwent compaction and the cortical layer of actin became more organised (Figure 24 (b)). The actin filaments within the cell also formed denser filament bundles, and the wisps of actin previously filling the apparent intracellular spaces, had retracted (arrowheads). This produced a clearing effect between cells.

Maximal contraction by ATP depletion

The specimens treated with sodium azide (10 mM) exhibited the effects of a maximal, and lethal, contraction of the cell due to depletion of ATP (Figure 24(c)). The actin filaments appeared highly compacted - more so than with U44619. The intercellular space was completely devoid of actin filaments (arrowheads) and the dense cortical actin filaments were replaced by filaments lying longitudinally or obliquely along the long axis of the cell.

These features were consistently seen across different sections cut from control, U44619-treated and azide-treated vessels. This suggested that progressive contraction or changes in SMC shape could be reflected not only in the filament patterns within the body of the cell, but also in compaction of the fine actin filaments found in the cytoplasmic extensions normally lying between cells. The

organisation of actin within the cell could therefore be classified in two ways: firstly by the transverse/oblique/longitudinal orientation of actin bundles within the cells and secondly by the degree of compaction of actin filaments at the cell margins, as demonstrated by the clearing of the intercellular spaces.

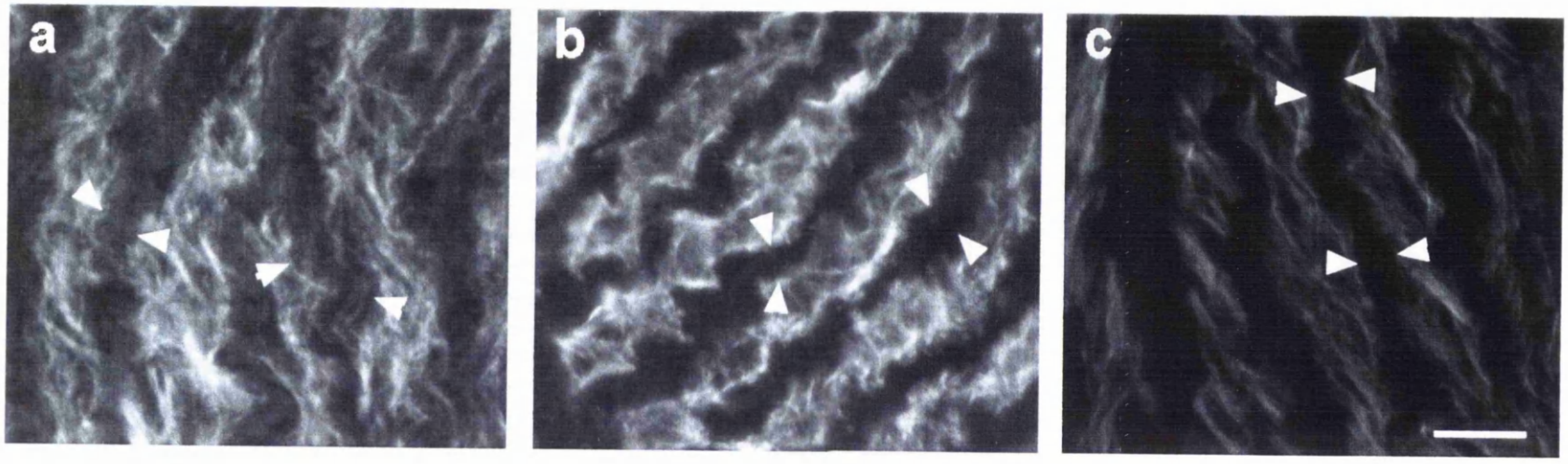

Figure 14 The effect of contraction on the appearance of the filamentous actin cytoskeleton, (a) control, (b) thromboxane mimetic U44619 (0.1μM) and (c) sodium azide (10 mM). The progressively stronger contraction of the SMCs in (b) and (c) is accompanied by orientation of actin filaments in the long axis of the cell and clearing of the intercellular spaces between cells (arrows). Bar corresponds to 5 μm.

4.2.2 *The appearance of the actin cytoskeleton during development*

As in the previous immunohistochemical studies, 3 day (n=3), 0 - 3 day hypoxic (n=3), 14 day old (n=3), and adult animals (n=3) were used in these experiments to reflect the stages of normal adaptation and to model persistent pulmonary hypertension of the newborn. In addition, non-breathing fetal piglets (n=3), and fetal piglets that had breathed for five minutes (n=3) were studied as were full-term newborn piglets that had not breathed (n=2) and newborn piglets that had breathed for five minutes before being killed (n=3). In this way the effect of labour and normal delivery on pulmonary arterial structure could be investigated by comparing the findings in fetal breathing piglets (born by caesarean section without labour) with those in the newborn breathing piglets (born after labour and by vaginal delivery). The immediate changes in pulmonary arterial structure with the onset of breathing and the extrauterine circulation could be assessed by comparing the findings in the vessels in the breathing fetal and newborn, with those in the vessels from the non-breathing fetal and newborn piglets. The choice of 5 minutes as a suitable time to kill the newborn breathing and the fetal breathing piglets was based on the results of previous experiments (Hall and Haworth, 1987). The assumption that these animals had completed the immediate phase of adaptation of the pulmonary circulation to the extra-uterine environment by 5 minutes of age was considered valid, not only on clinical grounds because the piglets had established regular respiration, become pink and begun to walk, but is also justified by the demonstration of the clear differences we found in the SMC actin cytoskeletal structure and its contractile function between birth in the absence of respiration and at 5 minutes of age with respiration.

The sections were scored in a semiquantitative manner, based on the degree of actin compaction. A highly compacted cytoskeleton, with clear space between cells was scored as (+++), and a poorly compacted actin cytoskeleton with extensive distribution of actin filaments in the space between cells was scored as (+) (Table 16 and Figure 25). There was very little variation between section.

The SMCs from the fetal non-breathing piglets showed an apparently disorganised actin filament arrangement within the cell, with many filaments filling the space between cells (+) (Figure 25 (f)). In the vessels from fetal animals that

had breathed for five minutes before death the actin within the SMCs had become much more compacted. The actin appeared to have become more concentrated at the cortex of the cell and there was significant clearance between the cells, although some wisps of actin remained between the cells (++) (Figure 25 (a)). Sections from newborn non-breathing piglets showed a similar degree of compaction of the actin cytoskeleton to the fetal breathing piglets (++) (Figure 25 (g)). Tissue sections from the newborn piglets that had breathed for five minutes showed a strongly compacted actin cytoskeleton, with hardly any filaments remaining in the spaces between cells (+++) (Figure 25 (b)). Thus, these sections demonstrated a shift from non-compacted actin to compacted actin following onset of breathing and establishment of the normal extrauterine circulation, both in the SMCs of both full-term and late fetal animals (Figure 25 compare (a) to (f) and (b) to (g)). The actin within the SMCs of tissue from the newborn non-breathing piglets was more compacted than that from the fetal non-breathing animals suggesting that some of the SMC actin compaction may have taken place during labour and vaginal delivery (Figure 25 compare (f) to (g)). Similarly although the fetal breathing piglets had been allowed to breath for the same length of time as the newborn breathing piglets, the SMC actin from the fetal breathing piglets was not as compacted as in that from the newborn breathing piglets. (Figure 25 compare (a) to (b)).

In view of the previous immunolabelling data showing reduced staining of anti-α SM actin, anti- β actin and anti-calponin antibodies at 3 days, it was particularly intriguing to note that using the present technique the SMCs within the inner media of the arteries in the 3 day old animals were seen to be completely filled with actin filaments. However, the appearances of the 3 day old pulmonary arteries were different from those in the newborn vessels. At 3 days the actin cytoskeleton was less compact and the actin within the cells appeared to be less organised. The filaments within the cells were fine and there were fewer thick bundles of actin than in sections taken from fetal and newborn breather animals. The spaces between cells also contained many wispy actin filaments (+) (Figure 25 (c)). By 14 days of age, there was more compaction of the actin cytoskeleton than in the younger animals (+/++) (Figure 25 (d)) and this was even more marked in the adult (Figure

25 (e)). Thus, 3 days after birth the actin cytoskeleton appeared to become disorganised, after which it became more compacted and denser with age.

The SMCs in the vessels of the hypoxic animals were filled with thick filaments and the space around the cells contained few actin filaments (++) (Figure 25 (h)). Their appearance was therefore in-between that of the normal newborn and 3 day old animals and similar in appearance to the tissue from the 14 day old animals.

The SMCs of the outer media had a similar degree of actin compaction at all ages (++) (data not shown). There were no other consistent differences in the appearances of individual cells of the inner and middle media at different ages.

Table 16. Changes in actin cytoskeleton compaction within SMCs of the inner media of the porcine intrapulmonary artery during postnatal adaptation.

		a	Fetal breather ++	f	Fetal non-breather +
		b	Newborn breather +++	g	Newborn non-breather ++
h	0-3 day hypoxic ++	c	3 day old piglet +		
		d	14 day old piglet +/++		
		e	Adult pig +++		

Figure 25. (opposite) Representative photomicrographs showing changes in actin cytoskeleton compaction within the SMCs of the inner media of the porcine intrapulmonary artery during postnatal adaptation. The sections demonstrate a shift from non-compacted to compacted actin filaments following the onset of breathing in near term fetal and newborn piglets. Although decompaction has occurred by 3 days of age there is progressive compaction with increasing age in normal animals. The animals exposed to hypobaric hypoxia retained a compacted cytoskeleton. Tissue sections from (a) a fetal animal that had breathed, (b) a newborn animal that had breathed, (c) a 3 day old piglet, (d) a 14 day old piglet, (e) an adult animal, (f) a fetal animal that had not breathed, (g) a newborn animal that had not breathed and (h) a piglet exposed to hypobaric hypoxia from birth to 3 days of age (arrowheads indicate actin filaments within the intercellular spaces) Bar corresponds to 10μm.

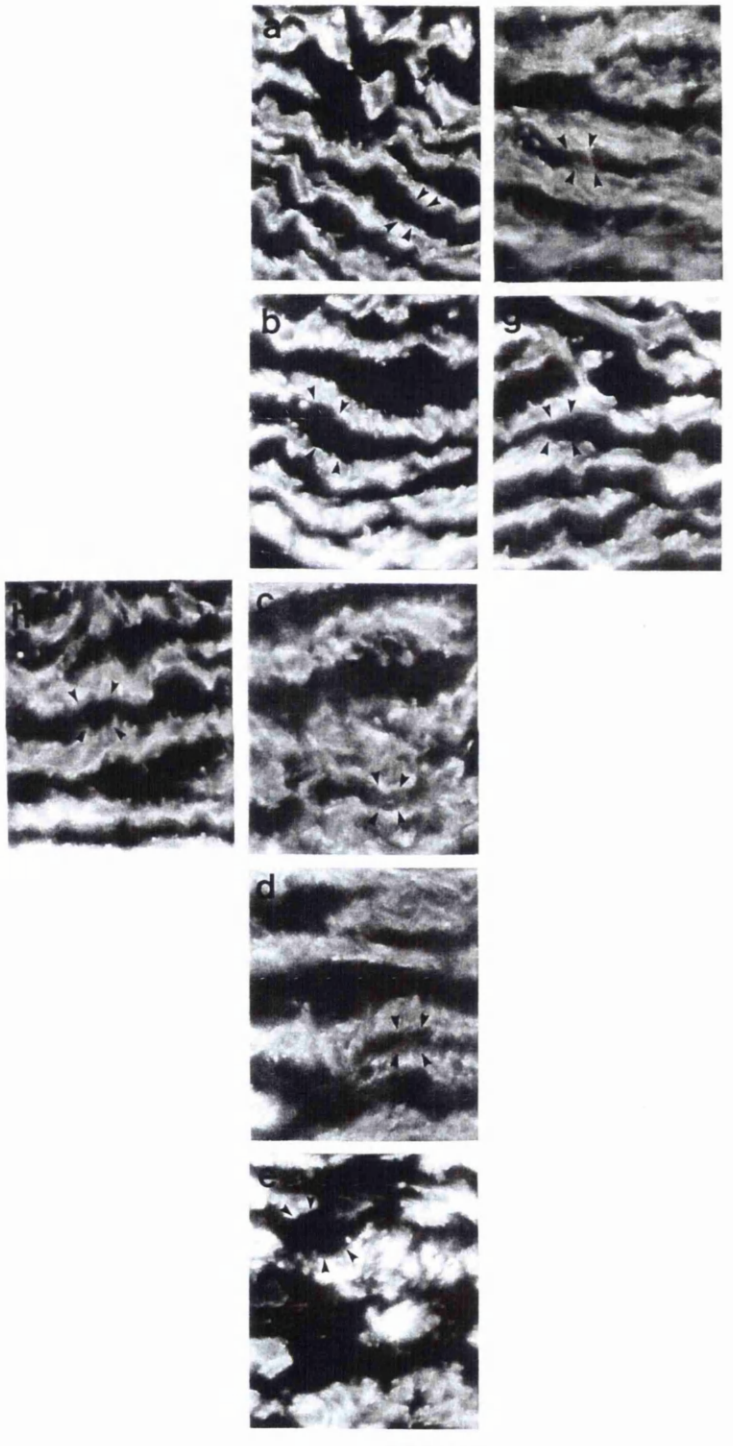
a
b
c
d

4.2.3 Summary

These experiments help interpret the immunohistochemical studies of cytoskeletal structure presented in **Chapter 3**.

The preliminary experiments comparing the effect of U46619 and sodium azide with that of an untreated segment of vessel from the same pulmonary artery demonstrated that the clearance of "space" between cells is an important feature which can be used to describe rearrangement of the actin cytoskeleton. However, the appearances of these pharmacologically contracted vessels was not used to infer that vessels from animals of differing ages were in a contracted or relaxed state as the appearances in normal vessels, although similar, might be obtained by different mechanisms of cytoskeletal organisation rather than simply by actin-myosin contraction.

The developmental studies indicated that the actin cytoskeleton became more compacted, following both normal vaginal delivery and the onset of respiration. However, at 3 days of age the actin cytoskeleton again became less compacted, then gradually became more compacted as the vessels matured in 14 day old and adult animals. The effect of hypoxia was to produce a degree of actin compaction intermediate between that seen at birth and 3 days of age. Furthermore, the stabilised-actin sections suggest that the change in α and β actin staining observed in the cryo-ultramicrotomy sections was due to a change in the form or organisation of filamentous actin within the cells at 3 days of age, from thick bundles to finer or shorter bundles of filaments. These finer structures were not resolved by the cryo-ultramicrotomy and immunostaining. The possibility that this cytoskeletal reorganisation was accompanied by a change in total actin or net depolymerisation to monomeric actin was addressed in the next series of experiments.

4.3 THE TOTAL AND MONOMERIC ACTIN CONTENT DURING POSTNATAL ADAPTATION

Using the actin-stabilised tissue sections, the transient reduction in amount of α and β actin and calponin immunostaining at 3 days of age was shown to be associated with a change in the appearance of actin filaments. The possibility that a change in total actin content, or an alteration in the monomeric/filamentous state of actin, could accompany these changes was investigated in the next series of experiments. The concentration of monomeric actin and total actin was assessed using a sensitive biochemical assay, described in **experiment 2.5.**

Fetal non-breathing piglets (n = 4); fetal breathing piglets (n = 3); newborn breathing piglets (n = 4); newborn non-breathing piglets (n = 2); newborn piglets exposed to hypoxia from 0 - 3 days (n = 3); 3 day old piglets (n = 4); 14 day old piglets (n = 4) and adult animals (n = 4) were examined. At each age, animals were taken from at least three different litters. Both lower lobe intrapulmonary arteries were used from each animal to obtain sufficient weight of tissue, except in the 14 day piglets and the adult pigs where a single intrapulmonary artery was sufficient.

Because the pulmonary arteries varied in size at the different ages, from fetus to adult, it was important to standardise the measurements of total actin to allow comparisons to be made. Since the proportion of collagen and extracellular matrix within the tissue was not know and might vary with age the actin content was standardised against protein soluble in guanidine hydrochloride/Triton X-100 and against DNA content, which reflect the cytosolic volumes and the number of nuclei present within the sample respectively. Wet weight was not used as it was too imprecise and the measurement of dry weight would prevent any subsequent biochemical analysis of the tissue samples.

4.3.1 Protein content of the tissue at different ages

The protein content estimated in these experiments was that fraction of protein which was initially soluble in 1% Triton X-100 and 0.5 M guanine hydrochloride (1:1 dilution of original tissue suspension with actin depolymerisation buffer), and remained soluble when diluted 10 fold with working buffer. The addition of guanidine hydrochloride chemically breaks down cytoskeletal filaments into individual proteins. Although this treatment does not render collagen and other extracellular matrix proteins soluble, it does reflect the total cytosolic components including the cytoskeletal filaments. It is therefore an appropriate approach to use in studying the porcine pulmonary artery which undergoes significant increases in collagen and elastin content during development .

In general the amount of soluble protein obtained from the pulmonary arteries was about 1.5 - 2 % of their wet weight (Figure 26). The values for tissue obtained from fetal animals which had and had not breathed were similar and were therefore pooled. Similarly, the values for newborn animals, breathing and non-breathing were also pooled. Within the individual age groups, the variation from each mean value was low and there were no statistically significant differences between age groups (Table 17).

4.3.2 DNA content of tissue at different ages

The DNA content of tissue was measured to give an estimate of the number of cells in the tissue (Figure 27 and Table 18). The values for tissue obtained from fetal animals which had and had not breathed were similar and were therefore pooled. Similarly, the values for newborn animals, breathing and non-breathing were also pooled. The mean DNA content of the tissue from fetal and newborn animals (breathing or not), and 0 - 3 day hypoxic piglets was the same, and the standard deviations small. There was no significant increase in DNA content in the tissue from 3 and 14 day old animals in relation to the fetal, newborn or hypoxic animals. In contrast, the adult values were lower than at 3 or 14 days ($p<0.02$), and also lower than in the tissue from fetal, newborn and hypoxic piglets ($p<0.001$).

Figure 26. Histogram showing the percentage of intrapulmonary artery obtained as soluble protein, in relation to wet weight of vessel, during development (error bars correspond to 1 SD).

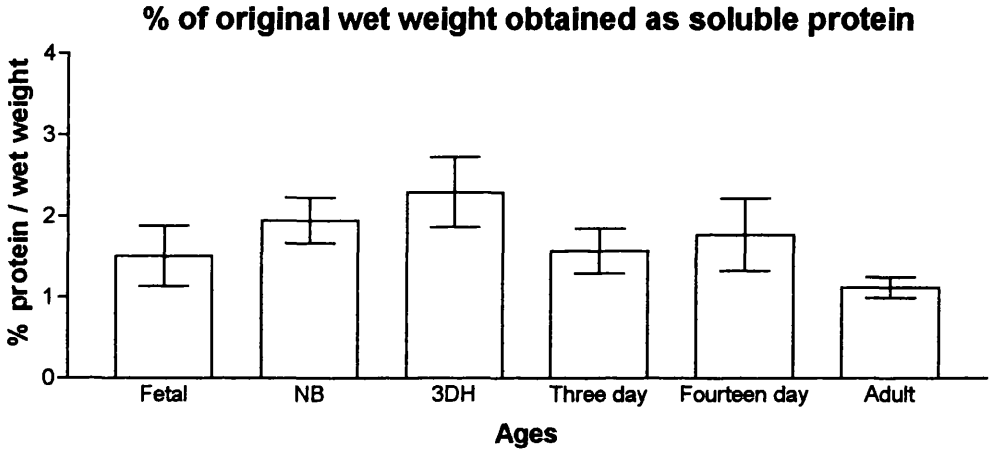

Table 17. Percentage of soluble protein in relation to wet weight of the intrapulmonary artery during development.

Age	Number of animals	Mean percentage	Standard deviation
Fetal	7	1.5	0.37
Newborn	6	2.0	0.28
0-3 day hypoxia	3	2.3	0.44
3 day normal	4	1.6	0.28
14 day normal	4	1.8	0.45
Adult	4	1.1	0.13

Figure 27 Histogram showing the DNA content of intrapulmonary artery, in relation to wet weight of vessel, during development
(error bars correspond to 1 SD).

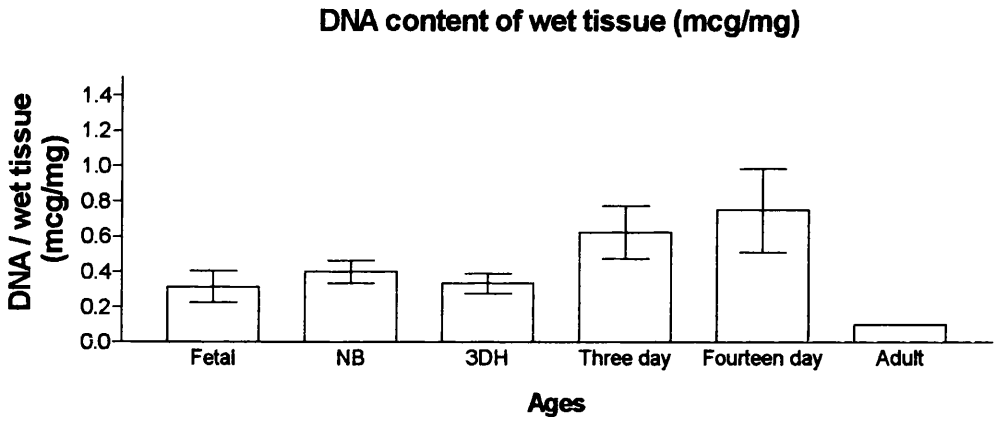

Table 18. DNA content in relation to wet weight of the intrapulmonary artery during development (μg DNA/mg vessel weight).

Age	Number of animals	DNA/Wt (μg/mg)	Standard deviation
Fetal	7	0.31	0.09
Newborn	6	0.40	0.06
0-3 day hypoxia	3	0.33	0.06
3 day normal	4	0.63	0.15
14 day normal	4	0.75	0.24
Adult	4	0.10	0

4.3.3 Standardised total actin content

Total actin, determined by the fluorometric assay, was standardised against DNA (Figure 28 and Table 19) and against soluble protein content (Figure 29 and Table 20). There was no statistically significant difference between the different age groups. However, the standardisation of the actin content with that of the DNA or protein content did lead to large standard deviation values for some age groups that would mask lesser changes. For example the mean adult values of actin although not statistically significant were relatively low when standardised for soluble protein but relatively high when standardised against DNA suggesting fewer, but larger, cells in the adult vessels.

4.3.4 Ratio of monomeric /total actin

The monomeric actin concentrations (μg/μl) were determined from the same lysed tissue suspensions used to determine total actin values. The ratio of monomeric actin to total actin was calculated and expressed as a mean percentage, and the variation of measurements around this value are described by the standard deviation.

The percentage of monomeric actin to total actin in the normal pulmonary arteries studied showed no significant change with age (Figure 30 and Table 21) However, there are trends which are open to speculation. The vessels from animals that had not inflated their lungs - fetal non-breathing and newborn non-breathing - had mean monomeric/total actin percentage of 19.5% (SD = 2.5%) and 18.6% (SD not calculated as n = 2) respectively, while those from the fetal breathing and newborn breathing animals had higher mean monomeric/total actin values of 23.4% (SD= 5.7%) and 26.8% (SD = 7.3%) respectively. Although not statistically significant, the mean values from tissue of animals which had not breathed are more alike than the values obtained from animals that did breath for five minutes before being killed. It is possible that the onset of respiration may be associated with an increase in the proportion of monomeric actin within the SMCs. It must be reiterated however, that the relatively small number of animals in this study do not

provide sufficient statistical power to detect a significant difference between the groups, given the large standard deviation of the results.

Figure 28. Histogram showing total actin content of intrapulmonary artery in relation to DNA content of the vessel during development (error bars correspond to 1 SD).

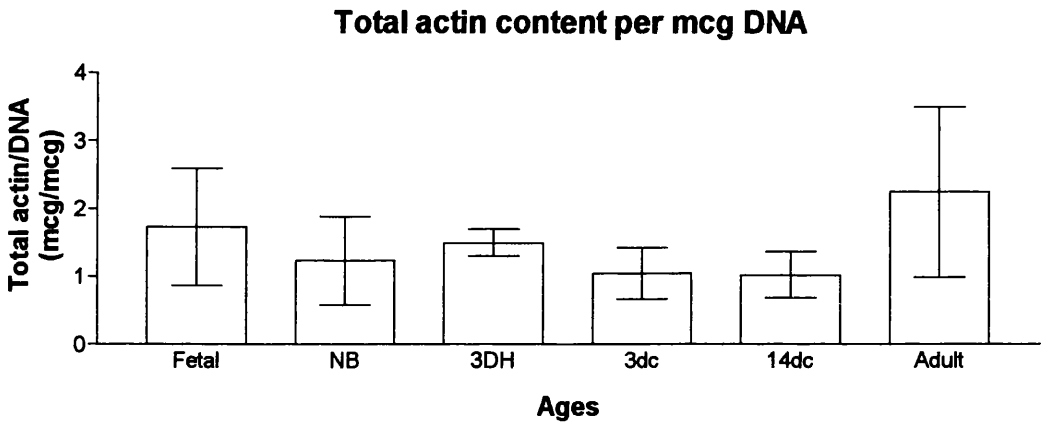

Table 19. Total actin content in relation to DNA content of the intrapulmonary arteries during development (μg actin/μg DNA).

Age	Number of animals	Total actin/DNA (μg/μg)	Standard deviation
Fetal	7	1.73	0.87
Newborn	6	1.23	0.65
0-3 day hypoxia	3	1.50	0.20
3 day normal	4	1.10	0.38
14 day normal	4	1.03	0.34
Adult	4	2.25	1.26

Figure 29. Histogram showing total actin content of intrapulmonary arteries, in relation to soluble protein content, during development
(error bars correspond to 1 SD).

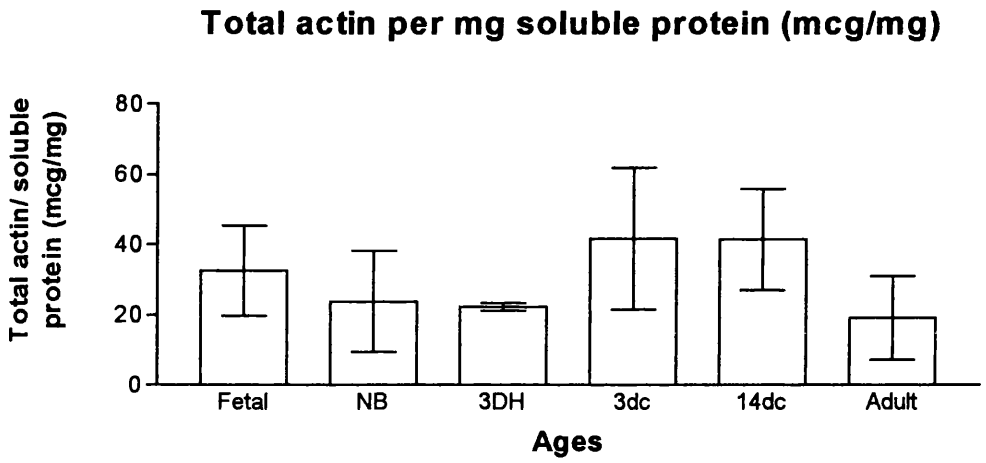

Table 20. Total actin content of intrapulmonary arteries, in relation to soluble protein content, during development (μg actin/mg protein).

Age	Number of animals	Total actin/Wt (μg/mg)	Standard deviation
Fetal	7	32.6	12.8
Newborn	6	23.8	14.4
0-3 day hypoxia	3	22.3	1.2
3 day normal	4	41.8	20.2
14 day normal	4	41.5	14.5
Adult	4	19.3	12.0

Figure 30. Histogram showing percentage of total actin in the monomeric form within the intrapulmonary arteries during development (error bars correspond to 1 SD).

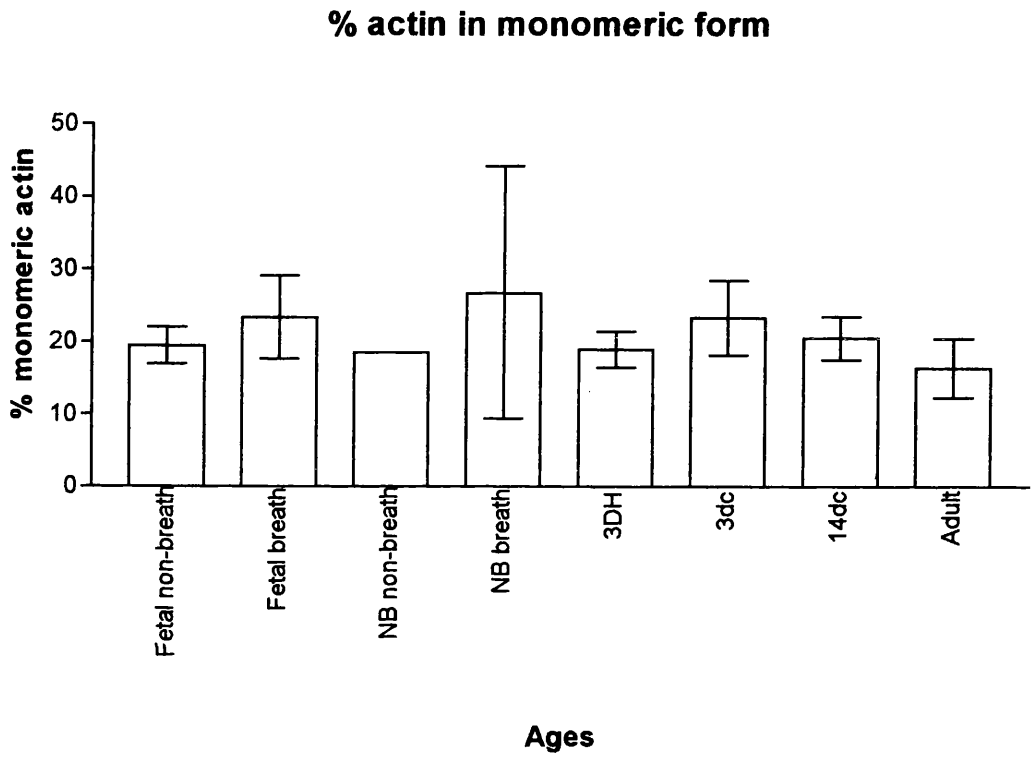

Table 21. Percentage of total actin existing in the monomeric form within the intrapulmonary artery during development.

Age	Number of animals	% monomeric actin	Standard deviation
Fetal non-breathing	4	19.5	2.5
Fetal breathing	3	23.4	5.7
Newborn non-breathing	2	18.0 & 19.2	No SD
Newborn breathing	4	26.8	17.4
0-3 day hypoxia	3	19.0	2.5
3 day normal	4	23.4	5.2
14 day normal	4	20.6	3.0
Adult	4	16.4	4.1

4.4 SUMMARY

These biochemical studies have demonstrated that there is probably no statistically significant change in the total actin concentration within the SMCs of the intrapulmonary artery during adaptation to the extra-uterine environment. However, the large standard deviations obtained with the standardised data does mean that small but significant changes will not be detected. These experiments were also able to demonstrate that there is no statistically significant change in the percentage of monomeric to total actin during adaptation to the extra-uterine environment.

The biochemical findings, together with the evidence from the stabilised-actin tissue sections, suggests that the transient reduction in the immunostaining pattern for α-smooth muscle actin, β-actin and calponin, confined to the inner part of the media at 3 days of age, could be due largely to a change in the form of actin, from thick bundles of filaments to finer bundles of filaments, rather than a change in the total actin content or a change in the proportion of actin existing in the filamentous state within the cell. However, it is possible that there is a transient depolymerisation of filamentous actin with the onset of breathing because the proportion of monomeric actin was greater in the pulmonary arteries of animals that had breathed, either fetal or newborn, than in those that had not breathed although the difference was not statistically significant. The intense staining of the pulmonary arteries of hypoxic animals with anti-α SM actin could also be explained, to some degree, by reorganisation of actin filament bundles, rather than by a change in the total amount of actin.

The phalloidin sections produced better resolution of filamentous actin than the cryo-ultramicrotomy sections possibly because the saponin detergent treatment allowed cytoplasmic contents to wash out, enhancing resolution of remaining actin filaments, and that the lighter formaldehyde fixation was responsible for the better resolution of fine structures with this method.

Thus, this work suggests that the SMCs in the inner part of the intact media have undergone phenotypic change, or a modulation of phenotype, as indicated by

the changing actin cytoskeletal organisation in the cells of this region. If there is no clear evidence of large scale depolymerisation of the filaments to monomeric actin, and total actin remains largely unchanged during this process, then the production of actin must presumably have continued relatively unchanged. It is possible that in the phase of growth and stabilisation, from 3 days of age onwards, the proportion of filamentous actin that is present as thick bundles within the SMCs increases until adulthood as suggested by the increase in actin antibody staining with age, and this can probably be considered as modulation, rather than change, of the SMC phenotype in the majority of cells. Other cells however, begin to express desmin and caldesmon which are markers of differentiation and may indicate change of phenotype. The change in actin organisation in the hypoxic animals may reflect modulation of phenotype, but this does not exclude a change in phenotype in some of the cells, suggested by the expression of desmin. The effect of these changes in actin cytoskeleton on the contractile function of the SMCs within the intrapulmonary artery were investigated in the next experiments (**Chapter 5**).

Chapter 5. Results: Contractile properties of the intact vessel wall

These experiments were performed to investigate the functional implications of the postnatal changes in the organisation of the SMC actin cytoskeleton seen by immunohistochemistry (**Chapter 3**) and on the phalloidin-stabilised actin sections (**Chapter 4**).

The contractile ability of isolated segments of intrapulmonary arteries was assessed by evaluating the ratio of wall stress generated passively by increases in resting strain, and actively following potassium chloride-induced contraction at these strains.

Four specific questions were addressed:

1. Is the contractile ability of the intrapulmonary artery the same during late gestation as in vessels at term, in newborn animals which have not breathed?
2. Does the contractile capacity of the pulmonary artery change during the establishment of respiration at birth, comparing vessels from animals that have and have not breathed?
3. Does the contractile capacity of the intrapulmonary artery change during postnatal development?
4. Does the reorganisation of the actin cytoskeleton, observed following exposure to hypobaric hypoxia, affect the contractile capacity of the intrapulmonary artery?

Tissues from breathing fetal piglets (n = 4), non-breathing fetal piglets (n = 8), breathing newborn piglets (n = 4), non-breathing newborn piglets (n = 2), 3 day old piglets (n = 6), 14 day old piglets (n = 7), hypoxic piglets 0 - 3 days old (n = 4), and adult pigs (n = 6) were used in these studies. The passive stress, and the active stress following a potassium chloride induced contraction, were calculated

from the forces recorded on a calibrated paper chart recorder (Figure 31), and measurements of the vessel rings according to the formula:

$$\text{Wall stress } (gcm^{-2}) = \frac{0.79\ F}{LPh\ S}$$

F= Force (grams)

L = Length of vessel ring (cm)

P = percentage wall thickness (Fraction)

h = hemicircumference of vessel ring (cm)

S = strain

In each preparation, stress data were plotted against increasing strain values. Typical stress-strain graphs of the intrapulmonary arteries of 14 day old piglets are shown in Figure 32, and are representative of the data obtained for the other age groups.

Figure 31. Original paper tracing indicating measurement of passive and active forces.

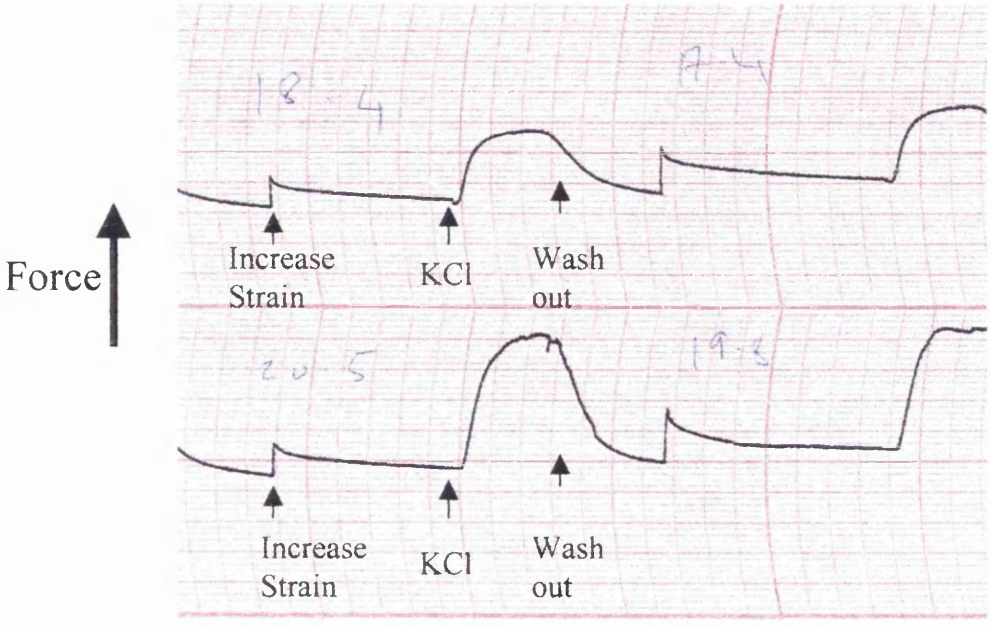

Figure 32. Individual active and passive stress- strain graphs for intrapulmonary arteries from 14 day old animals. The data from 14dc6 was not used due to technical failure during the experiment.

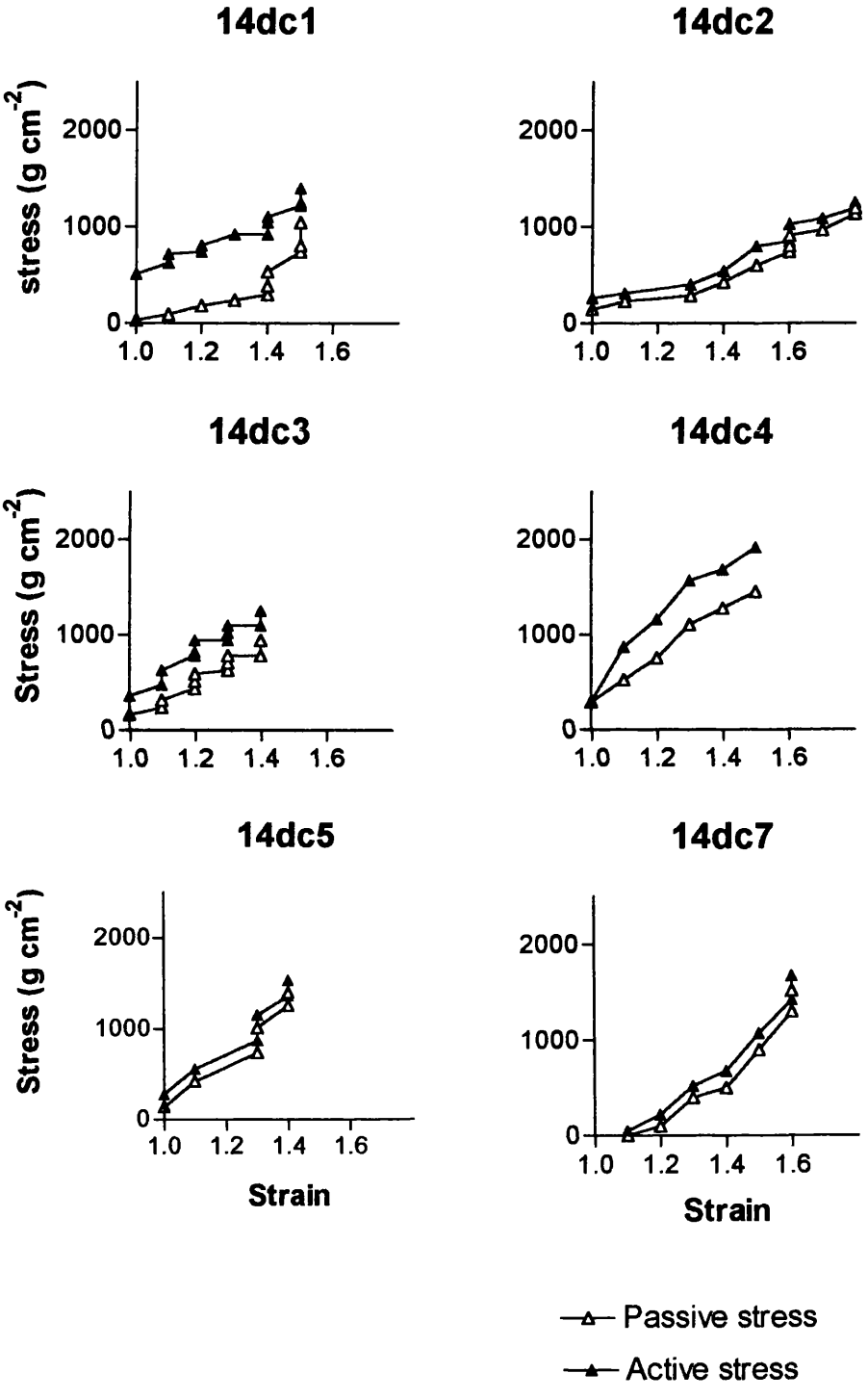

A feature of all the data sets was the great variability in the magnitude of passive and active stresses at increasing strain values. Because of this wide variation in stress values it was difficult to amalgamate data from individual animals of each age group. To overcome this problem the stress ratio at increasing strains was calculated.

The passive stress-strain data for intrapulmonary arteries from animals of different ages (see appendix for data and measurements obtained from histological rings) suggested a reasonable range of strains, at which to calculate stress ratio values, would be 1.3 - 1.7. This range of strains also contained more consistent stress values within each age group.

The stress ratio values were represented on scatterplots (Figure 33 to Figure 38). By calculating the mean of all stress ratio values between strains of 1.3 and 1.7 it was possible to compare the data from different age groups and these data is shown in Figure 39. The stress ratio values of the different groups were compared using a 2 way ANOVA statistical analysis, with the assistance of Dr S Greenwald (University of London).

5.1 CHANGE IN THE CONTRACTILE FUNCTION OF SMCS WITHIN THE INTACT MEDIA DURING THE PERIOD OF IMMEDIATE ADAPTATION TO EXTRA-UTERINE LIFE, AT BIRTH.

At all strain values between 1.3 and 1.7, the vessels from the fetuses that had breathed had significantly ($p < 0.05$) greater stress ratio values (mean value 1.9) than the vessels from fetuses that had not breathed (mean value 1.7) (Figure 33 and Figure 39). Both these groups of animals were born by caesarean section, and the fetuses which had not breathed, unlike the newborn animals which did not breathe, had no opportunity to gasp at birth. Similarly, at strains between 1.3 and 1.7, vessels from newborn animals that were allowed to breathe were capable of generating significantly more stress (mean value 1.6, $p < 0.0037$) than vessels from newborn animals that had been prevented from breathing (Figure 34 and Figure 39).

Figure 33. Stress ratios, at different strain intervals, obtained from the intrapulmonary arteries of late gestation fetal pigs that had been allowed to establish respiration, compared to the ratios in vessels from animals that had not been allowed to breathe.

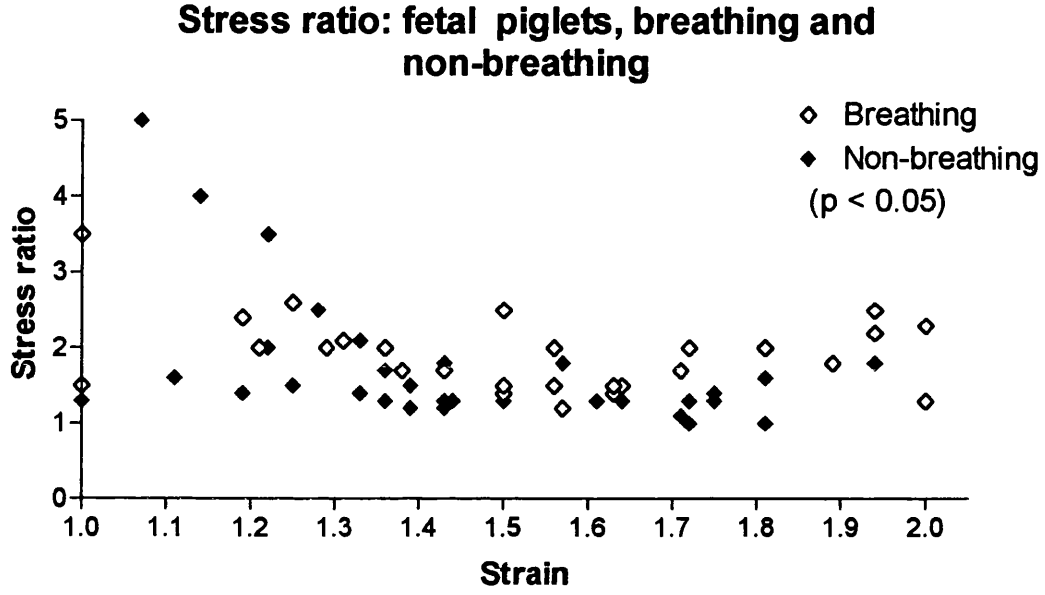

Figure 34. Stress ratios, at different strain intervals, obtained from the intrapulmonary arteries of term newborn piglets that had been allowed to establish respiration, compared to the ratios in vessels from animals that had not been allowed to breathe.

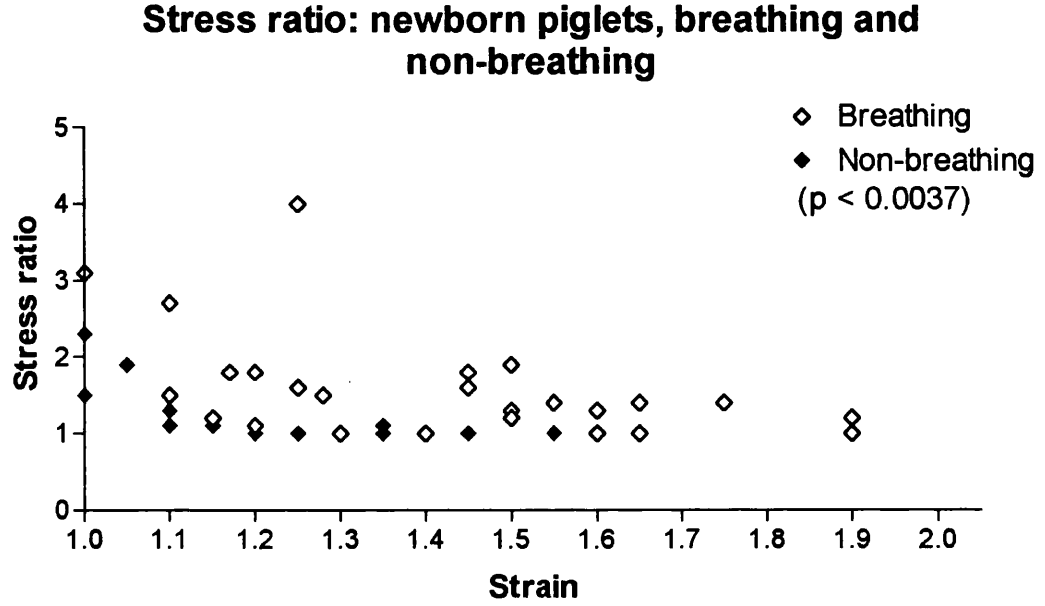

5.2 COMPARISON OF FETAL AND NEWBORN VESSELS

The newborn piglets were born at term and after a normal labour. In contrast, the fetal animals were born by caesarean section one week before the sow was due to farrow. Thus, comparison of the fetal and newborn piglets allowed an assessment to be made of whether any adaptation of the intrapulmonary arteries occurred during the last days of pregnancy and during labour, although the two processes could not be separated. The arteries from the breathing fetal piglets were capable of generating more stress at strain values of 1.3 to 1.7 than those from the breathing newborn piglets (mean stress ratio values 1.9 and 1.6 respectively, $p<0.007$) (Figure 35 and Figure 39). Similarly, the vessels from the non-breathing fetal piglets were capable of generating more stress (mean stress ratio value 1.7) than the vessels from the non-breathing newborn piglets (mean stress value 1.3, $p<0.0004$) (Figure 36 and Figure 39).

Figure 35. Stress ratios, at different strain intervals, obtained from the intrapulmonary arteries of late gestation fetal pigs that had been allowed to establish respiration compared to the ratios in vessels from term newborn animals that had also been allowed to breathe.

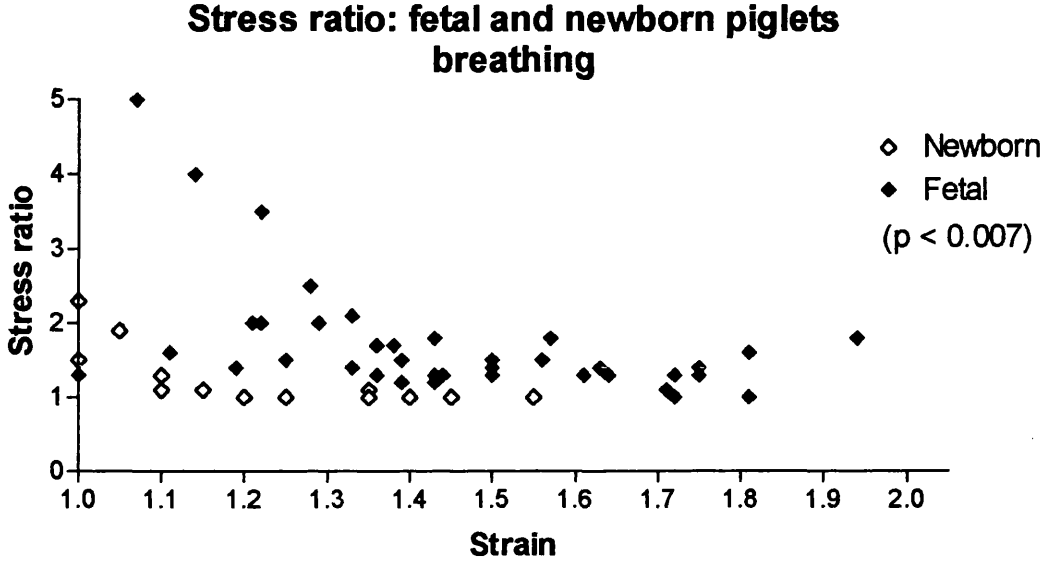

Figure 36. Stress ratios, at different strain intervals, obtained from the intrapulmonary arteries of late gestation fetal pigs that had not established respiration compared to the ratios in vessels from term newborn animals that had been prevented from breathing.

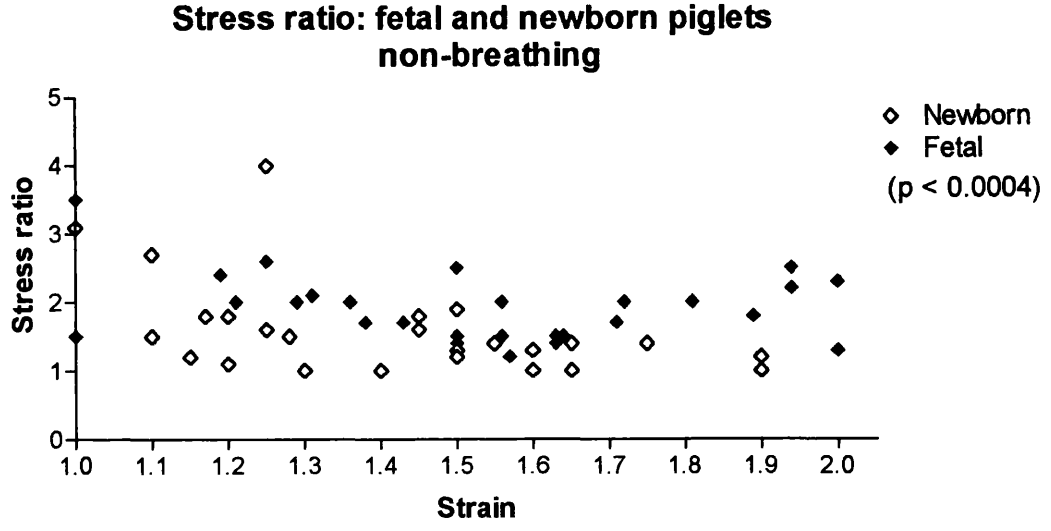

5.3 DEVELOPMENTAL CHANGES IN CAPACITY TO GENERATE STRESS.

The stress ratio values obtained from intrapulmonary arteries stretched between strains of 1.3 and 1.7 from newborn breathing piglets, 3 day old piglets (Figure 37), 14 day old piglets and adult pigs (Figure 38) were compared using a multiple ANOVA test. There was no statistically significant difference in the mean stress ratios of vessels from the newborn piglets which had breathed (mean stress ratio value 1.6), 3 day old piglets (mean stress ratio value 1.5) and 14 day old piglets (mean stress ratio value 1.9). However, the vessels from adult animals had a significantly greater mean stress ratio value (2.5) than those at any younger age ($p<0.001$) (Figure 39). This suggests that the adult vessels were capable of generating more wall stress.

5.4 EFFECT OF HYPOXIA ON ABILITY OF SMCS TO GENERATE WALL STRESS.

There was no significant difference between the stress ratios of vessels from the normal 3 day old piglets and the vessels obtained from the 0 - 3 day hypoxic piglets (Figure 37 and Figure 39).

Figure 37. Stress ratios, at different strain intervals, obtained from the intrapulmonary arteries of normal 3 day old piglets and animals that had been exposed to hypobaric hypoxia for 3 days from birth.

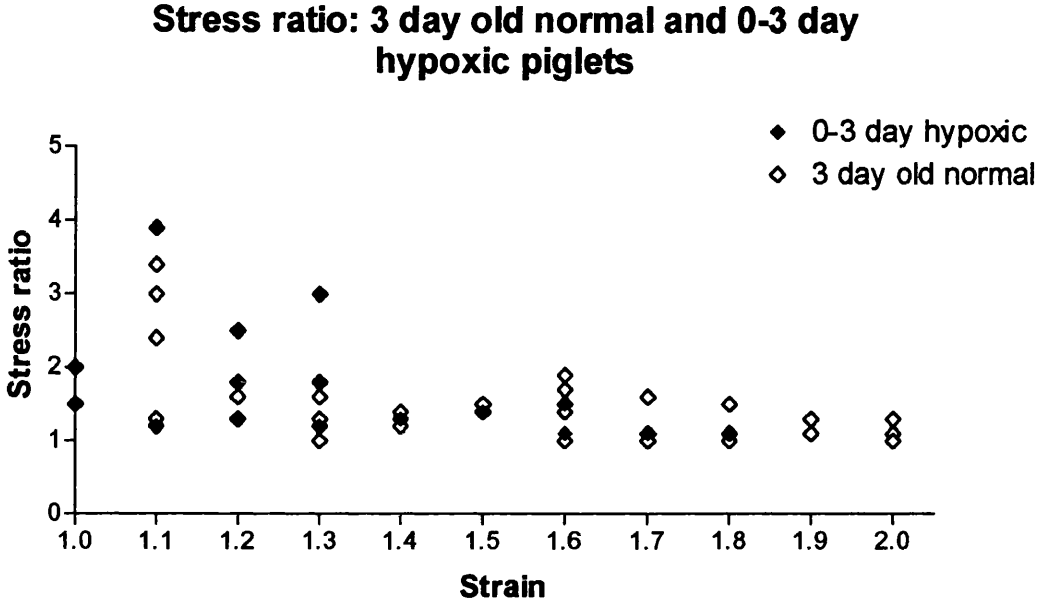

Figure 38. Stress ratios, at different strain intervals, obtained from the intrapulmonary arteries of normal 14 day piglets and adult pigs.

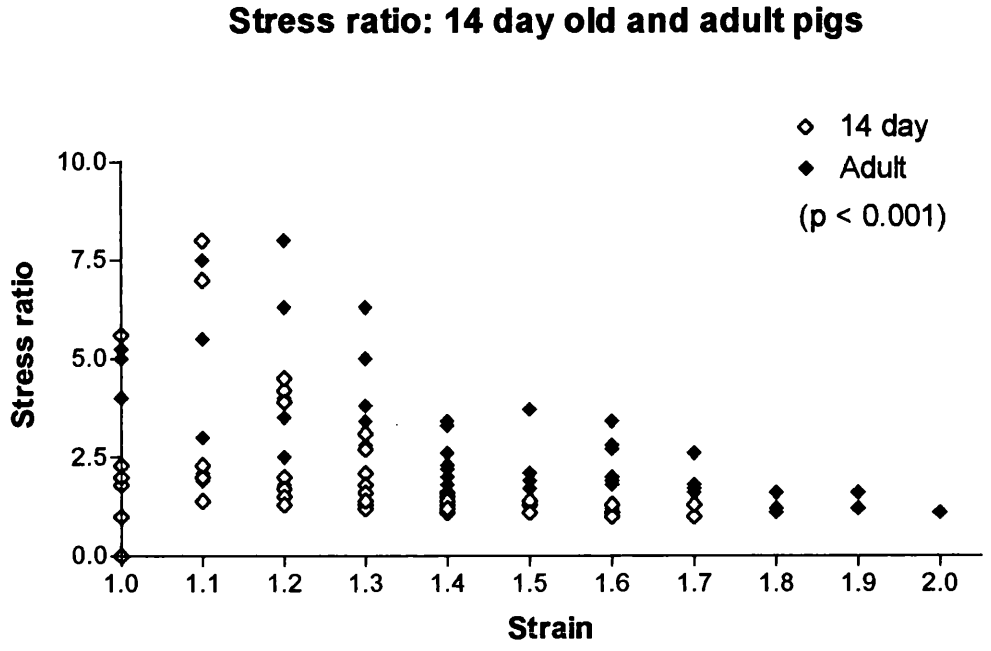

Figure 39. Mean stress ratio values, between stains of 1.3 - 1.7, of intrapulmonary arteries during postnatal adaptation. Stress ratio (SR) increases with greater actin compaction (AC) (see **Chapter 4.2.2**).

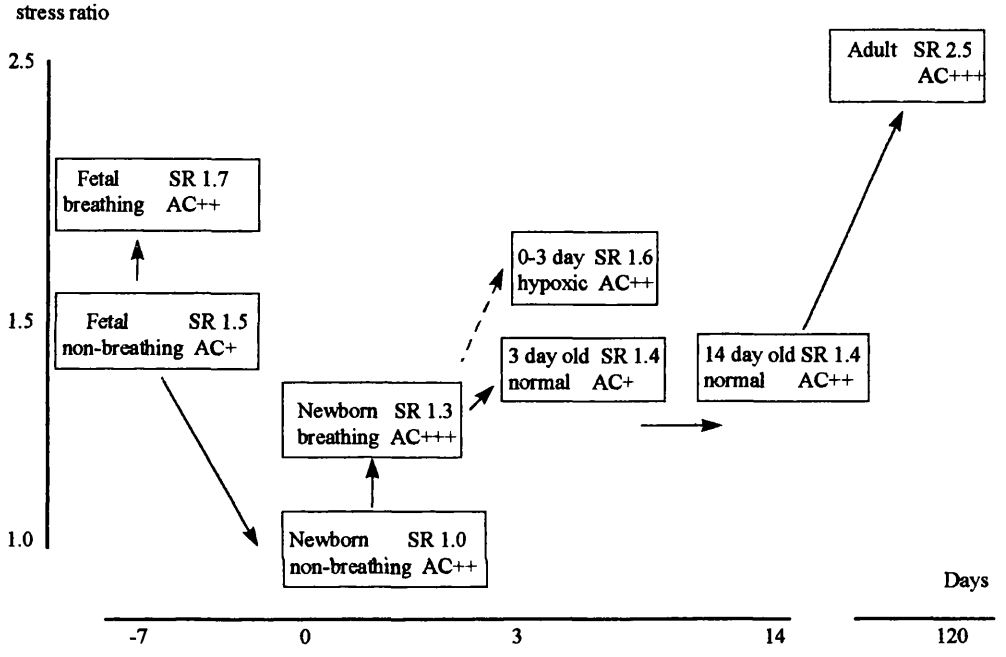

5.5 STRESS RATIO AND ACTIN COMPACTION

The degree of actin compaction seen within SMCs at each stage of development of the intrapulmonary area correlated well with the stress ratio values at each age. Thus, as the actin cytoskeleton was noted to be more compacted, the stress ratio values determined for the vessel were also increased (Figure 39).

5.6 QUANTIFICATION OF ELASTIN, COLLAGEN AND SMOOTH MUSCLE CONTENT OF VESSEL WALL

The composition of the vessel wall must be understood in order to interpret the demonstrable changes in wall stress when the SMCs are stimulated to contract. The same histological sections of intrapulmonary artery that were used to measure wall thickness for the functional studies of isolated intrapulmonary arteries were also analysed to determine the proportions of elastin, collagen and smooth muscle within the vessel wall.

Elastin van Geisen-stained sections from three different animals at each age were examined and photographs of the whole media taken randomly (Figure 40). Samples from these photographs were scanned and the proportions of elastin, collagen and muscle measured. The variation from the mean values is described by the standard deviation (Table 22 and Figure 41). The proportions of elastin, collagen and smooth muscle in the sections from the fetal and newborn (both breathing and non-breathing), 3 day old normal, the 0 - 3 day old hypoxic piglets 14 day old and adult pigs appeared the same with approximately 35 % muscle, 20 % elastin and 30 % collagen. The remaining approximately 15% was probably extracellular matrix. The wide standard deviations obtained with this data did not allow any statistical differences to be demonstrated. In part this is probably due to variation in the proportions of the elastin, collagen and smooth muscle within the sampled sections, but much of the variation is likely to be due to methodological limitations. Although this method had the advantage that the total of the elastin, collagen, extracellular matrix and smooth muscle staining areas must add up to 100%, differences in the intensity and hue of the staining probably led to significant variation in measurements.

Figure 40. Photomicrographs of 7 μm sections of tissue cut from adjacent intrapulmonary arteries to those used in mechanical studies. Stained with Millers elastin van Giesen, (a) newborn, (b) 14 day old, (c) adult pigs.
(Bar corresponds to 5 μm)

Figure 41. Histogram showing percentage of smooth muscle, elastin, collagen, and extracellular matrix within intrapulmonary arteries during development and following exposure to hypobaric hypoxia.

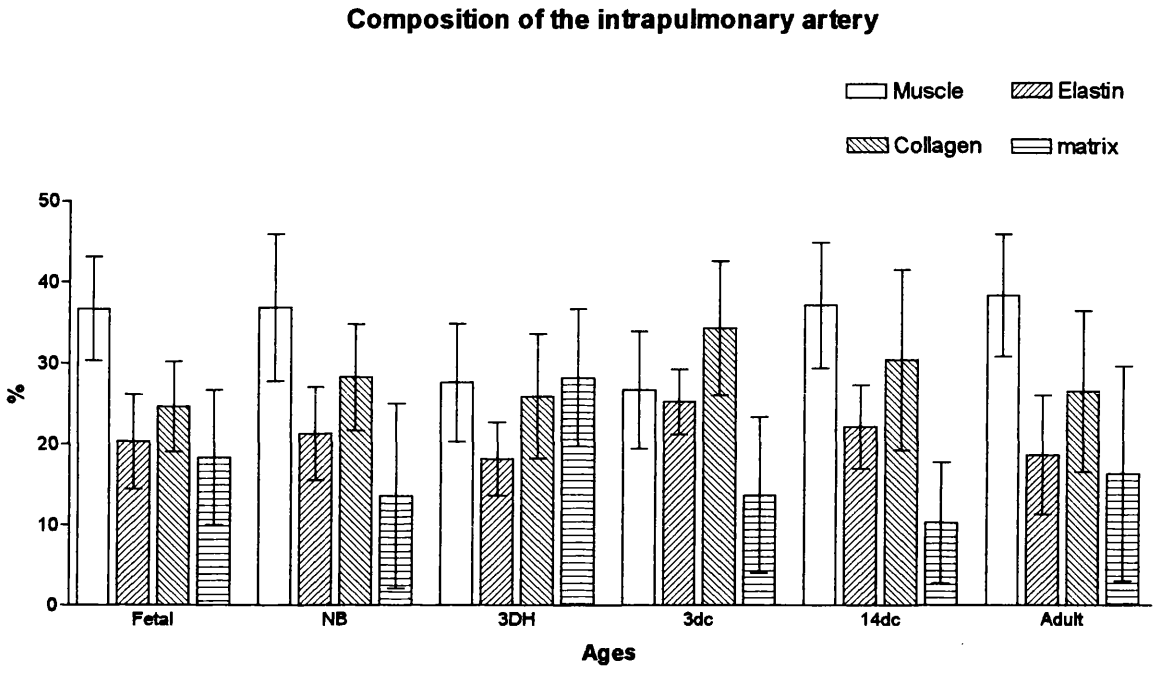

Table 22. Percentage of smooth muscle, elastin, collagen and extracellular matrix within the media of intrapulmonary arteries during development and following exposure to hypobaric hypoxia.

Ages	% Smooth muscle (SD)	% Elastin (SD)	% Collagen (SD)	% Matrix (SD)	Samples (n)
Fetal	37 (6)	20 (6)	25 (6)	18 (8)	42
Newborn	37 (9)	21 (6)	28 (7)	14 (11)	18
0-3 hypoxic	28 (8)	18 (5)	26 (8)	28 (8)	12
3 day old	27 (7)	25 (4)	34 (8)	14 (10)	12
14 day old	37 (8)	22 (5)	30 (11)	10 (8)	18
Adult	38 (8)	19 (7)	27 (10)	16 (13)	33

5.7 SUMMARY

The active : passive stress ratio, between strains of 1.3 - 1.7, changed during adaptation to extra-uterine life suggesting significant alterations in the contractile properties of the intrapulmonary conduit arterial wall (Figure 39). There was a decrease in the ability of the SMCs to generate wall stress between late fetal life and the newborn period. By contrast, the stress ratio was unchanged between breathing newborn piglets and those at fourteen days of age. By adulthood the vessels were capable of generating significantly more stress than at the younger ages (stress ratio 2.5). The stress ratio of vessels from animals exposed to hypoxia from birth until 3 days of age were not significantly different from the stress ratio of normal 3 day old piglets. In both fetal and newborn animals the stress ratio was lower in animals that had not breathed (stress ratio 1.7 and 1.3 respectively) than those which had (stress ratio 1.9 and 1.6 respectively).

Morphometric analysis of the composition of these vessels indicated that there was no significant change in the proportion of muscle, collagen and elastin within the vessel wall during adaptation to the extra-uterine environment. However, when the mean stress ratio values for each age were compared with the appearance of the actin cytoskeleton a close correlation between degree of actin filament compaction and mean stress ratio value was seen (Figure 39). These data indicate that the fall in stress ratio during late gestation, its increase during the initiation of respiration, and its increase in the late stages of continuing postnatal adaptation are associated with changes in the organisation of the actin cytoskeleton of the SMCs.

Chapter 6. Results: *Phenotypic variation of the pulmonary arterial SMCs during postnatal adaptation and production of defined SMC clones*

These experiments were designed to investigate if the changes in the actin cytoskeleton of SMCs in the inner half of the media at 3 days of age were due to modulation of an existing phenotype or to a change in the predominant SMC phenotype. In addition, the differences in α smooth muscle actin staining pattern between vessels from hypoxic animals and normal three day old animals were examined, to determine whether they related to modulation or a change of phenotype. To answer these questions, it was necessary to first characterise the pulmonary arterial SMCs within the vessel wall more fully, by studying them in culture. Following these initial studies, it became essential to produce clonal cell lines of the different morphological SMC phenotypes identified: firstly, to prove that the appearances were stable through several generations and hence that the appearances in primary culture were not a transient effect of tissue culture; and secondly to allow full characterisation of the morphological phenotypes by investigating potential differences in function.

6.1 DEFINITION OF SMOOTH MUSCLE CELL PHENOTYPES

In view of the marked and localised changes in the expression of different cytoskeletal proteins in the vessel wall at different ages, it was important to discover one or more characteristics, the possession or absence of which could be used to segregate cells into different phenotypes.

Cell phenotypes can be characterised in several ways, for example by genetic markers or protein expression, but we chose to characterise the cells

morphologically as preliminary experiments had indicated that the morphological appearance of cultured SMCs seen by phase contrast microscopy could be a useful characteristic.This was therefore used as the starting point for the studies described here. The SMCs were isolated by enzymatic digestion of connective tissue and grown for 72 hours on fibronectin-coated surfaces (**experiment 2.7.1 and 2.7.2**)

6.1.1 Smooth muscle cell phenotypes characterised by morphological features

Tissue from fetal (non-breathing), 3 day old, 14 day old, and 21 day old animals were used in these experiments to determine the SMC phenotype(s) present in the vessel wall during the process of postnatal adaptation, accepting that continued growth would occur after 21 days of age. Tissue from one adult animal was also studied. Cells were isolated from the intrapulmonary arteries of three unrelated animals at each of these ages and cells from vessels of three different animals which had been exposed to chronic hypobaric hypoxia were used. For each animal, the cells on three separate coverslips were examined. The initial strategy was to categorise cells based on cell shape. Criteria included the ability to identify the cell margins under phase contrast microscopy and the degree of cell polarity (longitudinal axis compared with transverse axis of the cell), ranging from polygonal (no longitudinal polarity) to spindle (extreme longitudinal polarity). There were no obvious differences in their nuclei or nucleoli. Four putative phenotypes were defined (Figure 42). The total number of cells were counted and the percentage of SMCs having a distinctive and different shape was determined.

Figure 42. Appearance of porcine intrapulmonary smooth muscle cells in primary culture. (a) epithelioid, (b) polygonal, (c) spindle/polygonal, (d) spindle shaped. Bar corresponds to 50 μm.

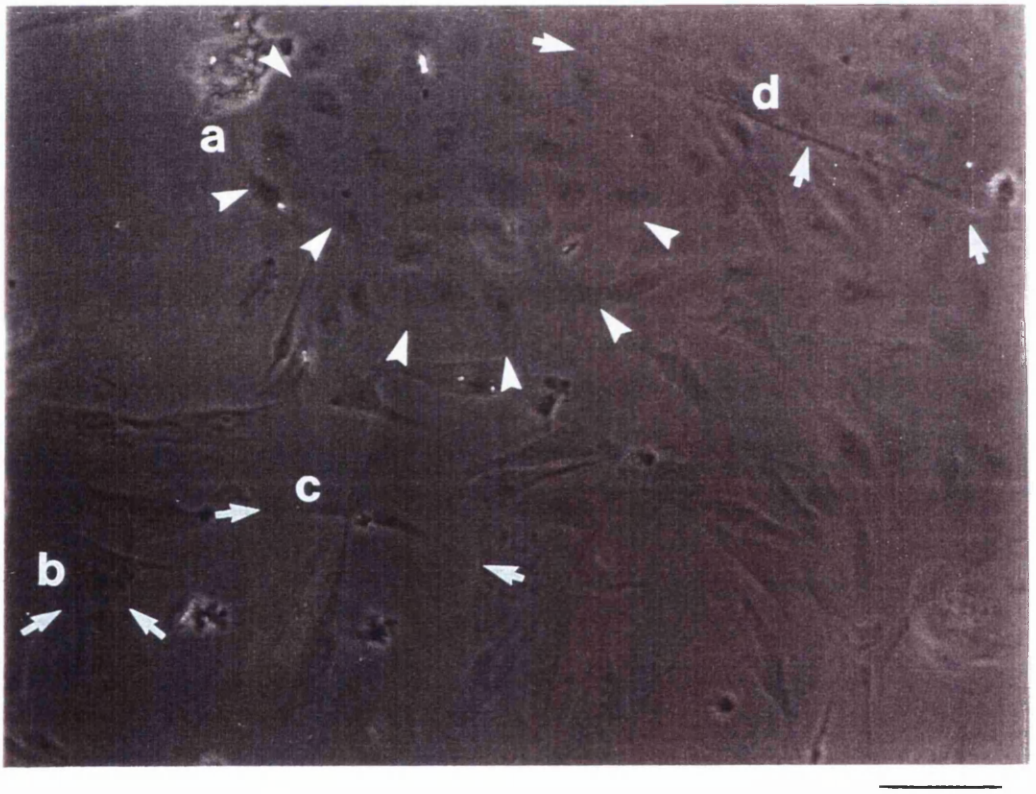

1. The epithelioid phenotype had a circular cell outline, low phase contrast edges and did not grow over other cells. Groups of the cells were usually seen, forming a monolayer. Since the intercellular margins were poorly seen, the rafts of cells gave a pseudo-syncitial appearance (Figure 42 (a)).

2. Polygonal cells demonstrated obvious refractile cell margins by phase contrast microscopy. They were seen singularly and in groups, growing over neighbouring cells, or sending fine cytoplasmic projections to more distant cells. There was no obvious long axis to the cells (Figure 42 (b)).

3. Spindle/polygonal-shaped cells also had clear cell margins by phase contrast microscopy, but had an obvious long axis to the cell which was 2- 3 times longer than the perpendicular short axis (Figure 42 (c)). These cells were also seen singularly and as rafts of cells, growing over each other.

4. The spindle-shaped cells were characterised by great length in relation to width (Figure 42 (d)).

When counting the cells it became apparent that the SMCs with an epithelioid appearance were easily identified as a homogeneous group, and the percentage of these epithelioid SMCs was consistent within each age group (Table 23). However, distinguishing between the polygonal, spindle/polygonal and spindle-shaped cells was more difficult as the appearances were less consistently different. Therefore at each age, the percentages of cells within these groups showed great variability. This may have been because of the different phenotypes actually comprising a single group, but could also have been due to limitations in the scoring of the different non-epithelioid phenotypes (Figure 43). It was decided that the epithelioid cells (epSMCs) comprised a distinct phenotype, and that the polygonal, spindle/polygonal and spindle cells could be considered together as a second phenotype, the spindle-shaped SMCs (spSMCs) (Figure 44). Tissue from the hypoxic animals produced similar groups of epithelioid and spindle-shaped

SMC phenotypes, but because the cytoskeletal appearances were abnormal in vivo within the intact vessel wall, they were named separately as hypoxic spindle-shaped SMCs (hyspSMCs) and hypoxic epithelioid SMCs (hyepSMCs).

Thus, on re-examining the original cell counts (Table 24 and Figure 44) it could be seen that the fetal intrapulmonary arteries produced 3.9 % (SE% = 0.4 %) of epithelioid cells in primary culture. Tissue from the 3 day, 14 day, and 21 day animals produced significantly higher ($p < 0.001$) percentages of epithelioid SMCs, (26.5 % (SE% = 0.9 %), 28.7 % (SE% = 0.6 %), and 28.3 % (SE% =0.8%) respectively) than the fetal arteries. The adult value of 21.7 % (SE% = 1.3 %) epithelioid cells is lower than that from the 3, 14, or 21 day old animal values ($p<0.01$) and significantly different from the fetal or hypoxic values ($p<0.001$). The tissue from hypoxic animals produced significantly more epithelioid cells (48.9 % (SE% = 1.2 %)) than tissue from the normal animals of any age ($p<0.001$).

Figure 43. Histogram showing percentage of each putative SMC phenotype during development of the intrapulmonary artery and following exposure to hypobaric hypoxia (error bars represent 1 SD).

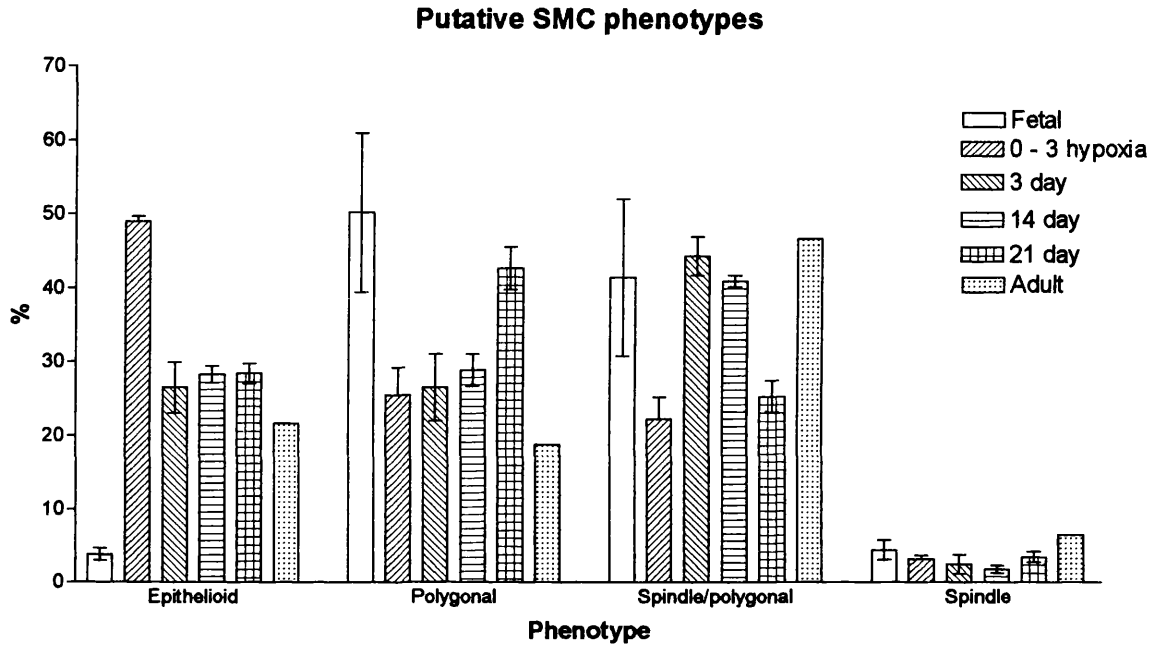

Table 23. Percentage of each putative SMC phenotype found in primary cell culture, during development of the intrapulmonary artery and following exposure to hypobaric hypoxia.

Age	Epithelioid (SD) %	Polygonal (SD) %	Spindle/polygonal (SD) %	Spindle (SD) %	Number animals
Fetal	3.8 (0.8)	50.2 (10.8)	41.5 (10.7)	4.4 (1.4)	3
0-3 hypoxic	49.0 (1.2)	25.5 (6.5)	22.3 (5.1)	3.2 (0.9)	3
3 day old	26.5 (3.5)	26.6 (4.5)	44.4 (2.6)	2.5 (1.3)	3
14 day old	28.3 (1.2)	28.9 (2.2)	41.0 (0.8)	1.8 (0.5)	3
21 day old	28.4 (1.4)	42.7 (2.9)	25.4 (2.1)	3.5 (0.8)	3
Adult	21.7	18.8	46.7	6.5	1

Figure 44. Histogram showing percentage of epithelioid and spindle-shaped SMC phenotypes seen in primary cell cultures obtained from the intrapulmonary artery during normal development and after exposure to hypobaric hypoxia (error bars represent 1 SE%).

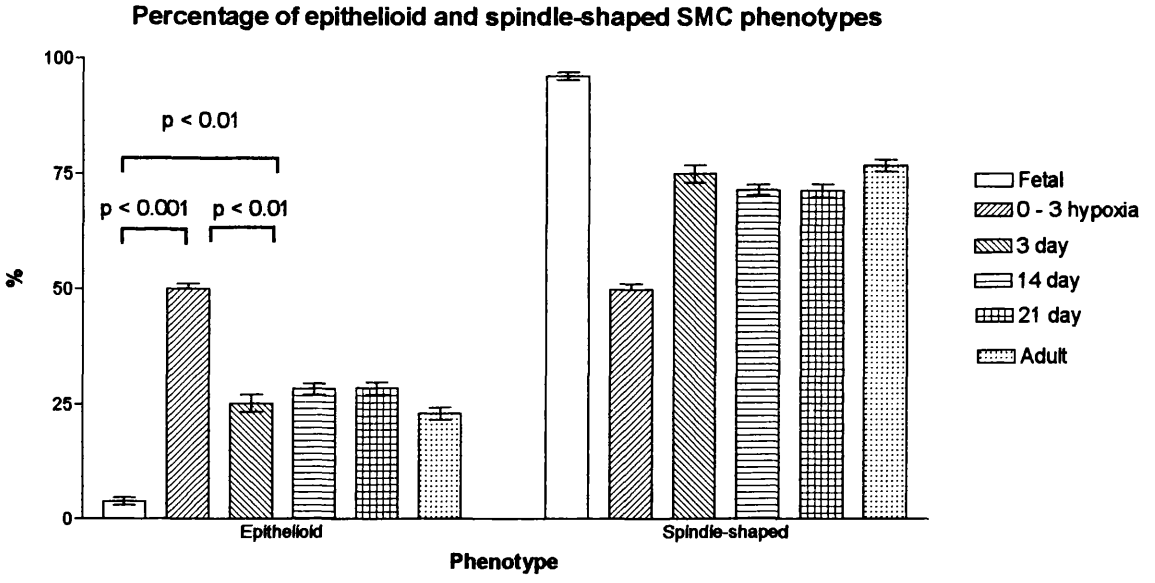

Table 24. Percentage of epithelioid and spindle-shaped SMC phenotypes seen in primary cell cultures obtained from the intrapulmonary artery during normal development and after exposure to hypobaric hypoxia.

Ages	% Epithelioid SMC (SE%)	% Spindle-shaped (SE%)	number of cells
Fetal	3.9 (0.4)	96.1 (0.4)	2067
0-3 day hypoxia	48.9 (1.2)	51.1 (1.2)	1818
3 day old	26.5 (0.91)	73.5 (0.91)	2374
14 day old	28.7 (0.6)	71.3 (0.6)	4948
21 day old	28.3 (0.8)	71.7 (0.8)	2969
Adult	21.7 (1.3)	78.3 (1.3)	953

6.1.2 *Effect of the plating substrate on smooth muscle cell morphology*

The previous experiments were carried out on fibronectin-coated coverslips. To ensure that the morphological appearance of the SMC phenotypes, viewed by phase contrast microscopy, was not determined by the cells having been grown on fibronectin, but was an inherent property of the cells, experiments were performed to determine the percentage of different SMC phenotypes growing on other commonly used cell culture substrates: glass, cell culture plastic, collagen IV, fetal calf serum, gelatin and laminin. The analysis was performed looking for the original four putative phenotypes to determine whether the different matrices had any effect on the degree of SMC polarity. These experiments were carried out on SMCs obtained from a single 14 day old piglet using the seven substrates listed above, and on SMCs obtained from a single adult animal using glass, fibronectin and collagen IV. Three coverslips were prepared with each substrate, and at least 200 SMCs counted on each coverslip.

The speed with which the cells settled on the coverslips varied. When fibronectin, laminin, collagen IV or FCS was used, cells settled and started to spread within four hours. Settling was slow when cells were plated on glass or cell culture plastic, and this would often not be complete even after 24 hours. Although the plating substance enhanced settling and spreading of all cell phenotypes, it did not change their morphological appearance. For both the 14 day old and the adult animals there was no difference between the proportions of the four putative SMC phenotypes obtained using the different plating substrates (Figure 45 and Figure 46, and Table 26). Therefore, fibronectin was considered a suitable substrate for culture of SMCs and was used for the subsequent experiments.

Figure 45. Histogram showing the effect of plating substrate on SMC phenotypes obtained from the intrapulmonary arteries of a 14 day old piglet (error bars indicate 1 SE%).

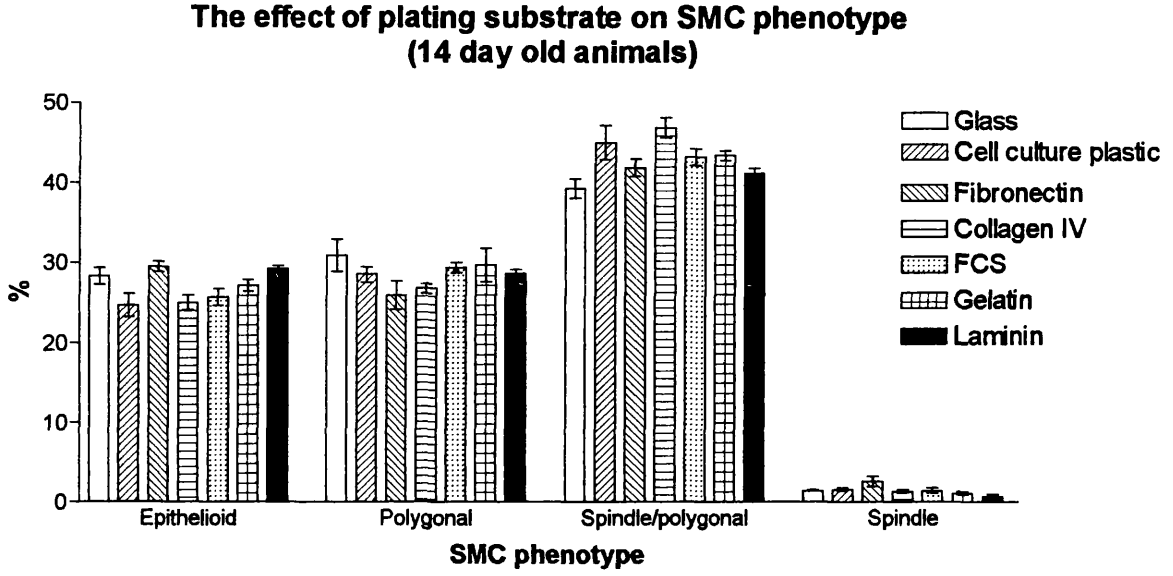

Table 25. The effect of plating substrate on SMC phenotypes obtained from the intrapulmonary arteries of a 14 day old piglet.

Substrate	Epithelioid % (SE%)	Polygonal % (SE%)	Spindle/ polygonal % (SE%)	Spindle % (SE%)	Number of cells
Glass	28.3 (0.9)	31.0 (0.9)	39.3 (1.0)	1.4 (0.2)	2627
Cell culture plastic	24.7 (0.9)	28.6 (0.9)	45.2 (1.0)	1.6 (0.2)	2573
Fibronectin	29.4 (0.9)	26.4 (0.8)	41.8 (1.0)	2.4 (0.3)	2823
Collagen IV	24.9 (0.9)	26.9 (0.9)	46.9 (1.0)	1.4 (0.2)	2419
Gelatin	29.3 (0.9)	28.8 (0.9)	41.3 (1.0)	0.6 (0.1)	2671
Laminin	27.6 (0.9)	29.8 (0.9)	43.5 (1.0)	1.1 (0.2)	2652
Fetal calf serum	25.8 (0.9)	29.4 (0.9)	43.4 (1.0)	1.4 (0.2)	2452

Figure 46. Histogram showing the effect of plating substrate on SMC phenotypes obtained from the intrapulmonary arteries of an adult pig
(error bars represent 1 SE%).

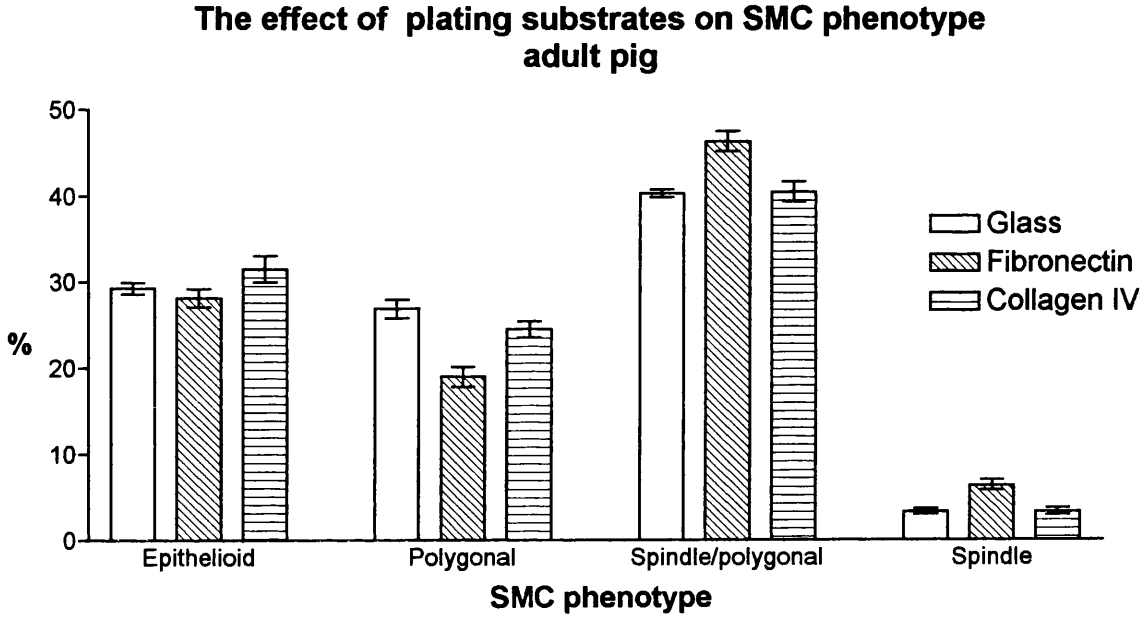

Table 26. The effect of plating substrate on SMC phenotypes obtained from the intrapulmonary arteries of an adult pig.

Substrate	Epithelioid % (SE%)	Polygonal % (SE%)	Spindle/ polygonal % (SE%)	Spindle % (SE%)	Number of cells
Glass	27.0 (1.5)	27.2 (1.5)	40.3 (1.7)	3.3 (0.6)	879
Collagen IV	31.4 (1.7)	24.7 (1.6)	40.6 (1.8)	3.3 (0.7)	754
Fibronectin	28.0 (1.5)	18.8 (1.3)	46.7 (1.6)	6.5 (0.8)	953

6.1.3 Expression of smooth muscle cell and endothelial cell-specific markers by epithelioid and spindle shaped SMCs

SMCs were isolated and cultured from the vessels of fetal, 0 - 3 day hypoxic, 3 day, 14 day, and adult animals, and were examined with the smooth muscle specific antibodies anti-α smooth muscle actin and anti- MHC SM1 isoform antibodies. After 72 hours in culture, the epithelioid phenotype SMC did not label with anti-α SM actin antibody at any age (Figure 47 (a)), but the spindle shaped SMCs showed varying degrees of staining for α SM actin (Figure 47 (b)). No SMCs, either epithelioid or spindle-shaped, labelled with anti-MHC SM1 antibodies at any age (Figure 47 (c) and (d)).

Although the nuclei of intrapulmonary arterial endothelial cells are larger than those of SMCs, the poor definition of the cell outline when viewed by phase contrast microscopy was common to both cell types. In order to prove that endothelial cells were not being mistaken for epithelioid SMCs, epithelioid SMC cultures from a 14 day old animal were exposed to the endothelial-specific antibodies, anti-CD31 and anti-von Willebrand factor. The findings were compared with those of immunostained endothelial cells isolated and cultured from the same intrapulmonary artery. No epithelioid SMCs labelled with either of these antibodies (Figure 47 (e)). However, the endothelial cells stained at the same time showed the labelling typically seen in cultured endothelial cells (Figure 47(f), (h), and control (g)).

Figure 47. Expression of SMC and endothelial-specific markers in porcine pulmonary arterial spindle-shaped and epithelioid phenotype SMCs, and in endothelial cells derived from the same artery. (a) - (d) phalloidin (red) was used to visualise the actin cytoskeleton. In (a) - (h) Hoechst 33258 (blue) was used to visualise the cell nucleus.

(a) Epithelioid SMCs do not stain for α smooth muscle actin.
(b) Spindle-shaped SMCs contain abundant α smooth muscle actin (green or yellow).
(c) Epithelioid SMCs do not stain for SM1 MHC isoform (green).
(d) Spindle-shaped SMCs do not stain for SM1 MHC isoform (green).
(e) Epithelioid SMCs do not label with anti-CD31 antibody or anti-von Willebrand factor antibodies.
(f) Isolated endothelial cells are positive for anti-CD31 antibody (green).
(g) Endothelial cells do not stain for α smooth muscle actin (green).
(h) Endothelial cells stain positively with anti-von Willebrand factor antibodies (red).
Where green labelling co-localises with red, a yellow colour is produced. Bar = 100μm

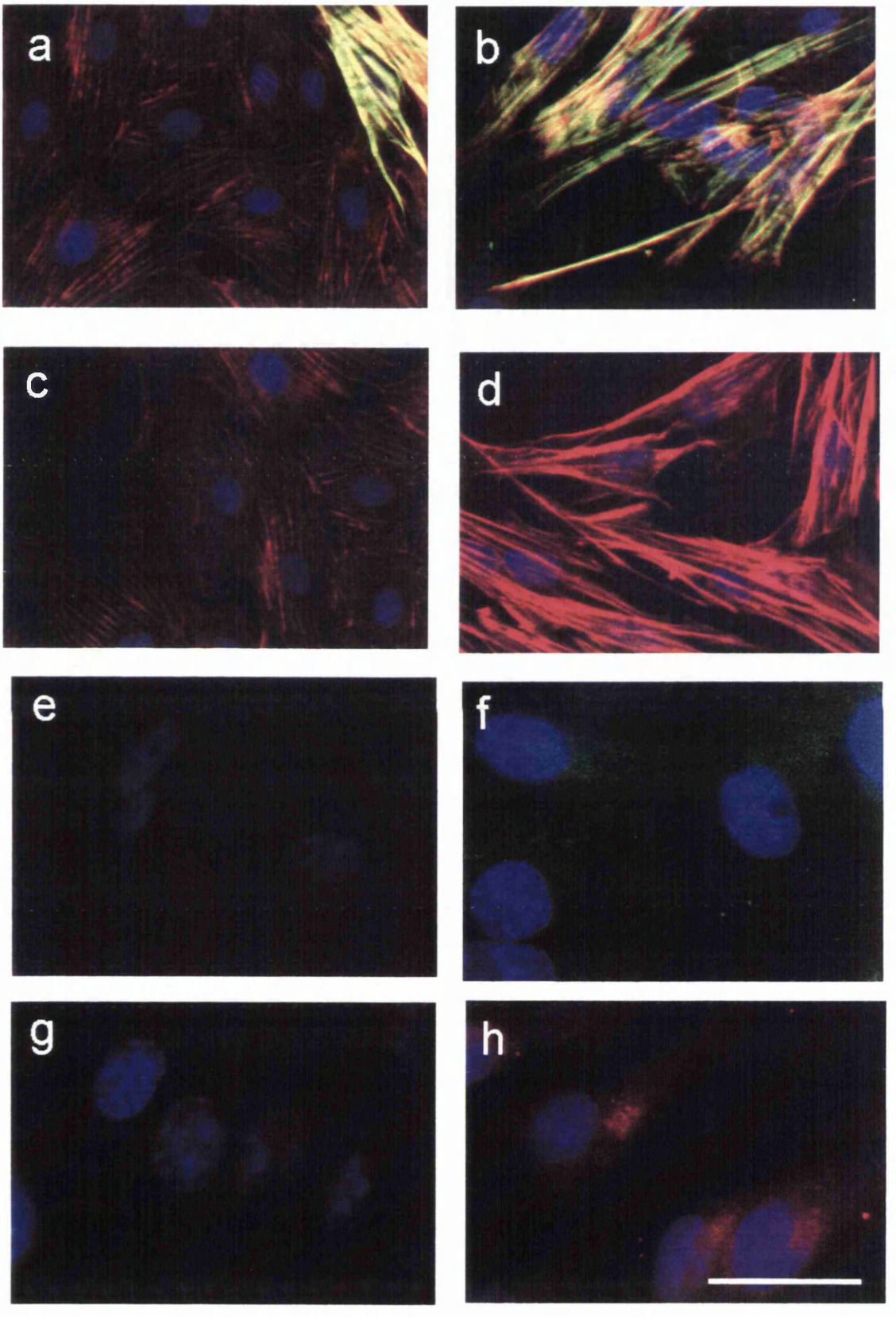
a
b
c
d
e
f
g
h

6.2 LOCATION OF SMOOTH MUSCLE CELL PHENOTYPES WITHIN THE ARTERIAL WALL

The absence of staining with anti-α smooth muscle actin by the epithelioid SMCs in primary culture was interesting as it suggested a parallel with the cells of the inner media at 3 days of age (**Chapter 3**). Experiments were therefore carried out to investigate whether the epSMCs might predominate in the inner half of the media and be responsible for the reduction in anti-α smooth muscle actin staining seen in the intact vessel wall. Tissue from two unrelated three day old animals and for comparison, tissue from one adult animal were used in this experiment.

When SMCs from the inner and outer portions of the media were cultured separately, there was no statistical difference in the percentage of epSMCs in the inner and outer halves of the media of the 3 day old, or adult animals (Figure 48 and Table 27). These data suggested that both epSMC and spSMC phenotypes occupy the inner half of the media and that after birth they both re-organise their actin cytoskeletal structure in response to a regional cue, rather than there being a phenotype-specific signal.

Figure 48. Histogram showing the percentage of epithelioid SMCs in different parts of the intrapulmonary artery wall in 3 day old and adult pigs (error bars represent 1 SE%).

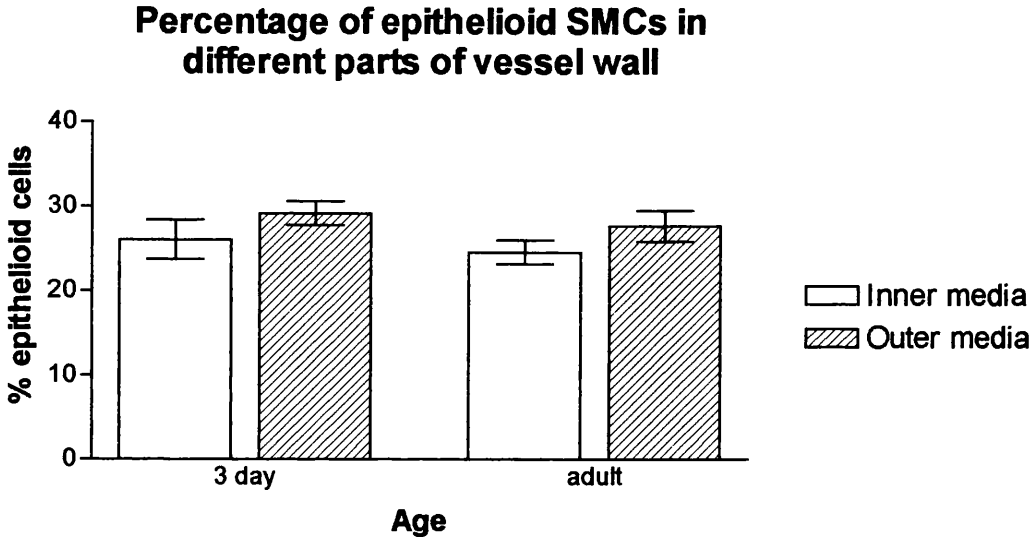

Table 27. Percentage of epithelioid SMCs in different parts of the intrapulmonary artery wall in 3 day old and adult pigs.

Region of media	% Epithelioid cells	SE%	Number of cells
Adult inner	24.6	2.3	348
Adult outer	27.2	2.4	339
3 day old inner	26.1	1.5	827
3 day old outer	29.2	1.6	824

6.3 PRODUCTION OF DEFINED CLONES OF SMOOTH MUSCLE CELLS

Dilutional cloning (Lemire et al., 1994) was necessary to produce these pure cell lines because both the epithelioid and spindle-shaped SMC phenotypes had been shown to be distributed throughout the whole media (Figure 48).

Three unrelated 14 day old piglets were used to generate epithelioid phenotype (epSMC) and spindle-shaped (spSMC) SMC clonal cell lines as detailed in **experiment 2.6** (Figure 14). This age was chosen as it seemed likely that any postnatal transitions in phenotype should have been completed at this stage. Tissue from one 0 - 3 day hypoxic piglet was available for production of hypoxic epithelioid (hyepSMC) and hypoxic spindle-shaped (hyspSMC) clones (Figure 15).

The spSMC clones appeared as "typical" SMCs with a fusiform shape and organised into parallel lines of cells within the culture dish. At confluence these lines produced the typical "hill and valley" appearance of SMCs in culture (Figure 49(f)). In contrast, the epithelioid and hypoxic epithelioid cells produced a monolayer of cells, and did not produce a hill and valley morphology (Figure 49(e) and Figure 50(b)). Unfortunately, as a result of building work, all the hypoxic spindle-shaped cells were infected with fungi and had to be discarded. Three of the five hypoxic epithelioid clones were used for migration studies and one clone survived to produce cells for other characterisation studies.

Figure 49. Appearances of epSMC and spSMC phenotypes during cloning procedure:

(a), (c) and (e) are an epSMC clone.

(b), (d) and (f) are a spSMC clone.

(a), (b) Appearance of cells at dilutional cloning step.

(c), (d) Appearance of cells when passaged onto coverslips.

(e), (f) Appearance of cells when grown to confluence in a 6 well plate.

Bar corresponds to 25 μm.

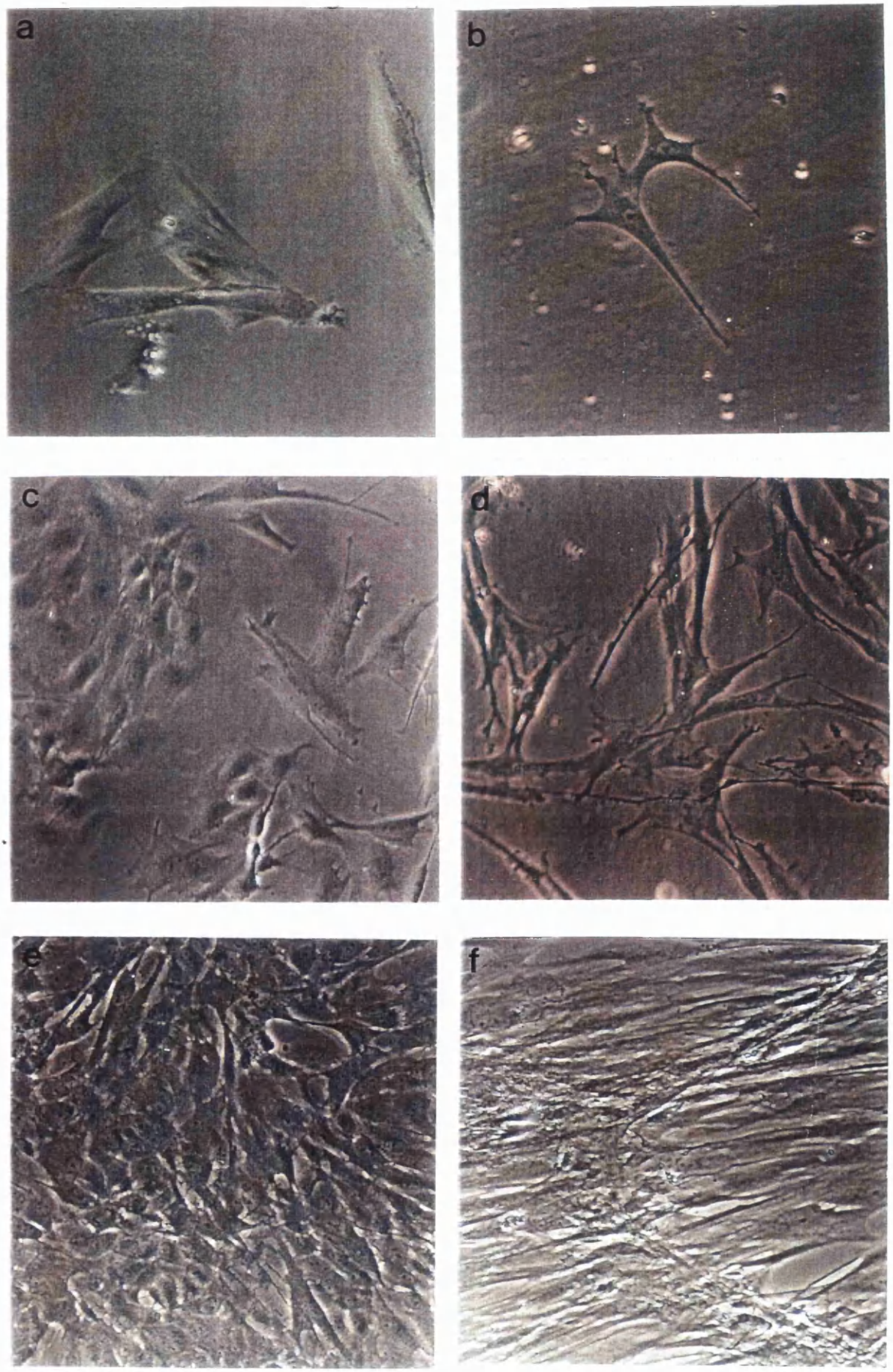
a
b
c
d
e
f

Figure 50. Appearance of hyepSMC and hyspSMC phenotypes during cloning procedure:

(a) Appearance of hyepSMC when passaged onto glass coverslip.

(b) Appearance of hyepSMC at confluence within a 6 well plate.

(c) Appearance of hyspSMCs on a glass coverslip.

Bar corresponds to 25 μm.


a


b

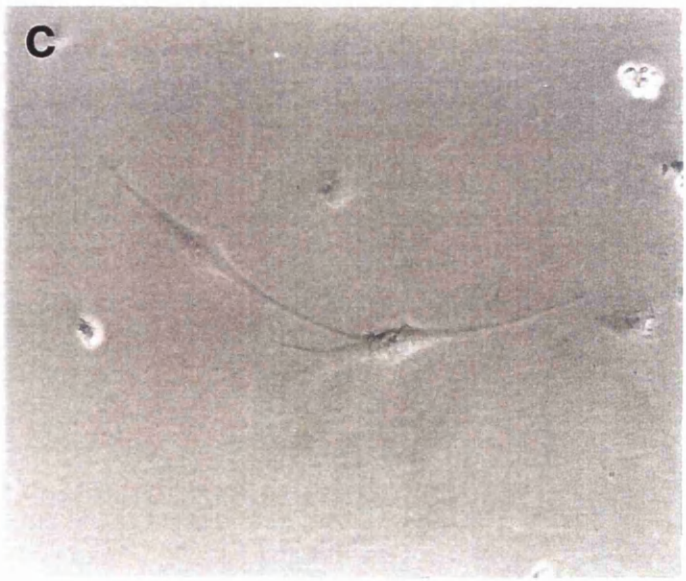
c

6.4 SUMMARY

The cloning of SMCs was performed by serial dilution (Lemire et al., 1994). This allowed production of a cell line from a single initial cell. Although a laborious method it was entirely satisfactory. Other selection methods of producing a single SMC phenotype colony, such as differential trypsinisation or different rates of cell adhesion, were not pursued, as they are subject to significant contamination with other phenotypes. Cells were cloned from 14 day old normal animals. In future experiments the experience gained in developing these methods must be directed towards isolating cells from younger animals. These cell culture studies have demonstrated that SMCs with two distinctive morphologies, epSMC and spSMC, can be derived from the normal porcine intrapulmonary artery at all ages from fetal to adult life. These morphological SMC phenotypes have been shown to retain their morphological characteristics through three passages of cells. The appearance of the SMC phenotypes was not significantly modified by the substrate on which they were grown. The spSMC phenotype behaves as a typical SMC in culture, producing a "hill and valley" appearance. The epSMC does not produce this hill and valley appearance, but remains as a monolayer. Two similar phenotypes, hyepSMC and hyspSMC, were obtained from the intrapulmonary arteries of a piglet exposed to chronic hypobaric hypoxia from birth - a model of persistent pulmonary hypertension of the newborn. It remains to be shown whether or not these hypoxic SMCs are identical in other respects to the epSMC and spSMC produced from the normal animal.

Since both epSMCs and spSMCs occur in both the inner and outer media, the changes in the actin cytoskeleton seen at three days of age within the inner part of the media do not appear to be caused by a single SMC phenotype. However, there appears to be a seven fold increase in the proportion of epSMCs contained within the whole media during the first three days of normal postnatal adaptation. In addition, exposure to hypoxia during the three days after birth produces a 12 fold increase in epithelioid phenotype cells obtained from intrapulmonary arteries which is a significantly greater increase than that seen vessels from normal animals ($p<0.001$).

Chapter 7. Results: *Characterisation of smooth muscle cell clones*

The SMC clones, epSMC, spSMC, and hyepSMC were subjected to a series of tests to examine their behaviour in culture. This was done in order to relate their appearance in culture to their appearance within the intact vessel wall, and to try and understand what different roles they might play in vivo based on their in vitro properties.

7.1 SERUM DEPENDENCE AND CONTACT INHIBITION

SMCs, like other mesenchymal cells, usually require 5 - 10% FCS to replicate in culture. The FCS provides micro-nutrients and growth factors essential to their well-being. In a reduced concentration of FCS they survive but do not replicate, and in the complete absence of serum they soon die. Other cells, notably those of neural crest origin are capable of serum independent growth. This experiment was designed to see if the epithelioid phenotype cells would behave like typical SMCs and be dependent on serum for replication.

Some cell types, for example endothelial or epithelial cells, have a reduced rate of replication when they are in contact with other cells. This is known as contact inhibition of replication. A particular feature of SMCs is that although they grow best across a clear surface, they are capable of growing and replicating over the top of each other - they do not exhibit contact inhibition of replication. The morphology of the different SMC phenotypes in culture (Figure 42) suggested that the epSMCs would show contact inhibition of replication.

A single epSMC clone and one spSMC clone from each of three different 14 day old piglets were used in these experiments, and for each epSMC or spSMC clone, three separate coverslips were tested in each set of conditions. A low power (X 10) digital image was acquired for each coverslip and the numbers of nuclei

staining with fluorescein/anti-BrdU antibody and the numbers staining with Hoechst 33258 counted (Figure 51 and Figure 52)

7.1.1 The effect of serum deprivation on cell replication

Following a 20 minute exposure to BrdU, 33.0% (SE% = 1.2 %) of non-confluent spSMCs growing in 10% FCS labelled positively for BrdU (Figure 52(a)). Non-confluent cells from the same clone grown in 1% FCS showed a three fold reduction ($p<0.001$) in BrdU positive cells to 10.1 % (SE% = 0.8 %) (Figure 52 (b)). A 7 fold reduction ($p< 0.001$), from 26.1 % (SE% = 1.4 %) to 4.0 % (SE% = 0.6 %), was similarly noted in confluent spSMC clones when grown in 10% and 1% respectively (Figure 52 (a) and (b)). This was the typical response expected of serum dependent SMCs.

In contrast, replication of epSMCs was not as dependent on high levels of FCS. Non-confluent cultures demonstrated a 43.5 % (SE% = 1.3 %) BrdU incorporation in 10% FCS (Figure 52(c)) and 38.5 % (SE% = 1.4 %) in 1% FCS ($p <0.01$) (Figure 52 (d)). Confluent cultures similarly showed 19.8 % (SE% = 1.2 %) incorporation when growing in 10% FCS (Figure 52 (c)), and 15.7 % (SE% = 0.8 %) in 1% FCS (Figure 52 (d)), again indicating only a minor degree of serum dependence ($p <0.01$). These data, although significantly different, demonstrate the replication of epSMCs are less influenced by serum deprivation than the spSMCs.

A single epithelioid clone from a 0 - 3 day hypoxic piglet (hyepSMC) was also studied. There was 48.4 % (3.7) and 44.6 % (3.9) BrdU incorporation in non-confluent cultures and 36.8 % (2.4) and 33.9% (3.9) in confluent cultures, when grown in 10% and 1% FCS respectively (Figure 52 (e) and (f)). The replication rates were not significantly different between cells grown in 1% or 10% FCS whether the cells were at confluence or not. Therefore these SMCs demonstrated serum independent replication.

7.1.2 The effect of confluence on cell replication

The greatest degree of contact inhibition was seen for epSMCs, such that for epSMCs growing in 1% FCS, contact with other cells reduced BrdU incorporation

from 38.5 % (SE% = 1.3 %) to 15.7 % (SE% = 0.8 %) (Figure 52(d)). This represented a 2.5 fold reduction in epSMC replication ($p < 0.001$). Growth in 10% FCS also produced a 2.2 fold reduction in replication ($p < 0.001$), with BrdU incorporation falling from 43.5 % (SE% = 1.3 %) to 19.8 % (SE% = 1.2 %) with confluence (Figure 52(c)).

Cell-cell contact in spSMCs growing in 1% FCS also resulted in a 2.4 fold reduction in replication ($p =<0.001$). For these cells, BrdU incorporation fell from 10.2% (SEM = 0.5%) in non-confluent cells to 4.1% (SEM = 0.3%) in confluent cells (Figure 52(b)). The presence of 10% FCS overcame the effect of contact on spSMCs. Under these conditions there was no significant reduction in replication, with 33.0% (SEM = 0.5%) of non-confluent cells compared to 27.5% (SEM = 3.2%) of confluent cells incorporating BrdU (Figure 52 (a)).

The hyepSMCs from the 0 - 3 day hypoxic piglet showed a reduction in replication rate with confluence when in low serum conditions ($p< 0.01$). In hyepSMCs grown in 1% FCS, 48.4% (SE% = 3.7 %) of non-confluent cells and 36.8 % (SE% = 2.4%) of confluent cells incorporated BrdU (Figure 52 (f)). In those cells exposed to 10% FCS there was no statistical difference found as, 44.6 % (SE% = 3.9 %) of non-confluent cells and 33.9 % (SE% = 3.6 %) of confluent cells took up BrdU (Figure 52 (e)).

Thus in summary, the spSMCs showed little contact inhibition, but a great degree of serum dependence. In contrast, the epSMCs showed little serum dependence but a large effect of contact inhibition. The epithelioid hyepSMCs were different from both these cell types, demonstrating a minor, although significant, degree of contact inhibition in low serum conditions but no significant contact inhibition in 10% FCS. The replication of hyepSMCs was not directly affected by the concentration of FCS.

Figure 51. Example of BrdU staining. The nuclei of all cells are labelled with Hoechst 33258 (blue) and the incorporated BrdU within replicating cells is labelled with fluorescein (green).

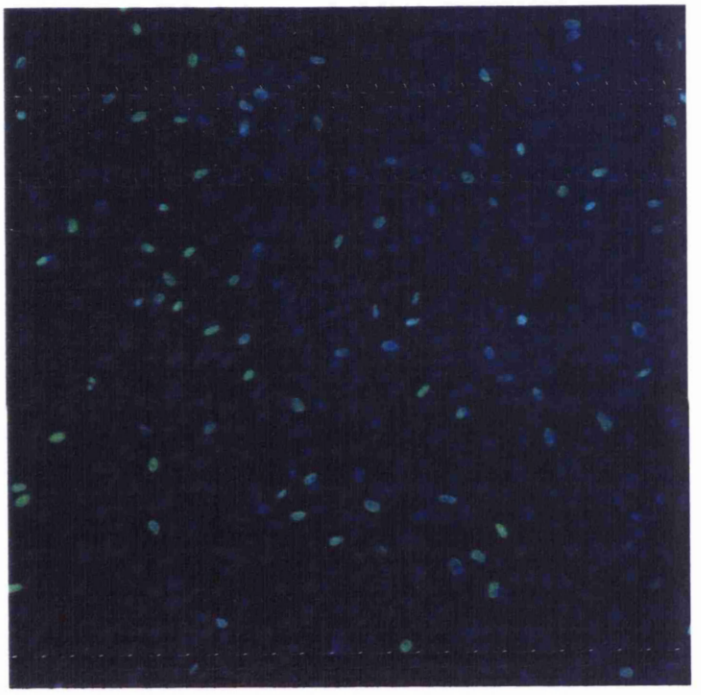

Table 28. The effect of serum deprivation and cell-cell contact on the replication rates of epSMC, spSMC and hyepSMC phenotypes.

Phenotype	%FCS	Cell-cell contact	% BrdU +ve cells	SE%	number of cells
spSMC	10%	non-confluent	33.0	1.2	1496
spSMC	10%	confluent	26.1	1.4	1026
spSMC	1%	non-confluent	10.1	0.8	1628
spSMC	1%	confluent	4.0	0.6	963
epSMC	10%	non-confluent	43.5	1.9	1378
epSMC	10%	confluent	19.8	1.2	1079
epSMC	1%	non-confluent	38.5	1.4	1304
epSMC	1%	confluent	15.7	0.8	2115
hyepSMC	10%	non-confluent	44.6	3.9	189
hyepSMC	10%	confluent	33.9	3.6	177
hyepSMC	1%	non-confluent	48.4	3.7	184
hyepSMC	1%	confluent	36.8	2.4	408

Figure 52. Histogram showing the effect of serum deprivation and cell-cell contact on the replication rates of epSMC, spSMC and hyepSMC phenotypes (error bars represent 1 SE%).

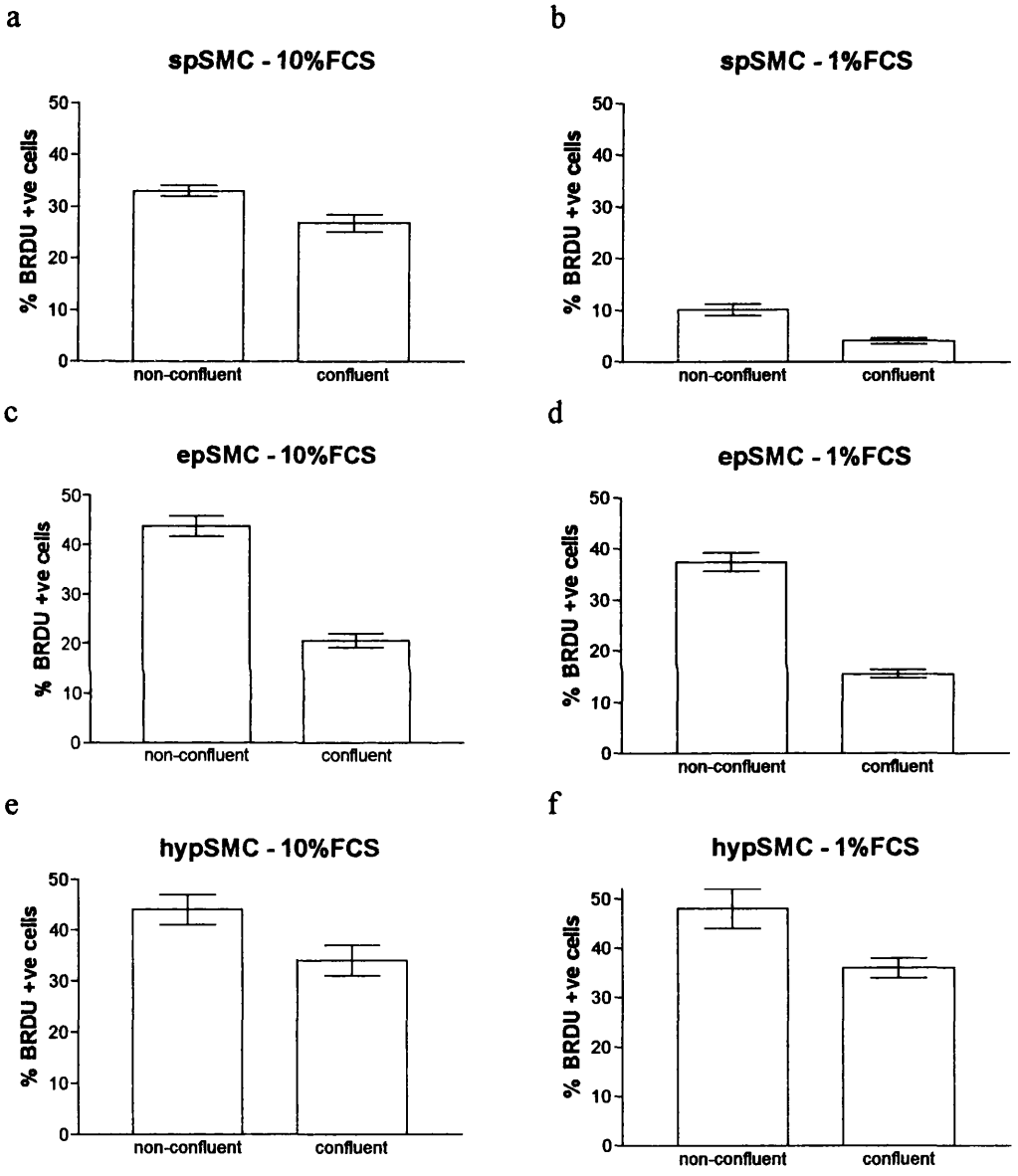

7.2 CELL MIGRATION - WOUND HEALING ASSAY

If a monolayer of confluent cells is damaged, the remaining cells fill the gap, either by movement and/or replication (Gabbiani et al., 1984a). These experiments were performed to analyse the movement of cells in culture in response to such a stimulus. They were carried out using clonal cell lines that had been passaged twice since primary culture, and had formed confluent monolayers on fibronectin-coated coverslips. A total of six coverslips were examined. Each coverslip contained an entire clonal population of either epSMCs or spSMCs derived from the intrapulmonary arteries of 14 day old piglets - animals A, B, and C (Figure 14) In addition three coverslips, containing three different hyepSMC clones were also examined. They were derived from the same artery of a single piglet (Animal D) exposed to chronic hypobaric hypoxia (Figure 15).

7.2.1 Spindle-shaped SMCs from the normal intrapulmonary artery (spSMC)

During the creation of the wound in the spSMC monolayers, the cells at the newly exposed edges were seen to retract. In one spSMC monolayer (spSMC-B) there was a further increase in the size of the monolayer during the first two hours of the experiment (Figure 56(a)). Apart from this, the behaviour of all three spSMC monolayers was similar. During the first few hours after injury, the leading edge of SMCs separated from the monolayer behind (Figure 53). The detached group of cells tended to separate from each another, but no migration towards the centre of the wound was seen. No other cells migrated out of the confluence of SMCs and the wound did not close during the 14 hours of the experiment. After 6 to 8 hours of the experiment refractile cells were seen to lift off the monolayer of all three spSMC clones. The monolayer of cells surrounding these refractile cells remained complete. As refractile cells were seen in areas of the monolayer distant from the wound it is unlikely that this represents lifting of cells physically damaged during the creation of the wound.

7.2.2 epithelioid SMCs from the normal intrapulmonary artery (epSMC)

In contrast to the spSMC monolayers, when an artificial wound was created in the epSMC monolayers, the SMCs at the edge of the wound only retracted a little way and the wound remained small (Figure 54). In order to properly compare cell migration between SMC phenotypes, a wound of a similar size to that with the spSMC monolayers was created. Within two hours of producing this wound there was spreading of epithelioid-shaped SMCs across the breach to reduce the diameter of the wound (Figure 56(b)). This not only involved SMCs at the wound edge migrating forward, but also migration of those cells in the rows behind (Figure 54). The epSMCs maintained cell contact with each other as they migrated across the wound and no separation of cells, as occurred with spSMCs was seen. During the 14 hour duration of the experiments two of the epSMC clones reduced the size of the wound by approximately 50% and one epSMC clone completely closed the breach (Figure 56(b)). As with the other SMC phenotypes, refractile spherical cells were also seen throughout the epSMC monolayers and occurred to the same extent as with the spSMCs.

7.2.3 Epithelioid SMCs from the intrapulmonary artery following hypoxia (hyepSMCs)

The production of the artificial wound in this monolayer was associated with a small degree of edge retraction which was similar to that of the epSMC monolayers, but not as marked as that seen with the spSMC monolayers. The hyepSMCs did not show any evidence of cell migration or separation of cells to heal the wound (Figure 55 and Figure 56 (c)). Lifting of refractile cells was seen with the hyepSMC monolayers with the same appearance and to the same extent as noted with the epSMC and spSMC monolayers.

7.2.4 Summary

These three morphological SMC phenotypes demonstrated three different migratory patterns in response to an identical stimulus. The epSMCs showed wound healing behaviour, by rapid spreading of the monolayer, without loss of

cell-cell contact. In contrast, the spSMC monolayers, comprised of "typical" SMCs showed migration of individual cells into the wound but the breach was not healed. Although this is a form of wound healing it was not as dramatic as that seen with the epSMCs. The hyepSMCs were different from both of the other SMC phenotypes, showing no evidence of individual cells separating from the monolayer and moving into the wound, or migration of the monolayer to close the wound. Lifting of cells was seen in all the different monolayers. This did not seem to be associated with the wound, but seemed to be a property of the SMCs in general as it occurred across the monolayers. It may have indicated replication of cells or lifting of cells in response to the culture conditions.

Figure 53. Serial photographs taken at two hour intervals, for a duration of 14 hours, showing the poor migration behaviour of spSMCs into an artificial wound created in the SMC monolayer. Arrow heads indicate separating cell.
Bar = 100 μm

Figure 54. Serial photographs taken at two hour intervals, for a duration of 14 hours, showing the migration behaviour of epSMCs into an artificial wound created in the SMC monolayer.
Bar = 100 μm

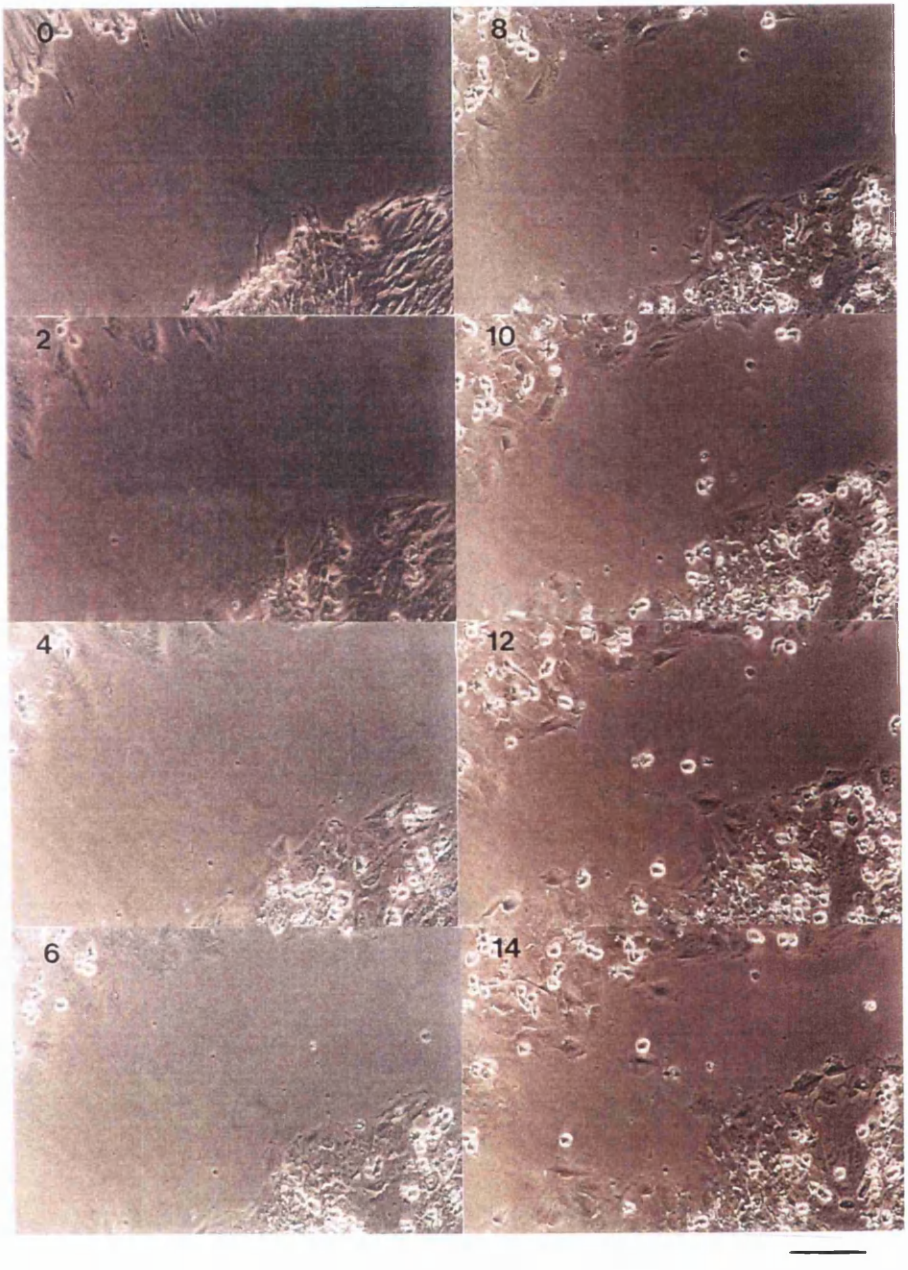

Figure 55. Serial photographs taken at two hour intervals, for a duration of 14 hours, showing the migration behaviour of hyepSMCs into an artificial wound created in the SMC monolayer.
Bar = 100 μm

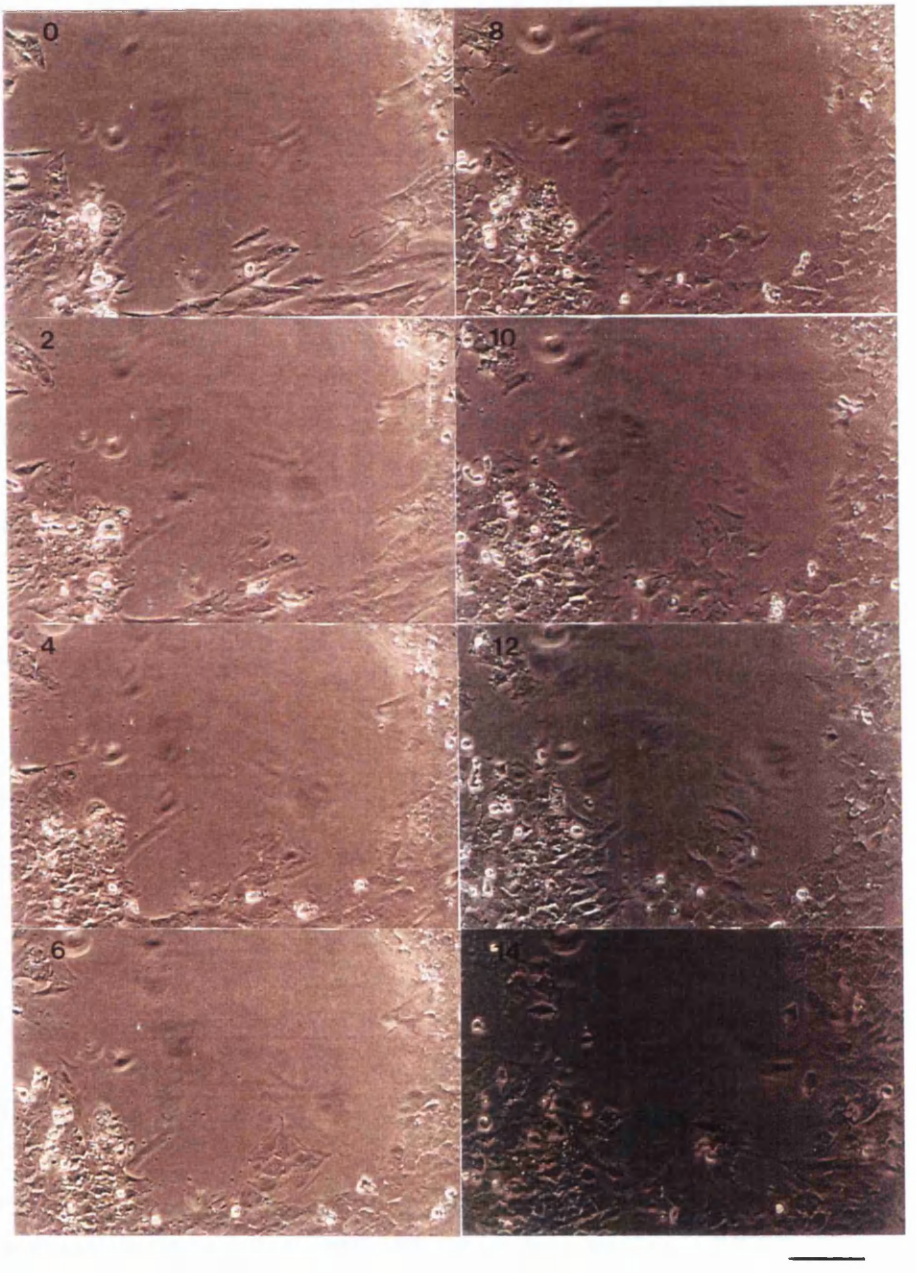

Figure 56. Graphs demonstrating the migration behaviour of individual SMC clones of epSMC, spSMC and hyepSMC phenotype, as indicated by a reduction in size of the artificial wounds in the cell monolayer:
(a) spSMC clones, from each 14 day old piglet A, B and C
(b) epSMC clones, from each 14 day old piglet A, B and C
(c) hyepSMCs Clone from 0-3 day hypoxic piglet D, coverslips 1, 2, and 3

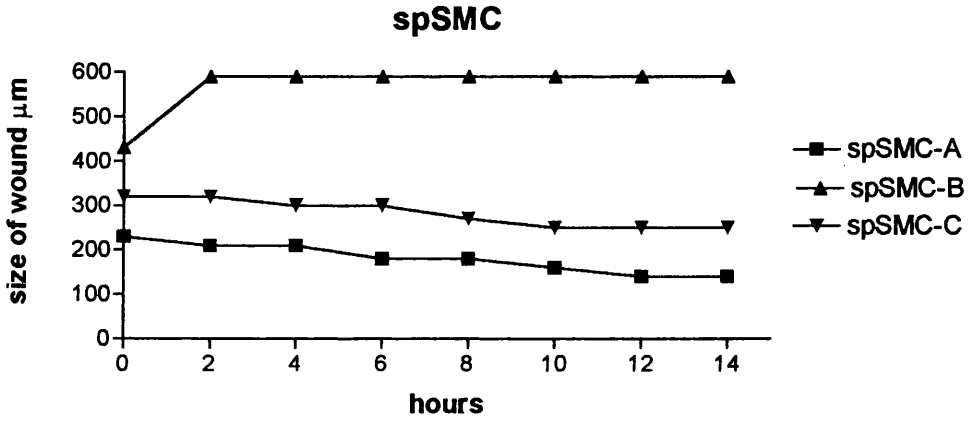

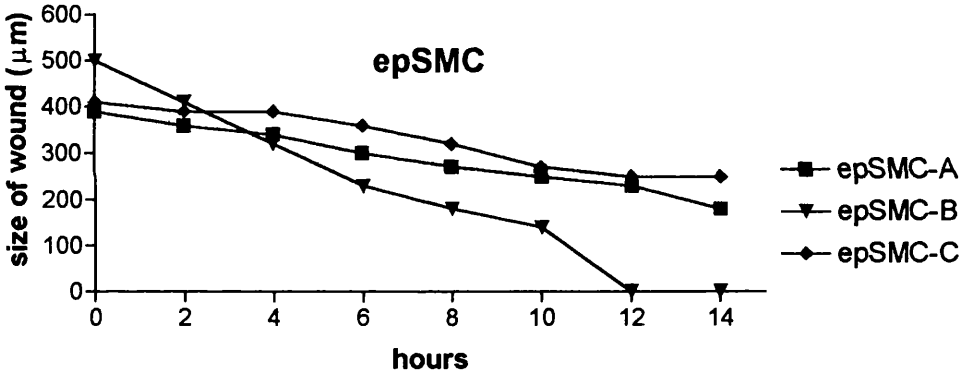

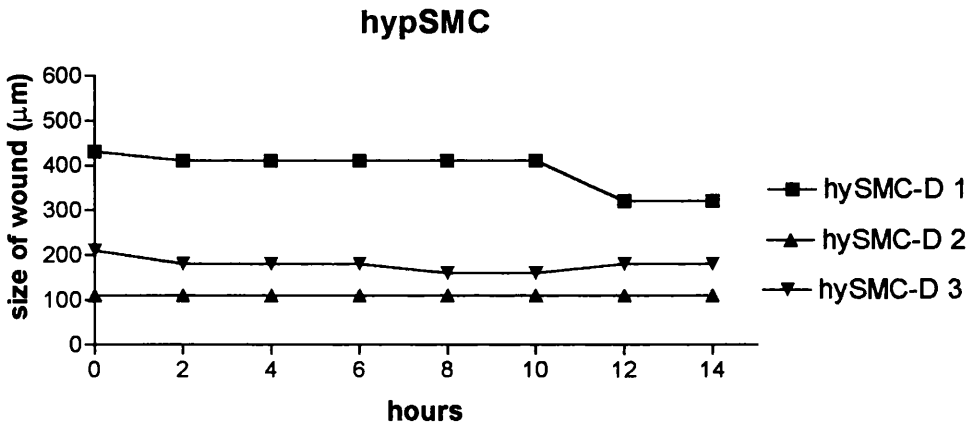

7.3 EXPRESSION OF CYTOSKELETAL PROTEINS BY IMMUNOCYTOCHEMISTRY

The clones of cells were examined by immunolabelling for the same cytoskeletal proteins as in the tissue sections from the whole vessel wall (**Chapter 3**). The aim of these experiments was not only to look for differences that would suggest specific SMC phenotypes in the cloned cells, but also to link expression of proteins within the intact vessel wall with those expressed in cultured cells.

7.3.1 General considerations

To allow identification of cellular architecture, the filamentous actin cytoskeleton of the cultured cells was identified by staining with rhodamine-phalloidin (red). The other cytoskeletal proteins of interest were labelled with fluorescein (green). The appearances of cells were therefore: red, no positive antibody staining; yellow, which was the combination of red (rhodamine-phalloidin) and green suggesting co-localisation of the antibody; or green, where there was a significant excess of the fluorescein, compared to the rhodamine phalloidin, which did not exclude co-localisation.

The appearances of the actin cytoskeleton, viewed with rhodamine-phalloidin, of the epSMCs and the spSMCs were different. The spSMCs generally had abundant stress fibres, which were orientated in the long axis of the cell. These appeared to be more prominent at the cell margins, although this could be artifactual (Keller and Bebie, 1996). The epSMCs generally had a more polygonal shape and although many of the stress fibres followed the long axis, other fibres lying parallel to other cell edges were seen to cross them. The stress fibres of the epSMCs appeared to be finer than those of the spMCs. The filamentous actin cytoskeleton of the hyepSMCs was similar to that of the epSMCs, as might be expected from their similar morphology.

7.3.2 Alpha smooth muscle actin

The spSMCs stained strongly with anti-α smooth muscle actin antibody (Figure 57 (a)). The staining produced a generally uniformly green colour, except for a few fibres at the cell periphery, suggesting most of the stress fibres were composed of α smooth muscle actin. The epSMCs (Figure 57(e)) also labelled throughout the cell with anti-α smooth muscle actin antibody but in contrast to the spSMCs, the staining at the centre of the epSMCs generally appeared more intensely green than the stress fibres at the periphery of the cells. The staining pattern of the hyepSMCs (Figure 57 (i)) was similar to the epSMCs, although the intensity of staining appeared greater in the hypoxic cells.

7.3.3 Beta actin

There was relatively little anti-β actin antibody labelling within the spSMCs which tended to be confined to stress fibres at the periphery of the cells. These areas of anti-β actin antibody labelling coincided with areas that did not stain intensely for α smooth muscle actin (compare Figure 57 (a) with (b)). Anti-β actin antibody labelled the central area of the epSMCs green and also produced some yellow in stress fibres running throughout the cell (Figure 57 (f)). This pattern was similar to that of the epSMCs with anti-α smooth muscle actin antibody. The hyepSMCs showed strong staining with anti-β actin antibody throughout the cell (Figure 57 (j)). The staining pattern was intensely green at centre the cell and yellow in the peripheral stress fibres.

7.3.4 Gamma actin

The spSMCs stained weakly with anti-γ actin antibody in many cells but more strongly in others, labelling stress fibres throughout the cell (Figure 57 (c)). A similar variability was seen in the epSMCs, with some cells staining strongly throughout the actin cytoskeleton and others only exhibiting weak staining (Figure 57 (g)). Interestingly, the majority of the stress fibres within the hyepSMCs stained well with anti-γ actin antibody (Figure 57 (k)).

7.3.5 Myosin heavy chain SM1 isoform

None of the phenotypes stained with the anti-SM1 myosin antibody (Figure 57 (d), (h), (I)). Whilst it is possible that the acetone fixation affected the epitope for the antibody, it is more likely that these cells do no express sufficiently large amounts of SM1 myosin heavy chain protein when in sub-confluent culture.

7.3.6 Desmin

Neither the spSMCs or the epSMCs labelled with the anti-desmin antibody (Figure 57 (m), (q)). In contrast, all the hyepSMCs labelled with the antibody showing a yellow/green staining pattern throughout the entire cytoplasm (Figure 57 (u)).

7.3.7 Vinculin

The anti-vinculin antibody produced punctate areas of staining at the end of stress fibres, revealing the focal adhesions, through which the SMCs attach to the fibronectin substrate (Figure 57 (n), (r), (v)). The density and size of the focal adhesions appeared to be similar in the spSMCs, epSMCs and hyepSMCs.

7.3.8 Calponin

The spSMCs, epSMCs and hyepSMCs all labelled with the anti-calponin antibody with a similar staining pattern in all three SMC phenotypes (Figure 57 (o), (s), (w)). In all cells there was strong staining in the central cytoplasmic portion of the cell and at the cell margins, but in general the antibody did not appear to co-localise with the filamentous actin cytoskeleton.

7.3.9 Caldesmon

The anti-caldesmon antibody labelled both the spSMCs and the epSMCs. Interestingly the staining was confined to the perinuclear area in both these SMC phenotypes (Figure 57 (p), (t)). No labelling was seen in the hyepSMCs (Figure 57 (x))

Figure 57. Immunocytochemical labelling of cultured SMCs. The cells in the first column are all spSMCs ((a) to (p)), those of the middle column all epSMCs ((e) to (t)) and the last column hyepSMCs ((i) to (x)). The filamentous actin cytoskeleton of all cells was labelled with rhodamine-phalloidin (red) and all nuclei with Hoechst 33258 (blue). The following antibodies appear green/yellow in the images:

(a) (e) (i) are labelled with anti-alpha smooth muscle actin antibody

(b) (f) (j) with anti-beta actin antibody

(c) (g) (k) with anti-gamma actin antibody

(d) (h) (I) with anti-SM1 antibody

(m)(q) (u) anti-desmin antibody

(n) (r) (v) anti-vinculin antibody

(o) (s) (w) anti-calponin antibody

(p) (t) (x) anti-caldesmon antibody

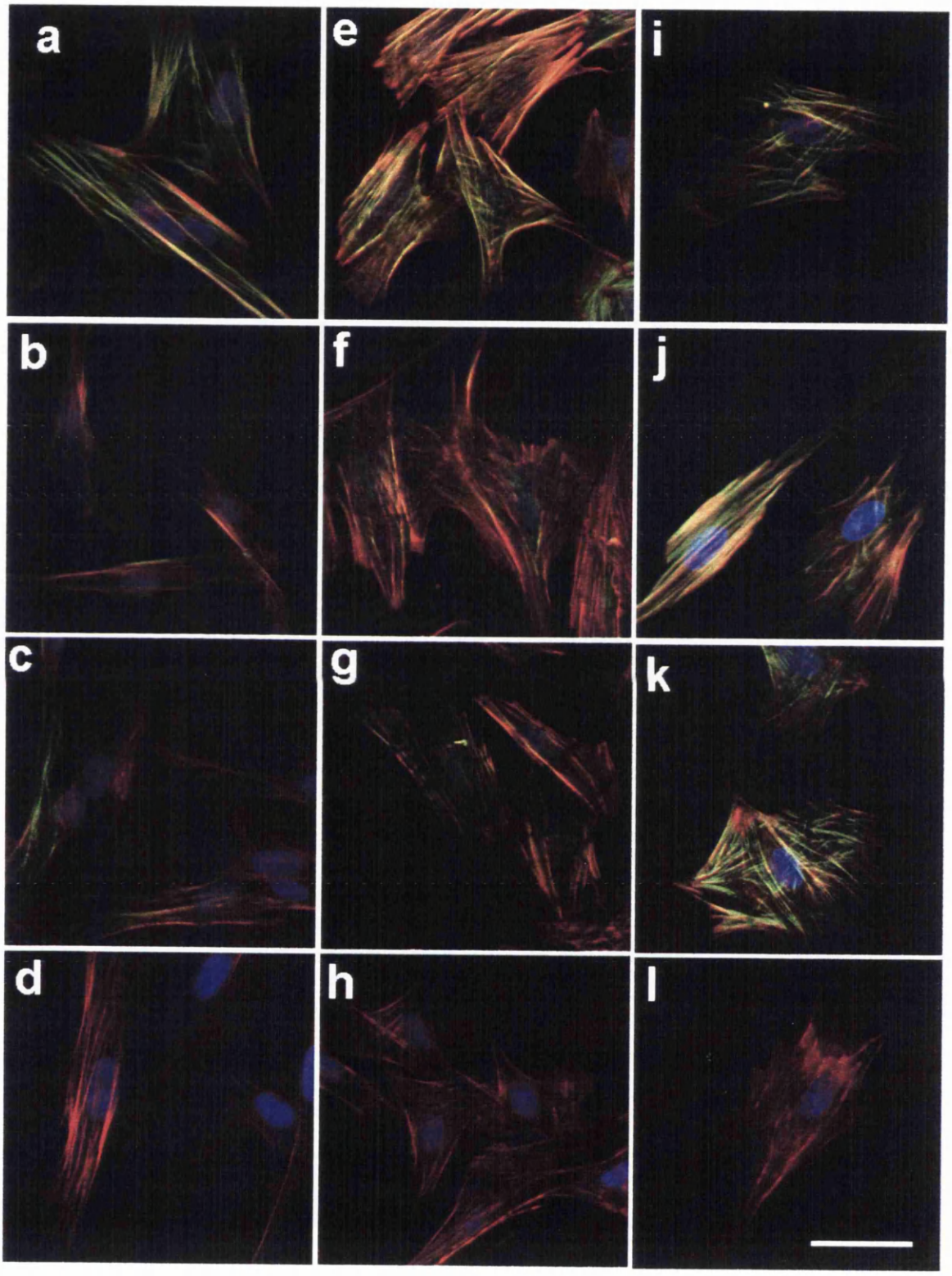
a
e
i
b
f
j
c
g
k
d
h
l

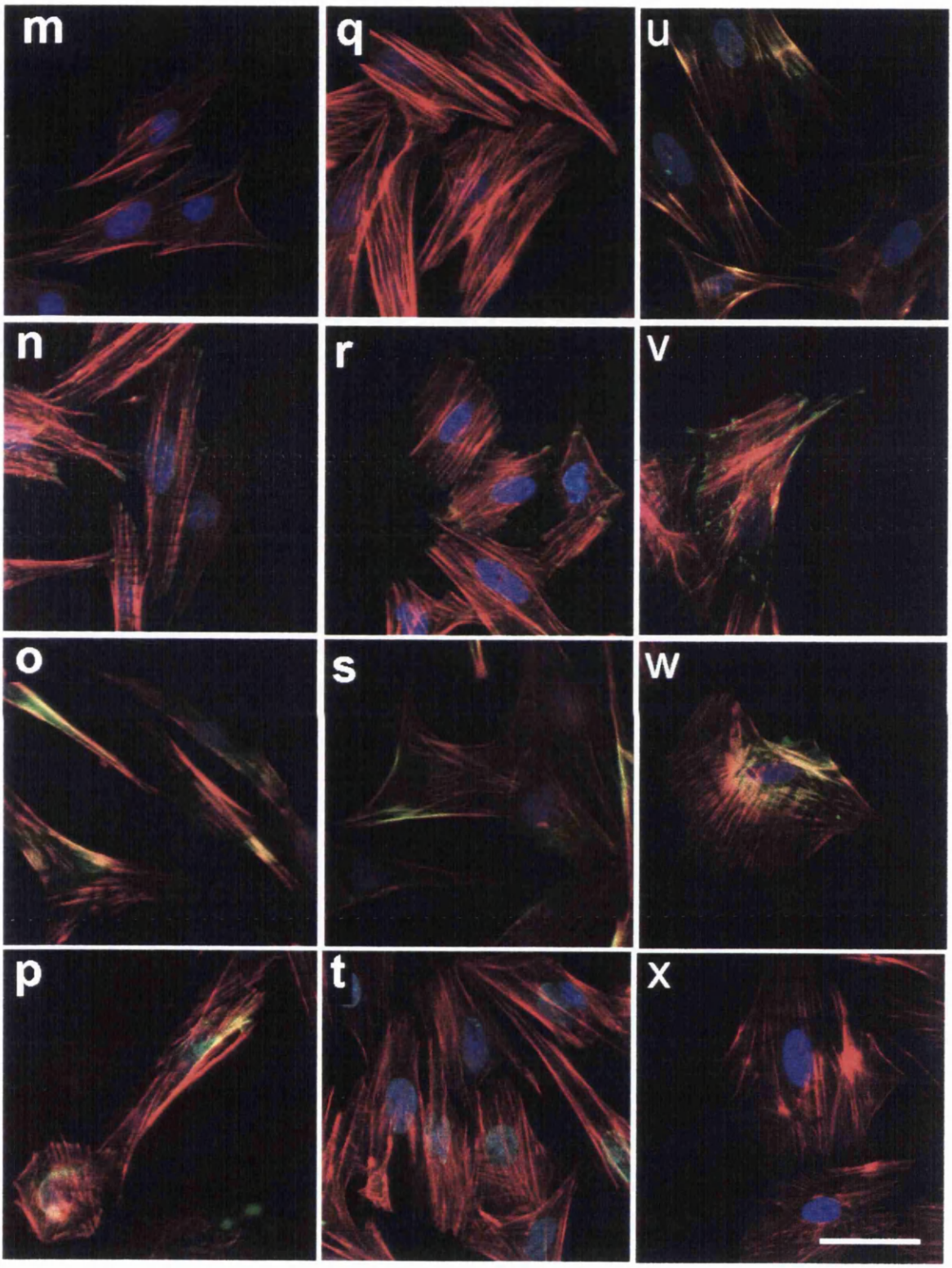
m
q
u
n
r
v
o
s
w
p
t
x

7.3.10 Summary of cytoskeletal staining patterns in clones of SMCs of different morphological phenotype

Table 29. The expression pattern of cytoskeletal proteins in cultured SMC clones obtained from intrapulmonary arteries of normal 14 day old piglets and from piglets exposed to hypobaric hypoxia from birth until 3 days of age. The staining pattern within individual cells is described from absent (-) to abundant (+++).

Cytoskeletal protein	spSMC	epSMC	hyepSMC
α smooth muscle actin	+++	++	+++
β actin	+	+	+++
γ actin	++	+	+++
SM1	-	-	-
Desmin	-	-	++
Vinculin	++	++	++
Calponin	++	++	++
Caldesmon	+	+	-

All the phenotypes contained α, β and γ actin (Table 29), but the possibility that the spSMCs contained more of these proteins than the epSMCs and that the hyepSMCs contained more than either the epSMC or spSMCs cannot be determined by immunostaining techniques alone and must also be addressed in the future by western blotting. It is possible that staining for actin isoforms was strongest when labelling thick actin filament bundles rather than thin actin filaments. The expression of desmin by the hyepSMCs but not the spSMCs and epSMCs mirrors the findings in the intact vessel walls from which these different SMCs were derived. Similarly the labelling with caldesmon of the spSMCs and epSMCs, but not the hyepSMCs mirrors the general staining characteristics of the intact vessel wall in normal 14 day old piglets and hypoxic piglets. Furthermore, it is particularly interesting to note that these normal and hypoxic cultured cells continue to differentially express desmin and caldesmon many weeks after being isolated from the vessel wall. Thus, desmin appears to represent a stable phenotypic marker of cultured hyepSMCs, and caldesmon a stable marker of both spSMCs and epSMCs derived from the intrapulmonary arteries of normal 14 day old piglets.

The lack of staining for the MHC SM1 isoform, limited perinuclear staining with anti-caldesmon and the spatial distribution of calponin were important findings because they indicate that these SMC phenotypes might not be capable of significant contraction in the culture environment.

Wrinkling experiments were performed to investigate if these SMC phenotypes were capable of contraction and relaxation in vitro.

7.4 GENERATION OF TENSION BY CULTURED SMCS

One of the key characteristics of SMCs is their ability to generate tension (Alberts et al. 1999). If SMCs are grown on a deformable silastic membrane, the contractile force generated by the cell can be observed by the appearance of wrinkles on the membrane surface (Harris et al., 1980). These experiments were carried out to compare the ability of the spSMCs, epSMCs and hyepSMCs to generate wrinkling of a standard silastic membrane. Because cells do not normally settle or spread well on a silastic membrane, the membranes were coated with fibronectin. As in the previous experiments, three epSMC and three spSMC clones derived from the pulmonary arteries of 14 day old piglets, and one hyepSMC clone were examined. Three different silastic membranes were examined for each clone of cells.

All three smooth muscle cell phenotypes (spSMC, epSMC and hyepSMC) were able to generate wrinkles on the silastic membranes, suggesting that they could generate a basal tension on the substratum to which they attach (Figure 58 (a) (b), Figure 59 (a) (b), Figure 60 (a) (b)). Potassium chloride, which causes contraction directly, and not via receptors, was added to each of the three clones of each SMC phenotype. There was no increase in wrinkling in any of the silastic membranes, from any of the three SMC phenotypes examined (Figure 58 (c), Figure 59 (c), Figure 60 (c)). This suggested that either the SMCs were in a maximally shortened state beforehand, or that they were not capable of contracting to potassium chloride. To test this, other silastic membranes containing the three SMC phenotypes were treated with sodium nitroprusside, which causes SMC relaxation via the nitric oxide pathway. Of the nine epSMC, nine spSMC and three hyepSMC membranes examined (Figure 58 (d) Figure 59(d), Figure 60 (d)), only one group of epSMCs showed a reduction in silastic membrane wrinkling (Figure 59 (d)).

This suggests that the wrinkling observed on the silastic membranes was not necessarily due to the contractile function of the SMCs but might simply be due to the effect of attaching to the substratum. In addition, since the SMCs in primary culture did not label with anti-SM1 MHC antibody, it is also possible that the SMCs in culture do not express sufficient smooth muscle-specific myosin to be

capable of contraction with potassium chloride, or relaxation with sodium nitroprusside on membranes with this degree of stiffness.

Figure 58. Appearances of spSMCs grown on fibronectin-coated silastic membranes in response to contractile and relaxant agonists.

(a) and (b), prior to treatment

(c) following exposure to potassium chloride

(d) following exposure to sodium nitroprusside.

Bar corresponds to 25μm

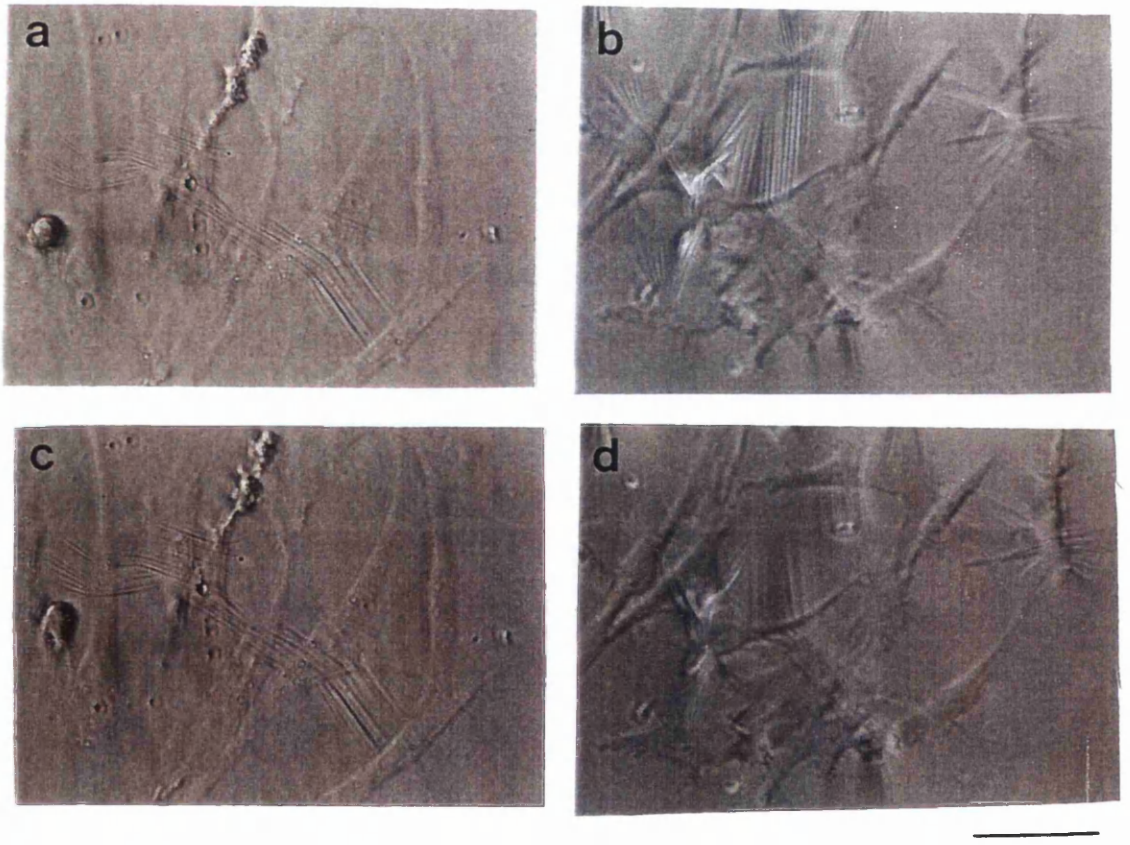

Figure 59. Appearances of epSMCs grown on fibronectin coated-silastic membranes in response to contractile and relaxant agonists.

(a) and (b), prior to treatment

(c) following exposure to potassium chloride

(d) following exposure to sodium nitroprusside.

Bar corresponds to 25μm

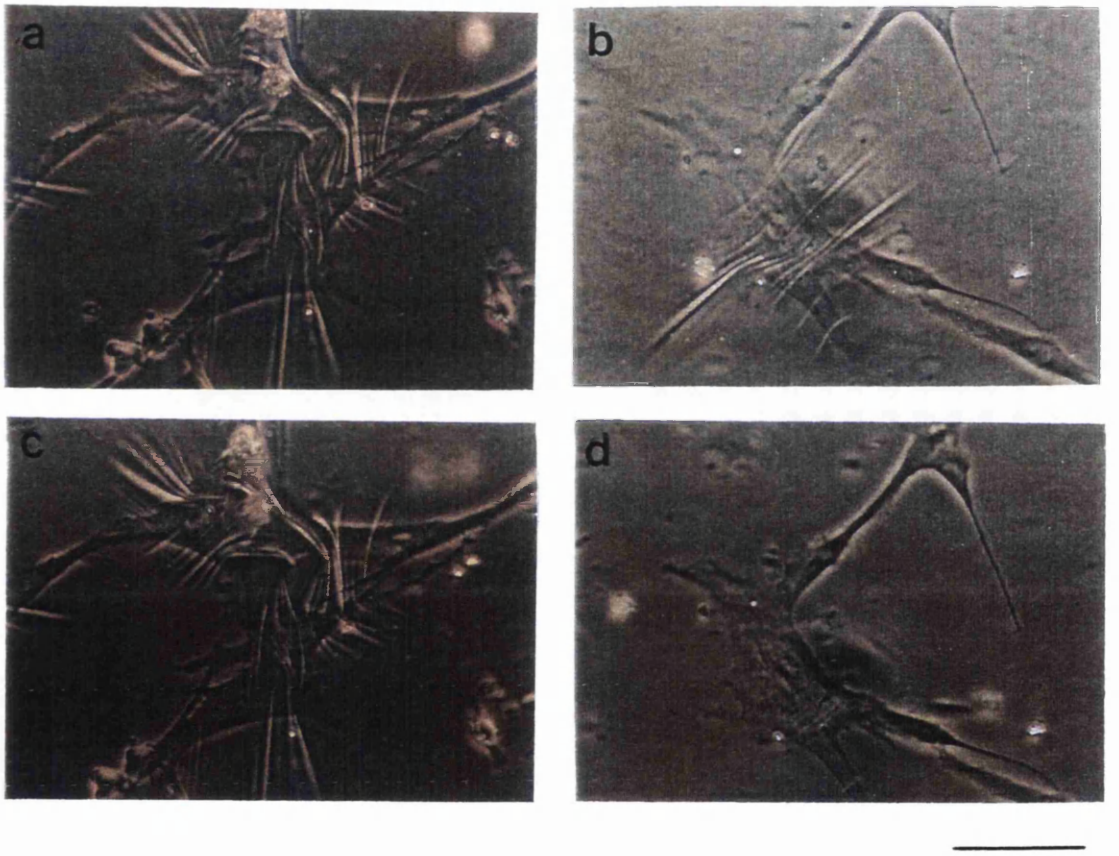

Figure 60. Appearances of hyepSMCs grown on fibronectin-coated silastic membranes in response to contractile and relaxant agonists.

(a) and (b), prior to treatment

(c) following exposure to potassium chloride

(d) following exposure to sodium nitroprusside.

Bar corresponds to 25μm

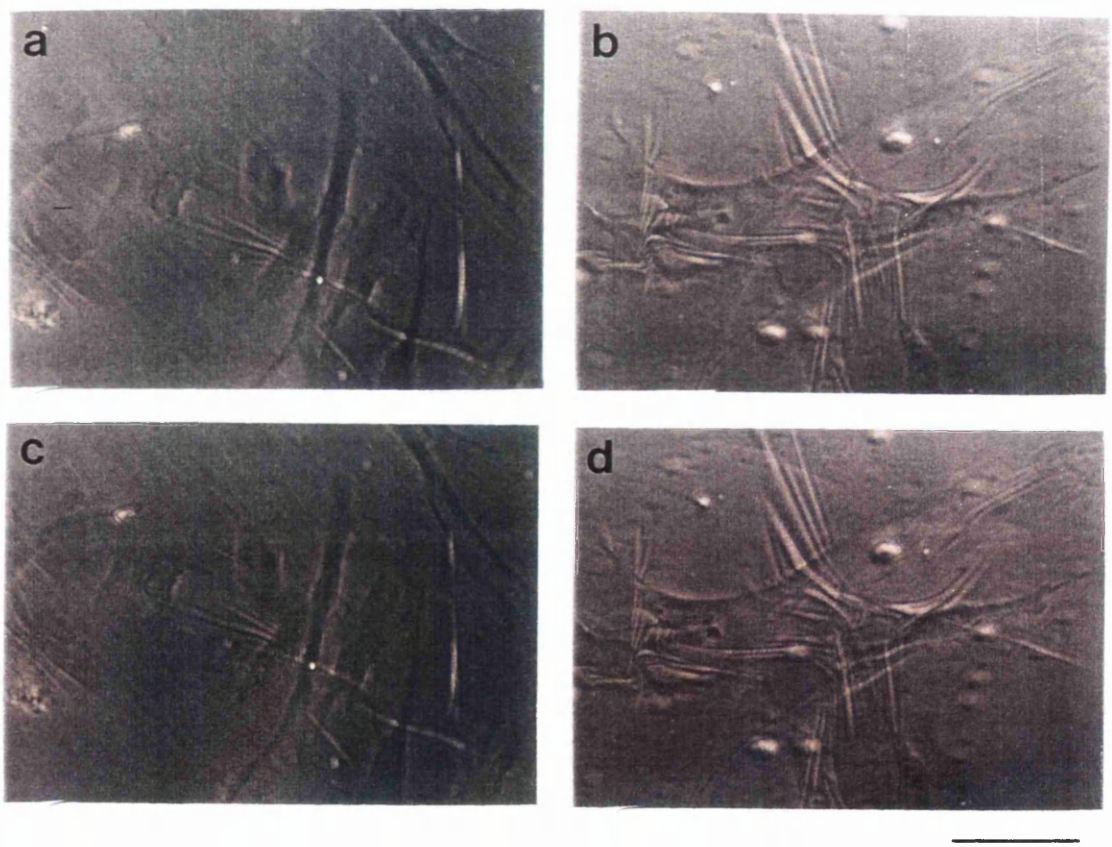

7.5 SUMMARY OF CHARACTERISATION EXPERIMENTS

Enzymatic digestion of tissue (**experiment 2.7.1**) was chosen as the method to isolate SMCs, rather than using the explant technique, on the theoretical basis that it would liberate all cells from the tissue without bias. In retrospect this judgement was correct. Considering the characteristics of the different SMC phenotypes which were obtained, it is clear that if the explant method had been used, selection of only one SMC phenotype would have occurred as the spSMCs would have separately migrated out whilst the epSMCs remained in contact with the explant. The experiments to characterise the SMC phenotypes further demonstrated that all 3 morphological SMC phenotypes studied have different properties from each other in cell culture. The epSMCs show significant contact inhibition when in confluent culture, but are relatively independent of FCS for replication. They are only able to migrate as a confluent monolayer. In contrast, the spSMCs are dependent on high levels of FCS for replication, but have little contact inhibition in comparison to the epSMCs. They do not migrate as a monolayer, but individual cells are able to migrate off separately. The limited number of studies in hyepSMCs suggest that these SMCs resemble the epSMCs, as might be expected from their shape, but that they are different from the epSMCs as their replication is independent of the concentration of FCS, they are only moderately inhibited from replicating by contact with other cells. They show no migration as a monolayer or as individual cells.

The hyepSMCs specifically contain desmin but not caldesmon, whilst the epSMCs and spSMCs contain caldesmon but not desmin. The expression of desmin, and the reciprocal pattern of caldesmon in these cells do follow the patterns seen in the initial cryo-ultramicrotomy sections and may be useful markers of SMC phenotype. Although all three morphological phenotypes express α SM actin they do not contain appreciable quantities of SM1 MHC isoform. This may explain why they did not contract well and failed to produce increased wrinkling in response to potassium chloride. Only one group of epSMCs relaxed with sodium nitroprusside.

Chapter 8. Discussion

Persistent pulmonary hypertension of the newborn (PPHN), is a serious disease process with significant mortality and morbidity, which is assumed to represent a failure of postnatal adaptation in newborn human infants (Haworth and Reid, 1976).

The cardiovascular system of the pig is similar in many respects to that of the human and therefore this animal is frequently used to model human disease. Previous studies from the Institute of Child Health have evaluated and compared the porcine pulmonary circulation with that of the human (Haworth and Hislop, 1981) and found it to be satisfactory for our purposes. The pathological changes of PPHN can be modelled by exposure of neonatal piglets to chronic hypobaric hypoxia (Haworth and Hislop, 1982). The studies described in this thesis were carried out to further the understanding of the events that surround the adaptation of the pulmonary circulation to the extra-uterine environment at the time of birth, and to understand the changes seen using the porcine model of PPHN.

The experimental approach taken was to investigate the cytoskeletal characteristics of individual cells and the contractile function of the SMCs within the intact vessel wall, and then to relate these findings to the properties of the SMCs isolated from the vessel wall and maintained in cell culture. A number of different approaches were used and these are discussed individually

The cytoskeletal protein composition of intrapulmonary arteries from normal animals during development (fetal, 3 day old, 14 day old and adult) and neonatal piglets exposed to hypobaric hypoxia for three days, were identified by immunolabelling of cryo-ultramicrotomy sections. A series of SMC cytoskeletal phenotypes were described on immunolabelling for α smooth muscle actin, β actin, γ actin, SM1 myosin heavy chain isoform, calponin, caldesmon and desmin. A maturational process was observed, whereby desmin and caldesmon containing SMC phenotypes became apparent across the entire media, progressing from outer to inner media, by the time of adulthood. In addition, a reduction in the staining for

α smooth muscle and β actins was noted to transiently occur within the inner part of the media at three days of age, which is in keeping with the concept of SMC phenotypic modulation (Chamley-Campbell et. al., 1979). Both normal changes in SMC phenotype and the modulation of SMCs within the inner media at three days were disturbed in piglets exposed to hypobaric hypoxia. The benefits and limitations of this histological technique and the implications of the results are discussed.

Further information regarding the organisation of the filamentous actin cytoskeleton within SMCs of the intact vessel wall was obtained by use of permeabilised and phalloidin treated tissue preparations. This together with biochemical methods of estimating total actin and monomeric actin content gave an insight into the changes in the actin cytoskeleton during development. In particular these studies suggested that the modulation of SMCs within the inner media at three days of age was probably not due to changes in total actin content, but related to reorganisation of the actin filamentous structure. In addition, it was also possible to show significant changes in the actin cytoskeleton during the onset of respiration at birth, and during the last week of gestation, including labour and vaginal delivery. The experimental methods used and these findings are discussed and the results then related to the cytoskeletal SMC phenotypes identified by immunostaining.

Having established the structural changes occurring in the intrapulmonary artery during normal development and following hypobaric hypoxia, the functional effects of these changes on contractile function were examined in isolated vessel segments. The ratio of stress generated by potassium chloride induced contraction was related to the passive stress generated at increasing strains and used to compare behaviour of vessels from animals of different ages. In this discussion the constraints of the method are addressed and the stress ratio information is related to the structural studies of the intact wall.

Having gained an understanding of the structure and contractile function of the intrapulmonary artery during development, vessels from fetal, three day old, 14 day old, adult and hypoxic piglets were dissociated and grown in cell culture conditions in order to identify morphological SMC phenotypes. Epithelioid and spindle-

shaped phenotypes were cultured from both normal and hypoxic animals. The proportion of epithelioid cells was found to increase during postnatal development, but these cells could not account for the changes in the inner part of the media at 3 days of age. The methods used to culture these cells and the results obtained are discussed in the light of information from studies of the intact vessel wall.

Pure cell lines of epithelioid and spindle-shaped SMCs from normal 14 day old animals and epithelioid phenotype SMCs from the intrapulmonary arteries of piglets exposed to hypobaric hypoxia were derived by dilutional cloning. The replicative, migratory and contractile properties of these cells are related to their cytoskeletal protein content. The limitations of the methods used and the clear differences in properties of the different SMC phenotypes are discussed in the light of the previous results presented within this thesis.

Finally, a summary of the thesis is presented and areas of future research are outlined.

8.1 IMMUNOFLUORESCENCE STUDIES OF CYTOSKELETAL SMC PHENOTYPE WITHIN THE INTACT WALL

These immunohistochemical experiments were designed to determine the cytoskeletal composition of smooth muscle cells within the media of the intact intrapulmonary artery. The aim was to attempt to identify different SMC phenotypes that might be involved in the structural and functional adaptation of the pulmonary arteries to the extrauterine environment.

The immunohistochemical examination of individual cells within the intact intrapulmonary artery wall using ultrathin sections (250 nm) was a technically difficult part of the study. This methodology was devised to improve on the appearances obtained from standard 10μm cryosections which produced an amalgamation of information from several SMCs within the thickness of the section. Ultrathin sections had the advantage of cutting through only a single cell. The use of anti-laminin antibodies to delineate the cytoplasm of SMCs within the intact media and the use of a digital camera were important and original

modifications without which the alterations in staining patterns within individual SMCs would have been difficult to detect. Although the immunolabelled ultrathin sections did not reveal the fine detail of actin organisation within the SMCs, which was seen later with the permeabilised phalloidin-stabilised sections, it did allow the cytoskeletal content to be determined simultaneously within many individual cells across the entire media. This was not possible with confocal microscopy as the laser beam used in this form of microscopy was not able to penetrate the dense tissue of the media in the intrapulmonary artery. Electron microscopy would have been an alternate technique which would have the resolution to demonstrate fine intracellular architecture. However, to survey such a large number of cells by immunoelectron microscopy would have been prohibitively time consuming.

Although only three animals from each of the selected ages provided tissue for examination, several sections, cut from different areas of the media, all showed similar results, strongly supporting the view that these are true and reproducible findings.

The choice of antibodies used on the sections was a balance between their availability and the likelihood of them differentiating between potentially different SMC populations. Smooth muscle specific myosin and alpha smooth muscle actin were used primarily to distinguish SMCs from other cell types, such as fibroblasts, that might be found in the vessel wall. In order to determine whether the reduction in α actin staining was associated with a change in the other SMC actin isoforms, antibodies directed against γ actin and β actin were also used. Caldesmon, desmin and calponin have been described as developmental markers for SMCs (Sobue and Sellers, 1991; Gabbiani, 1987; Gimona et. al., 1990).

The classification used for these cytoskeletal SMC phenotypes was modified from the VAD cytoskeletal protein classification of fibroblasts devised by Gabbiani, which was used to describe the transition of fibroblasts to myofibroblasts during wound granulation (Gabbiani, 1992). This classification was highly successful in the context of fibroblast-myofibroblast transitions because the cells expressed or did not express vimentin, desmin or α actin, rather than expressing all proteins in variable degrees. The published work describing SMC phenotypes in the pulmonary and systemic circulation have not used classifications in which

cytoskeletal proteins were the principle differentiating factors. Frid (Frid et. al., 1994), when examining the extra-pulmonary artery in developing calves, mainly differentiated SMCs on the basis of their orientation and position within the vessel wall. The only discriminating cytoskeletal protein was metavinculin, which was limited to cells with a longitudinal orientation in the outer part of the media. Similarly, classifications of putative SMC phenotype in human systemic vessels have not found cytoskeletal protein expression useful. In an immunohistological analysis of human aortas from individuals aged 14 to 83 years of age, almost all cells of the media labelled with both α smooth muscle actin and smooth muscle specific myosin. Cells contained within atheromatous plaques of some individuals expressed desmin and vimentin but not smooth muscle specific myosin (Babaev et. al.,1990). Similarly studies of SMC phenotypes in human embryos used shape after enzymatic dissociation coupled with transmission electron micrographs, and suggested ovoid cells predominated in the inner media and spindle-shaped cells were mainly found in the outer media (Mironov et. al., 1995).

The B/C/D/CD classification, devised for this thesis, effectively described the variation in cytoskeletal protein expression, within regions of the media and with age, in developing porcine intrapulmonary artery. It was particularly important as its descriptive nature avoided any inference that a particular cytoskeletal appearance might be associated with greater maturity or contractility.

8.1.1 SMC cytoskeletal phenotypes during normal development of the porcine intrapulmonary artery

Within the intact vessel wall, it was possible to identify four different cytoskeletal SMC phenotypes from intrapulmonary arteries of fetal through to adult animals using antibodies directed towards typical SMC proteins. These phenotypes were differentially localised, both spatially and temporally, within the intrapulmonary artery during normal development and following exposure to hypobaric hypoxia. The differences in cytoskeletal protein expression within the intrapulmonary artery of the pig are much clearer, than those seen in the developing calf main pulmonary artery (Frid et.al.,1994), developing human aorta (Mironov et. al., 1995), or rat aorta (Kocher et. al., 1995).

A finding common to the studies in this thesis, and those of others who have studied the bovine main pulmonary artery (Frid et al., 1994), or the developing rat aorta (Kocher et al., 1985), was that the overall maturity of the vessel is dictated by the spectrum of SMC phenotypes it contains, rather than the wall being composed of entirely immature or mature-appearing cells. For example, the appearance of most of the SMCs in the bovine intrapulmonary artery were similar in young and in adult animals, except for the appearance of metavinculin staining cells in the outer media in the adult. The results from this thesis similarly show that basic (B) phenotype cells are found throughout the media in younger animals, but these B SMCs are still scattered throughout the media of adult animals, accompanied by C/D/CD cells.

The B/C/CD classification of SMC phenotypes within the intact vessel wall was hampered by the technical inability to double-label caldesmon and desmin, because both antibodies were raised in mice. Thus although regional expression of both antibodies could be determined on serial sections, it was not possible to confirm whether the same cell contained both proteins. However, the existence of CD phenotype SMCs could be inferred because of the large numbers of cells staining for both antibodies on the sections. Thus, regions across the adult media, and within the outer media of younger animals, contained SMCs which labelled with caldesmon and/or desmin and could be designated as C, D or CD phenotype SMCs. The existence of C cytoskeletal phenotype SMCs was proven as they were identified in the mid media at 14 days of age in the absence of desmin staining. Similarly, the existence of D phenotype SMCs was proven when labelling for desmin but not caldesmon was seen following hypobaric hypoxia. In the future it will be necessary to overcome this technical problem by IgG subclass affinity purification of the two antibodies. Thus, if each antibody can be recognised exclusively by a different IgG specific reporter antibody it will be possible to dual label cells for both desmin and caldesmon.

It is not possible to say whether the B cell phenotype SMCs mature and sequentially express caldesmon and desmin under the effects of their environment, or whether replication of these B phenotype cells produces new SMCs bearing caldesmon or desmin. Linked proliferation/cytoskeleton expression studies have

not been reported to date in this system. In order to differentiate between these two possibilities, it would be necessary to label cells with a replication marker such as tritiated thymidine or BrdU in conjunction with antibodies to cytoskeletal proteins. This type of study has been successfully carried out to examine SMC changes in the bladder following partial outflow obstruction (Buoro et.al.1993), and during development of the embryonic chicken aorta (Lee et. al., 1997). Interestingly, these studies show that replication to produce new phenotypes, as well as differentiation of existing cells is possible. In the obstructed rabbit bladder serosal cells were seen to replicate, express smooth muscle myosin and α smooth muscle myosin and contribute to the remodelling of the bladder (Buoro et. al., 1993). In the developing chick aorta, expression of α actin, smooth muscle myosin and calponin followed rapid cell proliferation between days 4 to 12 of gestation (Lee et. al., 1997).

The different patterns of caldesmon and desmin expression, in SMCs within the media of the porcine intrapulmonary artery at different ages, described in this thesis indicates the two proteins probably have different regulatory pathways both can be expressed in the absence of the other. There is little information on the regulatory pathways of these two proteins, but their spatial expression patterns by immunogold electron microscopy of chicken gizzard, indicates they are distributed in different areas of the SMC. Desmin is seen primarily at the cellular periphery in association with the actin cytoskeleton, whilst caldesmon is associated with the contractile myosin-actin elements (Mabuchi et. al.,1996). Both the gene promoters for caldesmon and calponin have been identified and studied. The caldesmon promoter has marked similarities to other muscle protein promoters containing CArG and E-box motifs (Yano et. al., 1995) suggesting common upstream muscle specific signalling pathways. Desmin also has a MyoD (E-box) binding site but high expression depends additionally on a muscle-specific enhancer (Li and Paulin, 1991). Thus, desmin expression can be initiated by muscle specific pathways but requires secondary signalling for full expression.

As indicated in this thesis, regional variation in SMC cytoskeletal phenotypes was particularly evident within the porcine intrapulmonary artery. The outer part of the media in young animals contained a mixed population of SMC phenotypes

(C/D/CD) suggesting mature SMCs, which were then also found in the mid and inner parts of the media with increasing age of the animal, from 14 days to adulthood. Although a general increase in the expression of smooth muscle-specific cytoskeletal proteins can be easily understood, the reasons for the regional distribution of phenotypes and the "out-to-in" progression of SMC maturation with increasing age is not clear. The pulmonary circulation remains at low pressure with regard to the systemic circulation, but with age pulmonary arterial pressure increases as does cardiac output (Greenwald et. al., 1982). The effect of increasing pressure and flow is not only to increase the tension applied to the wall by hydrostatic pressure, but also to increase the shear stress on the endothelium due to flow (Nichols and O'Rourke, 1998). Thus progressive increase in numbers of caldesmon-positive cells is understandable, as with increasing age, the SMCs grow larger and have a greater content of contractile proteins as they function under increasing transmural pressures. This has also been seen in to occur in vivo, where cyclical stretch has been shown to produce an increase in caldesmon content in cultured rabbit aortic cells (Birukov et al., 1995). The increase in desmin expression with age can also be appreciated as its role appears to be in facilitating the transmission of stress through cells. In the desmin-null mouse the effect of mechanical forces on structures that do not contain desmin within their cells has been reported as dissection of the aorta and fibrosis of the right ventricle (Sjuve et al., 1998).

Although it would seem likely that the forces that act on a vessel wall are uniformly distributed across the media, work carried out on the rabbit aorta has shown that in the absence of any residual stress (see below), the stress found at the inner margin of the wall was up to seven times greater than average values (Chuong and Fung, 1983). It has been demonstrated that the differences in these stresses can be reduced if the vessel wall is pre-contracted (residual strain) and made taut by SMC tone (application of residual stress), prior to application of external forces (Chuong and Fung, 1983). Thus, if a vessel is cut open longitudinally it will spring open. This has been shown in the rat aorta and residual stress has also been demonstrated to increase with age (Badreck-Amoudi et. al. 1996). Although this work has not been performed on the pulmonary circulation, it

may present an explanation of why there is a progressive change in SMC cytoskeletal phenotype across the intrapulmonary artery with age. As wall stress increases with age, greater force would be applied to the inner areas of the vessel wall which would need to be modified to resist these forces and to generate greater residual stress in order to spread hydrostatic stress more evenly across the wall (Berry et. al., 1993). The expression of desmin and caldesmon, limited to the SMCs of the outer third of the media of the intrapulmonary artery in young animals, may also relate to the distribution of stress and strain in the vessel wall. It is in this region that dissecting aortic aneurysm occurs. This might suggest that although this is not the point of maximal stress in the wall, it is in this region that the balance between applied forces and the mechanical resilience of the vessel wall is most crucial.

8.1.2 Modulation of SMC cytoskeletal phenotype within the normal porcine intrapulmonary artery during adaptation to the extrauterine environment

The transient reduction in α smooth muscle actin and β actin staining pattern within the inner part of the media at 3 days of age is in keeping with the concept of modulation of the SMC phenotype (Chamley-Campbell et. al., 1979). A similar phenomenon may have been described in the embryonic chick aorta prior to elastogenesis (Bergwerff et. al., 1996). Histological studies of the developing chick aorta during early development, indicated a reduction of α smooth muscle actin staining within the inner media, followed by an increase in α smooth muscle actin staining and deposition of elastin. Similarly, the intimal proliferation seen in human atheroma and in endothelial injury models also show regions of SMCs in which α smooth muscle actin labelling is diminished (Babaev et. al., 1990; Orlandi et. al., 1994). The only other large-animal study which investigated SMC phenotypes during postnatal adaptation failed to demonstrate any transient modulation of cytoskeletal SMC phenotype within the bovine pulmonary circulation (Frid et al., 1994). They described multiple distinct SMC populations in the pulmonary arterial media of the developing bovine fetus, calves between 1 and 15 days of age, and

adult animals, primarily based on position within the vessel wall and expression of meta-vinculin. Their failure to show changes in cytoskeletal organisation or changes in expression of associated proteins during adaptation to the extrauterine environment is not surprising. The structure of the bovine pulmonary arteries is very different from that seen in human and porcine pulmonary arteries. In addition, they looked at the main extra-pulmonary arterial segment - possibly missing the significant maturational phenotypic changes and transient phenotypic modulation we found within the main intrapulmonary artery.

The purpose of this transient modulation of phenotype is difficult to explain. It may be that the highly specialised contractile SMC must alter its cytoskeletal organisation either to allow dilatation of the artery by spreading of cells, or to facilitate cell replication, or both. These possibilities have been demonstrated to occur in vitro. For example, a reduction in stress fibres was seen in cultured rabbit aortic SMCs in association with changing shape (Birukov et. al., 1993) and SMCs have been shown to undergo cytoskeletal disassembly prior to cell division, although this is not a prerequisite for replication (Owens, 1995). Modulation might also be limited to the inner part of the media at three days of age and not occur across the entire wall since at this time it is the lumen that is becoming larger, whilst the external diameter of the vessel remains unchanged (see Appendix). Further analysis of the vessel wall in the interval between 3 and 14 days will be necessary to answer this question, not only using the SMC markers already described but also using a marker of proliferation, such as proliferating cell nuclear antigen (PCNA).

The signals controlling the changes in SMC phenotype, and in particular the modulation at three days of age, are unknown and it is only possible to speculate on possible mechanisms. The change in distribution of the C/D/CD phenotype cells with age could easily be explained in terms of increasing wall stress and residual stress as discussed above. Alternatively, it is possible that the phenotypic modulation could occur in response to signalling via the adjacent endothelium, perhaps as a response to increasing flow and therefore shear stress (Hungerford and Little, 1999).

8.1.3 The effect of hypobaric hypoxia on the cytoskeletal phenotype and normal modulation of SMCs within the intact intrapulmonary artery

A key question in trying to understand persistent pulmonary hypertension of the newborn is whether the pulmonary arteries retain their fetal state, progress to an abnormal state, or are accelerated along their normal developmental pathway. Previous studies, using porcine hypobaric hypoxia as a model of human PPHN, as described in this thesis, have shown increased myofilament and connective tissue volume densities using electron microscopy, suggesting accelerated normal maturation (Allen and Haworth, 1986). However, findings from the same study also suggest the cells contained within the vessel wall fail to spread, and that the vessels do not increase lumen diameter and therefore retain a fetal appearance. The data from the immunolabelling studies contained in this thesis suggests that hypobaric hypoxia produces abnormal cellular behaviour and that the vessels develop abnormally. In the vessels exposed to hypobaric hypoxia SMCs expressing desmin in the absence of caldesmon were found throughout the media. This was not seen in any region of the media of normal vessels, at any age.

It is only possible to speculate as to what environmental signals might cause desmin to be expressed in the absence of other proteins such as caldesmon. One possibility is that desmin expression is preferentially up-regulated in response to contractile activity or stretch, a phenomenon which has been observed in cultured rat cardiac myocytes (Watson et. al., 1996). Alternatively, hypoxia may alter gene expression via oxygen sensing mechanisms, similar to those controlling erythropoietin production, either by the SMCs themselves or by the endothelium. For example, differential expression of angiogenic growth factor genes (both up and down regulation) has been demonstrated in cultured cells (Gleadle et. al., 1995). Endothelial dysfunction secondary to hypertension has also been noted to occur in the systemic circulation (Vanhoutte, 1996) and could also be responsible for inducing changes in SMCs within the media in the pulmonary hypertensive piglets described in this thesis. This dysfunction not only involves structural changes to the endothelial cells, with focal disruption to the basement membrane and incorporation of additional collagen and elastin, but also involves the signalling

pathways of the cells. Prostacyclin production is disrupted and nitric oxide synthase expression is lost (Stenmark and Mecham, 1997) in pulmonary hypertensive rats and pulmonary hypertensive calves.

Whatever mechanism is responsible for up-regulation of desmin expression, the effects of its absence in the desmin null mutant mouse (Galou et. al., 1997) would suggest that desmin probably plays a protective role within SMCs of the hypertensive pulmonary circulation and prevents cellular damage. These mice demonstrate a multi-system disorder involving the heart, skeletal muscle and smooth muscle within the great arteries. In the smooth muscle of the vasculature there is hypoplasia but importantly degeneration of the media accompanied by necrosis and calcification.

In addition to the appearance of the abnormal D phenotype cells, SMCs in the inner 2/3 of the media of hypoxic animals fail to undergo phenotypic modulation as seen in the normal 3 day old animals. This may be because phenotypic modulation is not possible in the D phenotype cells, perhaps due to a stabilising effect of the intermediate filaments on the actin cytoskeleton. Alternatively the phenotypic modulation may be inhibited by hypoxia sensing mechanisms (Gleadle et. al., 1995) or endothelial dysfunction (Vanhoutte, 1996) as discussed above.

8.2 APPEARANCE OF ACTIN FILAMENTS IN WHOLE TISSUE

Phalloidin stabilised and permeabilised intrapulmonary arteries were examined in order to gain more information about the arrangement of actin filaments within the inner media during cytoskeletal phenotypic modulation at three days of age, following hypobaric hypoxia, and throughout normal development including the onset of respiration at birth. This was necessary as the immunolabelling of ultrathin sections failed to provide sufficient resolution of actin filaments. Visualisation of the actin cytoskeleton has been extensively performed in cultured cells (Lawson, 1987) but has not been carried out in whole tissue. Having carried out the experiments reported in this thesis, it is clear that interpretation of the complex arrangements of filaments is very difficult in whole tissue as the boundaries between different cells can not be easily visualised, and the three dimensional

arrangement of filaments can not be easily understood. Despite this, it was possible to categorise the changes in the actin arrangement by describing the degree of actin compaction. This idea was based on the classical approach used when describing mitochondria when examined by electron microscopy. (Candipan and Sjostrand, 1984). In the same way mitochondria can be described as being compacted or orthodox in appearance, the actin cytoskeleton was described as having degrees of compaction. This method provided a useful classification with which to describe the appearance of the actin cytoskeleton. Although the results reported in this thesis allow an interpretation of the actin filament arrangements, the resolution afforded by scanning electron microscopy, with immunogold labelling, would undoubtedly improve the technique.

Hall and Haworth (1987) demonstrated that the distal intrapulmonary arteries become patent and accommodate an increasing pulmonary blood flow following birth with the onset of respiration. In the same study, they also showed that this dilatation also affected the larger proximal vessels. In this thesis, the phalloidin treatment of these same sized intrapulmonary arteries allowed investigation of the changes in actin filament patterns occurring around the time of birth. Both late fetal animals (one week prior to full-term) and full term piglets were studied, with the fetal animals being born by caesarean section and the term piglets being born following normal labour by vaginal delivery. This area of research is novel and the cytoskeletal changes during birth have not been previously published. The data presented in this thesis showed greater compaction of the actin cytoskeleton in newborn animals born following vaginal delivery and that had breathed, than in newborn animals that had never breathed. Similarly, fetal animals born by caesarean section and that had breathed, also demonstrated a greater degree of actin compaction than fetal animals that had never been allowed to breath. It is possible that these alterations in the actin cytoskeletal organisation with the onset of respiration are merely a result of dilatation of the intrapulmonary artery and stretching of the SMCs into a flatter shape. However, the work of Dawes and Strang (Dawes, 1968) indicated that lung inflation, oxygenation and pulmonary vasodilator therapy all individually effected an increase in pulmonary blood flow and are additive in their effects. This suggests that a variety of mechanisms above

simple distension of blood vessels and stretching of SMCs are all required for adaptation to the postnatal environment dilation at the time of birth. This therefore lends weight to the idea that mechanisms are in place within fetal intrapulmonary arteries that maintain the vessels and the actin cytoskeleton of the SMCs in a compact rigidly held form.

The rapidity of the changes that occur in the arrangement of the actin filaments suggests activation of a pre-existing mechanism as there is insufficient time for ne-novo gene transcription to occur. One such possible explanation for a rapid change in cell state with the onset of respiration might be release from a low energy expending state of persistent contraction or "latch state" (Hai and Murphy, 1992). This is similar to the "catch state" mechanism seen in the shell-hinge muscle of molluscs. The basis of the low energy persistent contraction in molluscs is slow cycling of cross linking between thick myosin containing filaments. (Bennett and Elliot, 1989), which is controlled by phosphorylation of proteins such as twitchin (Siegman et. al., 1998). Similar mechanisms have been demonstrated in chicken gizzard in which the force maintenance at low levels of myosin phosphorylation is maintained by cross linking which may be controlled by proteins such as calponin and caldesmon (Ruegg and Pfitzer, 1991).

Cytoskeletal remodelling could also be rapidly achieved by the activity of actin associated proteins. For example, induction of actin capping or severing proteins (Alberts et. al. 1999) or phosphorylation of Rho kinase , which induces stress fibre formation (Amano et. al., 1997) might be ways in which rapid cytoskeletal changes might occur.

The newborn piglets that did not breathe also exhibited greater actin compaction than the fetal animals that did not breathe. Similarly, the newborn piglets that did breath also exhibited a greater degree of actin compaction than the fetal animals that breathed. This finding suggests that there is a maturational effect, active in both animals that breathe or do not breathe, that occurs during the last week of pregnancy or during normal labour and vaginal delivery. This may relate to changes in the balance of humoral factors acting on the pulmonary circulation (see contractile studies, below).

The modulation of cytoskeletal SMC phenotype within the inner part of the media at 3 days of age, seen in the immunolabelling studies discussed above, was further investigated using phalloidin stabilised tissue sections. It was interesting to note that although the newborn breathing piglet exhibited marked actin compaction within SMCs of the intrapulmonary arteries, by three days of age the pattern of actin was relatively disorganised and non-compacted. However, although in the immunolabelled sections there appeared to be a paucity of α and β actin, the phalloidin stabilised sections revealed plentiful fine filaments filling the entire SMCs. It is difficult to explain why the antibodies to α and β action did not label the actin in these SMCs. A possible explanation may relate to the stabilising effect of phalloidin and one might postulate that the absence of phalloidin in the immunolabelled ultrathin sections may have permitted fine filaments to be washed off the tissue sections during immunostaining.

Between 3 days and adulthood the appearances of the actin cytoskeleton became more compacted once more, which might suggest that compaction of the actin cytoskeleton may be an indicator of SMC maturation or enhanced contractility.

The phalloidin stabilised sections taken from animals exposed to hypobaric hypoxia from birth to three days of age exhibited a degree of compaction intermediate to that seen in the newborn animals that had breathed (appearances when placed in hypobaric hypoxia) and that of normal three day old animals. Again this was surprising since the dense immunolabelling patterns seen with α, β and γ actin staining would have suggested a highly compacted actin cytoskeleton. Since the immunostaining patterns with α and β actin and the phalloidin stabilised appearances were so similar to those seen in sections from intrapulmonary arteries from fetal and 14 day old animals it is not possible to say whether hypobaric hypoxia produced a regression to the appearances of the fetal piglets, or that there was acceleration of the architecture towards 14 day old animals. However, the phalloidin stabilised appearances were certainly abnormal when they were compared to the normal three day old piglets.

8.3 TOTAL AND MONOMERIC ACTIN

The principle purpose of these experiments was to determine if there was any significant reduction in the total amount of actin, or in the proportion of actin in the filamentous state, within SMCs of the media, that might be of a sufficiently large magnitude to explain the reduction in actin immunostaining seen within the inner part of the media at 3 days of age.

The fluorometric method of actin measurement used in this experiment is a highly specific DNAse I inhibition assay which is able to detect as little as 20 ng of monomeric actin (Huang et. al., 1993). It has previously been used to assess total, filamentous and monomeric actin content in whole tissue from early gestation chick embryos (Nachmias et. al.,1992). The measurement of total actin in this chick study and the study in this thesis were complicated by the problems of standardisation, which is a requirement for any measurements taken throughout a developmental process. Nachmias et. al. (1992) estimated total cellular volume, a method which might be acceptable for early gestation embryos where there is relatively little extracellular connective tissue, but this would be totally unsuitable for the intrapulmonary artery which accumulates significant (Haworth and Hall, 1987) but unquantified amounts of collagen and elastin during development (Mills and Haworth, 1987; Crouch et. al., 1989). For the actin measurements contained in this thesis, a variety of possible denominating factors were considered for standardisation of results, but none were entirely satisfactory. Although measurement of dry weight is an accurate and reproducible method of standardisation, it was not possible to use dry weight as desiccation precluded biochemical analysis of the tissue. Total protein content of the tissue was hampered by large amounts of extracellular proteins, such as collagen and elastin, being present in the older animal, the amounts of which have been shown to increase with age (Mills and Haworth, 1987) but have not been directly quantified in the porcine intrapulmonary artery. The method used to standardise the actin concentration was to use a small aliquot of the tissue suspension used to measure total actin. This solution contained Triton X-100 with guanidine hydrochloride, which is a chemical combination used to render cytosolic proteins and glycosaminoglycans soluble, but does not solubilise elastin or collagen (Spina et.

al.,1983). This protein measurement was therefore used to give an indication of the actin content per unit of cytoplasm. DNA measurement was also performed in order to give an indication of actin content per cell. In practice, the measurement of DNA is relatively crude. Although spectrophotometric methods can be used to measure DNA they are limited by the need to separate the DNA from any protein, RNA, or interfering substances. This, like the assessment of dry weight, would preclude further biochemical analysis of tissue. The fluorometric method of Hoechst 33258 dye binding used in this thesis (LaBarca and Paigen, 1990) had the advantage of not requiring purification of DNA and not being influenced by the reagents used in protein extraction.

The standard deviations of the total actin content standardised against either DNA or solubilised protein content are relatively large for all ages of animal examined. This is probably due to a combination of variation in the actin assay, in the standardisation methods and by the of small quantities of tissue available for use. To maximise the quantities of tissue analysed in these actin studies, the entire middle segment of both left and right lung intrapulmonary arteries was used for each measurement, except in the largest animals. It was not considered acceptable to use other arteries of a similar size from different parts of the lung as these might not behave like the main intrapulmonary artery, which has been examined exclusively throughout this thesis, and cause further variation in results. The use of larger numbers of animals could also reduce the size of the standard deviations.

In contrast to these DNA and soluble protein standardised studies, the percentage of total actin in monomeric form generally had smaller standard deviations. This is probably because any variations in the behaviour of the assay would affect both monomeric and total actin readings to the same extent. It was interesting to note that the standard deviations of the percentage of actin in monomeric form were strikingly large in the fetal and newborn animals that had begun to breath. These animals have been shown in this thesis to have been undergoing reorganisation of the filamentous actin cytoskeleton within the SMCs of the intrapulmonary artery at this time. The wide variations in the percentage of monomeric/total actin might indicate that reorganisation of the actin cytoskeleton at these times were associated with a disturbance of the filamentous and

monomeric actin pools. Since actin filaments are dynamic structures (Alberts et. al., 1999), small changes in the proportion of monomeric actin might indicate large changes in filamentous structure.

Despite these methodological limitations, the experiments did help to exclude any large shift in the total actin content or the proportion of actin in the filamentous/monomeric form within the SMCs of the media at three days of age. Thus, since total actin remains relatively constant and there is no significant shift from filamentous to monomeric actin, the changes in immunostaining with α and β actin would appear to be due to reorganisation of the filamentous actin structure to finer filaments. It is possible that the reduction in immunostaining for the actin isoforms was as a consequence of the loss of short filaments from the tissue sections. In contrast to the rapid events occurring in the actin cytoskeleton at birth, slower changes in actin filament organisation would not necessarily be associated with large shifts of actin removed from filaments entering the monomeric actin pool.

8.4 CONTRACTILE PROPERTIES

The immunolabelling of ultrathin sections, and the experiments to visualise the filamentous actin cytoskeleton after phalloidin stabilisation, revealed a series of significant changes occurring to the cytoskeletal apparatus within SMCs of the intrapulmonary arteries between late fetal life and adulthood. Experiments on isolated segments of intrapulmonary artery were carried out to investigate the effects that these changes would have on the contractile potential of the SMCs within the intrapulmonary arteries.

8.4.1 Experimental considerations in the evaluation of the contractile potential of isolated intrapulmonary arterial rings

The study of the porcine pulmonary circulation requires methods of standardisation in order to compare the structure and function of vessels that are of different size. Strain and stress ratio were therefore used to allow comparison of the contractile properties of the intrapulmonary arteries. Strain, which is the ratio

of the intrapulmonary artery ring dimensions after deformation in comparison to the original dimensions, was used to assess the degree of vessel stretching. Stress, the quantity of force per unit cross sectional area that produces a deformation, was also calculated from the absolute force generated by the rings and their cross sectional dimensions.

It is recognised that the wall thickness of an artery is difficult to measure accurately, and a variety of methods have been described (Nichols and O'Rourke, 1998). Although the wall thickness of larger arteries can be measured from a knowledge of their tissue density, weight and outer dimensions, this was not possible in the very small intrapulmonary arteries. Similarly, although measurement of a flattened vessel with a Vernier micrometer can be performed in systemic vessels, this could not be carried out in intrapulmonary vessels, as the tissue was easily compressed. The method chosen for use in this thesis was microscopic measurement of fixed sections, taken from an adjacent segment of vessel to that which was used in the measurement of force. In order to overcome fixation artefact, which can easily approach 20% shrinkage (Dobrin, 1996), the ratio of wall thickness to external diameter was calculated from the histological sections and used in conjunction with the actual external diameter of experimental rings (where hemi circumference = π x external diameter/2).

Although it was hoped that absolute measurements of stress would be obtained, it was clear form the differing magnitude of results from individual experiments (Figure 32) that this would be difficult. Although the relationship between stress and strain was similar in all cases, variation in magnitude of force meant that the trends would be lost if the data was averaged. At the suggestion of Dr Steven Greenwald (University of London), this problem was overcome by evaluation of stress ratio. This is the ratio of stress developed during maximal contraction, with potassium chloride, in comparison to the stress developed by the ring at rest. The benefit of this ratio is that it allowed comparison of the different data derived from animals of the same age and also between animals of different ages. The calculations of stress ratio also removed the need to include individual measurements of wall thickness within the calculations.

The contractile potential of the vessels was measured during isometric contraction with potassium chloride in a traditional pharmacological organ bath (Stevens and Bromberger-Barnea, 1969). More complex methods of investigating contraction are available, such as by isotonic contraction or by examining vessels in vivo (Bank et. al., 1996). The in vivo measurement of stress is probably the most physiologically relevant method as the properties of isolated vessels are altered by their longitudinal retraction when removed from their native tissues (Dobrin and Mrkvicka, 1992). Furthermore, the reported studies refer to systemic vessels which are not subject to the cyclical changes in length which must occur in pulmonary vessels with each cycle of breathing. The effect of changes in length on removal from the lung was not addressed in this thesis.

As discussed previously in the methodology for these experiments, although the shape of vessel segments has been shown to alter passive mechanical properties, the active force development for both rings or cylinders of artery are similar, hence edge effects are minimal in this context (Cox, 1983). The length of rings used for these experiments were always greater than the diameter of the vessel.

8.4.2 Changes in stress ratio in fetal and term piglets associated with the onset of respiration

The contractile studies on fetal and newborn term piglets both indicated a significant increase in the ability to generate force, as manifest by an increase in stress ratio, with the onset of respiration. These changes in stress ratio were also seen to occur alongside an increase in the compaction of filamentous actin during this time in both the fetal and term piglets. This increase in contractile potential (stress ratio) in association with change in actin cytoskeleton might be suggestive of release from a state of persistent contraction or "latch state" (Hai and Murphy, 1992).

The stress ratios developed by fetal animals, both breathing and non-breathing were greater than the stress ratio values obtained from breathing and non-breathing term newborn piglets. Despite this fall in contractile potential, during the period of late gestation, labour and vaginal delivery, the actin cytoskeleton became more compacted. A possible explanation for this fall in stress ratio, during late gestation,

labour and vaginal delivery, may relate to the changing balance of humoral factors that are known to be involved in maintaining the fetal state. For example, in late gestation and neonatal lambs there is a marked increase in the synthesis of prostacyclin, a pulmonary vasodilator, within the endothelium and smooth muscle cells of the pulmonary circulation (Leffler et. al.,1984). The full term piglets investigated in this thesis, as well as being one week older than the fetal piglets, differed in that they had been born by normal vaginal delivery following labour. It is possible that the marked physiological changes that occur in labour, for example release of catecholamines, thyroid stimulating hormones, surfactant, as well as prostacyclin (Thorburn and Harding, 1994), may be responsible for the fall in stress ratio between fetal animals and newborn animals.

An important alternative explanation for these findings is the possibility that the appearances of actin cytoskeleton compaction are due to changes in the contractile ability of the SMCs. Thus, with the onset of breathing, the myosin-actin interaction is enhanced and then produces greater actin compaction which is seen on the phalloidin preparations. Even if this were the case, this mechanism still could not explain the fall in stress ratio which is accompanied by an increase in actin compaction and occurs between late gestation and vaginal birth after normal labour.

The results presented in this thesis may help to provide an explanation as to why human preterm infants have a relatively labile pulmonary vascular resistance. This is manifested as elevation of pulmonary arterial pressures during episodes of hypoxia or sepsis, and may also provide a link between elevated pulmonary arterial pressure and surfactant deficiency in respiratory distress syndromes affecting the newborn and preterm infant (Hamdan and Shaw, 1988).

8.4.3 Changes in stress ratio during postnatal development

The lack of differences in stress ratio values between intrapulmonary arteries from three day old piglets, and the newborn or fourteen day old piglets, suggests that modulation of SMC cytoskeletal phenotype in the three day old piglets does not significantly impair their function. The three day old intrapulmonary arteries demonstrate equivalent stress ratio values to the breathing newborn term piglets and the 14 day old piglets, despite the actin compaction scores of both the term

breathing piglets and the fourteen day old animals being higher than the three day old animals. It was only the adult vessels which demonstrated a substantial increase in stress ratio in combination with greater actin compaction. These data emphasise that whilst the pattern of the actin cytoskeleton during the onset of respiration at birth may be linked with contractile function, the postnatal progression of contractile function is dominated by other factors which augment the contractile process. This would not appear to simply involve the degree of immunostaining for actin isoforms or smooth muscle specific myosin as the expression pattern of these proteins bore no correlation to the contractile potential of the vessels. However, other accessory cytoskeletal proteins may be more relevant. For example, the immunolabelling studies in this thesis show that the combined expression of caldesmon and desmin only occur throughout the entire media in the adult. These and other proteins, such as tropomyosin which is involved in the calcium response of the troponin complex to actin filaments, play a key role in the generation of force (Alberts, 1999; Owens, 1995).

8.4.4 Changes in stress ratio following hypobaric hypoxia

These contractile studies indicated that there was no significant difference between the stress ratio values of intrapulmonary arteries from 3 day old piglets, newborn breathing piglets and vessels from piglets exposed to hypobaric hypoxia from birth. This demonstrated that, as with normal postnatal development, there was no relationship between contractile potential and the actin isoform staining patterns, smooth muscle myosin content, or actin compaction. Thus, in animals exposed to hypobaric hypoxia, the expression of desmin by SMCs, in the absence of caldesmon, may be an adaptation to protect the cells from mechanical disruption (Galou et. al., 1997).

8.5 QUANTIFICATION OF ELASTIN, COLLAGEN AND SMOOTH MUSCLE CONTENT OF THE VESSEL WALL

These morphometric studies were carried out in order to determine whether there was any change in the amounts of elastin, collagen and smooth muscle within

the intrapulmonary arteries that had been examined in the contraction studies, that might explain the changes in stress ratio during development. The experiment was not able to exclude changes in the proportion of collagen, elastin and smooth muscle as the results were associated with large standard deviations which made evaluation of differences difficult. However, from previous electron microscopic studies in the developing pig the proportions of elastin, collagen and smooth muscle probably do not change significantly during the first weeks of life (Haworth and Hall, 1987). However, although the mean values suggested that little change if any in the composition of the arteries was occurring during normal development in hypoxia there appeared to be a greater proportion of extracellular matrix present although this was not statistically significant. This has been previously noted to occur in several models of persistent pulmonary hypertension of the newborn (Morin and Stenmark, 1995).

Much of the variation in results which led to wide standard deviations was undoubtedly due to the staining methods used for morphometric analysis. Elastic van Gieson staining was used to identify elastin, collagen and smooth muscle on the histological sections as black, pink and brown. Some of the measurement difficulties were probably due to variable intensity of staining, although some variation in the results does also probably stem from natural variation in the composition of the vessel in different areas of the artery. In retrospect, it would have been better to stain individual components of the cell wall on a greater number of tissue sections, which has shown to yield acceptable results (Berry and Greenwald, 1976).

8.6 PHENOTYPIC VARIATION OF THE PULMONARY ARTERIAL SMCS DURING POSTNATAL ADAPTATION

The studies carried out on the intact porcine intrapulmonary artery, and discussed above, have suggested that significant changes in the SMC cytoskeleton occur around the time of birth and during the following days. Furthermore, SMCs within the intrapulmonary arteries of piglets exposed to hypobaric hypoxia, which is a model of persistent pulmonary hypertension of the newborn, develop abnormal

cytoskeletal appearances. In particular, the immunolabelling studies of cryo-ultramicrotomy sections, presented in this thesis, suggest the existence of several distinct cytoskeletal SMC phenotypes, based on their differential expression of caldesmon and desmin both in normal and hypoxic animals. The initial aim of the cell culture studies, described in this thesis, was to establish whether different morphological SMCs phenotypes might exist in the porcine intrapulmonary artery, and if they do exist, whether they are associated with SMC cytoskeletal phenotypic modulation seen in the inner part of the intact vessel media at 3 days of age.

8.6.1 Methods used to characterise morphological SMC phenotypes in cell culture

It was not possible to characterise the SMCs seen in primary cell culture by their expression of caldesmon or desmin, as had been carried out for the SMCs within the intact vessel wall. There were two main reasons for this. Firstly, it is recognised that when SMCs are seeded in primary tissue culture at sub-confluent density, the expression of many cytoskeletal proteins, for example caldesmon, calponin and smooth muscle specific myosin heavy chains, is reduced (Owens, 1995). Secondly, caldesmon and desmin are not useful for isolating different SMC phenotypes from a heterogeneous cell population because they can only be detected in fixed, i.e. dead, cells. This would therefore make derivation of cell lines, or any functional analysis of the SMCs impossible. An alternative characteristic of cells in tissue culture conditions was therefore chosen. Several published studies have shown that different morphological SMC phenotypes can be obtained from dissociated arterial wall. For example, when SMCs were dissociated from the human fetal aorta by use of an alcohol-alkaline solution, spindle-shaped, Y-shaped, stellate and spherical cell morphologies were obtained (Mironov et. al.,1995). Different morphological phenotypes were also observed when normal rat thoracic aorta (Bouchaton-Piallat et. al., 1996), or the intimal thickening which occurs fifteen days after endothelial denudation of rat thoracic aorta (Orlandi et. al., 1994) were dissociated and the cells maintained in tissue culture. Spindle-shaped cells predominated in the normal thoracic rat aorta, with occasional epithelioid cells (Bouchaton-Piallat et. al., 1996), whilst epithelioid cells

predominated in cultures produced from intimal thickening, which also contained occasional spindle-shaped cells (Orlandi et. al., 1994).

There are two main methods to produce SMCs for cell culture experiments. Either the use of enzymatic dissolution to obtain SMCs as described by Ives et. al. (1978), or the use of explant methods (Chamley-Cambell et. al., 1979). The enzymatic method was specifically chosen for use in these experiments to prevent bias in the proportion of different types of SMCs obtained. The results obtained from experiments conducted on pure SMC clones, discussed later in this chapter, indicated that this was correct and that if the explant method had been used to liberate cells from the intrapulmonary arteries, only classical spindle-shaped cells would have been obtained and the presence of other phenotypes would not have been suspected.

8.6.2 Morphological SMC phenotypes within the intrapulmonary artery during development

The initial scheme, used to classify the SMCs obtained from the porcine intrapulmonary artery, was designed to address the possibility that multiple morphological phenotypes might be present within the primary culture, as had been suggested by studies investigating human fetal aorta (Mironov et. al.,1995), as discussed above. The epithelioid cells were easily identified and their proportions were constant within preparations from different animals of the same age. The polygonal, spindle/polygonal and spindle-shaped cells were harder to prove as separate morphological phenotypes. After detailed observation, it was clear that the range of morphologies, from polygonal, polygonal/spindle-shaped to spindle shaped formed a continuum and that the exact shape depended on the motile state of the cell at the time of observation. This conclusion lead to the use of the spindle-shaped and epithelioid cell classification used in this thesis. The intrapulmonary arteries from the hypoxic animals also produced epithelioid and spindle-shaped SMC phenotypes. It is interesting to note that similar conclusions were reached concerning SMC phenotypes within the bovine extra-pulmonary artery. Although four phenotypes had been described in the intact vessel wall, differentiated by position and meta-vinculin expression (Frid et. al., 1994), only spindle shaped and

epithelioid morphological phenotypes were identified during cell culture experiments (Frid et. al., 1997).

An important initial concern was that the presence of epithelioid cells might be an artefact either due to contamination of the culture by endothelial cells or by the use of fibronectin as a plating substrate. It was relatively easy to exclude endothelial cell contamination, since none of the cultured cells labelled with the endothelial cell specific antibodies directed against von Willebrand factor or CD 31 ligand, and attempts to culture a pure primary isolate of intrapulmonary arterial endothelial cells in media designed for SMCs failed, as the cells would not settle within the cell culture system during the experimental time frame. In contrast, it was not initially possible to prove that the epithelioid cells seen in the primary cultures were actually SMCs as they did not express the typical smooth muscle cell markers smooth muscle specific myosin or α smooth muscle actin. Only by serial passaging of epithelioid cells, reported in the cloning cell culture experiments in this thesis, could they be induced to express α smooth muscle actin. This phenomenon of phenotypic modulation during cell culture has been extensively described before (Chamley-Campbell et. al., 1979; Owens, 1995). Experiments reported in this thesis also showed that neither the appearance or the proportions of the epithelioid and spindle-shaped SMC phenotypes were altered by different cell culture substrates. The effect of plating substrate on the degree of phenotypic modulation in classical spindle-shaped SMCs has been extensively investigated. It has been clearly shown that whilst different substrates may alter the proportion of SMCs expressing α smooth muscle actin and other smooth muscle specific proteins, they do not cause SMCs to change from spindle-shaped to the epithelioid phenotype (Owens et. al., 1986; Thyberg and Hultgardh-Nilsson, 1994). The majority of these studies have been performed using rat aorta, but the same results have been obtained using human vascular SMCs obtained from renal arteries (Palmberg et. al., 1985).

The experiments reported in this thesis, indicated that the proportions of epithelioid and spindle-shaped phenotypes within the porcine intrapulmonary artery changed during normal development, such that the percentage of epithelioid cells increased significantly from 3.9 % in the fetal animals to 28.3 % in the 21 day old

piglets and then fell to 21.7% in adult animals. This change in the proportion of phenotypes during development has not been reported before. However, the proportion of epithelioid phenotype SMCs derived from the normal media of the adult thoracic rat aorta has also been shown to be 20 % (Bochaton-Piallat et. al., 1996). The primary cell culture studies reported in this thesis also showed that the proportion of epithelioid cells obtained following hypobaric hypoxia was much higher than that seen in cell isolates from normal intrapulmonary arteries. The epithelioid cells obtained from intrapulmonary arteries of hypoxic animals approached 50% of the total number of SMCs isolated. It is only possible to speculate on the meaning of these findings, as this area of vascular biology has not been thoroughly investigated to date. An important possibility is that, rather than there being an increase in numbers of epithelioid SMCs within the vessel wall, there is a relative reduction in the number of spindle-shaped cells isolated or surviving in culture. Thus, one would need to speculate that many spindle-shaped cells would be viable in cultures derived from fetal vessels leading to a low level of epithelioid cells, but in older animals the spindle-shaped cells would be more fragile and therefore the epithelioid cells form a greater proportion of the cell population. This seems unlikely. However, if there is a real increase in the numbers of epithelioid cells present, this might be due to transformation of spindle-shaped cells into epithelioid cells either directly or following cell division, or due to programmed cell death of spindle-shaped SMCs.

Unfortunately there are no published data regarding proliferation or apoptosis of SMCs within the porcine pulmonary arterial media. However, some work has been carried out on the developing systemic circulation. Experiments on juvenile rabbits, in which carotid artery blood flow has been reduced, have indicated that significant reductions in SMC replication can occur rapidly, in association with significant levels of programmed cell death (Cho et.al., 1997). Work in the neonatal lamb has also suggested that during normal postnatal development the rates of programmed cell death varied in different systemic arteries. Rates were particularly high in the umbilical arteries as they regressed and the aorta as it remodelled (Cho et. al., 1995). These results indicate remodelling is associated with both proliferation and apoptosis within the systemic circulation. This is

probably similar to the situation in the postnatal normal pulmonary circulation, which although is a low pressure circulation, does receive a high blood flow. However, these data are harder to relate to the high pressure and relatively high flow circulation in hypobaric hypoxia or the high pressure low flow system in fetal life. In order to identify the role of proliferation and programmed cell death in the porcine pulmonary circulation, reliable markers of epithelioid and spindle-shaped phenotype will be required, in order to track the proportions of each cell type within the intact vessel wall and identify proliferation or apoptosis.

These cell culture experiments were also important in trying to understand the processes responsible for modulation of SMC cytoskeletal phenotype in the inner part of the media at three days of age. The discovery that epithelioid phenotype SMCs found within the intrapulmonary artery did not express α smooth muscle actin, whilst spindle-shaped SMCs grown within the same culture dish did express α smooth muscle actin was an exiting finding. This, in conjunction with the increase in the proportion of epithelioid SMCs between late fetal life and three days of age, led to speculation that the emergence of the epithelioid SMCs might be responsible for the reduction in α smooth muscle actin staining and the changes in actin filament organisation seen within the inner media of the normal intrapulmonary artery 3 days after birth. Separate cell culture of the inner and outer parts of the media disproved this suggestion since the proportion of both spindle-shaped and epithelioid phenotypes was the same in both parts of the media. This finding suggests that changes in the cytoskeletal protein expression in both epithelioid and spindle-shaped SMC morphological phenotypes are probably responsible for modulation of the B phenotype SMCs within the inner media at three days of age, and suggests the presence of a regional signal which affects both epithelioid and spindle-shaped morphological phenotypes. There are several mechanisms which could produce this effect, such as release of humoral mediators from the endothelium, or mechanical transduction via integrins to SMCs within the inner media (Stenmark and Mecham, 1997).

8.7 PRODUCTION AND CHARACTERISATION OF MORPHOLOGICAL SMC CLONES

Having identified two morphological SMC phenotypes within the porcine intrapulmonary artery, further experiments were then carried out to isolate pure colonies of the two cell types and investigate their properties, in order to try and understand their physiological roles.

The production of cell colonies derived from single cells by dilutional cloning (Lemire et. al., 1994) was simple and successful. However, cloning experiments of this type do exert a selection pressure, which is that only cells suited to the cloning conditions will replicate and produce colonies. Thus, one can not be sure the commonest, or the most physiologically relevant cells have been cloned. Despite this reservation, the clones that were produced did maintain their morphological features, through several weeks and rounds of cell division in the cell culture environment, and exhibited clear differences in behaviour which would suggest their properties were strongly related to their phenotype rather than as a result of the cell culture environment. Although at this stage the hypoxic epithelioid SMCs showed no difference in morphology to the normal epithelioid SMCs (epSMCs) they were examined as a separate phenotype (hySMCs). This proved to be an important step as both their characteristics were shown to be different to the classical spindle-shaped SMCs (spSMCs).

8.7.1 Serum dependence and contact inhibition of replication of SMC clones

Two related variables were used to investigate the replication potential of the different SMC phenotypes. Fetal calf serum, which is used as a general mitogen in tissue culture, and the effect of intercellular contact, were used in combination to understand the behaviour of the epSMCs, spSMCs and hySMCs.

Contact inhibition is a phenomenon often used to explain why the rate of cell growth is reduced when cells are surrounded by, and in intimate contact with other cells. In adult tissues contact inhibition is thought to be continually active, and loss of contact inhibition is associated with abnormal growth states such as that seen in tumours. In contrast embryonic cells and cells in continuously growing tissues are

not contact inhibited (Alberts et. al., 1999). Traditional smooth muscle cells generally behave like adult cells in vivo, but typically display little contact inhibition in vitro (Kato et. al.,1996). Fetal calf serum is an essential adjunct to cell culture in vitro and contains a cocktail of cytokines and growth factors essential for cell growth. Cells which are placed in cell culture media completely free of FCS die unless trace metals, and mitogens are specifically added.

All three SMC clones isolated from the porcine intrapulmonary artery, spSMC, epSMC and hySMC, demonstrated contact inhibition of replication when maintained with low concentrations of fetal calf serum (FCS). However, in the presence of 10 % FCS the spSMCs and the hySMCs completely overcame the effects of cell-cell contact and replication. In contrast, the epSMCs still demonstrated marked contact inhibition despite the presence of 10 % FCS. The underlying mechanism for this effect is not clear. It is possible that the FCS was acting as a general mitogen, acting, for example, via paracrine signalling, which was then able to modulate other direct cell adhesion effects as suggested by Faggotto and Gumbiner (1996). Interestingly although the epSMCs were constrained by cell-cell contact, they were also able to proliferate at the same high rates in low or high FCS concentrations, whilst the spSMCs replicated slowly in low FCS concentrations. This suggests the epSMCs are capable of autonomous cell division if released from contact inhibition whilst the spSMCs can only replicate rapidly if released from contact inhibition and also stimulated with exogenous mitogens. This difference in behaviour has been noted in rat aortic cells derived from fetal or adult animals. The adult derived cells, with a spindle-shaped phenotype, showed minimal replication in low serum conditions whilst epithelioid phenotype fetal cells continued to proliferate (Cook et. al., 1993). Similarly, the effects of contact inhibition were noted to only affect spindle-shaped SMCs, isolated from rat aorta, when the cells were held in low serum conditions (Kato et. al., 1996). This may suggest different roles for the two phenotypes in the intact vessel wall. For example, the epithelioid cells may behave in a similar fashion to fibroblasts, healing breaches in the media which would allow release from contact inhibition. Alternatively the different behaviours may possibly relate to different origins, for example neural crest or embryonic mesenchyme (Owens, 1995). The

hySMCs demonstrated little contact inhibition of replication and little stimulatory effect with fetal calf serum. This autonomous behaviour is interesting as it shows the hySMCs to have features of both the epSMC and the spSMC.

8.7.2 Cell migration- wound healing experiments

The different behaviours of the spSMC and epSMC SMCs from 14 day old animals and the hySMCs from hypoxia animals suggested that there may be differences in their wound healing behaviour. The experiment described in this thesis was based on the original method of Gabbianni et. al. (1984). It was interesting to see that , as would be expected, the epSMCs rapidly proliferated and spread to close a breach in their monolayer, whilst the spSMCs did not appear to show any wound healing activity. A similar experiment has been performed looking at the migratory potential of spindle-shaped rat aortic SMCs and epithelioid SMCs derived from experimental intimal proliferation following endothelial denudation. The results were similar to those presented in this thesis, such that epithelioid clones demonstrated twice as much migratory behaviour as spindle-shaped cells from the normal media (Bochaton-Piallat et. al.,1995).

It was noteworthy that the epSMCs did not separate from the cell raft whilst the spSMCs readily separated. This experiment illustrates the importance of enzymatic dispersion as a method for isolating SMCs. If explant techniques (Chamley-Campbell et. al., 1979) are used then the cells obtained in culture will depend on their motile behaviour. Thus, since the spSMCs are able to separate from a confluent raft of cells these will predominate. Conversely, although the epithelioid SMCs can replicate without inhibition, their inability to separate from the confluent raft of cells means that they will not leave the explant. The poor wound healing activity of the hySMCs was an unexpected finding, since their ability to proliferate was noted in the serum dependence/contact inhibition experiments (above). It would seem unlikely that this was due to a limitation of the culture system since all cell lines were treated identically. It is also unlikely that the presence of desmin, which was found in the hySMCs but not the spSMCs or epSMCs, would interfere with motility as SMCs containing desmin have been shown to be motile (Bochaton-Piallat et. al.,1996).

8.7.3 Expression of cytoskeletal proteins by immunohistochemistry

The aim of this experiment was to try and correlate the morphological appearance of the cells with the cytoskeletal profile of the vessels from which they originated. The immunohistochemical staining of cultured cells is a standard procedure. The main difficulty with trying to identify the expression pattern of cytoskeletal proteins in cultured SMCs, is the variable reduction in protein expression that is known to occur. Although re-expression of many proteins does occur over time, for example α smooth muscle actin and caldesmon, smooth muscle myosin is one of the last proteins to be re-expressed and usually only occurs when the cells are grown to over confluence (Owens, 1995). The epSMC, spSMC and hySMCs were immunolabelled with the same antibodies that had been used to establish the B/C/D/CD cytoskeletal phenotype classification within the intact wall. As expected, none of the cells from any of the three phenotypes expressed smooth muscle specific myosin. It was interesting to note that both the epSMCs and the spSMCs obtained from the normal 14 day old animals had identical patterns of cytoskeletal protein expression. Although the spSMCs may have stained more abundantly for α smooth muscle and γ actins, they both expressed calponin and caldesmon, but not desmin. In contrast, the hySMCs contained abundant α smooth muscle, β and γ actins, but also expressed desmin in the absence of caldesmon. Thus, the epSMCs and the spSMCs would be described as C phenotype SMCs, and the hySMCs as D phenotype SMCs using the B/C/D/CD classification described previously. This means that the expression pattern of cytoskeletal proteins within hySMCs mirrors the vessel wall from which they originated. However, this is not the case with the spSMCs and epSMCs obtained from the 14 day old animals. These would be expected to demonstrate some B, D or CD phenotype cells in addition to the C phenotype cells already identified. It is difficult to know how to interpret this finding. It is possible that that the cloning process selected only epithelioid and spindle-shaped cells that expressed caldesmon. It is also possible, but also less likely, that the expression of

caldesmon in these cells was secondary to the cell culture environment since the hySMCs did not express this protein when grown under the same conditions.

8.7.4 Generation of tension by cultured SMCs

The generation of tension by cultured cells can be identified by their ability to wrinkle silastic membranes (Harris et. al., 1980). Basal wrinkling is probably generated by the cells "pulling themselves down on to the substrate" (Chicurel et. al.,1998), whilst further contraction leading to additional wrinkling is due to cellular contraction (Murray et. al., 1990). The failure of the cultured SMCs to demonstrate contraction was disappointing, but in retrospect inevitable. The absence of sufficient smooth muscle specific myosin to produce immunostaining (see above) would mean that generation of force would be limited. In addition, although made with the same viscosity polysiloxane used by other workers (30,000 centipoise) (Murray et. al., 1990), it is possible that the silastic membranes used for the experiments may have been too stiff. In the future it will be important to repeat these experiments with modifications to answer these points. In particular, it will be necessary to use confluent SMCs which express smooth muscle myosin (Murray et. al., 1990), on a series of membranes of differing strengths.

8.8 SUMMARY OF THESIS

At the time of birth, with the onset of respiration there is an immediate and profound increase in the blood flow through the lungs. Changes to the pulmonary vasculature must occur immediately if normal gaseous exchange is to occur through the lungs. Although much is known about the physiological changes that occur at this time, relatively little is known about the changes within the pulmonary arteries that facilitate these events. Previous work in the pig has indicated that the massive increase in pulmonary blood flow following birth is associated with an immediate change in shape of the pulmonary arterial SMCs in vivo. The SMCs change from a "brick like" fetal appearance, which occludes the lumens of peripheral vessels and narrows the lumens of more proximal arteries, to cells with

large surface area to volume ratios which produced thinning of the vessel wall and make the vessel lumen larger (Haworth and Hislop, 1982; Hall and Haworth, 1987). The studies reported in this thesis focussed on the possibility that different smooth muscle cell phenotypes might be present in the main intrapulmonary artery and be associated with changes in structure and function of this vessel during postnatal adaptation. Furthermore, intrapulmonary arteries from animals exposed to hypobaric hypoxia, which is a model of persistent pulmonary hypertension of the newborn, were also investigated to determine whether smooth muscle cell phenotypes might be involved in the pathological changes found in PPHN.

Using the results reported in this thesis, the developmental progression of the intrapulmonary artery during late gestation, onset of respiration at birth, and through post natal development can be divided into a series of stages:

1. During the last week of gestation, including labour and normal vaginal delivery, there is a compaction in the form of the actin cytoskeleton within SMCs of the intrapulmonary artery associated with a reduction in their stress ratio values. It is speculated that this fall in contractile potential may be related to the changing balance of vasoactive mediators present within the arteries at this time (Stenmark and Mecham, 1997).
2. Within minutes of initial breathing, further compaction of the filamentous actin cytoskeleton occurs which is associated with significant increases in the stress ratio values of the intrapulmonary arteries. This same process occurs in fetal animals born by Caesarean section one week prior to term. This may represent release from a "Catch state" (Hai and Murphy, 1992).
3. Within the first days after birth, the pulmonary arteries further adapt to increase in blood flow. The outer dimensions of the intrapulmonary artery remain constant (see Appendix), but the lumen dilates. This is associated with modulation of the cytoskeletal SMC phenotype within the inner two thirds of the intrapulmonary arterial media seen at three days of age. This reduction in α smooth muscle actin, β actin and calponin immunolabelling is associated with further re-organisation of the filamentous actin cytoskeleton from thick to thin filaments, but not with any statistically significant change

in the total or filamentous actin pools. Contractile potential remains unchanged during this process.

4. In the weeks following birth, the effect of growth and maturation on the intrapulmonary artery is observed as a progressive increase in the proportion of SMCs within the wall immunolabelling for cytoskeletal proteins such as desmin and caldesmon. This maturation process proceeds from the outer to the inner regions of the media in the period between 14 days of age and adulthood and is associated with progressive compaction of the actin cytoskeleton and an increase in contractile potential.
5. Chronic neonatal hypobaric hypoxia was shown to interfere with normal adaptation of the porcine intrapulmonary artery to the extrauterine environment. The expected modulation of SMC phenotype at 3 days of age did not occur and an abnormal SMC phenotype, expressing desmin in the absence of caldesmon, was identified throughout the entire media. The contractile potential of these vessels was however not statistically different from that of arteries from newborn or three day old piglets.

The studies of SMCs within the intact pulmonary artery were carried further, by enzymatic dissociation and growth of the SMCs in controlled conditions in vitro. Two different morphological SMC phenotypes (epithelioid and spindle-shaped) were identified at all ages examined and their appearances shown to be independent of plating substrate. A seven fold increase in the proportion of epithelioid SMCs obtained by enzymatic digestion of intrapulmonary artery was seen to occur between late fetal life and 3 days of age. This increase in epithelioid cells was shown not to be responsible for the changes in the inner media at three days of age.

Pure lines of the epithelioid (epSMC) and spindle-shaped (spSMC) SMCs from normal 14 day old animals and epithelioid (hySMCs) from animals exposed to hypobaric hypoxia, were obtained by dilutional cloning and the properties of these cells examined. The spSMCs behaved like "typical" SMCs. Whilst they did not exhibit contact inhibition of replication when grown in 10% fetal calf serum (FCS), the rate of replication was reduced and contact inhibition of replication was evident

when grown in 1% FCS. Although limited in their capacity for wound healing, the spSMCs were able to separate from other cells and move individually. In contrast, the epSMCs were limited by contact inhibition both in high and low concentrations of FCS, but relatively independent of the mitogenic effects of FCS. The epSMCs moved as a monolayer to quickly heal an artificial wound suggesting an in vivo role in tissue repair. The cytoskeletal profile of the epSMCs and spSMCs were similar, as both phenotypes expressed α, β and γ actin together with caldesmon. The epithelioid phenotype SMCs (hySMCs) from hypoxic animals exhibited patterns of behaviour that were intermediate between the spSMCs and the epSMCs from the intrapulmonary arteries of 14 day old piglets. They were similar to the epSMCs in that their replication was unaffected by reduction of FCS within the culture medium. However, together with the spSMCs their replication was not strongly inhibited by contact with neighbouring cells. The migration of the hySMCs in response to an artificial wound was minimal with no separation of cells, a similar behaviour as exhibited by the spSMCs.

The significance of these phenotypes remains unclear, but the possibility that they may have different embryonic origins, or have different roles remains. For example, from the behaviour of the cells in culture conditions, it is possible that the epithelioid cells behave in a similar fashion to fibroblasts and are predominantly involved in wound healing and growth within the artery.

8.9 FUTURE STUDIES

The studies presented in this thesis suggest several avenues for further investigation. The immunolabelling of cryo-ultramicrotomy sections was limited by an inability to dual label with desmin and caldesmon antibodies. A possible way to overcome this technical problem is by IgG subclass affinity purification of the two antibodies. Thus, each antibody can be recognised exclusively by a different IgG subclass specific reporter antibody. This will then clearly establish the B/C/D/CD classification of cytoskeletal SMC phenotype within the intact vessel wall. The question of whether the B cell phenotype SMCs mature and sequentially express

caldesmon and desmin under the effects of their environment, or whether replication of these B phenotype cells produces new SMCs bearing caldesmon or desmin can be directly answered by linked BrdU/cytoskeletal protein expression studies as discussed above **(section 8.2)**.

Another important problem to be solved is the lack of a direct link between morphological SMC phenotypes in tissue culture and the SMCs within the original vessel wall. It might be possible to use anti-cellular retinol binding protein (CRBP) antibodies. Previous studies have linked specific SMCs within experimental intimal thickening of the rat aorta to the epithelioid phenotype SMCs seen in cell cultures obtained from these tissues (Neuville et al., 1997). Other proteins that might differentiate the morphological phenotype could be identified by two-dimensional gel electrophoresis of epithelioid and spindle-shaped SMCs.

It will also be interesting to examine the phalloidin stabilised preparations with scanning electron microscopy, as the higher resolution afforded by this technique may reveal additional information. The simultaneous immunolabelling of these sections using gold particles will allow information to be obtained regarding the localisation of different actin isoforms throughout the cell.

As discussed above, the contractile function of the cultured cells must be re-addressed, using more deformable silastic membranes and confluent SMCs which have re-expressed smooth muscle myosin.

The clones of different morphological SMC phenotype obtained from the intrapulmonary artery may provide an important tool in understanding the mechanisms responsible for hypoxic pulmonary hypertension. The first step must be to obtain cells from fetal animals and from age matched control animals (3 days of age). It should then be possible to compare the cell types with regard to protein expression (two dimensional electrophoresis) or gene expression (subtractive differential display).

Although the pig has proved useful for investigations so far, use of the model is limited by the size and expense of the animals - especially those piglets exposed to hypoxia. In future, it may be useful to also use a mouse or rat model. Although the smaller quantities of tissue available from rodent studies might necessitate modification of techniques, the advantages of using larger numbers of animals, and

increased opportunities for genetic studies, for example, gene knockouts, might outweigh this.

9. Bibliography

Abman, S.H., Wilkening, R.B., Ward, R.M. and Accurso, F.J. 1986. Adaptation of fetal pulmonary blood flow to local infusion of tolazoline. *Pediatr Res* **20**, 1131-1135.

Abman, S.H., Accurso, F.J., Wilkening, R.B. and Meschia, G. 1987. Persistent fetal pulmonary hypoperfusion after acute hypoxia. *Am J Physiol* **253**, H941-H948.

Abman, S.H., Shanley, P.F. and Accurso, F.J. 1989. Failure of postnatal adaptation of the pulmonary circulation after chronic intrauterine pulmonary hypertension in fetal lambs. *J Clin Invest* **83**, 1849-1858.

Abman, S.H., Chatfield, B.A., Rodman, D.M., Hall, S.L. and McMurtry, I.V. 1991. Maturational changes in endothelium-derived relaxing factor activity of ovine pulmonary arteries in vitro. *Am J Physiol* **260**, L280-L285.

Abu-Osba, Y.K., Manasara, K., Galal, O. and Rejjal, A. 1990a. Treatment of pulmonary hypertension of the newborn with magnesium. *Ped Res* **27**, 294A

Abu-Osba, Y.K., Rhydderch, D. and Balasundaram, S. 1990b. Reduction of hypoxia-induced pulmonary hypertension by magnesium sulphate in sheep. *Ped Res* **27**, 351A

Aikawa, M., Sivam, N., Kuro-o, M., Kimura, K., Nakahara, K., Takewaki, S., Ueda, M., Yamaguchi, H., Yazaki, Y., Periasamy, M. and Nagai, R. 1993. Human smooth muscle myosin heavy chain isoforms as molecular markers for vascular development and atherosclerosis. *Circ Res* **73**, 1000-1012.

Alberts, B., Bray, D., Lewis, J., Raff, M., Roberts, K. and Watson, J. (1999). The molecular biology of the cell,. Garland Press Ltd.

Allen, K.M. and Haworth, S.G. 1986. Impaired adaptation of pulmonary circulation to extrauterine life in newborn pigs exposed to hypoxia: an ultrastructural study. *J Pathol* **150**, 205-212.

Amano, M., Chihara, K., Kimura, K., Fukata, Y., Nakamura, N., Matsuura, Y. and Kaibuchi, K. 1997. Formation of actin stress fibres and focal adhesions enhanced by Rho-kinase. *Science* **275**, 1308-1311.

Amberger, A., Bauer, H., Tontsch, U., Gabbiani, G., Kocher, O. and Bauer, H.C. 1991. Reversible expression of sm α-actin protein and sm α-actin mRNA in cloned cerebral endothelial cells. *FEBS* **287**, 223-225.

Babaev, V.R., Bobryshev, Y.V., Stenina, O.V., Tararak, E.M. and Gabbiani, G. 1990. Heterogeneity of smooth muscle cells in atheromatous plaque of human aorta. *Am J Pathol* **136**, 1031-1042.

Badreck-Amoudi, A., Patel, C.K., Kane, T.P.C. and Greenwald, S.E. 1996. The effect of age on residual strain in the rat aorta. *J Biomech Eng* **118**, 440-444.

Bank, A.J., Wang, H., Holte, J.E., Mullen, K., Shammas, R. and Kubo, S.H. 1996. Contribution of collages, elastin and smooth muscle to in vivo human brachial artery wall stress and elastic modulus. *Circulation* **94**, 3263-3270.

Barclay, A., Barcroft, J., Barron, D. and Franklin, K. 1939. A radiographic demonstration of the circulation through the heart in the adult and in the foetus, and the identification of the ductus arteriosus. *Br J Radiol* **12**, 505-518.

Bennett, P.M. and Elliott, A. 1989. The "catch" mechanism in molluscan muscle: an electron microscopy study of freeze-substituted anterior byssus muscle of Mytilus edulis. *J Muscle Res Cell Motil* **10**, 297-311.

Bergwerff, M., DeRuiter, M.C., Poelmann, R.E. and Gittenberger-De-Groot, A.C. 1996. Onset of elastogenesis and downregulation of smooth muscle actin as distinguishing phenomena in artery differentiation in the chick embryo. *Anat Embryol* **194**, 545-557.

Berry, C.L. and Greenwald, S.E. 1976. Effects of hypertension on the static mechanical properties and chemical composition of the rat aorta. *Cardiovasc Res* **10**, 437-451.

Berry, C.L., Sosa-Melgarejo, J.A. and Greenwald, S.E. 1993. The relationship between wall tension, lamellar thickness, and intercellular junctions in the fetal and adult aorta: its relevance to the pathology of dissecting aortic aneurysm. *J Pathol* **169,** 15-20.

Birukov, K.G., Frid, M.G., Rogers, J.D., Shirinsky, V.P., Koteliansky, V.E., Campbell, J.H., and Campbell, G.R. 1993. Synthesis and expression of smooth muscle phenotype markers in primary culture of rabbit aortic smooth muscle cells: influence of seeding density and media and relation to cell contractility. *Exp Cell Res* **204**, 46-53.

Birukov, K., Shirinsky, V., Stepanova, O., Tkachuk, V., Hahn, A., Resink, T. and Smirnov, V. 1995. Stretch affects phenotype and proliferation of vascular smooth muscle cells. *Ped Res* **144**, 131-139.

Blank, R.S., Thompson, M.M. and Owens, G.K. 1988. cell cycle versus density dependence of smooth muscle alpha actin expression in cultured rat aortic smooth muscle cells. *J Cell Biol* **107**, 299-306.

Bochaton-Piallat, M., Ropraz, P., Gabbiani, F. and Gabbiani, G. 1996. Phenotypic heterogeneity of rat arterial smooth muscle cell clones. *Arterioscler Thromb Vasc Biol* **16**, 815-820.

Bochaton-Pillat, M., Gabbiani, F., Ropraz, P. and Gabbiani, G. 1992. Cultured aortic smooth muscle cells from newborn and adult rats show distinct cytoskeletal features. *Differentiation* **49**, 175-185.

Bohn, D., Tamura, M., Perrin, D., Barker, G. and Rabinovitch, M. 1987. Ventilatory predictors of pulmonary hypoplasia in congenital diaphragmatic hernia, confirmed by morphologic assessment. *J Pediatr* **111**, 423-431.

Buoro, S., Ferrarese, P., Chiavegato, A., Roelofs, M., Scatena, M., Pauletto, P., Passerini-Glazel, G., Pagano, F. and Sartore, S. 1993. Myofibroblast-derived smooth muscle cells during remodelling of rabbit urinary bladder wall induced by partial outflow obstruction. *Lab Invest* **69**, 589-602.

Campbell, J.H., Kocher, O., Skalli, O., Gabbiani, G. and Campbell, G.R. 1989. Cytodifferentiation and Expression of a-Smooth Muscle Actin mRNA and Protein during Primary Culture of Aortic Smooth Muscle Cells. *Arteriosclerosis* **9**, 633-643.

Candipan, R.C. and Sjostrand, F.S. 1984. An analysis of the contribution of the preparatory technique to the appearance of condensed and orthodox conformations of liver mitochondria. *J Ultrastruct Res* **89**, 281-294.

Capetanaki, Y., Milner, D.J. and Weitzer, G. 1997. Desmin in muscle formation and maintenance: knockouts and consequences. *Cell Struct Funct* **1**, 103-116.

Cassin, S., Dawes, G.S., Mott, J.C., Ross, B.B. and Strang, L.B. 1964. The vascular resistance of the foetal and newly ventilated lung of the lamb. *J Physiol* **171**, 61-79.

Cassin, S. 1987. Role of prostaglandins, thromboxanes and leukotrienes in the control of the pulmonary circulation in the fetus and newborn. *Semin Perinatol* **11**, 53-63.

Chamley, J.H. and Campbell, G.R. 1973. An analysis of the interactions between sympathetic nerve fibres and smooth muscle cells in tissue culture. *Dev Biol* **33**, 344-361.

Chamley-Campbell, J., Campbell, G.R. and Ross, R. 1979. The smooth muscle cell in culture. *Physiol Rev* **59**, 1-61.

Chen, C.S., Mrksich, M., Huang, S., Whitesides, G.M. and Ingber, D.E. 1997. Geometric Control of Cell Life and Death. *Science* **276**, 1425-1428.

Chicurel, M.E., Chen, C.S. and Ingber, D.E. 1998. Cellular control life in the balance of forces. *Curr Opin Cell Biol* **10**, 232-239.

Cho, A., Courtman, D.W. and Langille, B.L. 1995. Apoptosis (programmed cell death) in arteries of the neonatal lamb. *Circ Res* **76**, 168-175.

Cho, A., Mitchell, L., Koopmans, D and Langille, B.L. 1997. Effects of changes in blood flow rate on cell death and proliferation in carotid arteries of immature rabbits. *Circ Res* **81**, 328-337.

Chuong, C.J. and Fung, Y.C. 1983. Three-dimensional stress distribution in arteries. *J Biomech Eng* **105**, 268-274.

Clyman, R.I., Mauray, F. and Kramer, R.H. 1992. Beta 1 and beta 3 integrins have different roles in the adhesion and migration of vascular smooth muscle cells on extracellular matrix. *Exp Cell Res* **200**, 272-284.

Colebatch, H., Dawes, G., Goodwin, J. and Nadeau, R. 1965. The nervous control of the circulation in fetal and newly expanded lungs of the lamb. *J Physiol* **178**, 544-562.

Cook, C.L., Weiser, M.C.M., Schwartz, P.E., Jones, C.L. and Majack, R.A. 1993. Developmentally timed expression of an embryonic growth phenotype in vascular smooth muscle cells. *Circ Res* **74**, 189-196.

Cornfield, D.N., Stevens, T., McMurtry, I.F., Abman, S.H. and Rodman, D.M. 1993. Acute hypoxia increases cytosolic calcium in fetal pulmonary artery smooth muscle cells. *Am J Physiol* **265**, L53-L56.

Cox, R.H. 1983. Comparison of arterial wall mechanics using ring and cylindrical elements. *Am J Physiol* **244**, H298-H303.

Cremona, O., Savoia, P., Marchisio, P.C., Gabbiani, G. and Chaponnier, C. 1994. The α_6 and β_4 integrin subunits are expressed by smooth muscle cells of human small Vessels: A New localization in mesenchymal cells. *J Histochem Cytochem* **42**, 1221-1228.

Crouch, E.C., Parks, W.C., Rosenbaum, J.L., Chang, D., Whitehouse, L., Wu, L., Stenmark, K.R., Orton, E.C. and Mecham, R.P. 1989. Regulation of collagen production by medial smooth muscle cells in hypoxic pulmonary hypertension. *Am Rev Respir Dis* **140**, 1045-1051.

Darby, I., Skalli, O. and Gabbiani, G. 1990. Smooth muscle actin is transiently expressed by myofibroblasts during experimental wound healing. *Lab Invest* **63**, 21-29.

Daum, G., Hedin, U., Wang, Y., Wang, T. and Clowes, A.W. 1997. Diverse Effects of Heparin on Mitogen-Activated Protein Kinase-Dependent Signal Transduction in Vascular Smooth Muscle Cells. *Circ Res* **81**, 17-23.

Dawes, G.S., Mott, J.C., Widdicombe, J.G. and Wyatt, D.G. 1953. Changes in the lungs of the newborn lamb. *J Physiol* **121**, 141-162.

Dawes, G.S., Mott, J.C. and Widdicombe, J.G. 1954. The fetal circulation in the lamb. *J Physiol* **126**, 563-587.

Dawes, G.S. 1968. Foetal and neonatal physiology, Year book medical publishers, London.

DeRuiter, M.C., Poelmann, R.E., VanMunsteren, J.C., Mironov, V., Markwald, R.R. and Gittenberger-De-Groot, A.C. 1997. Embryonic endothelial cells transdifferentiate into mesenchymal cells expressing smooth muscle actins in vivo and in vitro. *Circ Res* **80**, 444-451.

Desmouliere, A., Rubbia-Brandt, L. and Gabbiani, G. 1991. Modulation of actin isoform expression in cultured arterial smooth muscle cells by heparin and culture conditions. *Arteriosclerosis and Thrombosis* **11**, 244-253.

Dobrin, P.B. 1978. Mechanical properties of arteries. *Physiol Rev* **58**, 397-460.

Dobrin, P.B., Mrkvicka, R. 1992. Estimating the elastic modulus of non-arterosclerotic elastic arteries. *J Hypertens Suppl* **10**, S7-S10.

Dobrin, P.B. 1996. Effect of histologic preparation on the cross-sectional area of arterial rings. *J Surg Res* **61**, 413-415.

Duband, J., Gimona, M., Scatena, M., Sartore, S. and Small, J.V. 1993. Calponin and SM22 as differentiation markers of smooth muscle: spatiotemporal distribution during avian embryonic development. *Differentiation* **55**, 1-11.

Ehler, E., Jat, P.S., Noble, M.D., Citi, S. and Draeger, A. 1995. Vascular smooth muscle cells of H-2K^{b}-tsa58 transgenic mice. *Circ* **92**, 3289-3296.

Enhorning, G., Adams, F.H. and Norman, A. 1966. Effect of lung expansion on the fetal lamb circulation. *Acta Paediatr Scand* **55**, 441-451.

Fagotto, F. and Gumbiner, B.M. 1996. Cell contact-dependent signalling. *Dev Biol* **180**, 445-454.

Fechheimer, M. and Zigmond, S.H. 1993. Focusing on unpolymerized actin. *J Cell Biol* **123**, 1-5.

Fike, C.D. and Kaplowitz, M.R. 1992. Pulmonary venous pressure increases during alveolar hypoxia in isolated lungs of newborn pigs. *J Appl Physiol* **73**, 552-556.

Fike, C.D. and Kaplowitz, M.R. 1994. Effect of chronic hypoxia on pulmonary vascular pressures in isolated lungs of newborn pigs. *J Appl Physiol* **77**, 2853-2862.

Fisher, S.A., Ikebe, M. and Brozovich, F. 1997. Endothelin-1 Alters the Contractile Phenotype of Cultured Embryonic Smooth Muscle Cells. *Circ Res* **80**, 885-893.

Fox, W.W. and Duara, S. 1983. Persistent pulmonary hypertension in the neonate: diagnosis and management. *J Pediatr* **103**, 505-514.

Frid, M., Dempsey, E.C., Durmowicz, A.G. and Stenmark, K.R. 1997. Smooth muscle cell heterogeneity in pulmonary and systemic vessels. *Arterioscler Thromb Vasc Biol* **17**, 1203-1209.

Frid, M.G., Printesva, O.Y., Chiavegato, A., Faggin, E., Scatena, M., Koteliansky, V.E., Pauletto, P., Glukhova, M.A. and Sartore, S. 1993. Myosin heavy-chain isoform composition and distribution in developing and adult human aortic smooth muscle. *J Vasc Res* **30**, 279-292.

Frid, M.G., Moiseeva, E.P. and Stenmark, K.R. 1994. Multiple phenotypically distinct smooth muscle cell populations exist in the adult and developing bovine pulmonary arterial media in vivo. *Circ Res* **75**, 669-681.

Fujita, H., Shimokado, K., Yutani, C., Takaichi, S., Masuda, J. and Ogata, J. 1993. Human neonatal and adult vascular smooth muscle cells in culture. *Exp Mol Pathol* **58**, 25-39.

Fulton, C. 1983. Macromolecular synthesis during the quick change act of Naegleria. *J Protozool* **30**, 192-198.

Furchgott, R.F. and Zawadzki, J.V. 1980. The obligatory role of endothelial cells in the relaxation of arterial smooth muscle by acetylcholine. *Nature* **288**, 373-376.

Gabbiani, G., Gabbiani, F., Heimark, R.L. and Schwartz, S.M. 1984a. Organization of Actin Cytoskeleton During Early Endothelial Regeneration *In Vitro*. *J Cell Sci* **66**, 39-50.

Gabbiani, G., Kocher, O., Bloom, W.S., Vanderkerckhove, J. and Weber, K. 1984b. Actin expression in smooth muscle cells of rat aortic intimal thickening and human atheromatous plaque. *J Clin Invest* **73**, 148-152.

Gabbiani, G. 1987. The cytoskeleton of rat aortic smooth muscle cells: normal conditions, experimental intimal thickening and tissue culture. *Acta histochemica* **XXXIV**, S33-S35.

Gabbiani, G. 1992. The biology of the myofibroblast. *Kidney International* **41**, 530-532.

Galou, M., Gao, J., Humbert, J., Mericskay, M., Li, Z., Paulin, D. and Vicart, P. 1997. The importance of intermediate filaments in the adaptation of tissues to mechanical stress: evidence from gene knockout studies. *Biol Cell* **89**, 85-97.

Gimola, Vandekerckove, Goethals, M., Herzog, M., Lando, Z. and Small, V. 1994. Cell motility and the cytoskeleton. *Journal* **27**, 108-116.

Gimona, M., Herzog, M., Vandekerckhove, J. and Small, J.V. 1990. Smooth muscle specific expression of calponin. *FEBS* **274**, 159-162.

Gleadle, J.M., Ebert, B.L., Firth, J.D. and Ratcliffe P.J. 1995. Regulation of angiogenic growth factor expression by hypoxia, transition metals and chelating agents. *Am J Physiol* **268**, C1362-C1638.

Glukova, M., Koteliansky, V., Fondacci, C., Marotte, F. and Rappaport, L. 1993. Laminin varients and integrin laminin receptors in developing and adult human smooth muscle. *Dev Biol* **157**, 437-447.

Gordon, J.B., Tod, M.L. and Wetzel 1999. Age dependent effects of indomethacin on hypoxic vasoconstriction in neonatal lambs lungs. *Pediatr Res* **23**, 580-584.

Greenwald, S.E., Berry, C.L. and Haworth, S.G. 1982. Changes in the distensibility of the intrapulmonary arteries in the normal newborn and growing pig. *Cardiovasc Res* **16**, 716-725.

Hai, C. and Murphy, R. 1992. Adenosine 5' triphosphate consumption by smooth muscle as predicted by the coupled four-state cross bridge model. *Biophys J* **61**, 530-541.

Halbower, A.C., Tuder, R.M., Franklin, W.A., Pollock, J.S., Forstermann, U. and Abman, S.H. 1994. Maturation-related changes in endothelial nitric oxide

synthase immunolocalization in developing ovine lung. *Am J Physiol Lung Cell Mol Physiol* L585-L591.

Hall, A. 1998. Rho GTPases and the actin cytoskeleton. *Science* **279**, 509-514.

Hall, S.M. and Haworth, S.G. 1987. Conducting pulmonary arteries: structural adaptation to extrauterine life. *Cardiovascular Res* **21**, 208-216.

Hall, S.M. and Haworth, S.G. 1992. Onset and evolution of pulmonary vascular disease in young children : abnormal postnatal remodelling studied in lung biopsies. *J Pathol* **166**, 183-194.

Halliday, A., Hunt, B., Poston, L. and Schachter, M. (Eds.) . 1998. An Introduction to Vascular Biology. Cambridge University Press.

Harris, A.K., Wild, P. and Stopak, D. 1980. Silicone rubber substrata: a new wrinkle in the study of cell locomotion. *Science* **208**, 177-179.

Harvey, W. 1628. Exercitatio anatomica de motu cordis et sanguinis in animalibus. *Francofurti: Fitzeri*.

Haworth, S.G., Hall, S.M., Chew, M. and Allen, K. 1987. Thinning of fetal pulmonary arterial wall and postnatal remodelling: ultrastructural studies on the respiratory unit arteries of the pig. *Virchows Arch A* **411**, 161-171.

Haworth, S.G. 1995. Development of the normal and hypertensive pulmonary vasculature. *Experimental Physiology* **80**, 843-845.

Haworth, S.G. and Hislop, A.A. 1981. Adaptation of the pulmonary circulation to extra-uterine life in the pig and its relevance to the human infant. *Cardiovasc Res* **15**, 108-119.

Haworth, S.G. and Hislop, A.A. 1982. Effect of hypoxia on adaptation of the pulmonary circulation to extra-uterine life in the pig. *Cardiovasc Res* **16**, 293-303.

Haworth, S.G. and Reid, L. 1976. Persistent fetal circulation: newly recognised structural features. *J Pediatr* **88**, 614-620.

Hayward, I.P., Bridle, K.R., Campbell, G.R., Underwood, P.A. and Campbell, J.H. 1995. Effect of Extracellular Matrix Proteins on Vascular Smooth Muscle Cell Phenotype. *Cell Biol Internat* **19**, 839-846.

Hedin, U., Bottger, B.A., Forsberg, E., Johansson, S. and Thyberg, J. 1988. Diverse Effects of Fibronectinand Laminin on Phenotypic Properties of Cultured Arterial Smooth Muscle Cells. *J Cell Biol* **107**, 307-319.

Hedin, U., Sjolund, M., Hultgardh-Nilsson, A. and Thyberg, J. 1990. Changes in expression and organisation of smooth-muscle-specific α-actin during fibronectin-mediated modulation of arterial smooth muscle cell phenotype. *Differentiation* **44**, 222-231.

Hill, M. and Gunning, P. 1993. Beta and gamma actin mRNAs are differentially located within myoblasts. *J Cell Biol* **122**, 825-832.

Hirokawa, N. and Tilney, L.G. 1982. Interactions between actin filaments and between actin filaments and membranes in quick-frozen and deeply etched hair cells of the chick ear. *J Cell Biol* **95**, 249-256.

Hirschi, K.K. and D'Amore, P.A. 1996. Pericytes in the microvasculature. *Cardiovasc Res* **32**, 687-698.

Hislop, A.A., Zhao, Y.D., Springall, D.R., Polak, J.M. and Haworth, S.G. 1995. Postnatal changes in endothelin-1 binding in porcine pulmonary vessels and airways. *Am J Respir Cell Mol Biol* **12**, 557-566.

Huang, Z., Yue, S., You, W. and Haugland, R. 1993. A fluorometric microplate-based assay of submicrogram monomeric actin by inhibition of deoxyribonuclease I. *Analytical Biochem* **214**, 272-277.

Huber, P. 1997. Caldesmon. *Int J Biochem Cell Biol* **29**, 1047-1051.

Hungerford, J.E. and Little, C.D. 1999. Developmental biology of the vascular smooth muscle cell: building a multilayered vessel wall. *J Vasc Res* **36**, 2-27.

Ingber, E. 1997. Tensegrity: the architectural basis of cellular mechanotransduction. *Ann Rev Physiol* **59**, 575-599.

Ives, H.E., Schultz, G.S., Galardy, R.E. and Jamieson, J.D. 1978. Preparation of functional smooth muscle cells from the rabbit aorta. *J Exp Med* **148**, 1400-1413.

Ivy, D.D., Kinsella, J.P. and Abman, S.H. 1994. Physiologic characterisation of endothelin A and B receptor activity in the ovine fetal pulmonary circulation. *J Clin Invest* **93**, 2141-2148.

Jahn, L., Kreuzer, J., Von Hodenberg, E., Kubler, W. and Franke, W.W. 1993. Cytokeratins 8 and 18 in smooth muscle cells: detection in human coronary artery, peripheral vascular, and vein graft disease and in transplant-associated atherosclerosis. *Arterioscler Thromb* **13**, 1631-1639.

Jain, M.K., Layne, M.D., Watanabe, M., Chin, M.T., Feinberg, M.W., Sibinga, N.E.S., Hsieh, C., Yet, S., Stemple, D.L. and Lee, M. 1998. *In Vitro* System for Differentiating Pluripotent Neural Crest Cells into Smooth Muscle Cells. *J Biol Chem* **273**, 5993-5996.

Jenson, L.T. and Host, N.B. 1997. Collagen: scaffold for repair or execution. *Cardiovasc Res* **33**, 535-539.

Jones, P.L. and Rabinovitch, M. 1996. Tenascin-C is induced with progressive pulmonary vascular disease in rats and is functionally related to increased smooth muscle cell proliferation. *Circ Res* **79**, 1131-1142.

Julian, D., Camm, A., Fox, K., Hall, R., Poole Wilson, P. 1996. Disorders of the pulmonary circulation in Diseases Of The Heart, Saunders.

Kapanci, Y., Ribauz, C., Chaponnier, C. and Gabbiani, G. 1992. Cytoskeletal features of alveolar myofibroblasts and pericytes in normal human and rat lung. *J Histo Cyto* **40**, 1955-1963.

Kato, S., Shanley, J.R. and Fox, J.C. 1996. Serum stimulation, cell-cell interactions, and extracellular matrix independently influence smooth muscle cell phenotype *in Vitro*. *Am J Pathol* **149**, 687-697.

Keller, H.U. and Bebie, H. 1996. Protrusive activity quantitatively determines the rate and direction of cell locomotion. *Cell Motil Cytoskeleton* **33**, 241-251.

Kelley, C., D'Amore, P., Hechtman, H.B. and Shepro, D. 1987. Microvascular pericyte contractility in vitro: comparison with other cells of the vascular wall. *J Cell Biol* **104**, 483-490.

Kinsella, J.P., Neish, S.R., Shaffer, E. and Abman, S.H. 1992. Low-dose inhaled nitric oxide in persistent pulmonary hypertension of the newborn. *The Lancet* **340**, 819-820.

Kinsella, J.P. and Abman, S.H. 1995. Recent developments in the pathophysiology and treatment of persistent pulmonary hypertension of the newborn. *Journal of Pediatrics* **126**, 853-864.

Kinsella, J.P. and Abman, S.H. 1998. Inhaled nitric oxide and high frequency oscillatory ventilation in persistent pulmonary hypertension of the newborn. *Eur J Pediatr* **157**, S28-S30.

Kitagawa, M., Hislop, A., Boyden, E.A. and Reid, L. 1971. Lung hypoplasia in congenital diaphragmatic hernia. A quantitative study of airway, artery and alveolar development. *Br J Surg* **58**, 342-346.

Kocher, O., Skalli, O., Cerutti, D., Gabbiani, F. and Gabbiani, G. 1985. Cytoskeletal features of rat aortic cells during development. *Circ Res* **56**, 829-838.

Kocher, O., Skalli, O., Bloom, W.S. and Gabbiani, G. 1994. Cytoskeleton of rat aortic smooth muscle cells. *Lab Invest* **50**, 645-652.

Kuro-o, M., Nagai, R., Tsuchimochi, H., Katoh, H., Yazaki, Y., Ohkubo, A. and Takaku, F. 1989. Developmentally regulated expression of vascular smooth muscle myosin heavy chain isoforms. *J Biol Chem* **264**, 9734-9737.

LaBarca, C. and Paigen, K. 1980. A simple, rapid and sensitive DNA assay procedure. *Anal Biochem* **102**, 344

Lawson, D., Harrison, M. and Shapland, C. 1997. Fibroblast transgelin and smooth muscle SM22α are the same protein, the expression of which is down-regulated in many cell lines. *Cell Motil Cytoskeleton* **38**, 250-257.

Lee, S.L., Hungeford, J.E., Little, C.D. and Iruela-Arispe, M.L. 1997. Proliferation and differentiation of smooth muscle cell precursors occurs simultaneously during development of the vessel wall. *Dev Dyn* **209**, 342-352.

Le Lievre, C.S. and Le Douarin, N.M. 1975. Mesenchymal derivatives of the neural crest: analysis of chimaeric quail and chick embryos. *J Embryol Exp Morphol* **34**, 125-154.

Lees-Miller, J., Heeley, D., Smillie, L. and Kay, C. 1987. Isolation and characterisation of an abundant and novel 22kDa protein (SM 22) from chicken gizzard smooth muscle. *J Biol Chem* **262**, 2988-2993.

Leffler, C.W., Tyler, T.L. and Cassin, S. 1978. Effect of indomethacin on pulmonary vascular response to ventilation of fetal goats. *Am J Physiol* **234**, H346-H351.

Leffler, C.W., Hessler, J.R. and Green, R.S. 1984. The onset of breathing at birth stimulates pulmonary vascular prostacyclin synthesis. *Paed Res* **18**, 938-942.

Lemire, J.M., Covin, S.W., Giachelli, C.M. and Swartz, S.M. 1994. Characterisation of cloned aortic smooth muscle cells from young rats. *Am J Path* **144**, 1068-1081.

Lemire, J.M., Potter-Perigo, S., Hall, K.L., Wight, T.N. and Schwartz, S.M. 1996. Distinct Rat Aortic Smooth Muscle Cells Differ in Versican/PG-M Expression. *Arterioscler Thromb Vasc Biol* **16**, 821-829.

Lewis, A.B., Heymann, M.A. and Rudolph, A.M. 1976. Gestational changes in pulmonary vascular responses in fetal limbs in utero. *Circ Res* **39**, 536-541.

Li, J., Sensebe, L., Herve, P. and Charbord, P. 1995. Nontransformed colony-derived stromal cell lines from normal human marrows. II. Phenotypic characterisation and differentiation pathway. *Exp Hematol* **23**, 133-141.

Li, L., Miano, J.M., Cserjesi, P. and Olson, E.N. 1996. SM22α, a marker of adult smooth muscle, is expressed in multiple myogenic lineages during embryogenesis. *Circ Res* **78**, 188-195.

Li, Z.L. and Paulin, D. 1991. High level desmin expression depends on a muscle-specific enhancer. *J Biol Chem* **266**, 6562-6570.

Li, Z., Colucci, G.E., Pincon, R.M., Mericskay, M., Pournin, S., Paulin, D. and Babinet, C. 1996. Cardiovascular lesions and skeletal myopathy in mice lacking desmin. *Dev Biol* **175**, 362-366.

Liddell, R., Syms, M. and McHugh, K. 1993. Hetrogeneous isoactin gene expression in the adult rat gastrointestinal tract. *Gastroenterology* **105**, 347-356.

Mabuchi, K., Li, Y., Tao, T., and Wang, C.L. 1996. Immunocytochemical localisation of caldesmon and calponin in chicken gizzard smooth muscle. *J Muscle Res Cell Motil* **17**, 243-260.

Malpighi M. 1661. De pulmonibus observationes anatomicae (Anatomical observations on the lungs).

Manderson, J.A., Mosse, P.R., Safstrom, J.A., Young, S.B. and Campbell, G.R. 1989. Balloon catheter injury to rabbit carotid artery. I. Changes in smooth muscle phenotype. *Arteriosclerosis* **9**, 289-298.

McHugh, K. and Lessard, J. 1988. The developmental expression of the rat α-vascular and y-enteric smooth muscle isoforms: isolation and characterisation of the rat y-enteric actin cDNA. *Mol Cell Biol* **8**, 5224-5231.

McKenzie, S. and Haworth, S.G. 1981. Occlusion of peripheral pulmonary vascular bed in a baby with idiopathic persistent fetal circulation. *Br Heart J* **46**, 675-678.

Mills, A.N. and Haworth, S.G. 1987. Pattern of connective tissue development in swine pulmonary vasculature by immunolocalisation. *J Pathol* **153**, 171-176.

Miner, J.H. and Sanes, J.R. 1994. Collagen IV alpha 3, alpha 4, and alpha 5 chains in rodent basal laminae: sequence, distribution, association with laminins, and developmental switches. *J Cell Biol* **127**, 879-891.

Mironov, A.A., Rekhter, M.D., Kolpakov, V.A., Andreeva, E.R., Polishchuk, R.S., Bannykh, S.I., Filippov, S.V., Peretjatko, L.P., Kulida, L.V. and Orekhov, A.N. 1995. Heterogeneity of smooth muscle cells in embryonic human aorta. *Tissue and Cell* **27**, 31-38.

Moessler, H., Mericskay, M., Li, Z., Nagl, S., Paulin, D. and Small, J.V. 1996. The SM22 promoter directs tissue-specific expression in arterial but not in venous or visceral smooth cells in transgenic mice. *Development* **122**, 2415-2425.

Morin, F.C. 1986. Hyperventilation, alkalosis, prostaglandins, and pulmonary circulation of the newborn. *J Appl Physiol* **61**, 2088-2094.

Morin, F.C., Egan, E.A. and Norfleet, W.T. 1988. Indomethacin does not diminish the pulmonary vascular response of the fetus to increased oxygen tension. *Pediatr Res* **24**, 696-700.

Morin, F.C.I., Egan, E.A. and Ferguson, W. 1988. Development of pulmonary vascular response to oxygen. *Am J Physiol* **254**, H542-H546.

Morin, F.C. and Stenmark, K.R. 1995. Persistent pulmonary hypertension of the newborn. *Am J. Resp Crit Care Med* **151**, 2010-2032.

Mosher, D. 1993. Assembly of fibronectin into extracellular matrix. *Curr Opin Str Biol* **3**, 214-222.

Moss, A.J., Emmanouilides, G. and Duffie, E.R. 1963. Closure of the ductus arteriosus in the newborn infant. *Paediatrics* **32**, 25-30.

Murray, T.R., Marshall, B.E. and Macarak, E.J. 1990. Contraction of vascular smooth muscle in cell culture. *J Cell Physiol* **143**, 26-38.

Nachmias, V.T., Philp, N., Momoyama, Y. and Choi, J.K. 1992. G-actin pool and actin messenger RNA during development of the apical processes of the retinal pigment epithelial cells of the chick. *Dev Biol* **149**, 239-246.

Nagai, R., Kuro, M., Babij, P. and Periasamy, M. 1989. Identification of two types of smooth muscle myosin heavy chain isoforms by cDNA cloning and immunoblot analysis. *J Biol Chem* **264**, 9734-9737.

Neuville, P., Benzonana, G., Redard, M., Gabbiani, F., Ropraz, P. and Gabbiani, G. 1997. Cellular retinol-binding protein-1 is expressed by distinct subsets of rat arterial smooth muscle cells in vitro and in vivo. *Am J Pathol* **150**, 509-521.

Newman, C.M., Bruun, B.C., Porter, K.E., Mistry, P.K., Shanahan, C.M. and Weissberg, P.L. 1995. Osteopontin is not a marker for proliferating human vascular smooth muscle cells. *Arterioscler Thromb Vasc Biol* **15**, 2010-2018.

Nichols, W.W. and O'Rourke, M.F. (1998). McDonalds Blood Flow in Arteries, Arnold.

Nicosia, R. and Villaschi, S. 1995. Rat aortic smooth muscle cells become pericytes during angiogenesis in vitro. *Laboratory Investigation.* **73**, 658-665.

Orlandi, H., Ehrlich, H.P., Ropraz, P., Spagnoli, L.G. and Gabbiani, G. 1994. Rat aortic smooth muscle cells isolated from different layers and at different times

after endothelial denudation show distinct biological features in vitro. *Arterioscler Thromb* **14**, 982-989.

Owens, G.K., Loeb, A., Gordon, D. and Thompson, M.M. 1986. Expression of smooth muscle-specific alpha isoactin in cultured vascular smooth muscle cells: relationship between growth and cytodifferentiation. *J Cell Biol* **102**, 343-352.

Owens, G.K. 1995. Regulation of differentiation of vascular smooth muscle cells. *Physiol Rev* **75**, 487-517.

Palmberg, L., Sjolund, M. and Thyberg, J. 1985. Phenotype modulation in primary cultures of arterial smooth-muscle cells: reorganization of the cytoskeleton and activation of synthetic activities. *Differentiation* **29**, 275-283.

Pantaloni, D. and Carlier, M. 1993. How profilin promotes actin filament assembly in the presence of thymosin β4. *Cell* **75**, 1007-1014.

Price, R.J., Owens, G.K. and Skalak, T.C. 1994. Immunohistochemical identification of arteriolar development using markers of smooth muscle Differentiation. *Circ Res* **75**, 520-527.

Raine, J., Hislop, A.A., Redington, A.N., Haworth, S.G. and Shinebourne, E.A. 1991. Fatal persistent pulmonary hypertension presenting late in the neonatal period. *Arch Dis Child* **66**, 398-402.

Redding, G.J., McMurtry, I. and Reeves, J.T. 1984. Effects of meclofenamate on pulmonary vascular resistance correlate with postnatal age in young piglets. *Pediatr Res* **18**, 579-583.

Roberton, N.R.C. (Ed). 1992. Textbook of Neonatology. Churchill Livingstone, Edinburgh.

Ross, R. 1986. The pathogenesis of atherosclerosis: an update. *N Eng J Med* **314**, 488-500.

Rothman, A., Kulik, T.J., Taubman, M.B., Berk, B.C., Smith, C.W.J. and Nadal-Ginard, B. 1992. Development and characterisation of a cloned rat pulmonry arterial smooth muscle cell line that maintains differentiated properties through multiple subcultures. *Circulation* **86**, 1977-1986.

Rovner, A.S., Murphy, R.A. and Owens, G.K. 1986. Expression of smooth muscle and nonmuscle Myosin Heavy Chains in Cultured Vascular Smooth Muscle Cells. *J Biol Chem* **261**, 14740-14745.

Rudolph, A.M. and Heymann, M.A. 1970. Circulatory changes during growth in the fetal lamb. *Circ Res* **26**, 289-299.

Ruegg, J.C. and Pfitzer, G. 1991. Contractile protein interactions in smooth muscle. *Blood Vessels* **28**, 159-163.

Sappino, A., Schurch, W. and Gabbiani, G. 1990. Differentiation repertoire of fibroblastic cells: Expression of cytoskeletal proteins as marker of phenotypic modulations. *Lab Invest* **63**, 144-161.

Schaller, M. and Parsons, J. 1993. Focal adhesion kinase: an integrin-linked protein tyrosin kinase. *Trends in Cell Biology* **3**, 258-262.

Siegman, M.J., Funabara, D., Kinoshita, S., Watabe, S., Hartshorne D.J. and Butler, T.M. 1998. Phosphorylation of a twitchin-related protein controls catch and calcium sensitivity of force production in invertebrate smooth muscle. *Proc Natl Acad Sci USA* **95**, 5383-5389.

Sjuve, R., Arner, A., Li, Z., Mies, B., Paulin, D., Schmittner, M. and Small, J.V. 1998. Mechanical alterations in smooth muscle from mice lacking desmin. *J Muscle Res Cell Motil* **18**, 415-429.

Sobue, K. and Sellers, J. 1991. Caldesmon, a novel regulatory protein in smooth muscle and non-smooth muscle regulatory systems. *J Biol Chem* **256**, 12115-12118.

Soifer, S.J., Kaslow, D., Roman, C. and Heymann, M.A. 1987. Umbilical cord compression produces pulmonary hypertension in newborn lambs: a model to study the pathophysiology of persistent pulmonary hypertension in the newborn. *J Develop Physiol* **9**, 239-252.

Soifer, S.J. and Heymann, M.A. (1997) Persistent pulmonary hypertension of the newborn. In: Hanson, M.A., Spencer, J.A.D. and Rodeck, C.H. (Eds.) Fetus and Neonate Physiology and clinical applications.

Somlyo, A.P. 1993. Myosin isoforms in smooth muscle: how may they affect function and structure? *J Muscle Res Cell Motil* **14**, 557-563.

Spina, M., Garbisa, S., Hinnie, J., Hunter, J.C. and Serafina-Fracassini, A. 1983. Age-related changes in composition and mechanical properties of the tunica media of the upper thoracic human aorta. *Arteriosclerosis* **3**, 64-76.

Stenmark, K., Fasules, J., Voelkej, Henson, N., Tucker, A., Wilson, H. and Reeves, J. 1987. Severe pulmonary hypertension and arterial adventitial changes in newborn calves at 4300m. *J Appl* **62**, 821-830.

Stenmark, K.R. and Mecham, R.P. 1997. Cellular and molecular mechanisms of pulmonary vascular remodelling. *Annu Rev Physiol* **59**, 89-144.

Stephens, N.L. and Bromberger-Barnea, B. 1969. Length-tension relationships of pulmonary artery and effects of carbon dioxide. *J Appl Physiol* **27**, 266-270.

Stevens, T., Cornfield, D.N., McMurtry, I.F. and Rodman, D.M. 1994. Acute reductions in PO2 depolarise pulmonary artery endothelial cells and decrease [Ca2+]i. *Am J Physiol* **266**, H1416-H1421.

Stevens, A. and Lowe, J. 1997. Human histology. Moseby, London.

Sun, H., Kwiatkowska, K. and Yin, H.L. 1995. Actin monomer binding proteins. *Curr Opin Cell Biol* **7**, 102-110.

Teitel, D.F., Iwamoto, H.S. and Rudolph, A.M. 1990. Changes in the pulmonary circulation during birth-related events. *Pediatr Res* **27**, 372-378.

Thorburn, G.D. and Harding, R. (Eds). 1994. Textbook of Fetal Physiology. Oxford University Press.

Thyberg, J. and Hultgardh-Nilsson, A. 1994. Fibronectin and the basement membrane components laminin and collagen type IV influence the phenotypic properties of subcultured rat aortic smooth muscle cells differently. *Cell Tissue Res* **276**, 263-271.

Tiktinsky, M.H. and Morin, F.C. 1993. Increasing oxygen tension dilates fetal pulmonary circulation via endothelium-derived relaxing factor. *Am J Physiol* **265**, H376-H380.

Topouzis, S. and Majesky, M.W. 1996. Smooth muscle lineage: diversity in the chick embryo. *Dev Biol* **178**, 430-445.

Vanhoute, P.M. 1996. Endothelial dysfunction in hypertension. *J Hypertens* **14**, S83-S93.

Watson P.A., Hannan, R., Carl, L.L. and Giger, K.E. 1996. Desmin gene expression in cardiac myocytes is responsive to contractile activity and stretch. *Am J Physiol* **270**, C1228-1235.

West, J. 1974. Respiratory physiology - the essentials. Williams and Wilkins, Baltimore.

Winder, S., Sutherland, C. and Walsh, M. 1991. Biochemical and functional characterisation of smooth muscle calponin. *Adv Exp Med Biol* **304**, 37-51.

Yamamoto, M., Yamamoto, K. and Noumura, T. 1993. Type 1 collagen promotes modulation of cultured rabbit arterial smooth muscle cells from a contractile to a synthetic phenotype. *Exp Cell Res* **204**, 121-129.

Yano, H., Hayashi, K., Momiyama, T., Saga, H., Haruna, M. and Sobue, K. 1995. Transcriptional regulation of the chicken caldesmon gene. Activation of gizzard-type caldesmon promoter requires a CArG box-like motif. *J Biol Chem* **270**, 23661-23666.

Chapter 10. Appendix: Data for Chapter 5, contractile properties of the intact vessel wall

Group	Strain	Stress Pas (g/cm2)	Stress Act (g/cm2)	ratio stress
Nbbrlla1	1.0	0	28	
Nbbrlla1	1.3	16	63	4.0
Nbbrlla1	1.5	113	217	1.9
Nbbrlla1	1.6	224	322	1.4
Nbbrlla1	1.7	270	374	1.4
Nbbrlla1	1.8	264	374	1.4
Nbbrlla1	1.9	407	490	1.2
NBbrlla2	1.0	0	42	
NBbrlla2	1.2	80	143	1.8
NBbrlla2	1.5	183	284	1.6
NBbrlla2	1.5	304	388	1.3
NBbrlla2	1.6	403	515	1.3
NBbrlla2	1.7	554	577	1.0
NBbrlla2	1.9	797	824	1.0
NBbrlla4	1.1	0	21	
NBbrlla4	1.1	62	93	1.5
NBbrlla4	1.2	109	130	1.2
NBbrlla4	1.2	159	181	1.1
NBbrlla4	1.3	245	245	1.0
NBbrlla4	1.4	291	291	1.0
NBlla5	1.0	33	105	3.1
NBlla5	1.2	89	161	1.8
NBlla5	1.3	152	231	1.5
NBlla6	1.0	0	32	
NBlla6	1.1	36	95	2.7
NBlla6	1.2	65	117	1.8
NBlla6	1.3	108	175	1.6
NBlla6	1.5	172	313	1.8
NBlla6	1.5	307	372	1.2
NBlla6	1.6	380	397	1.0
NBlla6	1.7	427	445	1.0
NBnblla1	1.0	39	58	1.5
NBnblla1	1.1	64	86	1.3
NBnblla1	1.3	170	170	1.0
NBnblla1	1.4	289	316	1.1
NBnblla1	1.6	362	362	1.0

Group	Strain	Stress Pas (g/cm2)	Stress Act (g/cm2)	ratio stress
NBnbIIa2	1.0	35	82	2.3
NBnbIIa2	1.1	86	160	1.9
NBnbIIa2	1.1	167	180	1.1
NBnbIIa2	1.2	242	255	1.1
NBnbIIa2	1.2	295	309	1.0
NBnbIIa2	1.4	363	379	1.0
NBnbIIa2	1.4	409	409	1.0
NBnbIIa2	1.5	424	424	1.0
FETbrIIa1	1.0	0	16	
FETbrIIa1	1.2	26	53	2.0
FETbrIIa1	1.3	35	70	2.0
FETbrIIa1	1.4	44	88	2.0
FETbrIIa1	1.4	62	105	1.7
FETbrIIa1	1.5	89	122	1.4
FETbrIIa1	1.6	124	145	1.2
FETbrIIa1	1.6	151	232	1.5
FETbrIIa1	1.7	186	307	1.7
FETbrIIa2	1.0	0	9	
FETbrIIa2	1.5	7	18	2.5
FETbrIIa2	1.6	15	30	2.0
FETbrIIa2	1.7	25	49	2.0
FETbrIIa2	1.9	36	63	1.8
FETbrIIa2	1.9	46	101	2.2
FETbrIIa2	2.0	57	133	2.3
FETbrIIa2	2.1	97	127	1.3
FETbrIIa2	2.1	110	190	1.7
FETbrIIa3	1.0	28	98	3.5
FETbrIIa3	1.2	83	199	2.4
FETbrIIa3	1.3	122	314	2.6
FETbrIIa3	1.3	183	384	2.1
FETbrIIa3	1.4	249	422	1.7
FETbrIIa3	1.5	314	460	1.5
FETbrIIa3	1.6	327	501	1.5
FETbrIIa3	1.6	431	589	1.4
FETbrIIa4	1.0	63	94	1.5
FETbrIIa4	1.6	102	153	1.5
FETbrIIa4	1.8	171	341	2.0
FETbrIIa4	1.9	122	304	2.5
FETbrIIa4	2.0	188	251	1.3
FETbrIIa4	2.1	200	467	2.3
FETbrIIa4	2.3	290	726	2.5
FETnbIIa1	1.0	0	25	
FETnbIIa1	1.1	9	46	5.0
FETnbIIa1	1.3	33	66	2.0
FETnbIIa1	1.4	49	85	1.8
FETnbIIa1	1.4	49	85	1.8
FETnbIIa1	1.5	76	102	1.3
FETnbIIa1	1.5	89	127	1.4

Group	Strain	Stress Pas (g/cm2)	Stress Act (g/cm2)	ratio stress
FETnblla2	1.0	0	30	
FETnblla2	1.2	24	48	2.0
FETnblla2	1.4	69	83	1.2
FETnblla2	1.7	1008	1008	1.0
FETnblla2	2.2	1268	1268	1.0
FETnblla2	2.7	1560	1560	1.0
FETnblla2	2.7	1593	1593	1.0
FETnblla3	1.0	0	8	
FETnblla3	1.1	10	39	4.0
FETnblla3	1.2	31	62	2.0
FETnblla3	1.3	44	87	2.0
FETnblla3	1.3	66	131	2.0
FETnblla3	1.4	104	138	1.3
FETnblla3	1.4	121	158	1.3
FETnblla3	1.4	146	170	1.2
FETnblla4	1.0	0	17	
FETnblla4	1.4	35	58	1.7
FETnblla4	1.6	53	93	1.8
FETnblla4	1.6	84	112	1.3
FETnblla4	1.7	117	131	1.1
FETnblla4	2.3	1185	1185	1.0
FETnblla5	1.0	0	24	
FETnblla5	1.1	22	35	1.6
FETnblla5	1.3	20	51	2.5
FETnblla5	1.3	37	79	2.1
FETnblla5	1.4	55	83	1.5
FETnblla5	1.4	86	109	1.3
FETnblla6	1.0	0	20	
FETnblla6	1.2	10	34	3.5
FETnblla6	1.3	53	74	1.4
FETnblla6	1.4	55	83	1.5
FETnblla6	1.5	98	125	1.3
FETnblla6	1.6	115	147	1.3
FETnblla6	1.7	150	191	1.3
FETnblla7	1.0	14	20	1.5
FETnblla7	1.2	20	28	1.4
FETnblla7	1.6	32	48	1.5
FETnblla7	1.6	38	55	1.4
FETnblla7	1.8	47	65	1.4
FETnblla7	1.8	74	74	1.0
FETnblla7	2.2	126	126	1.0
FETnblla8	1.0	11	14	1.3
FETnblla8	1.3	18	27	1.5
FETnblla8	1.4	15	24	1.7
FETnblla8	1.5	21	32	1.5
FETnblla8	1.6	29	40	1.4
FETnblla8	1.8	37	50	1.3
FETnblla8	1.8	32	51	1.6
FETnblla8	1.9	34	62	1.8
FETnblla8	2.1	44	73	1.7

Group	Strain	Stress Pas (g/cm2)	Stress Act (g/cm2)	ratio stress
3dhyula1	1.0	0	67	
3dhyula1	1.1	29	113	3.9
3dhyula1	1.2	72	128	1.8
3dhyula1	1.3	93	275	3.0
3dhyula1	1.3	120	212	1.8
3dhula2	1.0	0	28	
3dhula2	1.2	67	168	2.5
3dhula2	1.3	312	386	1.2
3dhula2	1.7	332	380	1.1
3dhula2	1.9	780	833	1.1
3dhylla3	1.0	20	40	2.0
3dhylla3	1.0	42	63	1.5
3dhylla3	1.1	69	80	1.2
3dhylla3	1.2	87	111	1.3
3dhylla3	1.4	110	138	1.3
3dhylla3	1.5	152	213	1.4
3dhylla3	1.6	236	361	1.5
3dhylla3	1.7	333	367	1.1
3dclla1	1.3	0	50	
3dclla1	1.3	78	105	1.3
3dclla1	1.6	97	162	1.7
3dclla1	1.8	325	487	1.5
3dclla1	1.9	467	616	1.3
3dclla1	2.1	616	883	1.4
3dclla1	2.2	828	981	1.2
3dclla2	1.2	76	102	1.3
3dclla2	1.6	0	0	
3dclla2	1.7	280	289	1.0
3dclla2	1.8	421	459	1.1
3dclla2	2.0	611	653	1.1
3dclla2	2.0	722	722	1.0
3dclla2	2.1	937	937	1.0
3dclla3	1.2	118	189	1.6
3dclla3	1.4	336	409	1.2
3dclla3	1.6	441	630	1.4
3dclla3	1.6	815	831	1.0
3dclla3	1.6	946	962	1.0
3dclla3	1.8	1150	1206	1.0
3dclla4	1.0	0	53	
3dclla4	1.1	118	157	1.3
3dclla4	1.3	236	236	1.0
3dclla4	1.6	428	428	1.0
3dclla4	1.7	823	823	1.0
3dclla4	1.7	1067	1098	1.0
3dclla4	1.8	1448	1530	1.1
3dclla4	1.8	1688	1915	1.1

Group	Strain	Stress Pas (g/cm2)	Stress Act (g/cm2)	ratio stress
3dclla5	1.0	0	32	
3dclla5	1.1	17	51	3.0
3dclla5	1.1	25	86	3.4
3dclla5	1.1	50	122	2.4
3dclla5	1.3	88	143	1.6
3dclla5	1.4	131	184	1.4
3dclla5	1.4	188	229	1.2
3dclla5	1.6	139	264	1.9
3dclla6	1.0	0	11	
3dclla6	1.1	0	24	
3dclla6	1.3	52	95	1.8
3dclla6	1.5	89	134	1.5
3dclla6	1.7	99	162	1.6
3dclla6	2.0	231	298	1.3
14dclla1	1.1	18	125	7.0
14dclla1	1.1	18	147	8.0
14dclla1	1.2	39	163	4.2
14dclla1	1.2	40	178	4.5
14dclla1	1.2	54	211	3.9
14dclla1	1.3	71	220	3.1
14dclla1	1.3	92	248	2.7
14dclla1	1.3	129	266	2.1
14dclla1	1.3	187	306	1.6
14dclla1	1.4	207	321	1.6
14dclla1	1.4	268	360	1.3
14dclla2	1.0	30	53	1.8
14dclla2	1.1	52	72	1.4
14dclla2	1.3	74	104	1.4
14dclla2	1.3	113	143	1.3
14dclla2	1.4	169	225	1.3
14dclla2	1.4	220	254	1.2
14dclla2	1.5	240	275	1.1
14dclla2	1.5	282	317	1.1
14dclla2	1.5	310	347	1.1
14dclla2	1.6	382	401	1.1
14dclla2	1.6	406	425	1.0
14dclla2	1.7	469	489	1.0
14dclla3	1.0	58	130	2.3
14dclla3	1.1	98	195	2.0
14dclla3	1.2	137	275	2.0
14dclla3	1.3	199	362	1.8
14dclla3	1.3	235	380	1.6
14dclla3	1.3	286	457	1.6
14dclla3	1.4	319	479	1.5
14dclla3	1.4	359	519	1.4
14dclla3	1.4	409	572	1.4
14dclla3	1.5	427	598	1.4
14dclla3	1.5	524	698	1.3

Group	Strain	Stress Pas (g/cm2)	Stress Act (g/cm2)	ratio stress
14dclla4	1.0	114	114	1.0
14dclla4	1.2	248	413	1.7
14dclla4	1.2	368	566	1.5
14dclla4	1.5	642	913	1.4
14dclla4	1.6	778	1026	1.3
14dclla4	1.7	943	1245	1.3
14dclla5	1.0	48	96	2.0
14dclla5	1.2	166	221	1.3
14dclla5	1.3	337	401	1.2
14dclla5	1.4	486	553	1.1
14dclla5	1.5	629	682	1.1
14dclla5	1.5	714	785	1.1
14dclla6	1.0	0	13	
14dclla6	1.1	31	69	2.3
14dclla6	1.2	134	175	1.3
14dclla6	1.3	180	243	1.4
14dclla6	1.4	347	414	1.2
14dclla6	1.5	518	568	1.1
14dclla6	1.5	627	689	1.1
adlla1	1.0	20	99	5.0
adlla1	1.3	25	124	5.0
adlla1	1.3	26	164	6.3
adlla1	1.4	63	208	3.3
adlla1	1.4	85	291	3.4
adlla1	1.5	129	476	3.7
adlla1	1.6	185	626	3.4
adlla1	1.6	287	775	2.7
adlla1	1.6	304	837	2.8
adlla1	1.7	373	961	2.6
Adlla2	1.0	0	126	
Adlla2	1.1	29	219	7.5
Adlla2	1.2	48	304	6.3
Adlla2	1.2	82	327	4.0
Adlla2	1.3	84	321	3.8
Adlla2	1.4	192	393	2.0
Adlla2	1.5	270	463	1.7
Adlla2	1.5	407	550	1.4
Adlla2	1.8	532	625	1.2
Adlla2	2.0	750	804	1.1
Adlla3	1.0	19	34	1.8
Adlla3	1.1	37	69	1.9
Adlla3	1.1	43	90	2.1
Adlla3	1.2	67	121	1.8
Adlla3	1.2	78	141	1.8
Adlla3	1.3	90	167	1.8
Adlla3	1.3	125	225	1.8
Adlla3	1.4	146	255	1.8

Group	Strain	Stress Pas (g/cm2)	Stress Act (g/cm2)	ratio stress
AdIIa4	1.0	8	34	4.0
AdIIa4	1.2	41	73	1.8
AdIIa4	1.3	55	155	2.8
AdIIa4	1.4	68	159	2.3
AdIIa4	1.4	117	211	1.8
AdIIa4	1.5	173	235	1.4
AdIIa4	1.6	290	345	1.2
AdIIa4	1.8	338	382	1.1
AdIIa5	1.1	11	60	5.5
AdIIa5	1.1	31	94	3.0
AdIIa5	1.2	37	129	3.5
AdIIa5	1.3	53	178	3.4
AdIIa5	1.4	83	194	2.3
AdIIa5	1.4	115	230	2.0
AdIIa5	1.5	133	273	2.1
AdIIa5	1.5	159	295	1.9
AdIIa5	1.6	155	311	2.0
AdIIa5	1.6	172	313	1.8
AdIIa5	1.7	214	370	1.7
AdIIa5	1.7	239	436	1.8
AdIIa5	1.9	331	543	1.6
AdIIa6	1.0	0	93	
AdIIa6	1.1	30	207	7.0
AdIIa6	1.2	129	324	2.5
AdIIa6	1.4	183	475	2.6
AdIIa6	1.5	275	590	2.1
AdIIa6	1.6	379	674	1.8

Histological measurements (mean values)

Age	external diameter (micrometre)	wall thickness (micrometre)	Percentge wall thickness
Fetal/NB	1240	142	23
3 days	1144	125	22
0-3 hypoxia	1309	144	22
14 days	2344	129	11
Adult	2750	138	10